Proceedings of the Nineteenth Annual Pacific Climate Workshop

Asilomar Conference Grounds
Pacific Grove, California
March 3-6, 2002

Edited by
G. James West and Nikki L. Blomquist

Technical Report 71
of the
Interagency Ecological Program for the
San Francisco Estuary

March 2003

PACLIM

Climate Variability
of the
Eastern North Pacific
and
Western North America

Single copies of this report may be obtained without charge from:

State of California
Department of Water Resources
P.O. Box 942836
Sacramento, CA 94236–0001

Proceedings of the Nineteenth Annual Pacific Climate Workshop

Asilomar Conference Grounds
Pacific Grove, California
March 3-6, 2002

Edited by
G. James West and Nikki L. Blomquist

Technical Report 71
of the
Interagency Ecological Program for the
San Francisco Estuary

March 2003

PACLIM

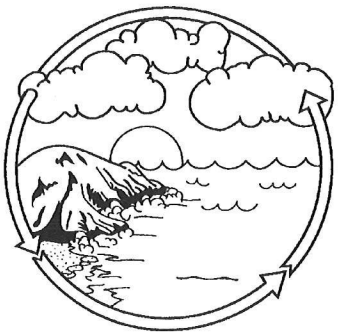

Climate Variability
of the
Eastern North Pacific
and
Western North America

Contents

Contents iii

Authors v

Statement of Purpose vii

Introductions ix

Acknowledgements xi

Was Water Year 2002 Wet Enough to Avoid Drought? 1
Maurice Roos

A 2,000-Year-Long Record of Climate from the Gulf of California 11
John A. Barron, David Bukry, and James L. Bischoff

Stratigraphic Evidence in Polar Ice of Variations in Solar Activity: Implications for Climate? 23
Gisela A.M. Dreschhoff

Looking for Recent Climatic Trends and Patterns in California's Central Sierra 35
Gary J. Freeman

Empirical Search for Clues to Process and Dynamics Underlying Climatic Change 49
Thor Karlstrom

Non-Precipitation Variability of the Western United States Snowpack .. 77
Mark Losleben

Is Streamflow Increasing in the Conterminous United States? 93
Gregory J. McCabe and David M. Wolock

The Effects of Galactic Cosmic Rays on Weather and Climate on Multiple Time Scales 99
Ed Mercurio

Suggested Research on the Effect of Climate Change on California Water Resources 121
Maurice Roos

A Holocene Record From Medicine Lake, Siskiyou County, California: Preliminary Diatom, Pollen, Geochemical, and Sedimentological Data 131
Scott W. Starratt, John A. Barron, Tara Kneeshaw, R. Larry Phillips, James L. Bischoff, Jacob B. Lowenstern, and James A. Wanket

Overture to a Landslide—A Seasonal Moisture Prerequisite 149
Raymond C. Wilson

The 400-Year Wet-Dry Climate Cycle in Interior North America and Its Solar Connection 159
Zicheng Yu and Emi Ito

Abstracts 165

Appendix A: Agenda 207

Appendix B: Poster Presentations 215

Appendix C: Participants 217

Authors

John A. Barron
Earth Surface Dynamics Program, MS910
U.S. Geological Survey
345 Middlefield Road
Menlo Park, CA 94025

James L. Bischoff
Earth Surface Dynamics Program, MS910
U.S. Geological Survey
345 Middlefield Road
Menlo Park, CA 94025

David Bukry
Earth Surface Dynamics Program, MS910
U.S. Geological Survey
345 Middlefield Road
Menlo Park, CA 94025

Gisela A.M. Dreschhoff
Department of Physics and Astronomy
University of Kansas
Malott Hall
1251 Wescoe Hall Drive
Lawrence, KS 66045

Gary J. Freeman
Pacific Gas and Electric Company
Mail Code N13C
PO Box 770000
San Francisco, CA 94177-0001

Emi Ito
Limnological Research Center
University of Minnesota
310 Pillsbury Drive S.E.
Minneapolis, MN 55455-0219

Thor Karlstrom
4811 SW Brace Point Drive
Seattle, WA 98136

Tara Kneeshaw
U.S. Geological Survey
345 Middlefield Road
Menlo Park, CA 94025

Mark Losleben
University of Colorado
818 County Road 116
Nederland, CO 80466

Jacob B. Lowenstern
U.S. Geological Survey
345 Middlefield Road
Menlo Park, CA 94025

Gregory J. McCabe
U.S. Geological Survey
P.O. Box 25046
Denver Federal Center, MS 412
Denver, CO 80225

Ed Mercurio
Hartnell College, Meteorology
156 Homestead Ave.
Salinas, CA 93901

R. Larry Phillips
U.S. Geological Survey
345 Middlefield Road
Menlo Park, CA 94025

Maurice Roos
California Department of Water Resources, retired
3310 El Camino Ave, Suite 200
PO Box 219000
Sacramento, CA 95821-9000

Scott W. Starratt
U.S. Geological Survey
345 Middlefield Road
Menlo Park, CA 94025 and

Department of Geography
University of California, Berkely
Berkeley, CA 94720

James A. Wanket
Department of Geography
University of California, Berkeley
507 McCone Hall
Berkeley, CA 94720-4740

Raymond C. Wilson
U.S. Geological Survey
345 Middlefield Road
Menlo Park, CA 94025

David M. Wolock
U.S. Geological Survey
4821 Quail Crest Place
Lawrence, KS 66049

Zicheng Yu
Department of Earth and Environmental Sciences
Lehigh University
31 Williams Drive
Bethlehem, PA 18015-3188

Statement of Purpose

In 1984, a workshop was held on "Climatic Variability of the Eastern North Pacific and Western North America." From it has emerged an annual series of workshops held at the Asilomar Conference Grounds at Pacific Grove, California, and the Wrigley Institute for Environmental Studies at Two Harbors, Santa Catalina Island, California. These annual meetings, which involve 80-100 participants, have come to be known as the Pacific Climate (PACLIM) Workshops, reflecting broad interests in the climatologies associated with the Pacific Ocean and western Americas in both the northern and southern hemispheres. Participants have included atmospheric scientists, hydrologists, glaciologists, oceanographers, limnologists, and both marine and terrestrial biologists. A major goal of PACLIM is to provide a forum for exploring the insights and perspectives of each of these many disciplines and for understanding the critical linkages between them.

PACLIM arose from growing concern about climate variability and its societal and ecological impacts. Storm frequency, snowpack, droughts and floods, agricultural production, water supply, glacial advances and retreats, stream chemistry, sea surface temperature, salmon catch, lake ecosystems, and wildlife habitat are among the many aspects of climate and climatic impacts addressed by PACLIM Workshops. Workshops also address broad concerns about the impact of possible climate change over the next century. From observed changes in the historical records, the conclusion is evident that climate change would have large societal impacts through effects on global ecology, hydrology, geology, and oceanography.

Our ability to predict climate, climate variability, and climate change critically depends on an understanding of global processes. Human impacts are primarily terrestrial in nature, but the major forcing processes are atmospheric and oceanic in origin and transferred through geologic and biologic systems. Our understanding of the global climate system and its relationship to ecosystems in the Eastern Pacific area arises from regional study of its components in the Pacific Ocean and western Americas, where ocean-atmosphere coupling is strongly expressed. Empirical evidence suggests that large-scale climatic fluctuations force large-scale ecosystem response in the California Current and, in a very different system, the North Pacific central gyre. With such diverse meteorologic phenomena as the El Niño–Southern Oscillation and shifts in the Aleutian Low and North Pacific High, the eastern Pacific has tremendous global influences and particularly strong effects on North America. In the western United States, where rainfall is primarily a cool-season phenomenon, year-to-year changes in the activity and tracking of North Pacific winter storms have substantial influence on the hydrological balance. This region is rich in climatic records, both instrumental and proxy. Recent research efforts are beginning to focus on better paleoclimatic reconstructions that will put present day climatic variability in context and allow better anticipation of future variations and changes.

The PACLIM Workshops address the problem of defining regional coupling of multifold elements as organized by global phenomena. Because climate expresses itself throughout the natural system, our activity has been, from the beginning, multidisciplinary in scope. The specialized knowledge from different disciplines has brought together climatic records and process measurements to synthesize and understand the complete system. Our interdsciplinary group uses diverse time series, measured both directly and through proxy indicators, to study past climatic conditions and current processes in this region. Characterizing and linking the geosphere, biosphere, and hydrosphere in this region

provides a scientific analogue and, hence, a basis for understanding similar linkages in other regions and for anticipating the response to future climate variations. Our emphasis in PACLIM is to study the interrelationships among diverse data. To understand these interactive phenomena, we incorporate studies that consider a broad range of topics both physical and biological, time scales from months to millennia, and space scales from single sites to the entire globe.

Introductions

Editor's Introduction

G. James West, U.S. Bureau of Reclamation

The Nineteenth Annual PACLIM Workshop was held at the Asilomar State Conference Grounds at Pacific Grove, California. The stunning and easily accessable location of the workshop has served well for conferences on climate of the eastern Pacific. Attended by more than 100 registered participants (see Appendix C, Attendees), the workshop included 38 scheduled talks and 28 poster presentations. This year's primary themes were climatic influences on oceanic biology and solar influences on climate. The special session on Climate and Oceanic Biology was chaired by John McGowan (see below). The remaining talks consisted of a diverse range of issues ranging from modern climate change and variability to paleoclimate reconstruction (see Appendix A, Agenda). On the first evening, Kelly Redmond gave us the weather and climate for the "PACLIM YEAR" PY2002, Maury Roos presented his annual California Water Year report and Jeff Severinghaus spoke on the role of the sun in climate variation. Monday evening's speaker, Richard Wilson, provided interesting information on the sun's variability. Poster presentations were displayed throughout the entire meeting and time was set aside on Tuesday evening for their presentation and discussion (see Appendix B, Poster Presentations).

All presenters were invited to expand their abstracts into a manuscript for inclusion in the Proceeding volume, and nearly all presentations are included in manuscript or abstract form. In this Proceedings volume, 13 papers are presented full-length. The abstracts submitted to the meeting are printed in a following section. The papers are not formally peer reviewed and editorial comments are generally limited to grammar, spelling, punctuation, and format. Editorial comments on the content on some submittals have been offered, but it is the responsibility of the author(s) for any errors of fact or logical inconsistencies.

Special Session Introduction—Climate and Oceanic Biology

John McGowan, Scripps Institution of Oceanography

The background for the special session on Climate and Oceanic Biology is the observation that the earth's atmosphere and oceans are warmer now than at any time since reliable instrumental measurements began. We can expect the warming to continue. A great deal of effort is being devoted to understanding the physics of the warming and in picking apart the details of the carbon cycle. But it is the consequences of such climatic variability to the biology of the oceans that concerns a rather small group of biologists and this, after all, is or should be of major importance. This research is a new kind of ecology. Most biologists are unprepared for study on the time/space scales of the phenomenon, but somehow we must find our way.

The special session is an attempt to gather together those biological oceanographers concerned about the consequences of change, to report on the status of their research, and to determine if there is common ground among us.

PACLIM, a personal view

G. James West

After four great years of sharing the editorship of the PACLIM Proceedings, it is time for me to pass the torch. I've thoroughly enjoyed interacting with my co-editors, the authors, and participants during this time. It's been a positive experience and I've learned a lot. Thanks to Ray Wilson and Lauren Buffaloe who guided a then-neophyte editor through the intricacies of turning a collection of papers into a finished document. A special thanks goes to my wife, Katherine, who helped in so many ways and did a lot of work on the volumes, too. Thanks for the privilege of letting me have the opportunity of being part of PACLIM.

Acknowledgements

PACLIM workshops are produced by volunteers who always manage to put together a topically interesting and timely gathering of a wide range of researchers. The 2002 workshop had more than 100 participants and attendees, many for the first time, continuing the tradition started almost two decades ago by providing an inviting forum for new ideas, information, and concepts.

For 2002, thanks go to the following institutions and people: **USGS**: Mike Dettinger, Program Chair and Charles Perry; **Long Beach City College**: Janice Tomson, Meeting Organizer; **Scripps Institution of Oceanography**: Dan Cayan, Program Chair Emeritus and John A. McGowan, Emeritus; and **Center for Climate/Ocean Resources**: Gary Sharp.

Sponsorship and funding for the workshops come from a wide variety of sources. This year's PACLIM Workshop was sponsored by: U.S. Geological Survey Water Resources Division, Bill Kirby; NOAA Office of Global Programs, Roger Pulwarty and Harvey Hill; CALFED Bay-Delta Science Program, Sam Luoma; U.S. Navel Postgraduate School, Tom Murphree; State of California Department of Water Resources, Zach Hymanson.

For the fifth year Mike Dettinger chaired and organized the meeting and maintained the Web site. As she has done previously, Janice Tomson did a superb job of planning, organizing, and supervising the operation of the meeting — getting us there; getting us fed, watered, and roomed; and, with her Long Beach City College students, doing all the other numerous things that need to be done to make a successful meeting. Lucenia Thomas, USGS Water Resources Division, arranged travel and assisted in the meeting organization. Tom Murphee, Naval Postgraduate School, provided and set up the audio-visual equipment. The seven meeting moderators are also greatly acknowledged. Finally, we thank all our speakers and poster presenters (listed in agenda) for their contributions and enthusiasm.

For the editing, production and printing of the proceedings, thanks go to the California Department of Water Resources and the U.S. Bureau of Reclamation's Interagency Ecological Program for the Sacramento-San Joaquin Estuary. The production of this volume was performed by my co-editor, Nikki Blomquist, who I thank for her special expertise and knowledge. Katherine West assisted in editing the papers.

The precedents for the 2002 volume were established by the previous editors of the PACLIM Proceedings: Dave Peterson (1984-1988), with the able assistance of Lucenia Thomas; Julio Betancourt and Ana MacKay (1989-90); Kelly Redmond and Vera Tharp (1991-1993); Caroline Isaacs and Vera Tharp (1994-1996); Ray Wilson and Vera Tharp (1997); Ray Wilson and Lauren Buffaloe (1998); and G. James West and Lauren Buffaloe (1999-2001).

G. James West
U.S. Bureau of Reclamation
Sacramento, California

Was Water Year 2002 Wet Enough to Avoid Drought?

Maurice Roos[1]

Water year (WY) 2000-01, October 2000 through September 2001, was dry in northern California with statewide runoff only about half average. It was driest in the northeastern region of the State (remember the news about the Klamath Project troubles). For most water users, however, reservoir storage from the previous good years helped take up some of the slack. But, as the water year ended, storage was about 10% below average and more than 20% behind the previous year (in September 2000). There was much concern that a second dry year would plunge California into drought.

Let's take a look at the major parameters of water supply for this year to see how we did. The situation looked fairly good at the end of March with a 95% of average snowpack and runoff forecasts at 80% of average overall. But the spring (and summer) was dry and the actual snowmelt runoff turned out to be about 70% and the water year amount about 75% of average. Table 1 shows the figures for WY 2002 along with previous years, including the last critical dry year of 1994. (For the river runoff percentages in the table, I have continued to use the 1946-1995 average to enable comparison with last year's report. The Snow Surveys program has updated the current averages, using 1951-2000 figures which are about 5% wetter due to inclusion of 5 relatively wet years.) The first figure shows the distribution of precipitation by hydrologic areas for the water year. Note the "dry south more moderate north" pattern; this is a reversal of the previous winter's pattern, which was quite dry in the north.

Figure 2 shows a comparison of estimated monthly statewide precipitation compared to average for the water year. Summer deficits do not really mean much, because normal amounts are quite small anyway. Approximately 75% of our average annual precipitation comes during the five months, November through March. In WY 2001-02, two of the wet months were well above average (November and December), while all the other months were below average. January and February were quite dry at about half normal. The wetness of November and December provided about half of a full season supply, enough excess to make up a major share of the deficits in the rest of the year and ensure adequate, but not ample, supplies for most users.

Figure 3 and 4 show northern Sierra monthly and accumulated precipitation during the year. Figure 5 shows the snowpack water content for the three sections of the State from snow sensors. Note the rapid melting in April and the lower buildups in the southern Sierra. Figure 6 shows the April through July runoff, in percent of average. The overall statewide average was about 70%. Note the dropoff at the southern end of the Sierra, particularly the Kern River at 46%.

1. Presented at the Pacific Climate Workshop in Pacific Grove, March 3, 2002, with statistics updated in October 2002.

Table 1: Percentage of average (unless noted)

	2002	*2001*	*2000*	*1999*	*1998*	*1997*	*1994*
Statewide							
Precipitation	80	75	100	95	170	125	65
April 1 snowpack	95	60	100	110	160	75	50
Runoff	75	50	95	110	175	145	40
Reservoir storage, Sept. 30	87	89	111	118	136	104	73
Reservoir storage, maf	19.4	(19.3)	(24.2)	(25.6)	(29.6)	(22.7)	(15.9)
Regional							
Northern Sierra Precipitation	93	66	113	110	165	138	64
8 Station Index, inches	46.3	(33.0)	(56.7)	(54.8)	(82.4)	(68.7)	(31.8)
Sacramento River	81	54	104	117	174	141	43
Unimpaired runoff, maf	(14.6)	(9.8)	(18.9)	(21.2)	(31.4)	(25.4)	(7.8)
San Joaquin River	72	57	103	104	183	167	45
Unimpaired runoff, maf	(4.1)	(3.2)	(5.9)	(5.9)	(10.4)	(9.5)	(2.5)

Note: 1996-1995 averages for runoff

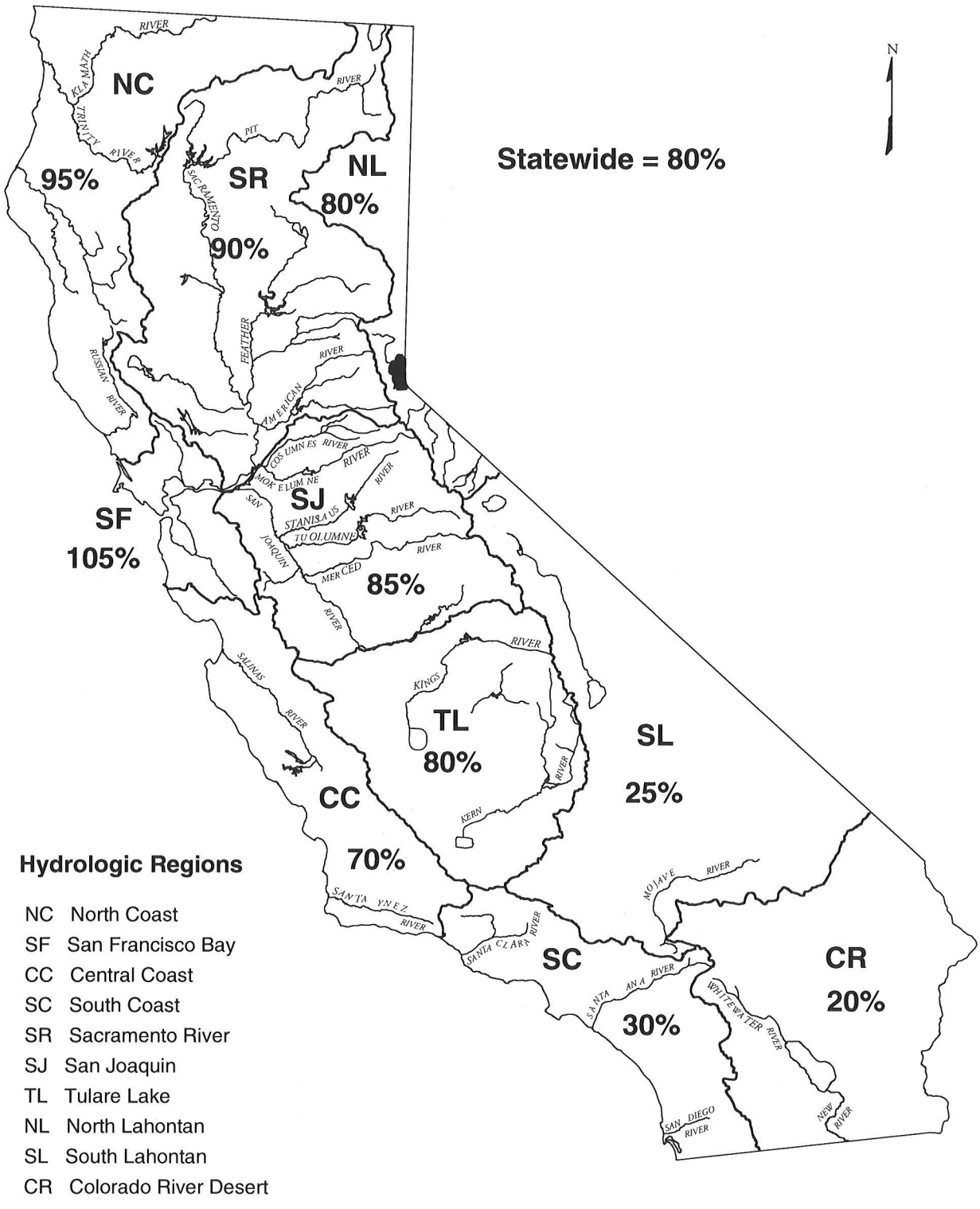

Figure 1 Water year 2002 precipitation in percent of average (by hydrologic region)

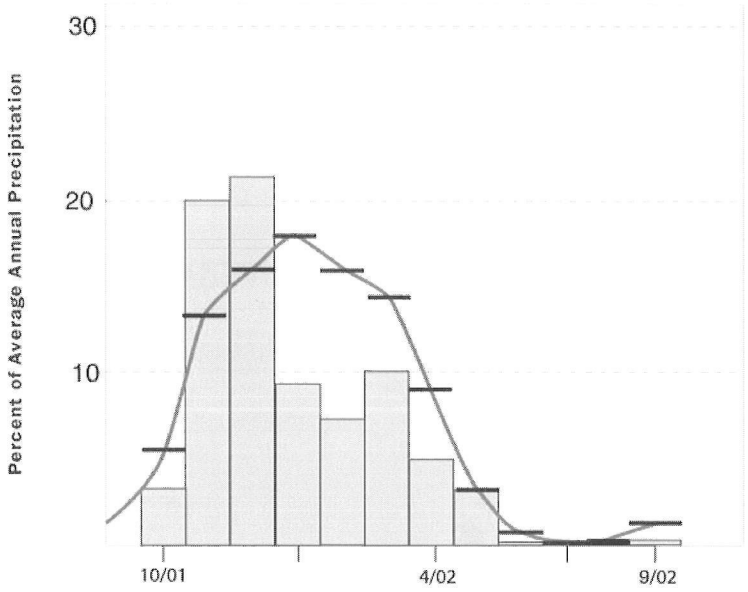

Figure 2 Estimated WY 2002 monthly precipitation pattern

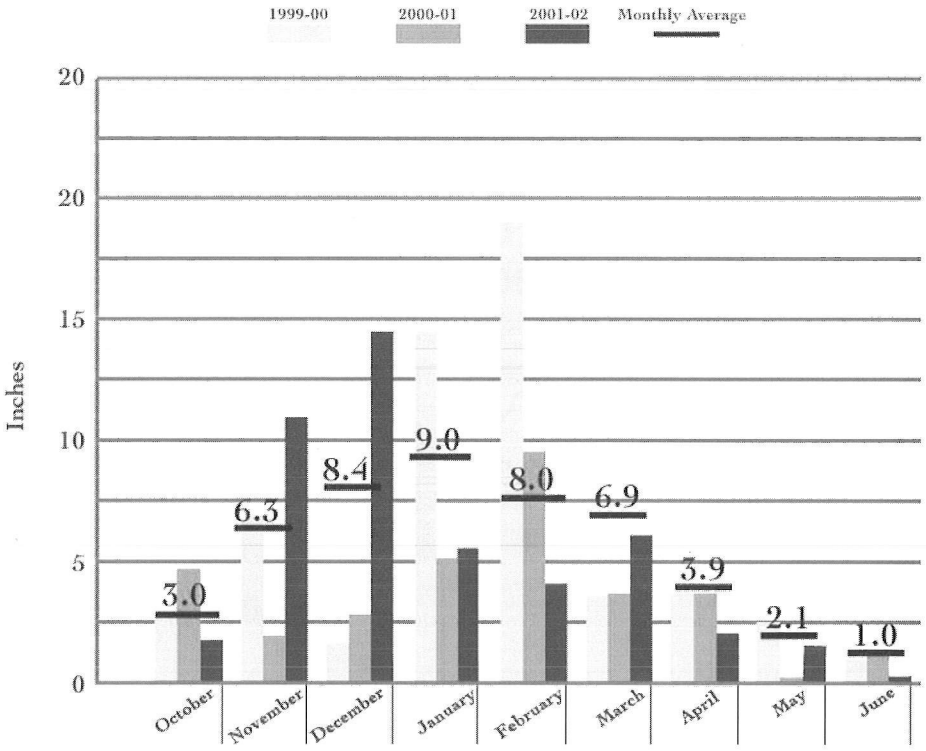

Figure 3 Northern Sierra monthly precipitation, in inches

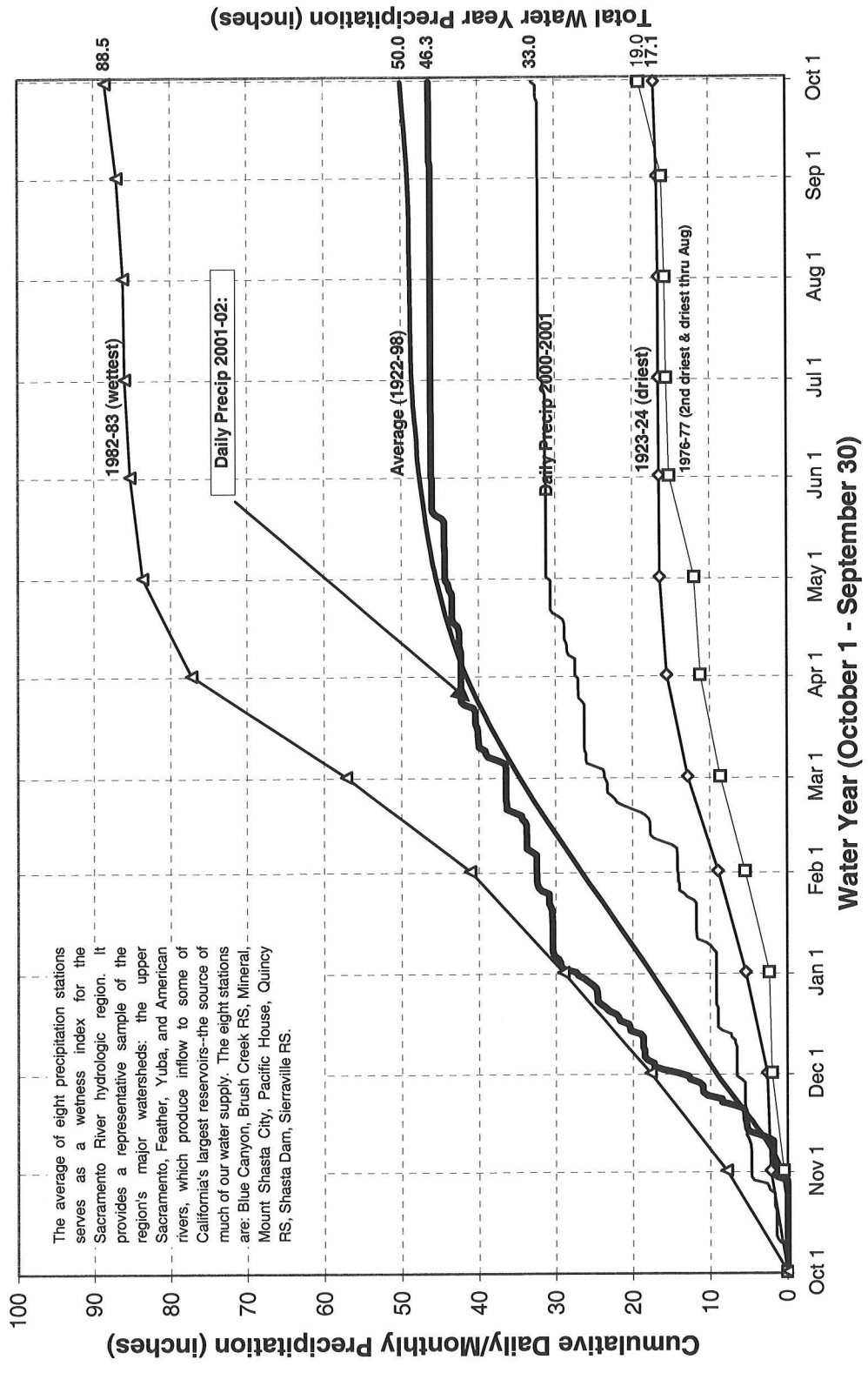

Figure 4 Cumulative northern Sierra precipitation, WY 2002, in inches

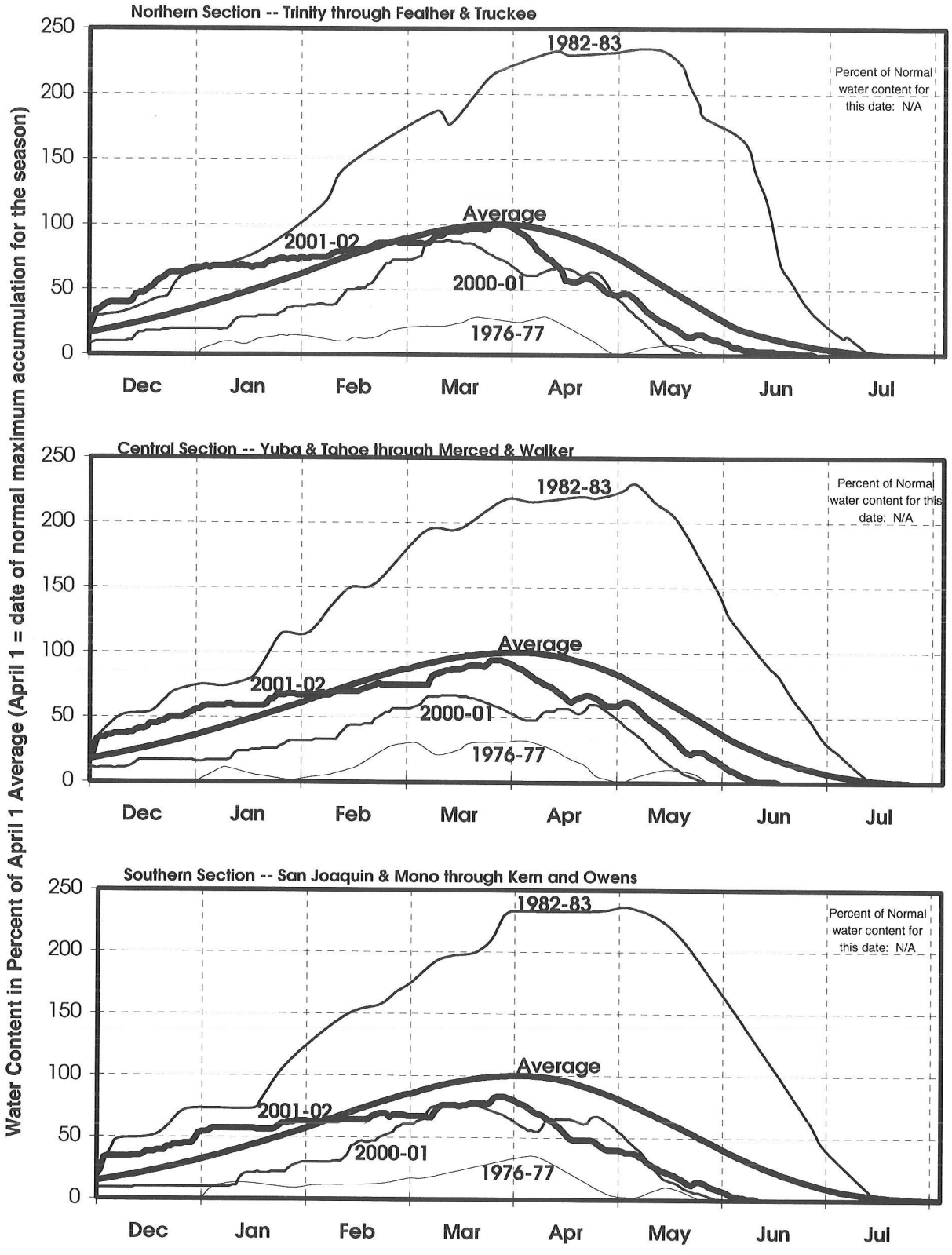

Figure 5 Snow water content in percent of April 1 average

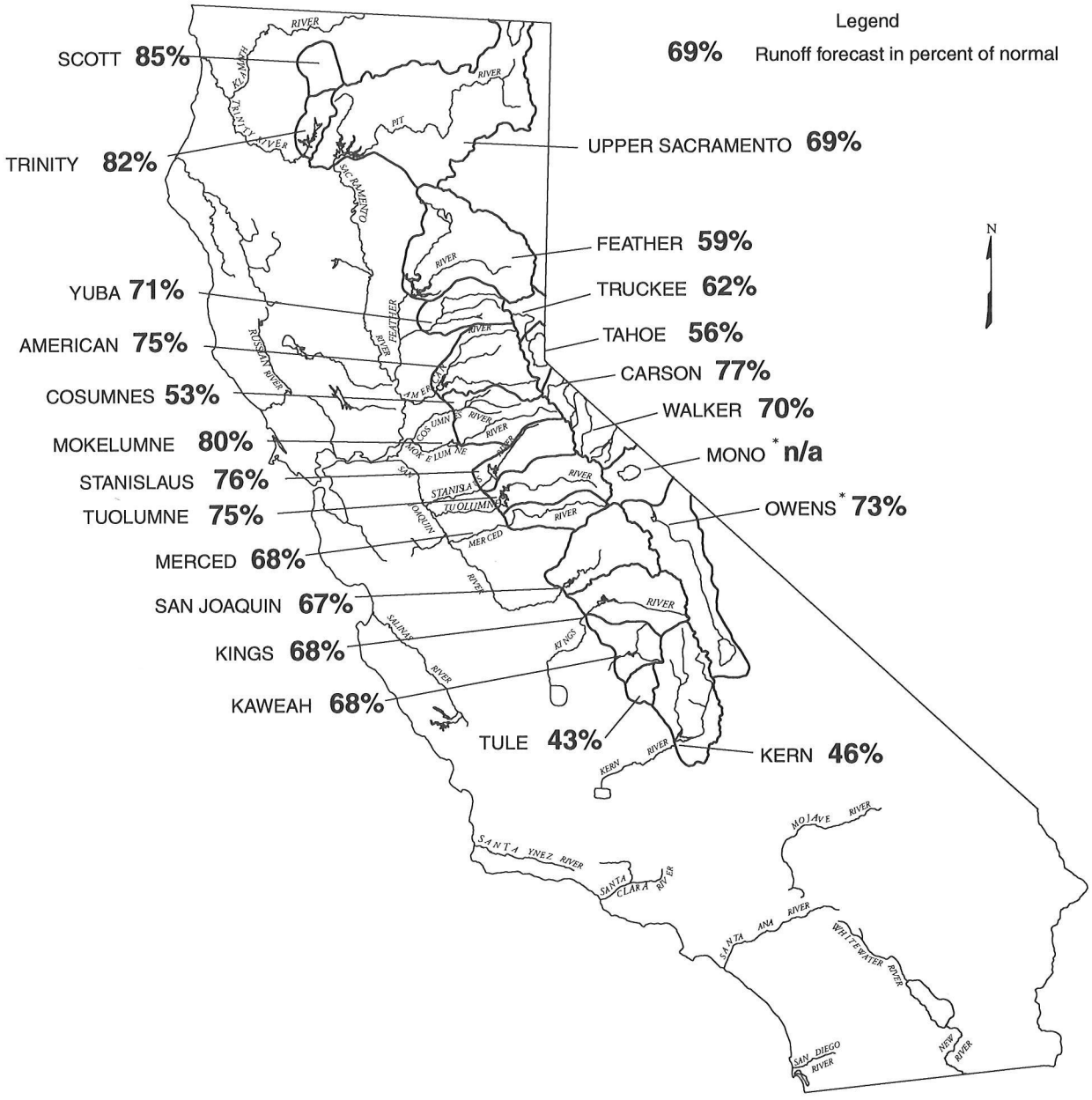

Figure 6 Estimated actual April through July unimpaired runoff for WY 2002

The snowpack started out with a wintry blast reaching nearly 1.5 times normal for the date on January 1, and 60% of a full April 1 pack. Since then the increase was pretty nominal for two months with a final boost in March which brought the pack to 95% of the average seasonal amount on April 1. That compares well with 2001 when some early melting of a smaller pack eventually left 60% on April 1. Winter runoff this year was about 80% of average at the end of March, double the 40% of the previous year.

Reservoir storage overall recovered to average by April 1 which boded well for water supply. For the SWP, an initial allocation of 20% of entitlements was made on November 30. In mid-January this

was upped to 45%. In late March the allocation was raised to 60%. In May, 5% more was added. A final adjustment in August raised the 2002 allocation to 70%. The 70% is 2.89 million acre-feet (maf) out of 4.13 maf entitlements. Last year's entitlement deliveries were 39%. On March 6, 2001, the allocation was only 25% of entitlements.

For the CVP, the mid-February allocation of San Joaquin Valley west side project agricultural deliveries was 55%, compared to an eventual 52% in 2001. Urban users south of the Delta would get 80%. These numbers did not change much for the February median projection which called for 60% and 85% respectively. Wildlife refuges were to get 100%, as did water rights holders and Sacramento Valley CVP users. San Luis reservoir was about 95% full in early March, so the problem for the summer was conveyance south of the Delta and the constraints on exports. Eventually the CVP was able to deliver 70% for west side agriculture and 95% of the urban users south of the Delta.

Things were not quite as good for the east side of the San Joaquin Valley. Near Fresno, the Friant (Millerton) allocations were 912 thousand acre-feet (taf), 61% of the long term average of 1500 taf. The 912 taf was 100% of Class 1 water, and 8% of Class 2 water. Stanislaus River CVP project users received 15 taf, only 10%.

The next two charts (Figures 7 and 8) illustrate the recent history of Sacramento and San Joaquin River runoff. Earlier in the spring we were predicting a "below normal" water year for 2002. But as below normal precipitation continued, in the May 1 DWR Bulletin 120 report on "Water Conditions in California", the water year classification was lowered to "dry". Estimated actual water year runoff for the Sacramento and San Joaquin River systems turned out to be about 3% under the May 1 forecasts. Estimated actual April through July runoff was about 5% under the May 1 forecast.

Water storage at the end of the water year for the past several years is shown on Figure 9. In-state major reservoir storage at the end of WY 2002 totaled about 19.4 maf, some 87% of average, virtually the same as the year before. That is the lowest since 1994 when the reservoirs held about 15.9 maf. In 1992 at the end of the 6 year drought, storage had dropped to 12.7 maf. So there is some carryover available for WY 2003. Another big question for 2003 is how much interim surplus will be available to southern California from the Colorado River. In recent years California has been using up to 0.8 maf of surplus over its long term entitlement of 4.4 maf.

Now to go back to the initial question: Was the year wet enough to avoid drought? My answer is "yes" for this year, but it was not wet enough to build a reserve cushion for next year. So we live one year at a time and hope the following winter will be a little wetter.

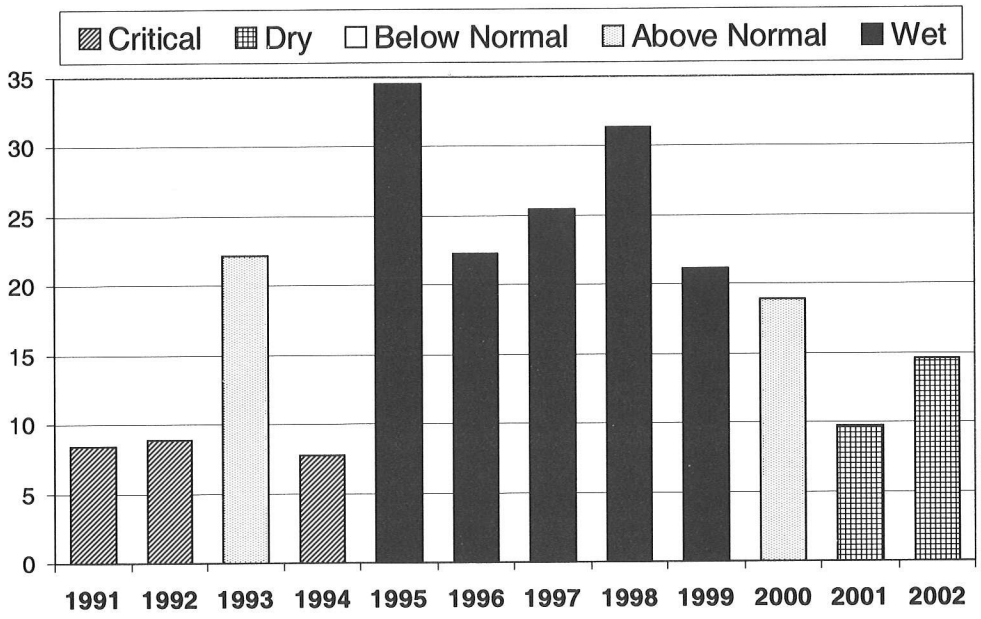

Figure 7 Sacramento River system runoff, in maf

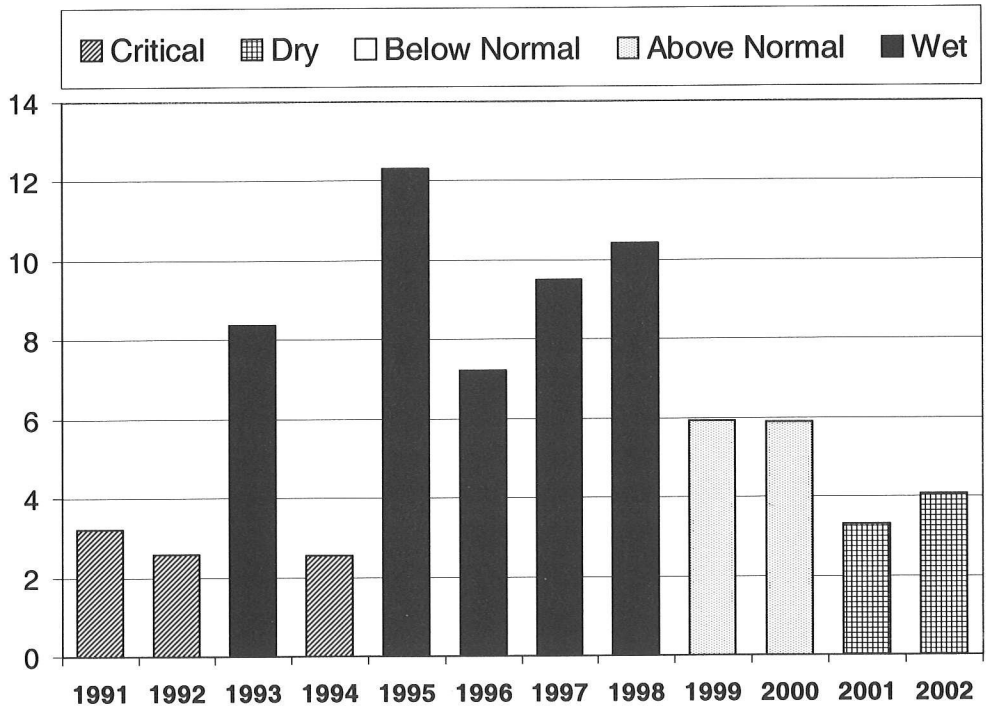

Figure 8 San Joaquin River system runoff, in maf

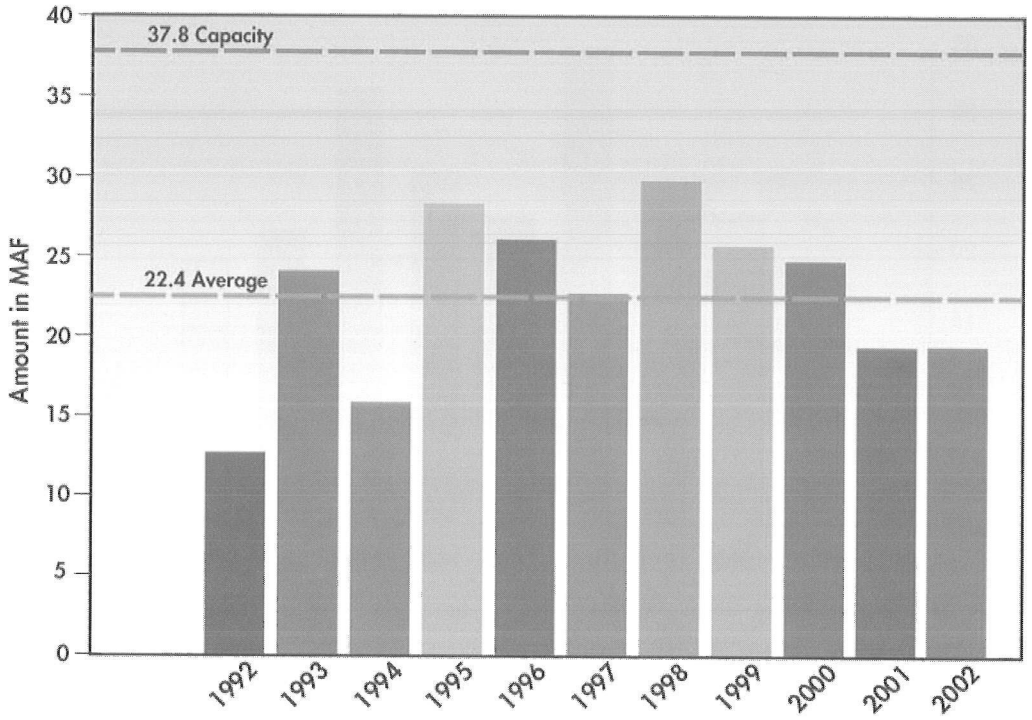

Figure 9 Storage in 156 major in-state reservoirs on October 1, 2002

A 2,000-Year-Long Record of Climate from the Gulf of California

John A. Barron, David Bukry, and James L. Bischoff

Abstract

High resolution study (samples every ca. 37 yr) of the diatoms, silicoflagellates, and geochemistry of Kasten Core BAM80 E-17 yields a detailed record of climatic and paleoceanographic change for the past 2,000 years for the eastern Guaymas Basin, a region of very high diatom productivity within the central Gulf of California.

Roughly every 200 years, intervals enriched in diatoms alternate with intervals characterized by higher terrigenous material and total organic carbon (TOC), suggesting solar forcing. The record of percent biogenic silica is remarkably similar to the radiocarbon production curve, with increased diatom production occurring during sunspot minima. It is suggested that solar minima coincide with an increase in the strength or duration of late fall/winter northwest winds blowing down the Gulf due to atmospheric cooling above northwest Mexico.

A prolonged interval of dramatically warmer sea surface temperatures (SST) that is marked by a two-fold increase (above normal background fluctuations) in the relative abundance of the tropical diatom *Azpeitia nodulifera* occurs between ca. 910-1140 AD, corresponding to the Medieval Warm Period. This interval is interrupted by a brief period (ca.1020-1100 AD) of reduced *A. nodulifera* and enhanced diatom production.

Introduction

The climate of the Gulf of California (referred to elsewhere as "the Gulf") region is divided into a mid-latitude, winter phase and a subtropical, summer phase. During the winter, prevailing surface winds are northwesterly, along the mean pressure gradient, causing an overturn of the water column, upwelling of nutrients and enhanced phytoplankton production. This pattern is punctuated by brief southerly winds lasting a few days caused by an anticyclone that often resides over the southwestern United States (Bandon-Dangon and others 1991). During the summer, winds blow steadily from the south, resulting in a monsoonal climate of increased rainfall.

Thunell's (1998) sediment trap studies in the Guaymas Basin reveal that the peak flux in biogenic silica, which is overwhelmingly diatoms, occurs in November to December, coincident with the onset of northwest winds. A secondary peak occurs in early spring, coinciding with a period of coastal upwelling that is stronger along the mainland coast than it is off the coast of Baja California (Santamaria-del-Angel and others 1994). Such conditions produce anoxic bottom conditions and some of the most rapidly accumulating biogenic sediments in the world.

High resolution studies of the latest Holocene in the Guaymas Basin have focused on Kasten core BAM80 E-17, which was taken by the R/V Matamoros of Oregon State University in 1980 at 27.920°N and 111.610°W beneath 620 m of water. Over 450 cm of varved, diatom-rich sediment

was recovered in this core. Murray (1982) used varve counting to estimate the sedimentation rate of BAM80 E-17 at 0.23 cm/yr; however, he noted that three radiocarbon dates on benthic foraminifers suggested a sedimentation rate of 0.13 cm/yr. Subsequent varve counting by Karlin (1984) yielded a sedimentation rate of 0.135 cm/yr that conforms more closely to the sedimentation rate suggested by radiocarbon dating.

Murray (1982) studied the downcore variability of silicoflagellate assemblages over the entire length of BAM80 E-17 at 5 cm intervals. He found major cycles in the relative percentages of *Octactis pulchra*, a silicoflagellate that he considered to be indicative of upwelling and high productivity, and *Dictyocha messanensis*, a silicoflagellate that is more common outside of the Gulf on the Pacific coast of southern Baja California.

Schrader and Baumgartner (1983) estimated decadal variations of productivity levels during the past 500 years in a number of Kasten cores from the central Gulf of California. They used *O. pulchra* to estimate productivity with a chronology based on varve counts and silicoflagellate assemblage changes. Schrader and Baumgartner (1983) compared their results with a tree-ring record from the Sierra Madre Occidental and concluded that drier continental conditions showed a good match with intervals of increased productivity (higher upwelling).

Julliet-Leclerc and Schrader (1987) used oxygen isotopes from the biogenic silica of diatoms to infer sea surface temperature (SST) variations in the eastern Guaymas Basin over the past 3.000 years. Their data for Kasten core BAM80 E-13, which was dated by ^{137}Cs isotopes and varve counting, suggested to them that SSTs warmed as much as 13°C during the past century. Subsequently, Julliet-Leclerc and others (1991) revised their SST estimates, calling for a ca. 8°C increase during the past century. Such a warming, however, seems rather extreme compared to the <3°C maximum warming in SSTs predicted for the past 300 yr in the Guaymas Basin by the alkenone studies of Goñi and others (2001).

For the 450 cm-long record of BAM80 E-17, Julliet-Leclerc and Schrader (1987) appear to have used a sedimentation rate of ca. 0.15 cm/yr in plotting their SST record for the past 3,000 years. They observed a total temperature amplitude of ca. 8°C over the 3,000 yr-long record with highest SSTs (17°C) occurring at the core top and approximately 3,000 years ago. Julliet-Leclerc and Schrader (1987) suggested that northwesterly winds (=upwelling and low SSTs) were at their maximum between 2,000 and 1,500 yr BP, which would presumably correspond to ca. 2,200 to 1,660 yr BP, if Karlin's (1984) sedimentation rate of 0.135 cm/yr was used.

A high resolution study of diatoms, silicoflagellates, and geochemistry on the same samples would reveal much about the interrelationships between these various proxies. At the same time, a paleoclimatic record of the past 2,000 yr from BAM80 E-17 should be very valuable both for synthesizing the late Holocene paleoceanographic history of the Gulf of California and for comparisons with high resolution records from the Pacific coasts of Baja and Alta California.

Materials and Methods

Samples were taken at 5 cm-intervals from the upper 250 cm of BAM80 E-17, corresponding to a sampling interval of ca. 37 yr, according to Karlin's (1984) sedimentation rate of 0.135 cm/yr. The approximate 1 cm-thickness of each sample and the varved nature of the sediments means that each sample represents on the order of seven years of deposition. Samples were taken vertically across the varves and homogeneous splits were used for siliceous microfossil and geochemical studies.

Geochemistry

Bulk ICP-AES geochemical analyses were performed on these samples following total sample dissolution after metaborate fusion. The following elements were analyzed: Na, Mg, Al, Si, P, K, Ca, Ti, Cr, Mn, Fe, Sr, Y, Zr, Nb, and Ba. Weight percent biogenic silica was estimated from the analyses by using the Si/Al ratio to factor out the terrigenous (non biogenic) silica. Our data indicate that the average sea floor terrigenous sediment in the central Gulf of California is very similar to the average for Pacific pelagic clay which has a Si/Al ratio of 3.30. Silica in excess of this ratio is deemed biogenic. Calcium carbonate percent was determined for the same samples by acidification and measurement of evolved CO_2 by coulomtery. Total carbon was determined on a separate aliquot by combustion at 1000°C and coulometric measurement of evolved CO_2. Organic carbon was calculated as the difference between total carbon and $CaCO_3$ carbon.

Diatoms

Following Sancetta (1995), counts of diatoms were made at 500X, ignoring small diatoms that strongly dominate the sediment assemblages and mask subtle changes, such as *Chaetoceros spores* and *Thalassionema nitzschioides*. In addition, small and delicate taxa (*Fragilariopsis*, *Rhizosolenia*, *Thalassiosira*) were not counted in order to reduce bias caused by differential dissolution. Rather, larger centric diatoms demonstrating clear environmental preferences according to the sediment trap studies of Sancetta (1995), and sediment fabric studies of Pike and Kemp (1997) and Kemp and others (2000) were counted, including *Actinocyclus curvatulus*, *A. octonarius*, *Actinoptychus* spp., *Azpeitia nodulifera*, *Cosinodiscus radiatus*, *Cosinodiscus* spp. (mainly large-diameter forms such as *C. asteromphalus*, *C. granii*, and *C. oculus-iridis*), *Cyclotella* spp. (mainly *C. littoralis*), *Roperia tesselata*, and *Stephanopyxis palmeriana*. At least 200 diatoms per sample were counted while making random traverses across the microscope slide at 500X.

Silicoflagellates

Silicoflagellate slides were systematically tracked across an upper, middle and lower area to obtain a representative count of 200 specimens for the samples. Counts were typically made at magnification 250X, with 500X used in checking questionable identifications. All whole specimens and half specimens with apical structures intact were counted. Lesser fragments were not counted.

Results

For the purposes of this report, only selected geochemical, diatom and silicoflagellate data are displayed. Complete tables of the data collected are available on request from the authors.

Geochemistry

As indicated by earlier studies by Karlin and Levy (1985), the dominant sediment components of BAM80 E-17 are biogenic silica (mainly diatoms) alternating in cycles with intervals with greater amounts of terrigenous components (e.g., Fe, Ti, Mg, Al) and organic carbon. These cycles mirror yearly varves, with diatoms enriched during the late fall-early spring phase of strong northwest winds (November-May) and detritus enriched during the summer phase (June-September) of monsoonal rainfall and decreased diatom production. Weight percent $CaCO_3$ is very low (<0.5%) except in the topmost 20 cm of BAM80 E-17, where it ranges between 2 and 6%. This suggests that substantial

pore water dissolution of $CaCO_3$, possibly due to oxidative decomposition of organic matter, occurs below the 20 cm depth (Karlin and Levy 1985).

Biogenic Silica Production

The record of weight percent biogenic silica for the past 2,000 yr. in BAM80 E-17 is shown on Figure 1, where it is compared with the $\Delta^{14}C$ radiocarbon production curve (Stuiver and others 1998). Intervals of increased $\Delta^{14}C$ are thought to coincide with the sunspot minima, because an increase in solar activity (more sunspots) is accompanied by an increase in the "solar wind," which reflects cosmic rays and reduces ^{14}C production. These cycles in ^{14}C production and, by inference, in solar activity, have periodicities of about 200 years, which are termed Suess Cycles by Damon and Sonnett (1991).

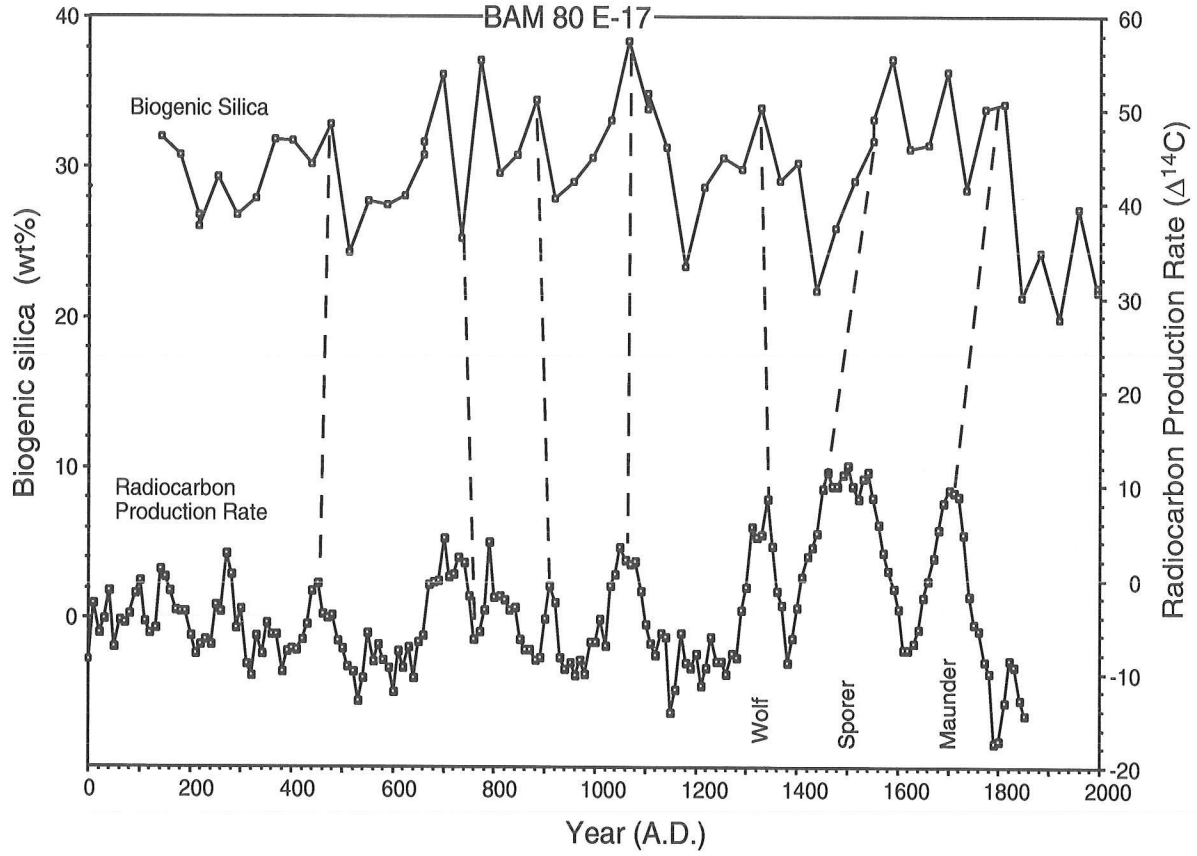

Figure 1 Record of weight percent biogenic silica in BAM80 E-17 and possible correlation (dashed lines) with radiocarbon production rate (Stuiver and others 1998). Shaded intervals show selected sunspot minima.

The biogenic silica record of the past 2,000 years in the eastern Guaymas Basin appears to bear remarkable resemblance to $\Delta^{14}C$ radiocarbon production curve, with peaks in biogenic silica coinciding with sunspot minima (Figure 1). This correlation seems to be especially good between

ca. 450 and 1350 AD; however, after ca. 1400 AD, the peaks in wt.% biogenic silica appear to be 60-80 yr younger than those in the radiocarbon production cure. Such an offset implies a possible acceleration in sedimentation rates in the topmost 85 cm of BAM80 E-17, which might be expected from reduced compaction and increased water content near the top of the core. If such a correlation is correct, it is possible that some surface sediments may not have been recovered by BAM80 E-17, a suggestion made by Julliet-Leclerc and Schrader (1987).

We hypothesize that during periods of reduced solar activity (sunspot minima), increased winter cooling of the North American continent leads to intensification of northwest winds down the axis of the Gulf, leading to increased upwelling and enhanced diatom production. Recently, Shindell and others (2001) used a general circulation model (GCM) to predict a 1 to 2 °C cooling of winter temperature for the North American continent during the Maunder Minimum (ca. 1680). Citing the effect of a dimmer Sun on the Arctic Oscillation/North Atlantic Oscillation, they argued that reduced solar activity reduced the strength of the westerly winds, which resulted in lower continental winter temperatures. Increased winter cooling of northwest Mexico would likely deepen the atmospheric low there, resulting in an enhanced pressure gradient down the Gulf and an increase in resulting northwest winds.

Support for this hypothesis comes from Thunell's (1998) report of the biweeky averages of biogenic silica accumulating in a sediment trap in the eastern Guaymas Basin between the summer of 1990 and the end of 1996. His data reveal greatly enhanced opal production in the period from 1994 through 1996 compared to period between late 1990 and late 1993. Thunell (1998) infers that the 1994-1996 increase in opal production was due to a decrease in ENSO strength during these years. However, this period displays better correlation with an interval of decreased solar activity (see http://science.nasa.gov/ssl/pad/solar/sunspots.htm) rather than reduced ENSO as measured by the NINO3 index (http://rainbow.ldgo.columbia.edu/ees/data/elnino3.htm).

Dean (2000) demonstrated that Ti concentrations in sediment samples from a box core collected in the Gulf of California off the west coast of Mexico between the mouths of the Rio Yaqui and Rio Mayo, two of the largest rivers draining the west slope of the Sierra Madre Occidental, exhibit striking cycles over the last 200 years with an average period of about 10 years, coinciding almost exactly with 10- to 12-year cycles of precipitation as reconstructed from tree rings (Fritts 1991). Dean (2000) concluded that these cycles reflect rainfall cycles, as Ti is concentrated in the detrital sediments deposited during the summer monsoonal rains rather than in the biogenic silica-rich sediments deposited during the winter. However, the strong negative correlation between weight percent Ti and biogenic silica in BAM80 E17 (r^2= -0.752) suggests that Dean's (2000) Ti cycles may actually be biogenic silica cycles operating to dilute a constant terrigenous supply, if variations in seasonal biogenic silica production are greater than variations in terrigenous input, as is implied by Thunell's (1998) sediment trap data.

Diatoms and Environment

Figure 2 shows the relative percentage contribution of selected diatom groups during the past 2,000 yr. in BAM80 E-17. Sancetta's (1995) sediment trap data in the eastern Guaymas Basin reveal the environmental and seasonal preferences of these diatom taxa. *Azpeitia nodulifera*, a tropical species, is only present in the modern eastern Guaymas Basin during ENSO-like conditions. On the other hand, *Roperia tesselata* is a late winter-early spring taxon indicative of waters that are well mixed by northwest winds. Sancetta (1995) concludes that *Coscinodiscus radiatus* is more common in the

mixed waters of the winter, whereas the mostly large-diameter taxa tabulated as *Coscinodiscus* spp. (*C. asteromphalus*, *C. granii*, and *C. oculus-iridis*) are associated with the stratified, low nutrient waters of the summer-early fall that are deposited in the late fall when the thermocline breaks down after the onset of northwest winds (Kemp and others 2000). *Cyclotella* spp. (mostly *C. littoralis*) are coastal taxa that are thought to be indicative of low production in warm, stratified, and nutrient limited waters of the summer and early fall.

The relative abundances of most of these diatom groups appear to fluctuate within generally well-constrained limits (horizontal dashed lines on Figure 2). An exception is the tropical diatom, *Azpeitia nodulifera*, which rises to 36% to 57% of the diatom assemblage, maximum values for the 2000 yr-long BAM80 E-17 record, between ca. 920 and 1020 AD. This interval, centered on 1000 AD, recalls the Medieval Warm Period (MWP). In their recent, detailed compilation of Northern Hemisphere tree ring records for the past 1,200 years, Esper and others (2002) report that "the warmest period" of the MWP covers the interval 950-1045 AD, a period that closely matches this *A. nodulifera* abundance peak in BAM80 E-17. Closer to the Gulf of California, Baumgartner and others (1992) report a major peak in the numbers of Pacific sardine, which is indicative of warmer SSTs, in the Santa Barbara Basin during the interval from ca. 960 to 1040 AD. It is therefore possible that the peak *A. nodulifera* abundances between ca. 920 and 1020 AD in the BAM80 E-17 record represent a regional, anomalously warm event, possibly associated with the MWP.

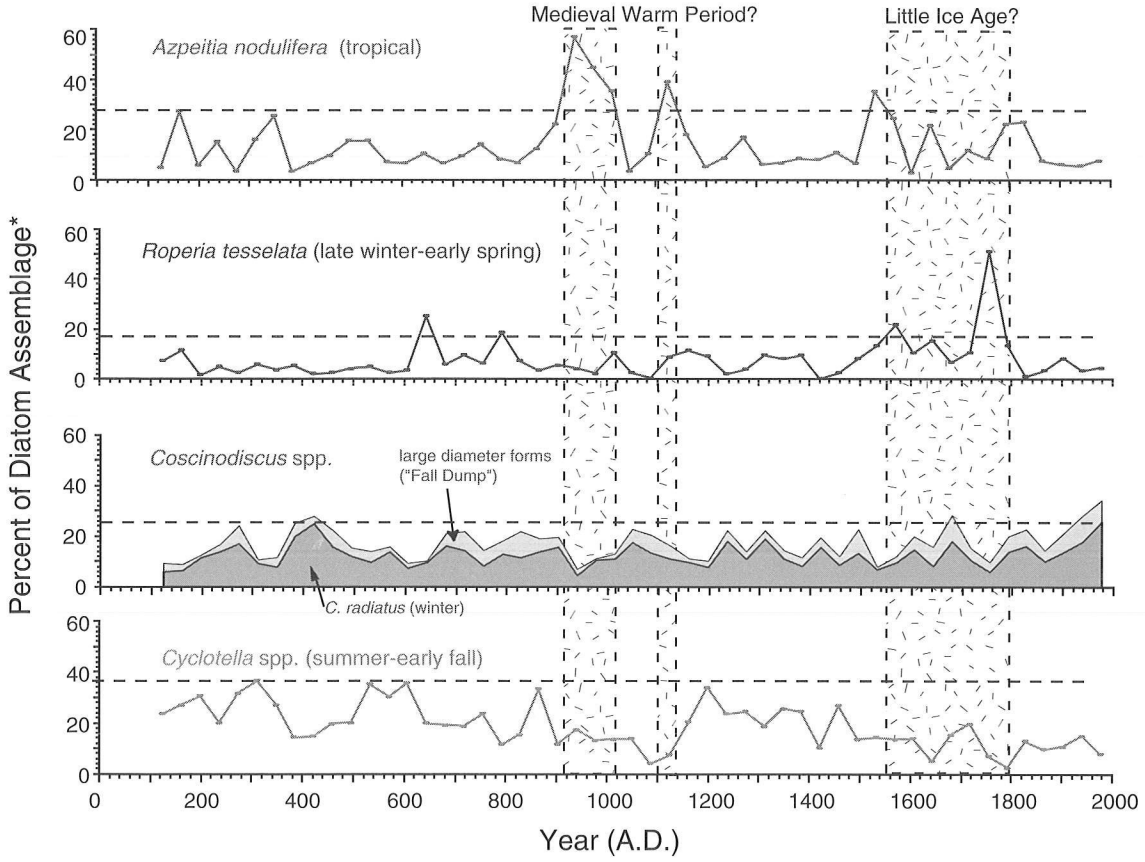

Figure 2 Relative percentage contribution* of selected diatom taxa in the BAM80 E-17 record and inferred expression of the Medieval Warm and Little Ice Age. (* -diatom counts exclude smaller taxa).

This event is followed by reduced numbers of *A. nodulifera* between ca. 1050 and 1090 AD, an interval that coincides with a peak in biogenic silica production (Figure 1). Baumgartner and others (1992) report greatly reduced numbers of Pacific sardine in the Santa Barbara Basin between ca. 1060 and 1130 AD, suggesting possible region wide cooling of SSTs.

Shortly thereafter, between ca. 1100 and 1140 AD, *A. nodulifera* again increases to >25% of the diatom assemblage of BAM80 E-17, while percent biogenic silica falls by >15% (Figure 1), indicating a return to warmer SSTs. This second return to warmer SSTs in the Guaymas Basin is matched by only moderate increases in the Pacific sardine biomass in the Santa Barbara Basin (Baumgartner and others 1992), suggesting that this warm event was more limited in extent or expression.

Cyclotella spp. display reduced abundances during the broader part (920-1150 AD) of this MWP, compared to the periods immediately proceeding or following it (Figure 2). Although Sancetta (1995) concludes that *Cyclotella* spp. are indicative of low diatom production in warm-stratified, nutrient-limited waters, it is also likely that these small, relatively delicate diatoms might be selectively removed from sediments characterized by reduced diatom production and increased dissolution of biogenicsilica.

Increased occurrences of *Roperia tesselata*, a late winter-early spring diatom indicative of waters that are well mixed by northwest winds, characterize the interval between ca. 1550 and 1800 AD (Figure 2), a period that closely matches the Little Ice Age according to Grove (1988) (1550-1850 AD). This same interval is marked by sustained higher percentages of biogenic silica (>30%) (Figure 1), suggesting increased diatom production, presumably due to strengthened northwest winds during the winter. Other diatom groups do not appear to show any unusual change in relative abundance during this period.

Silicoflagellates and Environment

Murray and Schrader (1983) studied plankton and surface samples from the Gulf of California in order to determine the present-day geographic distribution of silicoflagellate taxa and to relate assemblages to various water masses. Taken with the earlier studies of Poelchau (1976), the studies of Murray and Schrader (1983) reveal the environmental preferences of silicoflagellate taxa. Tropical silicoflagellates include *Dictyocha calida*, *D. ampliata*, (grouped with *D. calida* by Poelchau 1976), and *D. perlaevis* (*D.* sp. *A* and *D.* sp. *B* of Murray and Schrader 1983). *Dictyocha stapedia* (*D. messanensis* of Murray and Schrader 1983) is a cosmopolitan form that dominates the silicoflagellate assemblage of Pacific stations west of the Baja California peninsula. *Dictyocha* sp. aff. *D. aculeata* appears to be an endemic Gulf variant of a taxon that is associated with the modern California Current. *Octactis pulchra* is associated with high levels of primary productivity in surface waters, supporting the observations of Schrader and Baumgartner (1983). The sediment trap data of Sancetta (written comm. 2001) confirm that *O. pulchra* is most abundant during the late fall to winter period of high primary productivity.

The relative percentage contributions of these environmental-indicator silicoflagellates in the BAM80 E17 record of the past 2000 yr are plotted on Figure 3. Because it may be argued that smaller, more delicate forms of *O. pulchra* are more likely to be preserved during periods of higher biosilica production, these small forms have been differentiated from the main *O. pulchra* populations. Similarly, in intervals where small *O. pulchra* are reduced, the largest silicoflagellates,

D. sp. aff. *D. aculeata* and large *O. pulchra* (four times the size of the small form), are most abundant and give another index for reduced upwelling conditions.

The intervals between ca. 920-1020 AD and 1100-1140 AD, that are suggested by the diatom data (Figure 2) to be an expression of the MWP, are not marked by increases in the tropical silicoflagellates *Dictyocha calida*, *D. ampliata*, and *D. perlaevis* (Figure 3). Rather, these intervals are characterized by two peaks (>10%) of *D.* sp. aff. *D. aculeata* along with distinct reductions in the abundance of the small form of *O. pulchra*. A similar coincidence of increased *D.* sp. aff. *D. aculeata* and reduced number of the small form of *O. pulchra* marks the topmost part of BAM80 E-17, identified here as the post-1880 AD interval. This same interval is marked by reduced biogenic silica (Figure 1) and may be representative of a modern interval of reduced productivity in the Gulf of California that has been suggested by the silica oxygen isotope studies of Julliet-Leclerc and Schrader (1987). Thus, silicoflagellates suggest that the interval indicated by diatoms to be an expression of the MWP was not marked by increased incursions of tropical silicoflagellates into the central Gulf of California, but rather was characterized by greatly reduced productivity, similar to that of the past century.

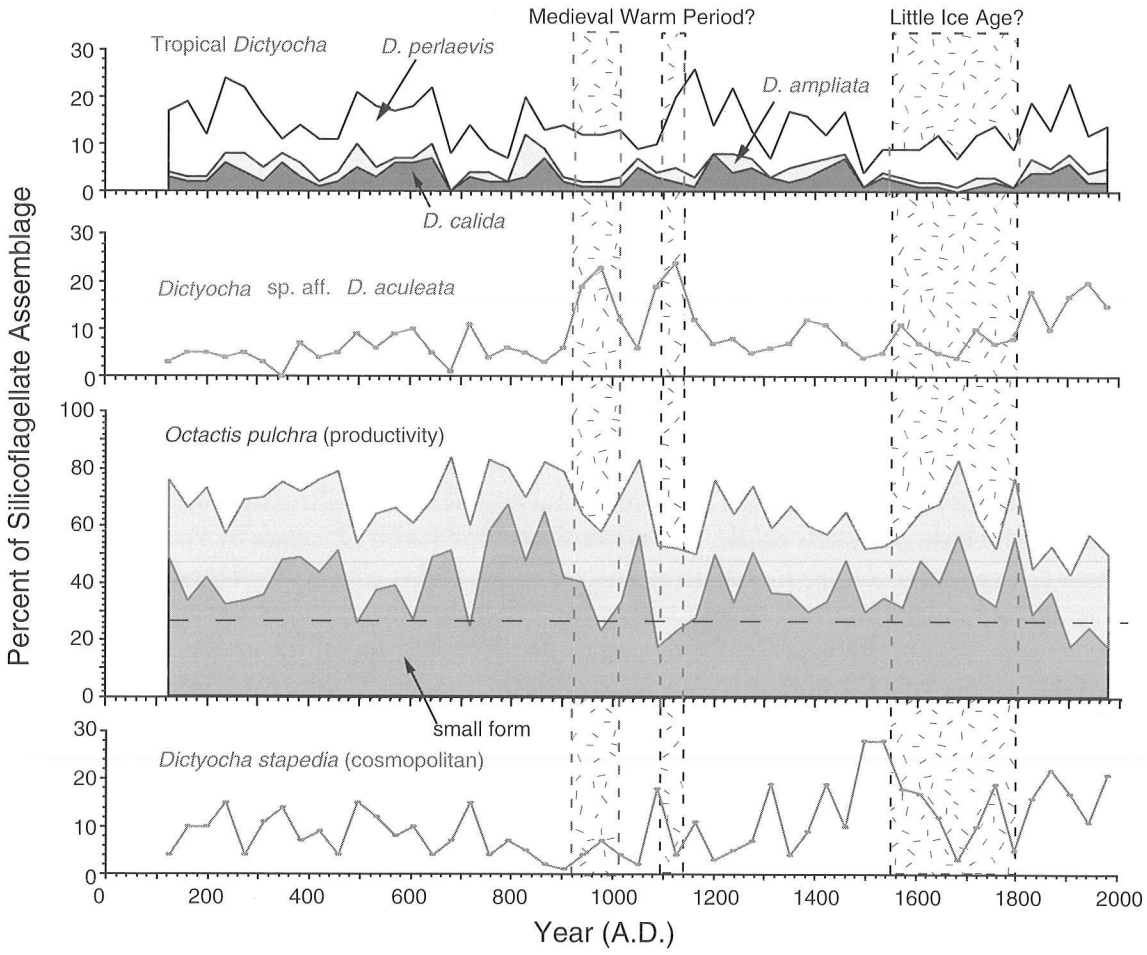

Figure 3 Relative percentage contribution of selected silicoflagellate taxa in the BAM80 E-17 record and possible expression of the MWP and the Little Ice Age

The interval of the Little Ice Age (ca. 1550-1800 AD), on the other hand, coincides with increased abundances of the small form of *O. pulchra* and generally reduced abundances of *D.* sp. aff. *D. aculeata* (Figure 3), suggesting increased productivity. As with the biogenic silica data (Figure 1) and the diatom (*R. tesselata*) (Figure 2) data, however, this interval does not really stand out as being different from other intervals of increased biogenic silica production during the past 2,000 years.

Conclusions

- During the past 2,000 years, the record of percent biogenic silica in eastern Guaymas Basin core BAM80 E-17 bears a striking resemblance to the radiocarbon production curve, suggesting that diatom production increases during sunspot minima.
- In support of this conclusion, the sediment trap data of Thunell (1998) for the years 1990-1996 appear to show a stronger correlation of years of increased biogenic silica flux with years of decreased solar activity rather than with years of reduced ENSO strength.
- Increased abundance of the tropical diatom *Azpeitia nodulifera* between ca. 920 and 1020 AD and again between ca. 1100 and 1140 AD is suggested to be a representation of the MWP. Although tropical silicoflagellates do not increase in relative numbers during these intervals, greatly increased numbers of the large silicoflagellate *Dictyocha* sp. aff. *D. aculeata* and reduced numbers of the small form of *Octactis pulchra* are evidence of reduced productivity.
- Increases in the relative abundance of the late winter-early spring diatom *Roperia tesselata* occur between ca. 1550 and 1800 AD, an interval associated with the Little Ice Age. Percent biogenic silica is relatively high (>40%) during this entire period, suggesting enhanced winter time siliceous phytoplankton production associated with strengthened northwest winds. Silicoflagellate data also supports increased productivity during this period.

Acknowledgments

We are grateful to the core laboratory of the College of Ocean and Atmospheric Sciences, Oregon State University for providing the samples used in this study. This manuscript benefited from the reviews of Scott Starratt and Mary McGann of the U.S. Geological Survey.

References

Bandon-Dangon A, Dorman CE, Merrifield MA, Wianat CD. 1991. The lower atmosphere over the Gulf of California. Journal Geophysical Research 96(C9):16,877-16,896.

Baumgartner T, Soutar A, Ferreira-Bartrina V. 1992. Reconstruction of the history of Pacific sardine and northern anchovy populations over the past two millennia from sediments of the Santa Barbara Basin, California. CalCOFI Reports. 33:24-40.

Damon PE, Sonnett CP. 1991. Solar and terrestrial components of the atmospheric ^{14}C variation spectrum. Pages 360-388 in The Sun in Time. Sonnett CP, Giampapa MS, Matthews MS, editors. The University of Arizona Press, Tucson, Arizona.

Dean WE. 2000. Sun and Climate. U.S. Geological Survey Fact Sheet 0095. www.geology.cr.usgs.gov/pub/fact-sheets/fs-0095-00/fs-0095-00.pdf.

Esper J, Cook ER, Schweingruber FH. 2002. Low-frequency signals in long tree-ring chronologies for reconstructing past temperature variability. Science 295:2250-2253.

Fritts HC. 1991. Reconstructin large-scale climate patters from tree-ring data. University of Arizona Press, Tucson AZ. 286pps.

Goñi MA, Hartz DM, Thunell RC, Tappa E. 2001. Oceanographic considerations in the application of the alkenone-based paleotemperature Uk'37 index in the Gulf of California. Geochimica et Cosmochimica Acta 65:545-557.

Grove JM. 1988. The Little Ice Age. Methuen, London, UK, 498 pp.

Julliet-Leclerc A, Schrader H. 1987. Variations of upwelling intensity recorded in varved sediment from the Gulf of California during the past 3,000 years. Nature 329:146-149.

Julliet-Leclerc A, Labeyrie LD, Reyss JL, Schrader H. 1991. Temperature variability in the Gulf of California during the last century: a record of recent strong El Niño. Geophysical Research Letters 18(10):1889-1892.

Karlin R. 1984. Paleomagnetism, rock magnetism and diagenesis in hemipelagic sediments from the Northeast Pacific Ocean and the Gulf of California. Ph.D. Thesis, Oregon State University, Corvallis, Oregon, 246 pp.

Karlin R, Levi S. 1985. Geochemical and sedimentological control of magnetic properties of hemipelagic sediments. Journal Geophysical Research 90(B12):10,373-10,392.

Kemp AES, Pike J, Pearce RB, Lange C. 2000. The "Fall dump"—a new perspective on the role of a "shade flora" in the annual cycle of diatom production and export flux. Deep-Sea Research II, 47:2129-2154.

Murray D. 1982. Paleo-oceanography of the Gulf of California based on silicoflagellates from marine varved sediments. M.S. Thesis, Oregon State University, Corvallis, Oregon, 129 pp.

Murray D, Schrader H. 1983. Distribution of silicoflagellates in plankton samples from the Gulf of California. Marine Micropaleontology 7:517-539.

Pike J, Kemp AES. 1997. Early Holocene decadal-scale ocean variability recorded in Gulf of California laminated sediments. Paleoceanography 12(2):227-238.

Poelchau HS. 1976. Distribution of Holocene silicoflagellates in North Pacific sediments. Micropaleontology 22(2):164-193.

Sancetta C. 1995. Diatoms in the Gulf of California: Seasonal flux patterns and the sediment record for the last 15,000 years. Paleoceanography 10(1):67-84.

Santamaria-del-Angel E, Alavrez-Borrego S, Muller-Karger FE. 1994. Gulf of California biogeographic regions based on coastal zone color scanner imagery. Journal Geophysical Research 99 (C4):7411-7421.

Schrader H, Baumgartner T. 1983. Decadal variation of upwelling in the central Gulf of California. Pages 247-276 in Coastal Upwelling Part 2. J. Thiede and E. Suess, editors. Plenum Publishing Corporation, New York, New York.

Shindell DT, Schmidt GA, Mann ME, Rind D, Waple A. 2001. Solar forcing of regional climate change during the Maunder Minimum. Science 294:2149-2152.

Stuiver M, Reimer PJ, Bard E, Beck JW, Burr GS, Hughen KA, Kromer B, McCormac FG, Plicht JVD, Spurk M. 1998. INTCAL98 radiocarbon age calibration, 24,000-0 cal BP. Radiocarbon 40:1041-1083.

Thunell RC. 1998. Seasonal and annual variability in particle fluxes in the Gulf of California: A response to climate forcing. Deep-Sea Research I 45:2059-2083.

Stratigraphic Evidence in Polar Ice of Variations in Solar Activity: Implications for Climate?

Gisela A.M. Dreschhoff

Introduction

The earth may be viewed as a satellite orbiting the sun where the space occupied by the sun-earth system consists largely of ionized gas and charged particles. Effectively, the solar atmosphere or corona expands outward as the solar wind, which collides with the earth's magnetosphere and atmosphere, forming the magnetopause. The term bow shock indicates the region of the abrupt drop in speed of the supersonic solar wind. The real, non-idealized solar wind includes interplanetary shock waves and high-speed plasma streams, which are accompanied by large scale flows of different levels of turbulence. Figure 1 outlines roughly the complex phenomena operating in the inner heliosphere. The degree to which energy and momentum of the solar wind are coupled to the magnetosphere is a function of the variations in solar activity, and in turn functions as a modulator of the upper polar atmosphere. It is made visible by the display of the aurorae, which are formed by electron precipitation and ionization processes in the upper atmosphere in both polar regions of the earth. Figure 2 shows the general configuration of the auroral oval in the northern hemisphere.

Within the polar region energetic charged particles have essentially full and prompt access to the polar atmosphere. In fact, they are able to affect significantly the polar stratosphere as the stopping region for such solar energetic particles. For this reason it is appropriate to consider the extent to which ionization in the polar atmosphere may have affected the concentrations of nitrate compounds found in the stratigraphic layers of the polar ice sheets. Nitrate ion (NO_3^-) can be produced by proton bombardment through ionization of oxygen and nitrogen followed by chemical reactions in the solid state in the cold winter polar atmosphere (Zeller and Dreschhoff 1995). Trace amounts of nitrate (parts per billion) present in Antarctic and Greenland snow and ice are generally considered to have been incorporated in the snow as gas phase compounds or tropospheric and terrestrial dust blown aerosols. Little consideration has been given to processes, which involve non-gas phase nitrate production in the middle and upper atmosphere. In fact, it has been found that measurable quantities of non-gas phase nitrate are removed from the polar atmosphere by gravitational sedimentation. There is no reason to doubt that these processes take place (Dreschhoff and Zeller 1998). Furthermore, nitrates being removed from the gas-phase are much less subject to photolysis by solar ultra-violet during spring conditions. Such solid nitrate-containing particulates would tend to be deposited, and would tend not to be subject to numerous changes within the depositional environment as are gas-phase components.

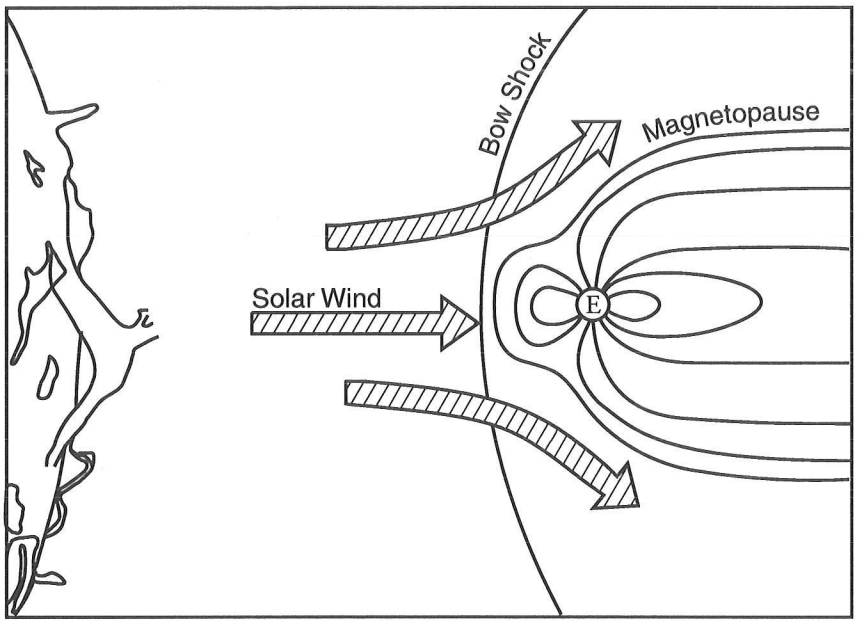

Figure 1 Sketch (not to scale) of an active sun, the earth and its magnetic field being exposed to the stream of charged particles from the sun. The solar wind will undergo dramatic changes in flux and level of turbulence according to variations in solar activity.

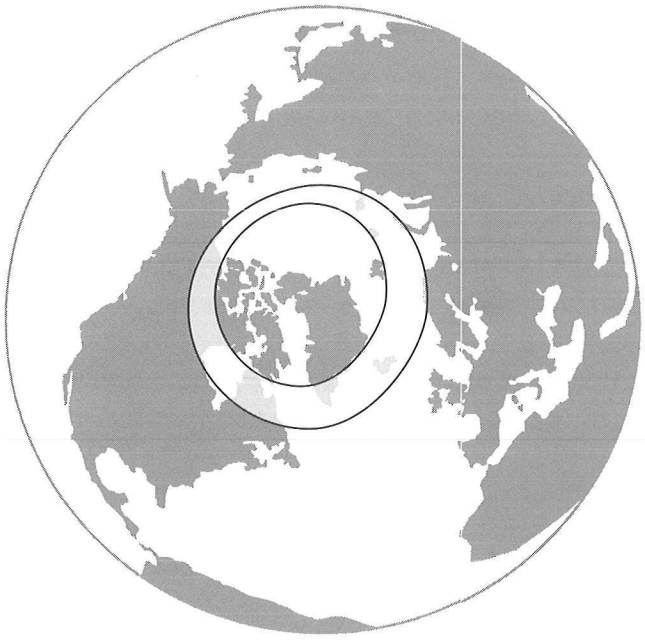

Figure 2 The auroral oval forms an irregular circle around the geomagnetic poles in the northern and southern hemisphere. Highly accelerated electrons from the magnetosphere interact with the upper atmosphere to form the luminous aurora as indicated by the hatched area for the northern hemisphere.

If the solar particle flux in the past was substantially larger, the interaction with the upper polar atmosphere may have played a very important role in atmospheric dynamics as well as nitrate production in the polar stratosphere with subsequent fallout to the surface of the polar ice sheets. On the other hand, for periods of very low solar activity with basically no sunspots visible on the solar surface and a very reduced corona or solar atmosphere, the solar wind would have been much less dense, resulting in less intense interactions at the earth. In fact, recent observations have shown that the waxing and waning of the magnetosphere involves dramatic changes, extending its location sunward to beyond the orbit of the moon for an extremely low density solar wind (Lazarus 2000). Similar conditions could have existed for the period of the Maunder Minimum (about 70 years), which has also been associated with the Little Ice Age on the earth.

A 3200-Year Record of Polar Ionization Variations

Owing to the interest in the variations in solar activity and the problem involved in their influence on the earth's climate, the original principal effort was concerned with time periods for which solar, geomagnetic or historical climate information was available. For this reason, experimental work was focussed on the evaluation of ice cores of approximately 100 meters in length, representing time scales of 3200 years, 1200 years, and 430 years, depending on the precipitation condition at the specific drill sites on the polar ice sheets. These sites were the South Pole, the south geomagnetic pole at Vostok Station, and Summit in Greenland, respectively. By analyzing trace levels of nitrate it was possible for the first time to test the hypothesis of polar nitrate production in association with ionization events taking place in the polar atmosphere (Zeller and Parker 1981).

Firn cores (cores of highly compacted snow) from the South Pole (108 m) and from Vostok Station (101 m) on the high polar plateau of Antarctica were analyzed for trace levels of nitrate. Sequential chemical analyses were made on the entire core from the South Pole, each representing approximately semi-annual accumulation increments of snow. In the case of the Vostok core, completely sequential data points were generated as well, each representing approximately annual accumulation increments of snow. Time series were constructed from the nitrate concentration data based on average annual accumulation (Parker and others 1982), and the entire South Pole data are compared with the equivalent time period of the Vostok data. Both curves revealed pronounced oscillations in nitrate variability as shown in Figure 3. By applying a cubic spline fit to both time series, the broad periods of maxima and minima displayed in the data show a close anticorrelation with the cosmogenic ^{14}C -record for the equivalent time period. Based on these results, these oscillations appeared to reflect changes in solar activity that have occurred in the past twelve hundred years. In fact, both nitrate records show the period of known reduced solar activity, the Maunder Minimum from about 1645-1715 with very low nitrate values. Other periods of varying solar activity, particularly the Medieval Maximum, are clearly displayed in a general rise in average nitrate concentrations.

Extending the cubic spline fit to the annual data of the complete Vostok core, periods lasting several hundred years of lower and higher average nitrate concentrations are seen throughout the approximately 3200 years of record, as shown in Figure 4. Approximate historic time periods known from climatic records and ^{14}C variation studies are indicated on the graph. Although the dating of the ice cores, i.e. the years BP, were only approximate, the apparent coincidence of nitrate concentrations, solar activity, and climate information could not be dismissed. For this reason the research was directed to more fully delineate the signal of nitrate concentrations in polar snow and their relationships to solar activity.

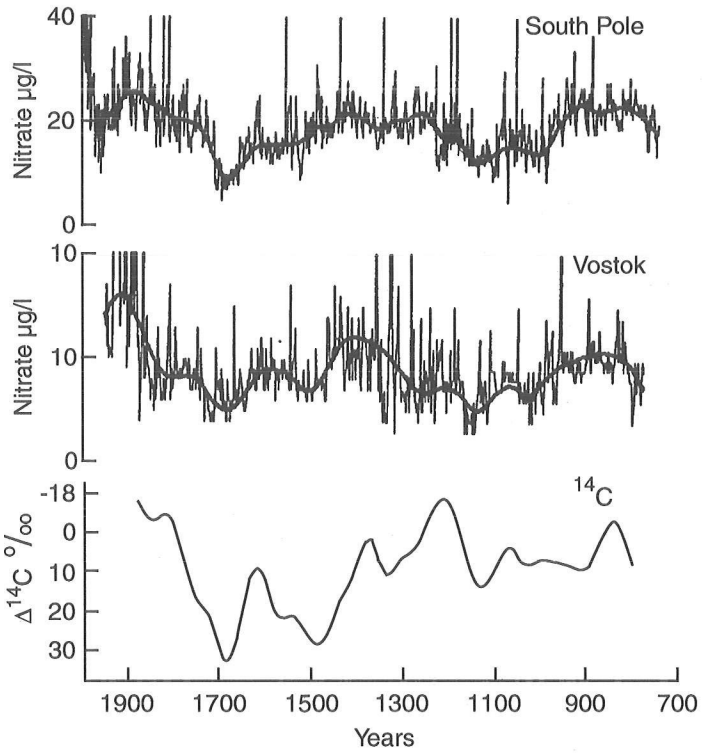

Figure 3 Plots of the nitrate concentrations for the South Pole and Vostok cores with smoothed curves superimposed. A comparison is shown with a ^{14}C-curve adapted from Eddy (1977).

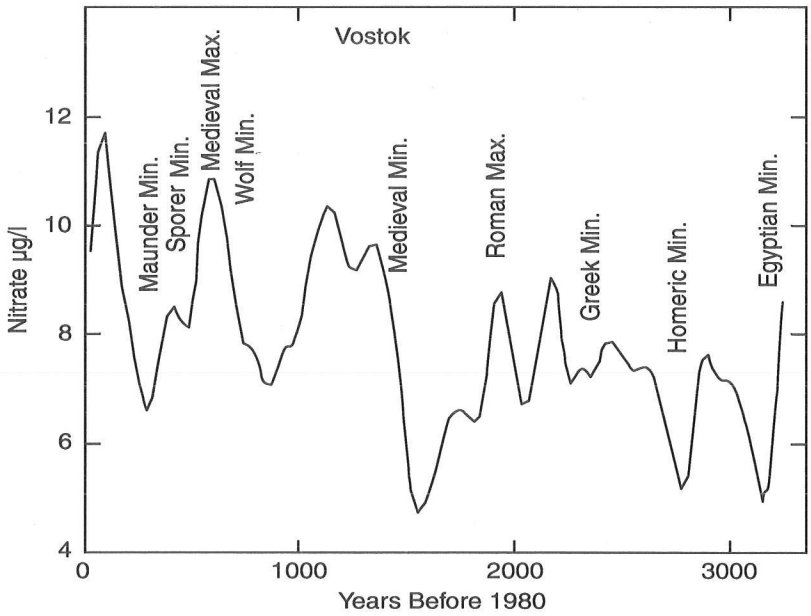

Figure 4 Cubic spline fit (S=100) to the nitrate concentration data for the complete Vostok core with historic solar and climate data superimposed using the terminology by Eddy (1977).

A 430-Year Record of Solar Proton Events

As seen in the investigation of longer-term records of >1000 years, it seems evident that proton irradiation can alter the composition of the polar atmosphere by formation of nitrate ion. Furthermore, relatively rapid fallout of the ionization products to the surface of the polar ice sheets is to be expected due to the atmospheric conditions specific to the polar regions (Dreschhoff and Zeller 1998). These include the chemical and dynamical containment vessel of the polar winter vortex, the penetration of stratospheric air into the tropopause, as well as significant mass transport from the stratosphere to the troposphere. In our investigation it was found that the total nitrate signal consists of a background from a number of sources on which are superimposed large nitrate anomalies or impulsive events. For this reason, the primary concern of this investigation was an ultra-high-resolution examination of the ice cores. The measurements of 1.5 cm increments along the entire snow or ice sequences were performed under tightly controlled experimental procedures (Dreschhoff and Zeller 1990; 1994). Making use of two firn sequences from Antarctica, representing about 80 years and most of the instrumental era of satellites and ground-based geophysical measurements, it was found that the largest nitrate anomalies (several standard deviations above the mean) are associated with large fluence solar proton events (Shea and others 1993).

This investigation was extended to include the equivalent time period from the 430-year record of data from the central Greenland ice sheet. A one to one correlation was demonstrated between the largest solar proton fluence events that have been observed since continuous recording of cosmic radiation and the corresponding thin nitrate layers for the event date (McCracken and others 2001a). Further evaluation of the data series includes the total of 430-years of nitrate impulsive events, which provided the possibility to delineate a signal of detailed solar activity well beyond the known geophysical record for the period 1561-1991. The determination of time along the entire ice core was accomplished by making use of the known volcanic eruptive episodes as described by Zeller and Dreschhoff (1995). A clearly defined seasonal nitrate signal (background of annual variation) assisted in the estimate of time and functioned as a quality control as well. Due to metamorphic processes in the uppermost few meters of snow where gas-phase nitrate may undergo extensive changes induced by pressure differentials at the snow surface (Gjessing 1977), the nitrate record does contain many smaller, short-term anomalies. They are frequently accompanied by electrical conductivity enhancements showing essentially an identical time profile, and are not part of the evaluation procedure of solar cosmic rays.

Integrated concentrations of nitrate impulsive events above the background and of time duration <2 months were determined. This resulted in the identification of a total of 70 large impulsive nitrate events for the time period between 1561 and 1950. These events were determined to correspond to major solar proton events characterized by an energy of > 30 MeV and omnidirectional fluence of $> 2 \times 10^9$ cm^{-2}. The highly correlative, high probability nature of impulsive nitrate and solar proton events is exemplified by one of the largest solar eruptive events that occurred in historical times. In September 1859, Carrington observed what is still today a classical case of special event on the surface of the sun. It induced a period of exceptional interplanetary and geomagnetic disturbances. The impulsive nitrate event identified in our record, and shown in Figure 4, coincides within ±2 months with the unusually large solar eruptive event and white light flare (Zeller and Dreschhoff 1995; McCracken and others 2001a). Another feature seen in Figure 4 is the series of large ionization events, which have been identified in the stratigraphic snow layers of the 1890s. The nitrate anomalies were of exceptional strength or amplitude, and these conspicuous occurrences coincide with similarly large

peaks in high-resolution cosmogenic data, which consist of the high frequency components of secular variations of atmospheric ^{14}C (Peristykh and Damon 1999).

Based on this type of results it was concluded that the impulsive nitrate events or nitrate anomalies are reliable indicators of the occurrence of large fluence solar proton events, and that they may even provide a quantitative measure of these events. In fact, McCracken and others (2001a), demonstrated that the probability for a one-to-one correlation to occur by chance was $< 10^{-6}$. Furthermore, by evaluating the high-resolution nitrate data along the entire core in terms of their frequency distribution in time, it was found that a whole series of nitrate anomalies had occurred prior to the beginning of the Maunder Minimum (Dreschhoff and Zeller 2002). In fact, McCracken and others (2001b), identified a total of five periods in the vicinity of 1610, 1710, 1790, 1870, and 1950, when large >30 MeV proton events with fluence greater than $2x10^9$ cm^{-2} were up to eight times more frequent than in the modern era of satellite observations. In addition, it was found that there is a well-defined Gleissberg periodicity (approximately 80 years) in large fluence solar proton events, with six well-defined minima, two in close association with the Maunder and Dalton minima in solar sunspot number. One main conclusion is that the present "satellite" era is a recurrence of this series of minima, and the present Gleissberg cycle is one of the least effective in the production of large fluence solar proton events on earth. It is conceivable, that the earth could have experienced much higher fluence events in the past, or could be exposed to such again in future time periods.

Discussion and Conclusions

In summary, the nitrate confined to thin, stratigraphic layers in the polar ice sheets reflects a signal of ionization (a) of individual solar proton event injections into the polar stratosphere, and (b) the ionization density of the auroral zone. In addition, the information we have gained from the > 3,000-year nitrate record from Vostok Station, Antarctica shows a close, although non-quantitative, relationship with historic climate information (see Figures 3 and 4). Such a relationship seems to be conceivable, particularly in view of some investigations that have been conducted in Antarctica, the results of which are a measure of the geo-effectiveness of solar charged particles.

Troshichev (2001), reported the occurrence of abrupt tropospheric temperature changes (heating at h<5 km and cooling at h>8 km) recorded near Vostok on the high polar plateau during solar proton events and Forbush decreases.

Upper atmosphere investigations clearly showed the thermospheric response to the energy and momentum input from the solar wind. Hernandez and others (1990) found that the upper atmospheric dynamics are related to a number of forcings, such as tidal effects and possibly local auroral heating. High winds, which are superimposed on the tidal variation, can be generated through the coupling of high-speed ions in the lower ionosphere and surrounding neutral atmosphere. The initiation of large-scale circulation and its strength would be dependent on the variable ionization density of the ionosphere. It has even been suggested that tremendous movement of mass and energy via a giant pole-to pole Hadley cell cannot be excluded (Smith and others 1989).

From numerous investigations it is well known that global climate change has not yet been linked quantitatively to solar activity in terms of variations in solar luminosity. Without feedback mechanisms to amplify the effect, irradiance changes are too small, and the complexity of this relationship has been reviewed by Rind (2002). On the other hand, Pap (2003) points out that while the sun's radiative output will affect the earth's global thermal environment, in the past it could have been even larger than is known from the relatively short instrumental era of irradiance measurements.

Based on this type of data, the assumption that solar activity cannot account for a measurable degree of climate change may have to be reconsidered. In fact, long-term trends, signaling fundamental changes taking place deep within the sun, may have to be taken into account in evaluating climate change. This may well be the case for the upward trend, beginning ~1900, for the aa index of geomagnetic activity. It signals increased geoeffectiveness of the solar wind. In addition, since the solar wind is the agent which carries the solar magnetic field out into the heliosphere, this signal also shows that the general solar magnetic field has doubled during the last ~100 years (Lockwood and others 1999). Parker (1999) discusses these findings from the point of view of the observed changes in mean temperatures on earth, which leads him to state that this "reinforces the likelihood that the sun has had a hand in the general warming of our climate".

It is noticed that the rise of the general solar magnetic field coincides with the timing of the large impulsive nitrate events in the late 1800s (see Figure 5). These unusual events were associated with solar cycle 13 of rather small sunspot numbers. Investigating this time period further, it was found that cycle 13 and the preceding cycle 12 coincided with discontinuities in the temporal distribution of the sunspot record and the aa index (Dreschhoff and others 1999). The two records were analyzed by determining the number of years between each maximum of annual sunspot numbers and annual aa index from cycle 11 to 22. The shift of the aa index maximum (cycle 12 and 13) from preceding to following the sunspot maximum is clearly seen in Figure 6. The result indicates that during the period

of cycle 12 and 13, the ascending phase of sunspot activity was dominant in producing magnetic storms on earth. However, beginning at the turn of the century (~1900), the descending phase became dominant, most likely due to coronal hole development which persists for long periods of time and may result in recurrent magnetic disturbances on earth.

If, in fact, proton irradiation of the polar atmosphere results in the formation of impulsive nitrate events, as our data suggest, they mirror not only the changes taking place in minor constituents in the atmosphere, but possibly fundamental processes taking place in the corona and within the sun. This interpretation may be supported when the observations reported by Lockwood and others (1999) are combined with the most recent helioseismic data of the deep interior of the sun. It becomes possible to learn more and more about the details of the interior of the sun as an oscillating body of plasma, where violent solar activity is driven by turbulence deep within the sun. In fact, the helioseismic images show very complex regions of rapidly evolving magnetic vortex structures beneath the active regions on the solar surface (Showstack 2002). These plasma vortices can reach to great depths, such as the boundary of the convection and radiative zone, the tachocline. The tachocline is the location where the solar dynamo operates, which would ultimately be responsible for the increase in field strength of the general magnetic field of the sun. It may even be permitted to speculate that feedback mechanisms may involve the entire sun, possibly via g-mode activity, since the g-mode oscillations even penetrate the core (Hellemans 1998). Despite the new insights, however, that have been gained about the physical properties of the deep interior, the sun remains a very complex object, and the sun's detailed influence on the global climate of the earth remains hidden.

Nevertheless, it is noted that two independent data sets lead to strong suggestions that solar activity plays a major role in the evolvement of climate change on earth. The doubling of the sun's coronal or general magnetic field relates to the average temperature increase on the earth (Parker 1999). Perry and Hsu (2000) build their investigation on the premise "that the cyclic variations in the sun's total energy output occurring simultaneously at different scales of time are ultimately responsible for global climate variations, and can explain both gradual and abrupt changes in climate on a global scale".

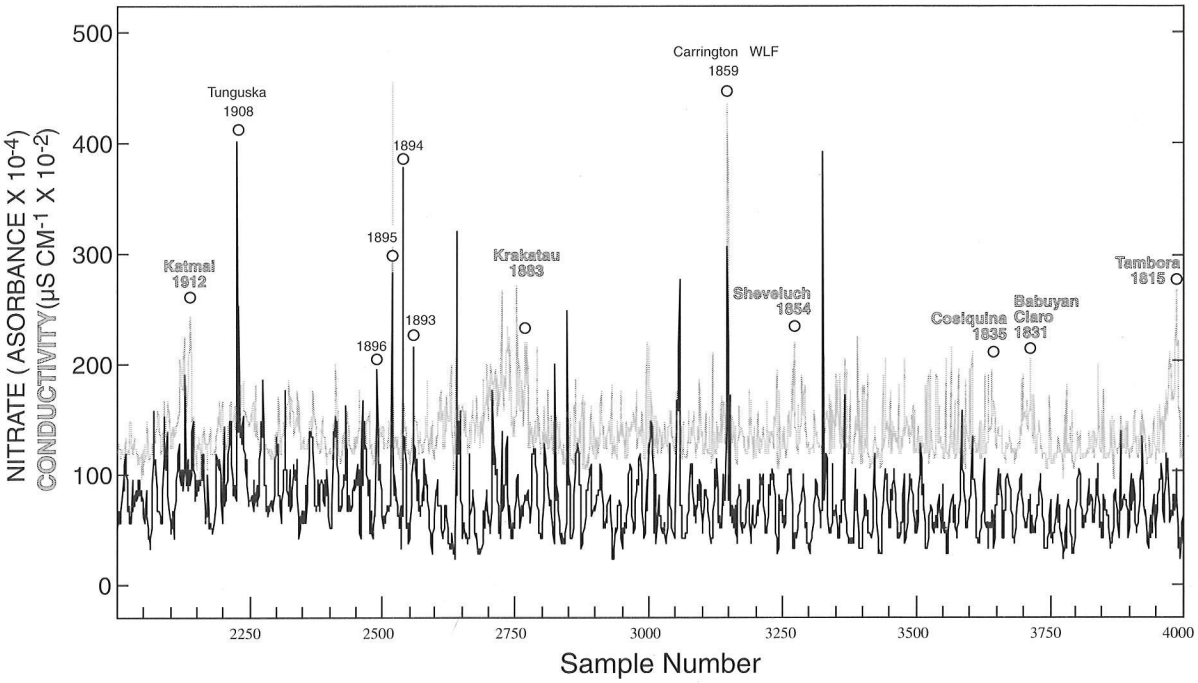

Figure 5 Nitrate (bottom) and conductivity (top) records from the central Greenland ice sheet for a 100-year period, beginning with the Tambora eruption 1815 (deposit 1816). (Absorbance units 100 x 10^{-4} = 20.4 µg/l NO_3 - N). Known volcanic eruptive events are indicated as well as the years of impulsive nitrate events including the White Light Flare (WLF) observed by Carrington.

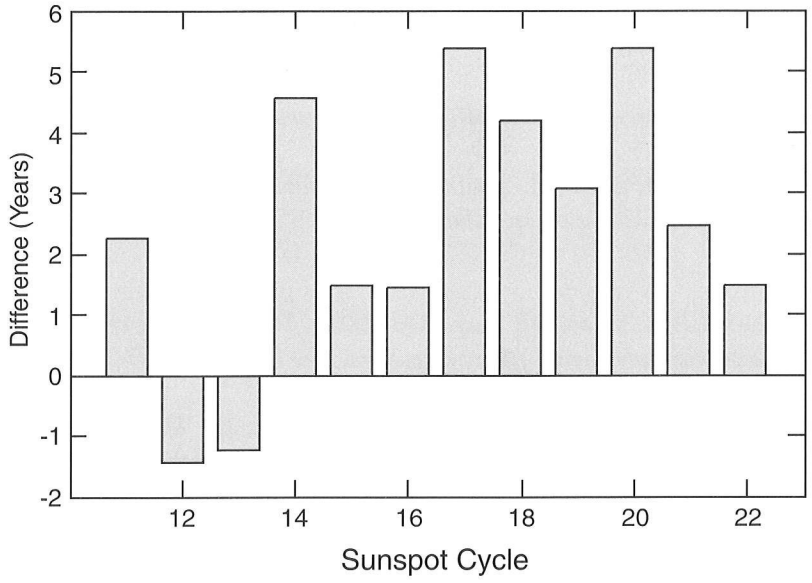

Figure 6 Temporal relationship of the annual sunspot numbers at maximum to the maximum of the annual aa index plotted as Differences in Years. A phase shift is noted for cycles 12 and 13, where negative figures indicate that the aa index maximum precedes the sunspot maximum.

References

Dreschhoff G, Zeller EJ. 1990. Evidence of individual solar proton events in Antarctic snow. Sol. Phys. 127:333-346.

Dreschhoff G, Zeller EJ. 1994. 415-year Greenland ice core record of solar proton events dated by volcanic eruptive events. Inst. Tertiary-Quaternary Studies, TER-QUA Symposium Series 2:1-24.

Dreschhoff G, Zeller EJ. 1998. Ultra-high resolution nitrate in polar ice as indicator of past solar activity. Solar Physics 177:365-374.

Dreschhoff G, Shea MA, Smart DF. 1999. Solar wind parameters and records in the Sun-Earth system. 26th Int. Cosmic Ray Conf. 7:139-142.

Dreschhoff GAM, Zeller EJ. 2002. A signature of the solar wind in the inner heliosphere and in the ice caps of the Earth. Inst. Tertiary-Quaternary Studies, TER-QUA Symposium Series 3:125-161.

Eddy JA. 1977. Climate and the changing sun. Climatic Change 1:173-190.

Gjessing YT. 1977. The filtering effect of snow, isotopes and impurities in snow and ice. Symposium Proceedings of the Grenoble Symposium Aug./Sept. 1975, Int. Assoc. of Hydrological Sciences 118:199-203.

Hellemans A. 1998. Seeking the sun's deepest notes. Science 280 (26 June):2047.

Hernandez G, Smith RW, Kauffman SD. 1990. South Pole mesospheric and lower-thermospheric dynamics. Antarctic Journal of the U.S. 25 (5):278-279.

Lockwood M, Stamper R, Wild MN. 1999. A doubling of the sun's coronal magnetic field during the past 100 years. Nature 399 (3 June):437-439.

Lazarus AJ. 2000. The day the solar wind almost disappeared. Science 287 (24 March):2172-2173.

McCracken KG, Dreschhoff GAM, Zeller EJ, Smart DF, Shea MA. 2001a. Solar cosmic ray events for the period 1561-1994. 1. Identification in Polar Ice, 1561-1950. J. Geophys. Res.106 (A 10):21,585-21,598.

McCracken KG, Dreschhoff GAM, Smart DF, Shea MA. 2001b. Solar cosmic ray events for the period 1561-1994. 2. The Gleissberg Periodicity. J. Geophys. Res. 106 (A10):21,599-21,609.

Pap J. 2003. Solar irradiance variations from UV to infrared [abstract]. In: West GJ, Blomquist N, editors. Proceedings of the nineteenth annual Pacific Climate Workshop; March 3-6, 2002. Sacramento: CA Dept. of Water Resources. p182.

Parker BC, Zeller EJ, Gow AJ. 1982. Nitrate fluctuations in Antarctic snow and firn: potential sources and mechanisms of formation. Annals of Glaciology 3:243-248.

Parker, EN. 1999. Sunny side of global warming. Nature 399 (3 June):416-417

Peristykh AN, Damon PE. 1999. Cosmogenic isotope evidence of very high solar flare activity at the end of XIX century. 26th Int. Cosmic Ray Conf. 6:264-267.

Perry CA, KJ Hsu. Geophysical, archeological, and historical evidence support a solar-output model for climate change. Proc. Nat. Acad. Sci. 97(23):12433-12438.

Rind D. 2002. The sun's role in climate variations. Science 296 (26 April):673-677.

Shea MA, Smart DF, Dreschhoff G, Zeller EJ. 1993. The flux and fluence of major solar proton events and their record in Antarctic snow. 23rd Int. Cosmic Ray Conf. 3:846-849.

Showstack R. 2002. Helioseismologists release new findings about the solar subsurface. EOS, Transactions, America Geophysical Union 83 (5):1.

Smith RW, Meriweather JW, Hernandez G, Rees D, Wickwar V, de la Beaujardiere O, Killeen TL. 1989. Mapping the wind in the polar thermosphere. EOS, Transactions Geophysical Union 70 (11):161.

Troshichev OA. 2001. Influence of solar activity on processes in the south polar lower atmosphere. International SCOSTEP Newsletter 4 (2):11-17.

Zeller EJ, Parker BC. 1981. Nitrate ion in Antarctic firn as a marker of solar activity. Geophys. Res. Lett. 8 (8):895-898.

Zeller EJ, Dreschhoff G. 1995. Anomalous nitrate concentrations in polar ice cores — do they result from solar particle injections into the polar atmosphere? Geophys. Res. Lett. 22 (18):2521-2524.

Looking for Recent Climatic Trends and Patterns in California's Central Sierra

Gary J. Freeman

Introduction

Pacific Gas & Electric Company's (PG&E) water management team has historically assumed that future years, as a group of three or more successive years, were subject to the same level of climatic randomness characteristic of the past 25-50 years. There is increasing ongoing analysis that indicates that this may not always be the best assumption for future planning. With approximately 38% of its long term average annual hydroelectric generation derived from aquifer outflow, typical historic practice at PG&E, with regard to forecasting future seasonal runoff beyond the current year, has focused almost entirely on analyzing the current baseflow trend for the volcanic watersheds in northern California, such as in the Pit, McCloud, and upper North Fork Feather River watersheds. Historic climate randomness is then assumed for future seasonal precipitation and a multi-year baseflow forecast for a number of years forward is made for these northern watersheds. For the mid-to-high elevation headwaters, which overlay the central Sierra granites, the baseflow effect of prior years, is relatively minimal, and seasonal year-to-year randomness for historic precipitation has been assumed for input to multi-year runoff forecasts.

No attempts at PG&E have previously been made to utilize historic climate oscillation and trends as possible input to predict overall likelihood for precipitation in successive groups of upcoming years. Relatively recent analysis however, cautiously suggests that there may be relatively short precipitation cycles, which are approximately 14-16 years in length, and possibly longer term cycle and trend movements, which, while not necessarily helpful for defining wetness or dryness in the following year, may possibly provide helpful insight to better anticipate wetness for successive groups of years in terms of three or more years as a group. The apparent non-random subtle reflections of climatic cycling and trending was first noticed from the natural multi-year smoothing that accompanies baseflow trends and cycles of the large northern California volcanic springs that continuously contribute water as diminishing echoes of past wetness. Manga (1999) discusses timescales and groundwater discharge from the Cascade volcanics, which include those in northern California's Hat Creek drainage. A portion of the water, which is now emerging from underground storage to become surface runoff, may have come from seasonal precipitation that occurred many decades in the past. In this paper, an array of monthly and seasonal groupings of historic precipitation, snowpack and runoff are analyzed to reveal possible subtle signs of climatic oscillation and trending. While no attempt is made here to forecast future cycles of wetness based on observations of historic data, or being able to define the wetness for any given 1-2 years specifically, there may be potential for anticipating future wetness in terms of using successive groups of three or more years.

Repeating Climate Patterns in Wetness During the Past 100 Years

Recurring approximate 15-year oscillations in aquifer outflow rates from springs that contribute a large proportion of annual runoff into the Pit and McCloud rivers in northern California (Freeman 2001) provide possible clues that there may be multi-year periodicity to overall climate wetness and dryness as characterized by groups of successive years. This paper will illustrate some specific examples of precipitation, snowpack, and runoff that appear to support periodicity in wetness and dryness with amplitudes at about 7-8 years, and wetness and dryness, peaks and valleys respectively, utilizing three- and five-year grouped averages, each peak and valley being repeated approximately every 15 years. Some longer-term trends are also explored in this paper.

During either the wet or dry period, specific years were frequently observed to vary significantly from the three- or five-year average, but the group as a whole remained in relative harmony with the historic 15-year frequency. A review of aquifer outflow rates was utilized to identify the wet and dry amplitude peaks and valleys in terms of initially typing historic years. When applied to the 107-year, 1895 through 2001 Lake Spaulding precipitation record, grouping the year types into regular successive wet and dry three-year peaks and valleys according to rates of aquifer outflow, a relatively close matching relationship was found with the precipitation record. The apparent 15-year periodicity between successive recurring wet peaks and successive recurring dry valleys can be observed in Figure 1 for the 107-year period studied.

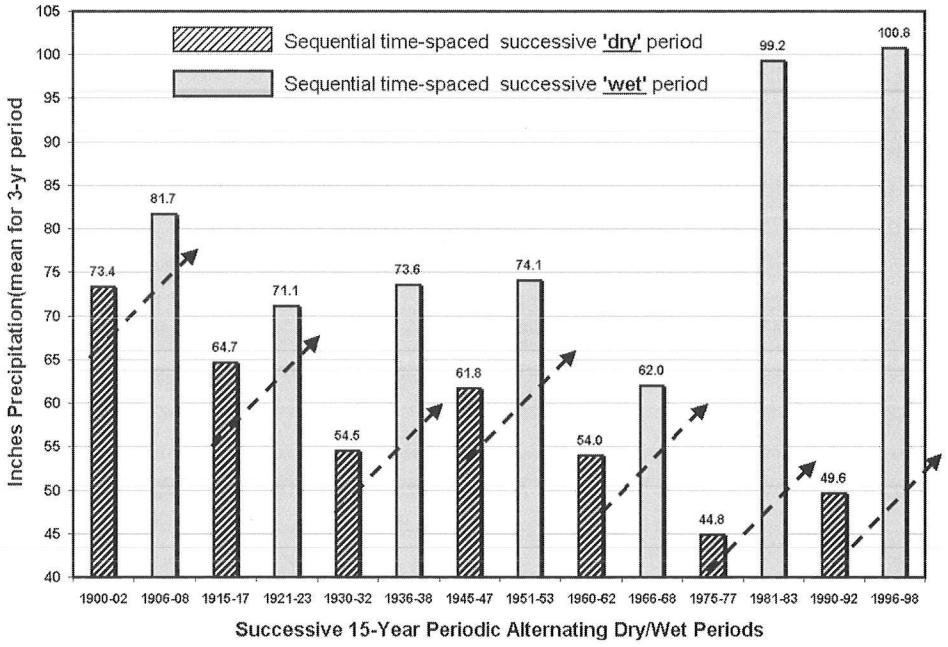

Figure 1 Lake Spaulding periodic oscillation of successive, sequential, time-spaced 3-year wet and dry groups of years. A sometimes subtle, but regular, oscillation appears to regularly repeat itself in terms of reaching a relative wetness maximum for the grouped years approximately every 15 years.

When other precipitation stations in both the central Sierra and southern Cascades near Mt. Shasta are combined and a five-year moving average smoother applied, the wet and dry oscillation again appears in a regular periodic manner, with some implied likelihood that the next dry valley for these three climate station will occur in or about 2005-2007 (Figure 2).

Spectral analysis can be applied to smoothed moving averages to reveal possible periodicity in wetness and dryness. This approach may reveal periodicity and show indication of the interval length, but in terms of prediction, this approach does not readily type the years into wet or dry groups such that the oscillation can be meaningfully extended forward in time from a specific year. Forecasts of periods, which reflect future periods of wetness and dryness based on past climate history, can be charted with possible implication that if the observed pattern continues, one may gain some skill for determining wet and dry groups of years forward of the present point in time. Such skill would be especially helpful for planning based on multiyear estimates of hydropower, water supply, and other longer-range hydro resource needs.

While individual years within the 3-5 year group are somewhat random in terms of being wet or dry, their moving average especially for the groupings reveals a somewhat regular oscillating pattern. A centered five-year moving average smoother was applied to the 1950 through 2001 Water Year flow for the east branch of the North Fork Feather River near Rich Bar, USGS 11403000 (Figure 3). This 52-year runoff record shows both the approximate 15-year periodicity in runoff and a possible longer-term trend toward increasing variance between high and low runoff periods.

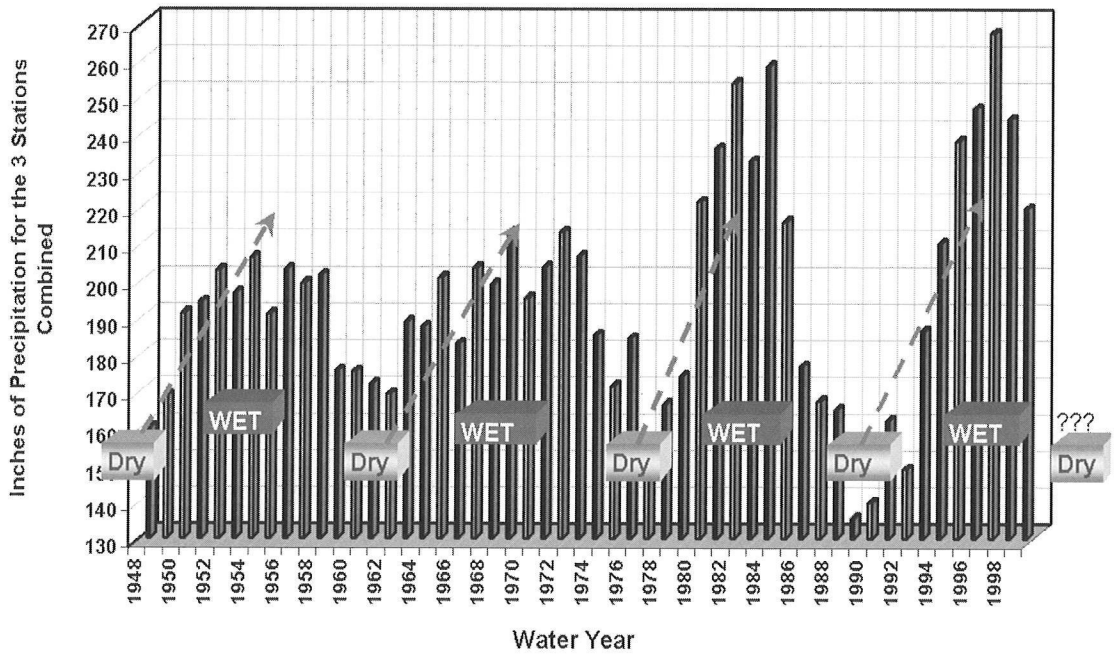

Figure 2 A five-year centered moving average smoother was applied to the combined water year precipitation of two central (Salt Springs, Lake Spaulding) and one northern California (Pit PH#5) climate stations. A regular periodic oscillation in wetness may provide some implied likelihood for predicting future wetness as a grouped set of years. In the past 30 years, two approximately 15-year oscillation periods, there appears to be increased difference between wetness and dryness amplitude compared with prior oscillations.

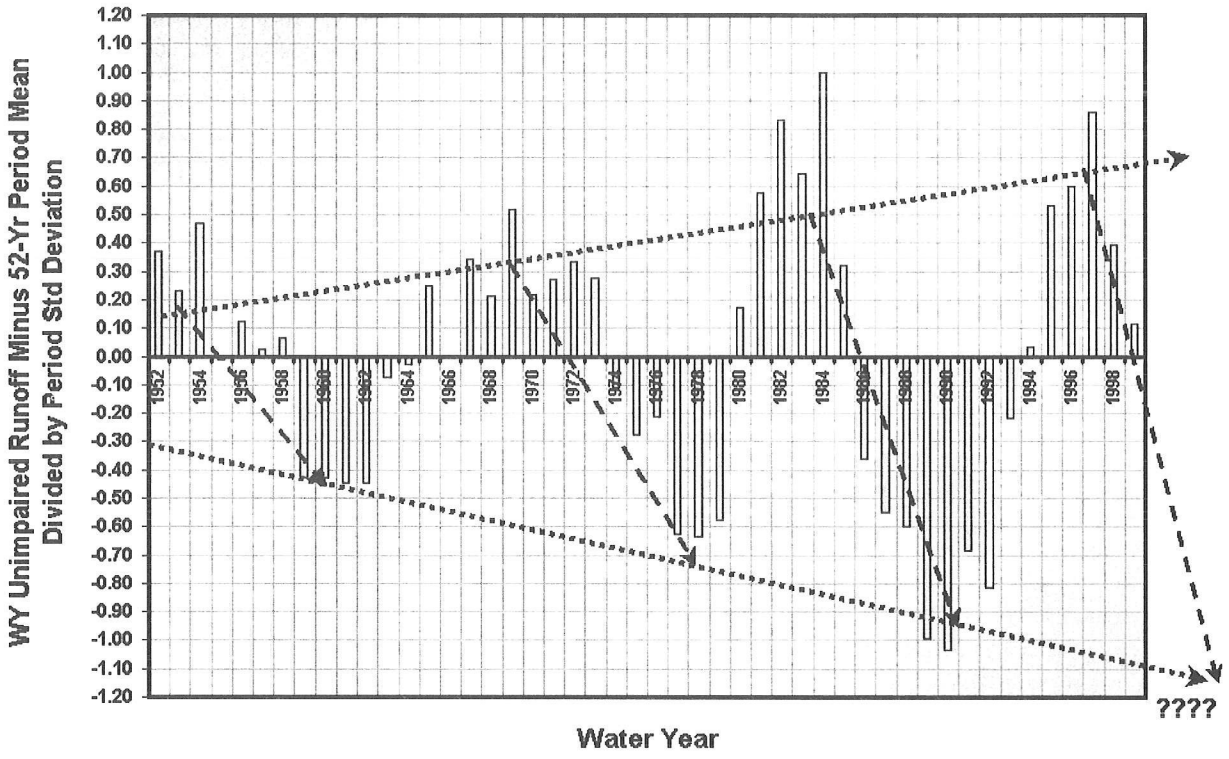

Figure 3 Recurring periods of greater and lesser-unimpaired runoff during the past 52 years on the east branch of North Fork Feather River. Increased period variability since about the mid-1970s, for the 52-year period, shows an increased variance in amplitude in recent years. Centered 5-year moving average applied.

Periods Within the Year also Show Recurring Runoff Patterns with Possible Long-Term Trends

In addition to the longer-term periodicity, there also appear to be trends and cycles (although less regular) that show up within the water year. The longer-term trend may possibly be due to earlier melt of the snowpack. The March runoff for the east branch of the North Fork Feather River (Figure 4) has increased while the May runoff (Figure 5) has decreased. Such trend change over the relatively brief span of approximately 50 years has potential to impact efficiently scheduling the water for hydroelectric production. The hydroelectric facilities were designed based on a runoff pattern for the Feather River typical of the early to mid-20th century. During the past 50 years the March runoff from the east branch of the North Fork Feather River, which represents about one-third the average annual runoff for the North Fork Feather River at Lake Oroville, has in recent years approximately doubled in quantity. In terms of hydroelectric scheduling, March flow releases from the large upstream storage reservoirs, Lake Almanor and Bucks Lake, have greatly decreased in recent years. This has in part resulted from an ongoing hydro scheduling practice to avoid when possible, the spill of upstream stored water from Lake Almanor past hydroelectric powerhouses along the lower reaches of the river that are already running at full capacity from the unimpaired east branch of the North Fork Feather River's March runoff. The approximate 15-year oscillation of grouped annual runoff observed in both the March and May months is most likely related to the similar wet/dry oscillation in annual precipitation. Seasonal precipitation amounts show an almost direct correlation with

snowpack amount and therefore snowmelt runoff, which will in turn likely affect March and May runoff amounts. This observed shift in runoff timing has in general within the past 15-20 years supported a relatively recent practice by water planners for reduced draft from both Lake Almanor and Bucks Lake during the January through March period, while the late winter and early spring uncontrolled sidewater flows from low elevation headwater areas, which have trended upward in recent years, are being increasingly utilized to run power houses downstream of these two lakes.

The November through February period was divided by the combined November through February period and the April through July period utilizing the monthly computed unimpaired flow for the Yuba River at Smartville, as computed by the California Department of Water Resources, for the 102-year period 1901 through 2002. The data was standardized with a centered five-year moving average smoother and is shown in Figure 6. Figure 6 reveals a positive upward drift in the November through February flows compared with the April through July snowmelt period.

Increased winter runoff is reflective of an increased proportion of precipitation falling as rainfall over the watershed during the November through February period. The record period used was 1901 through 2002 (102 years).

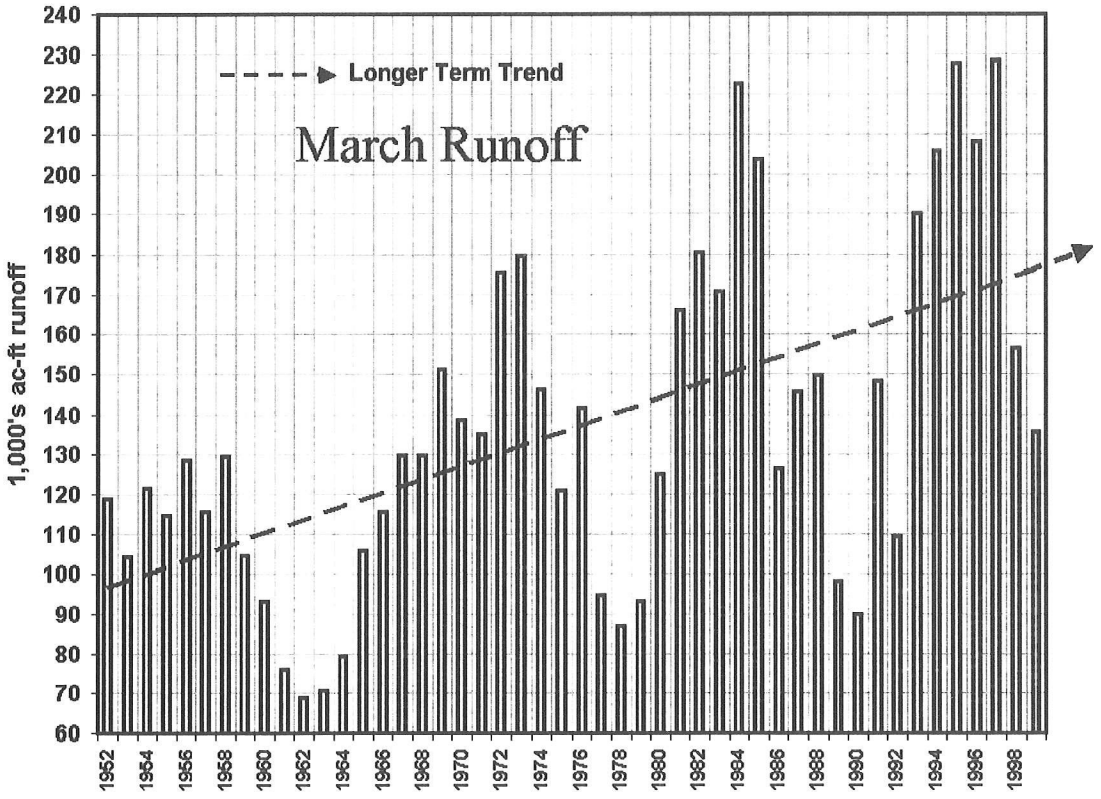

Figure 4 March unimpaired runoff for the east branch of the North Fork Feather River. Both a relatively short-term 14-16 year oscillation and longer-term trend toward increased March runoff in recent years appear on the chart. Centered 5-year moving average applied.

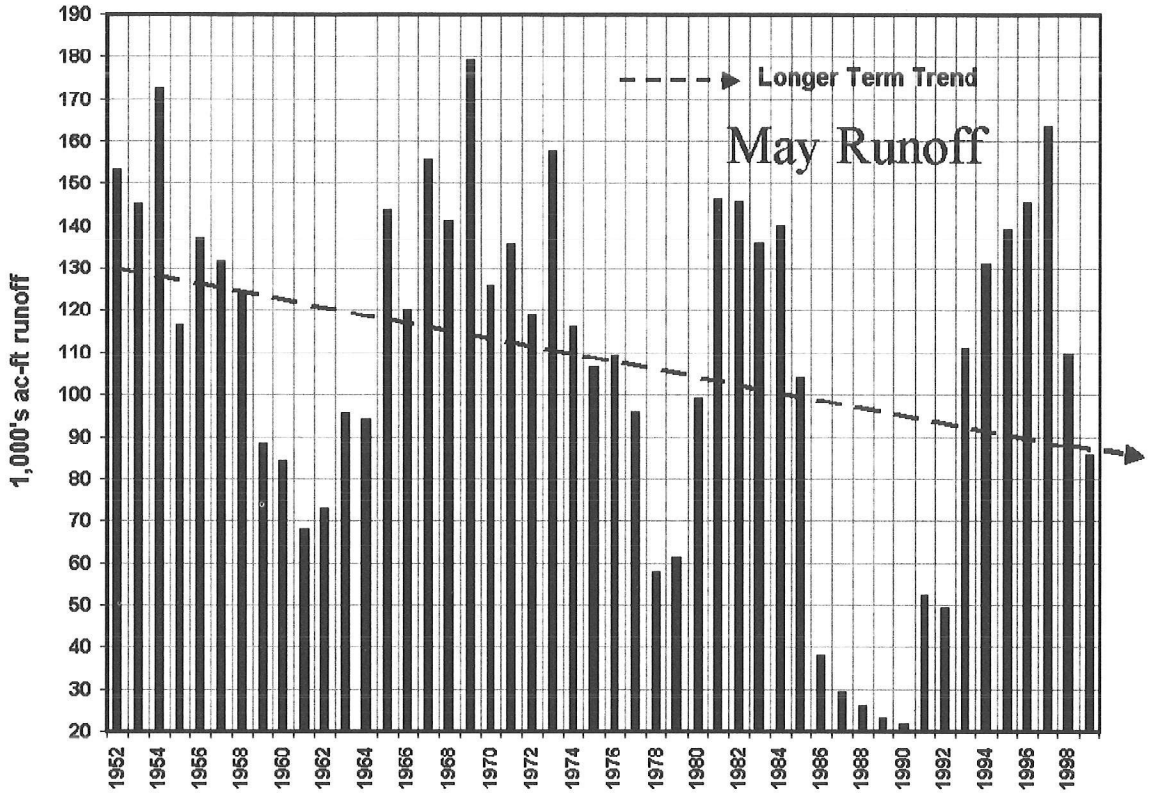

Figure 5 May unimpaired runoff for the east branch of the North Fork Feather River. Both relatively short-term 14-16 oscillation cycles and a longer-term trend toward decreased May runoff appear on the chart. Centered 5-year moving average applied.

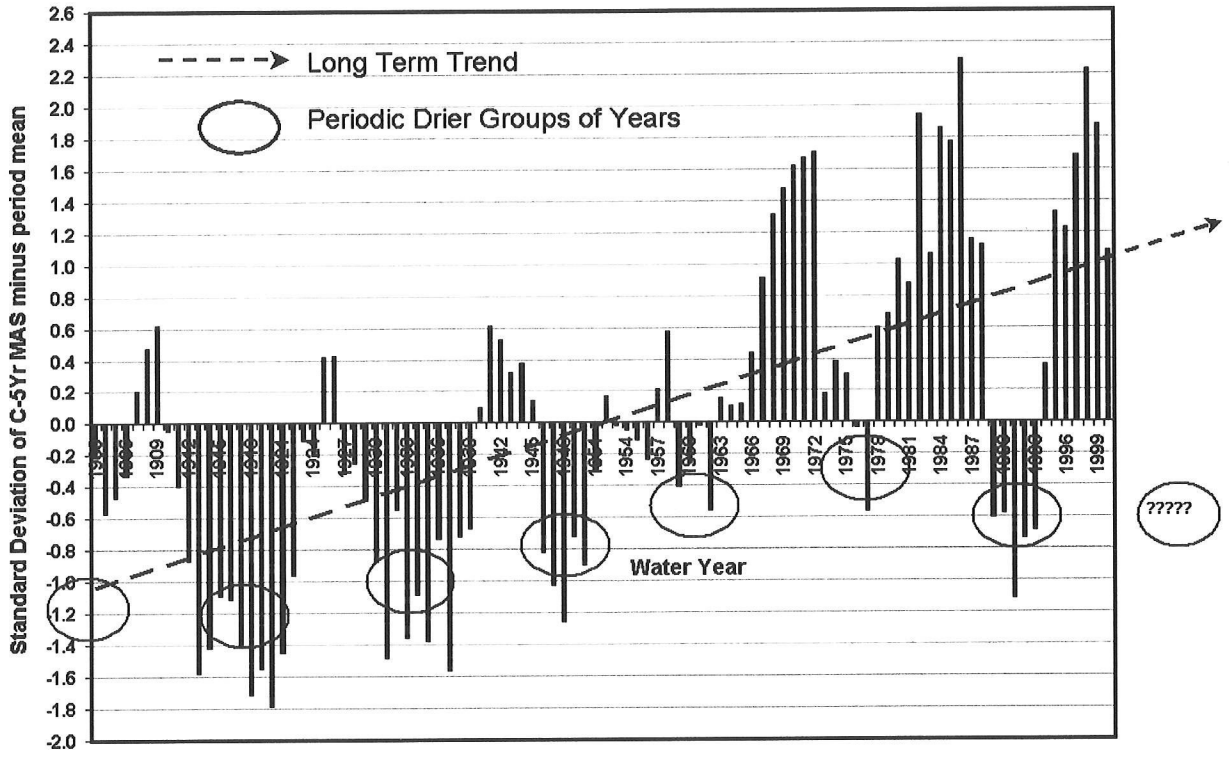

Figure 6 A drift in flow timing for the unimpaired runoff of the Yuba River at Smartville. Increased winter runoff in recent years appears reflective of an increased proportion of the annual precipitation falling as rainfall over the watershed during the November through February period. Record period used was 1901 through 2002 (102 years).

A continuous shift of the April through July runoff into the winter months November through February was observed from the data analyzed. With winter runoff in the Sierra largely produced from frontal type winter storms, the magnitude of winter runoff is mainly dependent upon quantity of winter rainfall produced runoff. If such is the case then it should revel itself when charted over the past 102 years. Figure 7 illustrates an increased frequency of large rain-produced runoff events in the second half of the 20th century compared with earlier years. This appears consistent with recent research findings, which forecast a shift in spring snowmelt runoff to increased rainfall produced winter runoff (Cayan and others 2001). Figure 8 displays the November through February averages for the two periods. There was a 17% increase in the period averages for November through February runoff.

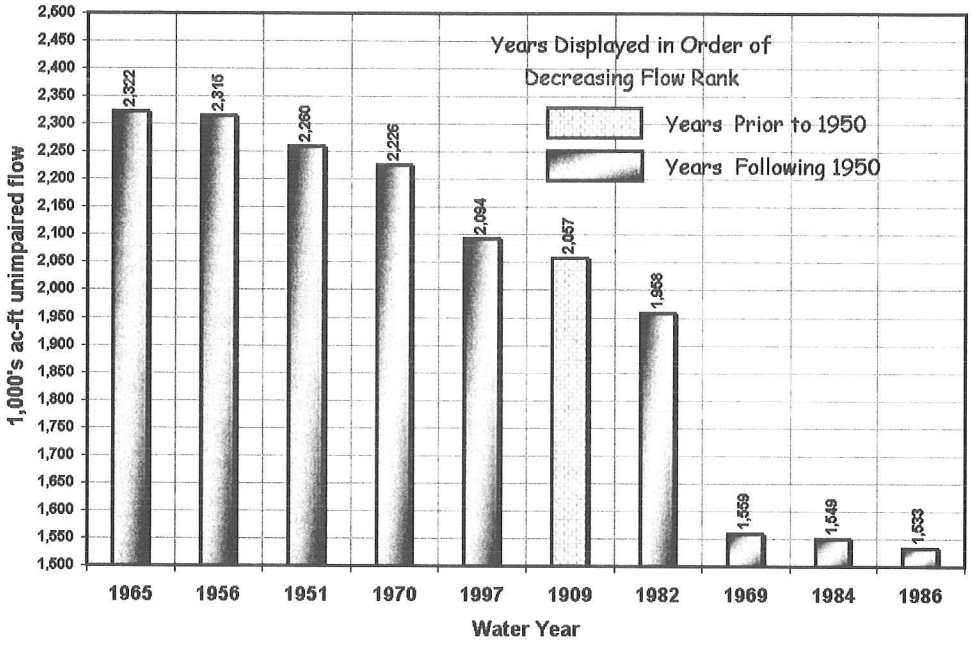

Figure 7 For the period 1901 through 2000, Yuba River at Smartville, only one year in the ten years of November through February unimpaired flows, which exceed 1,500,000 af, occurs prior to 1950. Recent years appear to have higher likelihood for more flow during the 4-month November through February winter period.

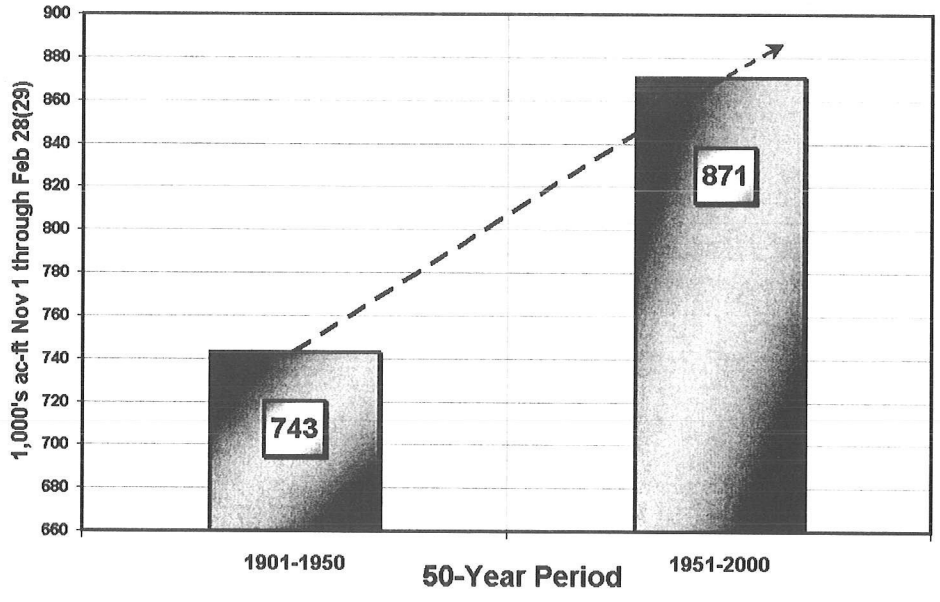

Figure 8 The mean flow of two successive November through February 50-year periods for the Yuba River at Smartville. There is a 17% increase in the more recent period.

The California Sierra Snowpack

California's snowpack likewise shows recurring patterns similar to that for both runoff and precipitation. A single snow course at Meadow Lake (#66) in the central Sierra at the 7,200 foot elevation readily revels relative consistency in regular recurring oscillation between wet and dry groups of years as shown in Figure 9. While no attempt is made here to explain a cause for the observed recurring multiyear oscillation, a significant amount of the seasonal snowpack variability may be explainable with indices of Pacific Ocean Climate such as PDO (McCabe and Cayan 2001).

In order to test that the centered five-year moving average produced pattern was not simply a moving average "produced-aberration", regularly spaced discrete groups of years were also charted to verify alternating wet/dry periods. This is displayed in Figure 10. The regularly occurring highs and lows are readily identifiable, but in some cases are relatively subtle and could possibly be easily overlooked unless one was specifically looking at the appropriate successive regularly occurring time blocks.

Seasonal snowpack is closely related to both precipitation amount and freezing levels for winter and spring storms. The author found that for moderate to high elevation snow courses in the central Sierra, the April 1 snow water equivalent exhibit oscillation patterns closely resembling those of both precipitation and runoff.

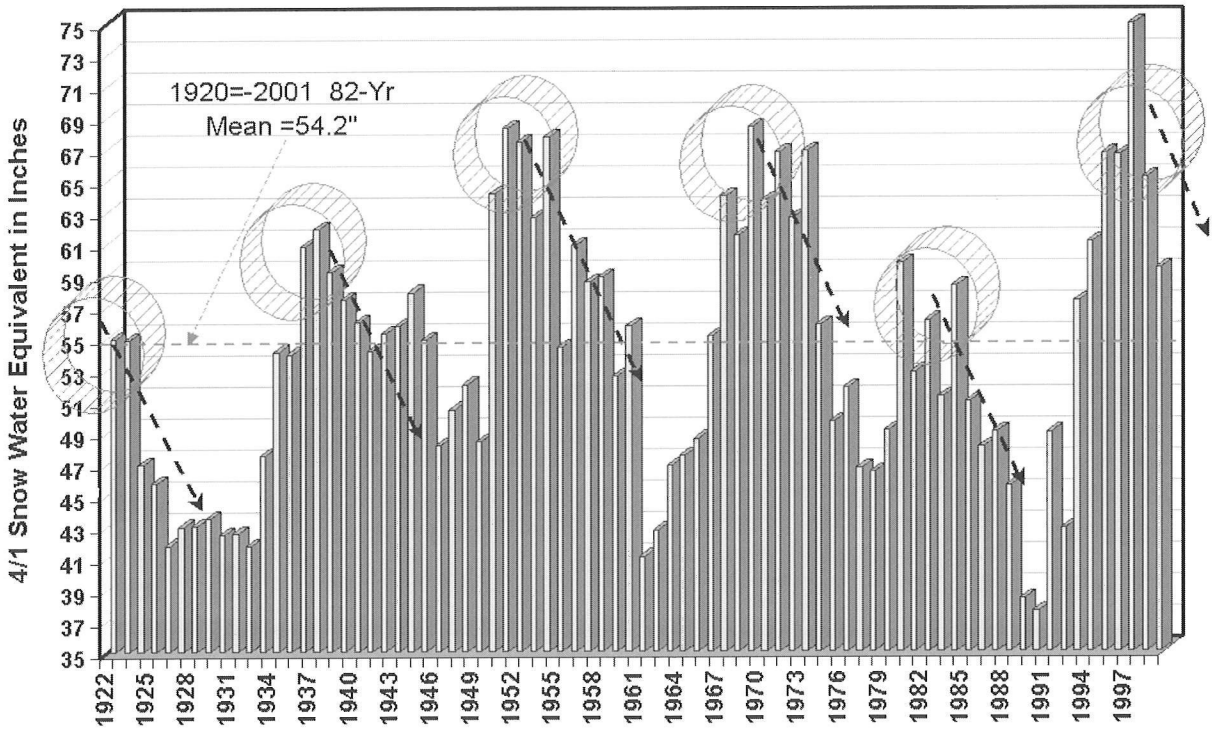

Figure 9 Meadow Lake snow course #66 in California's central Sierra Yuba River headwaters reveals a periodic oscillation in April 1 snow water equivalent (SWE) between periods of relative wetness and dryness. This snow course at the 7,200 foot elevation, unlike others at lower elevations, has not seen a reduction in snow water equivalent during the second half of the 20th century. Centered 5-year moving average applied.

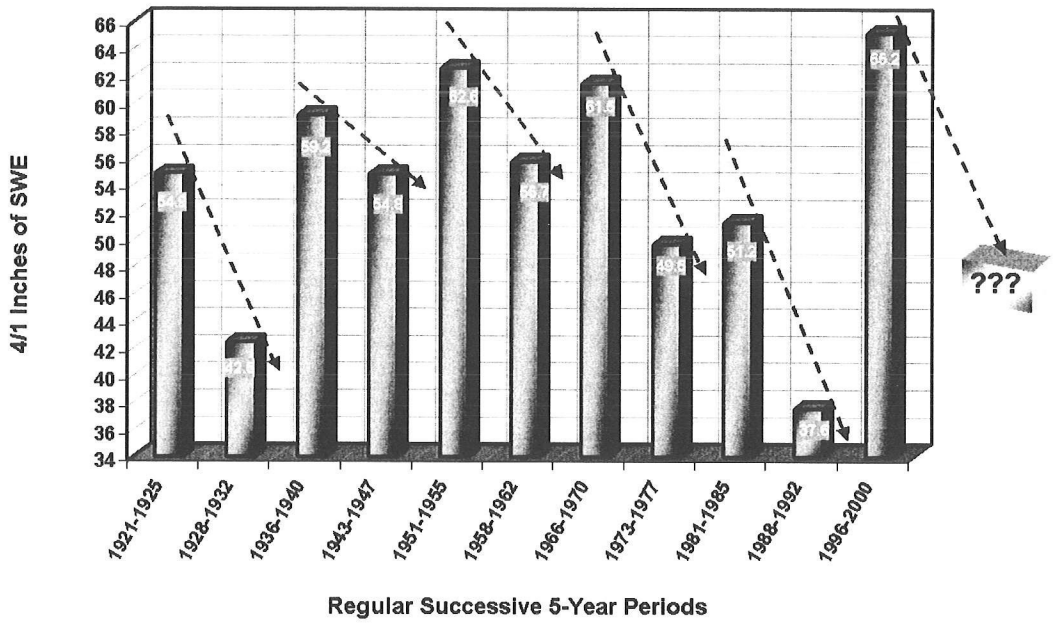

Figure 10 Meadow Lake #66 snow course — April 1 Snow Water Equivalent (*same original basic data set as used for Figure 10*). Discrete, successive 5-year groupings of regularly spaced years charted to show sometimes subtle, but regular, periods of wetness and dryness.

Comparison of the April 1 snow water equivalent for two snow courses on the south Yuba watershed for the period 1948 through 2002 — Lake Spaulding at the 5,200 foot elevation and Meadow Lake at the 7,200 foot elevation — reveals a downward trend for Lake Spaulding, the lower elevation snowpack (Figure 11). Meadow Lake, however, at the 2,000 foot higher elevation, approximately 10 miles northeast of Lake Spaulding, displays a near level trend line for the same 55-year period. The Lake Spaulding April 1 snow water equivalent is examined for a longer period (Figure 12). The April 1 snow water equivalent decreases from a mean of 24.4 inches for the 37-year period 1929 through 1965 to 19.8 inches for the 37-year period 1966 through 2002. This equates to a 19% drop in the mean for the more recent of the two periods (Figure 12). This long-term decreasing trend in low elevation snowpack and consequent decline in melt produced runoff appears consistent with that described elsewhere (Roos 1991).

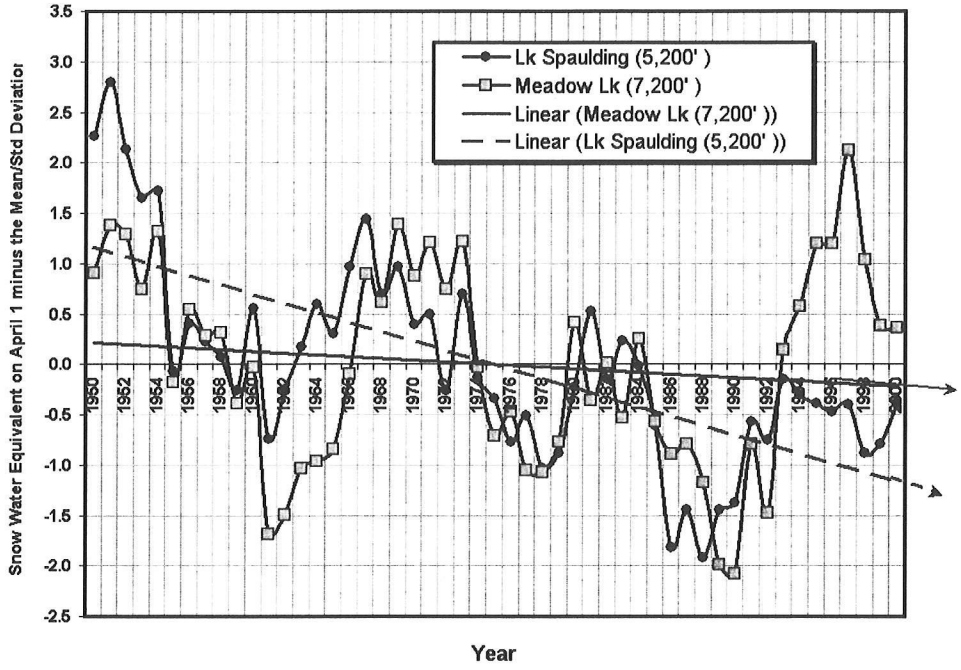

Figure 11 A comparison of the April 1 snow water equivalent for the two snow courses, Lake Spaulding #85 at the 5,200 foot elevation and Meadow Lake #66 at the 7,200 foot elevation in the headwaters in central California's Yuba River headwater drainage. Trend lines for each of the snow courses show a much steeper decline in recent years for the lower elevation Lake Spaulding snow course.

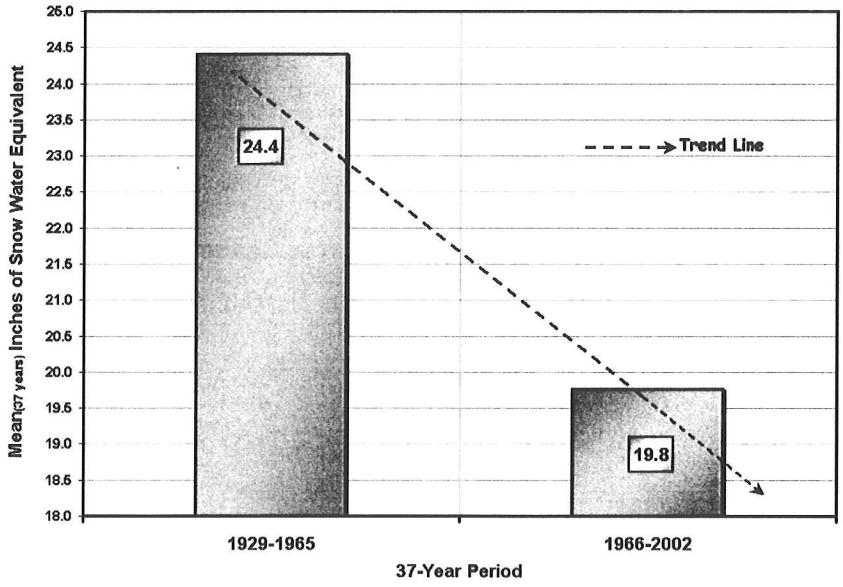

Figure 12 The April 1 snow water equivalent mean for two successive 37-year periods at the Lake Spaulding #85 snow course at the 5,200 foot elevation in California's central Sierra. This decrease in the April 1 SWE mean represents a 19% drop from the earlier period. No significant decline was observed to have occurred in the nearby snow course at Meadow Lake, which is 2,000 feet higher in elevation. The decline in low elevation snow in recent years may be indicative of a higher snowfall line with winter storm systems.

Conclusions

Analysis of historic hydrometeorological data reveals patterns that may have use in predicting future tendency toward wet or dry multiyear periods. If substantiated from additional research, such patterns may have potential use for long-range hydroelectric planning. Planning future outage schedules for hydroelectric facilities and reservoir carryover storage targets for multi-year storage reservoirs such as PG&E's Lake Almanor could benefit from increased skill in predicting upcoming years to have increased likelihood for more or less annual inflow. PG&E is already able to forecast approximately 40 % of its annual generation several years forward by making a baseflow forecast of anticipated relatively firm aquifer outflow from springs, which provide large relatively stable daily flows of the High Cascade and flood basalts of northern California. The apparent bimodal approximate 15-year oscillation pattern does not appear to provide much insight into predicting any given year's wetness in the future, but seems more useful for defining multi-year groupings as being in a wet or dry period as a grouping of three or more years. From the limited analysis presented here, precipitation, snowpack, and unimpaired runoff all appear to reflect this approximate 15-year oscillation in the central Sierra. The aquifer outflow of springs in northern California slightly lags these cycles and provides a natural moving average smoother of prior years annual precipitation variance.

Longer-term trends in apparent distribution shift of monthly runoff from the April through July snowmelt runoff period into the November through February period may be occurring from a trend toward reduced low elevation snowpack, possibly from an increased frequency of slightly warmer winter frontal storm cells during the second half of the 20th century. Since most of PG&E's hydroelectric system was designed based on historical flows prior to the mid-1960s, increased winter flows of higher magnitude are posing new challenges in monthly hydroelectric scheduling for reservoirs primarily designed to accommodate pre-1960s snowmelt quantities and annual year-to-year variance. Warmer conditions may shift reservoir filling from the late spring-early summer period toward holding additional water later into the winter-early spring period to increase assurance of filling from snowmelt. There is growing research that this trend is likely to continue (Knowles and others 2001; Snyder and others 2001). The reality of the limited observations discussed in this paper must await further, more thorough research, but the patterns and trends being observed tend to hint at possibility of a bimodal stochastic resonance effect. Regardless of the underlying forcing causes, the observed regularity of patterns appears helpful in making longer-range multiyear planning decisions.

References

Cayan D, Dettinger M, Hanson R, Brown T, Westerling A, Knowles N. 2001. Investigation of climate change impacts on water resources in the California region. http://meteora.ucsd.edu/~meyer/acpi_progress_jun01.html

Freeman G. 2001. The impacts of current and past climate on Pacific Gas & Electric's 2001 hydroelectric outlook. In: Proceedings of the eighteenth annual Pacific Climate Workshop. West GJ, Buffaloe LD, editors. Tech Report 69 of the Interagency Ecological Program for the San Francisco Estuary. Sacramento; CA Dept. of Water Resources. p 21-37.

Knowles N, Cayan D. 2001. Potential effects of global warming on the Sacramento/San Joaquin watershed and the San Francisco estuary. Submitted to Geophysical Research Letters.

Manga M. 1999. On the timescales characterizing groundwater discharge at springs. Journal of Hydrology 219(1999) 56-69.

McCabe G, Dettinger M. 2001. Primary modes and predictability of year-to-year snowpack variations in the Western United States from teleconnections with Pacific Ocean climate. In: Proceedings of the eighteenth annual Pacific Climate Workshop. West GJ, Buffaloe LD, editors. Tech Report 69 of the Interagency Ecological Program for the San Francisco Estuary. Sacramento; CA Dept. of Water Resources. p 47-56.

Roos M. 1991. A trend of decreasing snowmelt runoff in northern California. 59th Western Snow Conference, Juneau, AK p. 29-36.

Snyder MA, Bell J, Sloan L. 2001 Climate responses to a doubling of atmospheric carbon dioxide for a climatically vulnerable region. Geophysical Research Letters, Vol. 29, No. 11, 10.1029/2001GLO14431.

Empirical Search for Clues to Process and Dynamics Underlying Climatic Change

Thor Karlstrom

Abstract

Early analyses of high-resolution time series suggested correlation of longer term ice-age trends with latitude controlled solar insolation (The Milankovitch [1941] Climate Model); of shorter term trends with globally synchronous tidal forces (the Pettersson Climate Model); and of the associated processes such as geomagnetism, volcanism and higher frequency changes in solar output (cf Karlstrom 1961). Most paleoclimatologists now accept geometric solar insolation as the modulator of the Ice Ages, but most also assume that the waxing and waning of the much larger Northern Hemisphere ice sheets determined parallel climatic and associated glacial changes in the Southern Hemisphere. Over the past 10 years increasing attention has focused on the pervasive patterns of secondary oscillations so characteristic of the instrumental and paleoclimatic records; few researchers, however, have analyzed the possible phasing of these oscillations with either lunar or solar perturbations (Notable exceptions are listed below). The purpose of this paper is to provide time-series correlations that strongly suggest cause-and-effect relations between solar/lunar perturbations and climate, volcanism, cosmic rays and solar/earth magnetism. The presented correlations focus in on orbital perturbations of the solar system (varying both tidal force and insolation) as the operational energy system within which past climatic and associated process changes have been concurrently modulated (evidently with occasional non-linear phase reversals) at yearly to millennial scales. Although much work remains to be done, sufficient clues are now available to focus research into those critical areas likely to enhance understanding of the multi-factors underlying climatic change.

Introduction

In the absence of a generally accepted theory of past climatic change, paleoclimatic research necessarily concentrates on the empirical evidence of past climates in the search for clues relating to underlying process and dynamics. Early analysis of radiometrically, varve- and tree-ring-dated time series (Karlstrom 1955, 1956, 196l and 1976; Karlstrom and others 1976) suggested correlation of : l) the longer term Ice-age trends with latitudinal changing summer solar insolation (the Milankovitch Climate Hypothesis: M. Milankovitch 1941); 2) superposed shorter fluctuations with globally synchronous changes in tidal forces generated by orbital relations between Sun, Moon and Earth (The Pettersson Climate Hypothesis: O. Pettersson 1912-1930) and 3) of associated processes such as volcanism (atmospheric dust and aerosols), geomagnetism and sunspots (intrinsic or geometrically induced changes in the solar constant).

Paleoclimatologists with few exceptions now accept the geometric Solar Insolation Climate Hypothesis for the Ice Ages. Many assume, however, that the waxing and waning of the much larger Pleistocene ice sheets of the Northern Hemisphere determined parallel climatic and glacial changes in the Southern Hemisphere. Within the last ten years an increasing number of researchers have turned

their attention to the pervasive patterns of yearly, decadal, centennial and millenial oscillations in their paleoclimatic and instrumental time series. Relatively few, however, have analyzed the possible phasing of these oscillations with solar or lunar perturbations. For notable exceptions, however, see, among others, Abbott 1900; Clough 1905; Douglas 1919-1936; Willett 1961; Brier 1968; Fairbridge 1968; Michell and others 1979; Currie and others 1981-1990; Wood 1985; Friis-Christensen and Lassen 1991; Burroughs 1992; Sanders 1995; Keeling and Whorf 1997; and Berry and Hsu 2000. A major breakthrough relating to correlation of geometric solar perturbations with geomagnetism, cosmic rays, and climate (primarily cloud cover and precipitation), at scales ranging from the decadal sunspots to the millennial long solar-insolation trends, is most recently summarized in Mercurio (2001).

The purpose of this paper is to provide time-series correlations that strongly suggest cause-and-effect relations between solar/lunar perturbations and climate, volcanism, cosmic rays and solar/earth magnetism. The presented correlations focus in on orbital perturbations of the solar system (causing variations in both tidal force and insolation) as the operational energy system within which past climatic, volcanic and geomagnetic changes have been concurrently modulated (evidently with occasional non-linear phase reversals) at yearly, decadal, centennial and millenial scales.

Much work remains in refining our understanding of underlying physical linkages as well as of the dynamics of associated atmospheric circulation patterns resulting in characteristic regional variability. Nonetheless, significant clues are now available that should provide critical focus for further research, hopefully leading to the development of more sophisticated General Circulation Models (GCM) that incorporate the critical factors of cloud cover, geomagnetism, cosmic rays and tidal forcing, along with other definable natural changes such as atmospheric CO_2, methane and ozone.

The Search for Climatic Change Clues

Clue Search #1— Higher Latitude Glaciations and the Obliquity Cycle versus Mid-latitude Glaciations and the Precessional Insolation Cycle—If the Milankovitch's climate mechanism (summer half-year solar insolation) modulated Pleistocene Glaciations, as now accepted by most researchers, higher latitude glaciations should theoretically follow the ca. 40,000-year Obliquity Insolation Cycle which predominates in both polar regions. On the other hand, glaciations in mid latitudes should largely reflect the ca. 20,000-year Precessional Cycle characterized instead by opposing trends across the Equator.

Figures 1 and 3 show high-latitude glacial and collated records that phase well with the Obliquity Cycle, and thus with my Cook Inlet Alaska chronology (Karlstrom 1961, 1964, 1968). In contrast, the North American mid-continental ice sheets as well as mountain glaciers terminating in the warmer mid latitudes, correlate with glacioeustatic sea-level records and, in turn, with the higher frequency Precessional Insolation Cycle (Figure 4). As shown in Figures 1 and 2, the amplitudes of the Alaska and Siberia glacial records follow more closely the Pacific- rather than the Atlantic- Ocean isotope record.

Current dating problems with the Southern Hemisphere glacial records make inter-hemispheric correlations less certain. But as shown in Figure 4, the Chile glaciations, as dated by Clapperton and others (1992), are evidently in opposition to their Northern Hemisphere counterparts, or again consistent with direct correlation with local Precessional trends. The same anti-phase relations occur between the Southern Hemisphere lake-level fluctuations of eastern Africa and Australia and those of

the North American Southwest (Street and Groves 1979). The classic Northern Hemisphere "Little Ice Age" (correlative of the Alaskan Glaciation) is evidently absent in southern middle and lower latitudes because of opposing insolation trends. In the Northern Hemisphere insolation trends indicate cooling since 10,000 years BP; in the Southern Hemisphere the contemporaneous trend is towards warming.

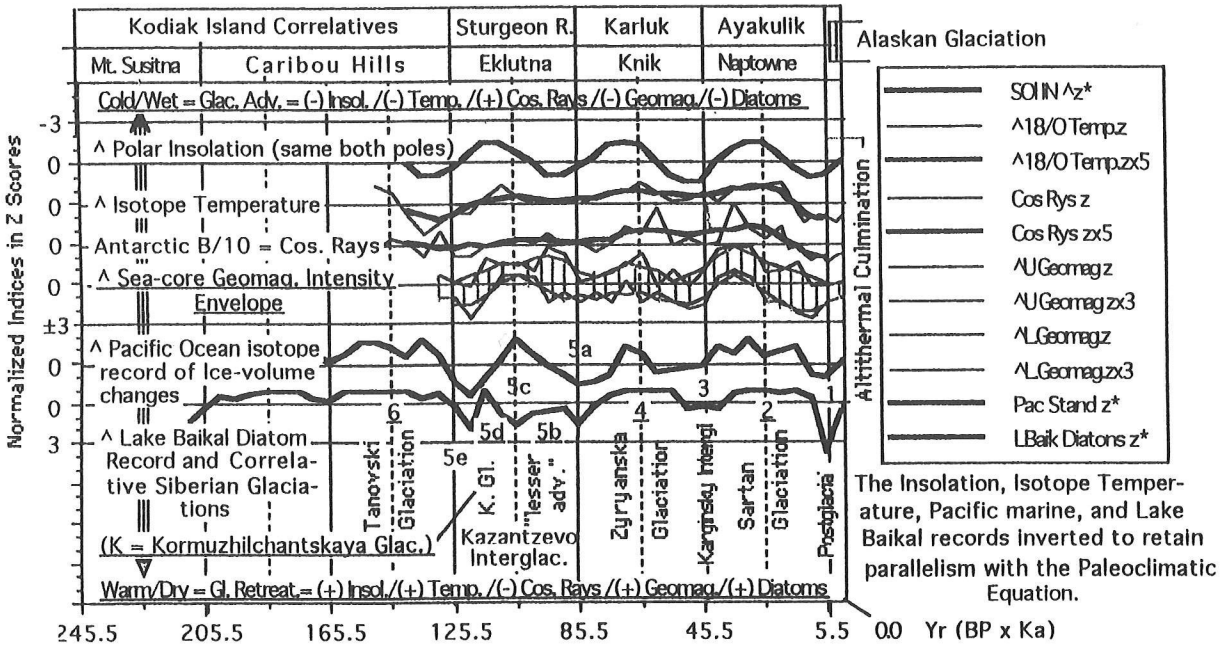

Figure 1 Marine records, cosmic rays, geomagnetism, high-lat. glaciations and the obliquity cycle Cook Inlet and Kodiak Island, Alaska Glaciations (Karlstrom 1961, 1964, 1968). Correlation of isotope temperature and ice volume, cosmic rays, geomagnetic intensity, Baikal Lake record and high latitude glaciations with the polar obliquity insolation cycle. These records are positioned on the author's timescale of interglacial culminations (Karlstrom 1961) assuming a 4,500-year response lag between insolation and glacial retreat. Insolation indices from Verneke (1972); the temperature, cosmic ray and geomagnetic indices from Mercurio (2001); the "standard" marine isotope record of the equatorial Pacific Ocean from Chuey and others (1987); and the Lake Baikal record and time correlations with the Siberian glacial record from Karabanov and others (1998). See Figure 2 for a direct comparison of the above "standard" Pacific Ocean isotope record with the equatorial Atlantic Ocean. Note confirmation of the general validity of the Cook Inlet glacial time frame by striking parallelisms with comparably high-latitude Siberian and Antarctica records and with the cosmic ray and geomagnetic records; all evidently directly modulated by solar insolation dominated in upper latitudes by the Obliquity Cycle. Also see Figure 3.

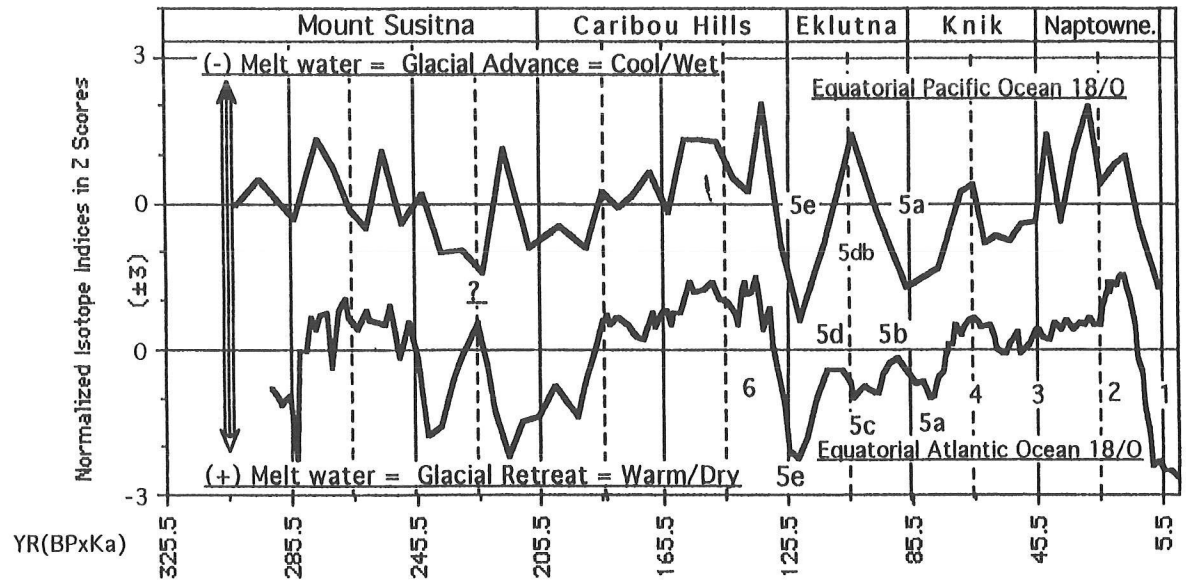

Figure 2 Two standard pleistocene marine isotope records. Cook Inlet, Alaska Glacial Chronology (Karlstrom 1961). Two "standard" marine ice age chronologies on timescale of the obliquity insolation cycle (ca. 40,000-years) and its 2/1 (ca. 20,000-years) resonance assuming a response lag of ca. 4,500 years (Karlstrom, 1961). Isotope indices of an Equatorial Pacific Ocean core from Chuey and others (1987); the Equatorial Atlantic record from Martinson and others (1987). Both chronologies are fine-tuned to the Milankovitch N 60° Lat. Climatic Model assuming corresponding response lags. The records differ mainly in (1) out-of-phase relations ca. 225,000 yrs. BP and (2) post-125,000 yr. glacial amplitudes. These differences suggest either heterogenieties in the global record or remaining operational or sampling difficulties. Note the tendency for near in-phase oscillations with the Obliquity 2/1 (ca. 20,000-year) Resonance. Most researchers continue to correlate terrestrial paleoclimatic records with Martinson and others isotope record on the assumption that it reflects a global climatic signal. Many terrestrial records appear to contradict this assumption and to support instead the Insolation/Tidal-resonance Model which requires opposing longer term climatic trends in the two hemispheres because of precessional effects, but globally synchronous secondary climatic oscillations because of modulating tidal forces. Modified from Figure 28 in Karlstrom (1995).

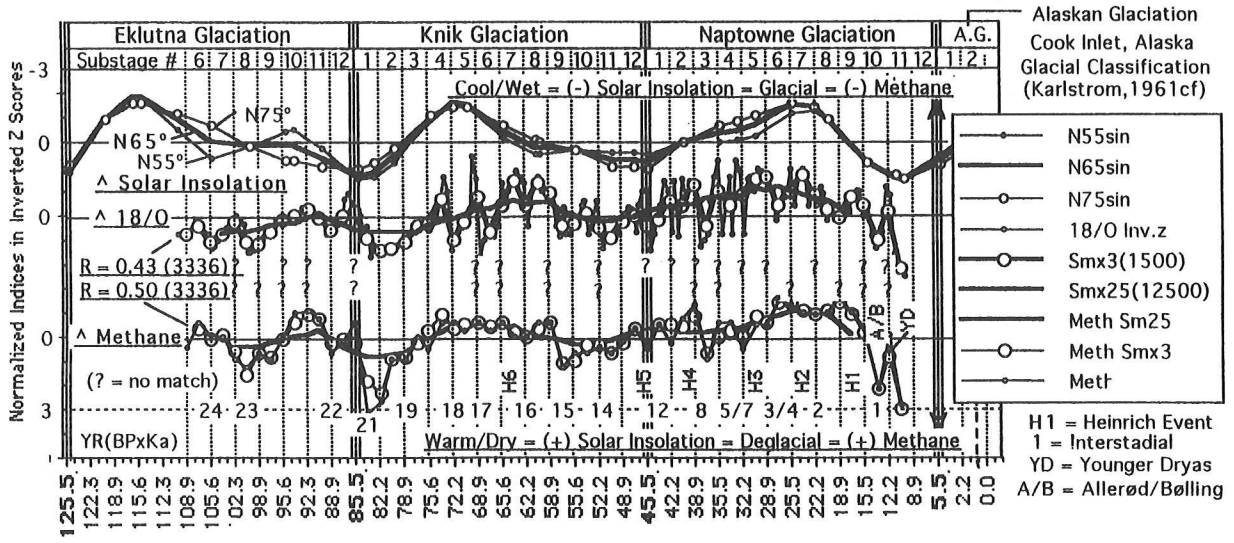

Figure 3 Greenland ice-core isotope temperature, methane and north 60° latitude insolation. Correlation of Greenland GISP2 Ice-core record (N 60° L.) with Upper N. Latitude Solar Insolation on timescale of the 3336-year Substage Cycle and its x12 (40,032 yr.) superharmonic. Isotope- and methane-indices and dating of marine Heinrich Events (cold) and terrestrial Bølling/Alerød (warm) and Younger Dryas (cold) events by correlation with the GISP2 time frame (Brooks and others 1996). Their ice-core indices are replotted at 500-year intervals thus filtering out secondary cycles of less than 1000-years. Brooks and others correlate their GISP2 record with the N 60° Lat. solar insolation dominated by the Obliquity Cycle but slightly modified by precessional trends that predominate in lower latitudes (see Figure 4). Note the striking parallelism with the comparable-latitude Cook Inlet Alaska glacial record; also note the general positive correlation between glaciation and green-house methane gas, which emphasizes the important role of past climatic (nonanthropogenic) changes in determining the greenhouse-gas content of the atmosphere (Karlstrom 1995); and finally, note the lace of correlation between GISP2 secondary oscillations and the Substage Cycle which may result from differing response functions or from remaining uncertainties in dating.

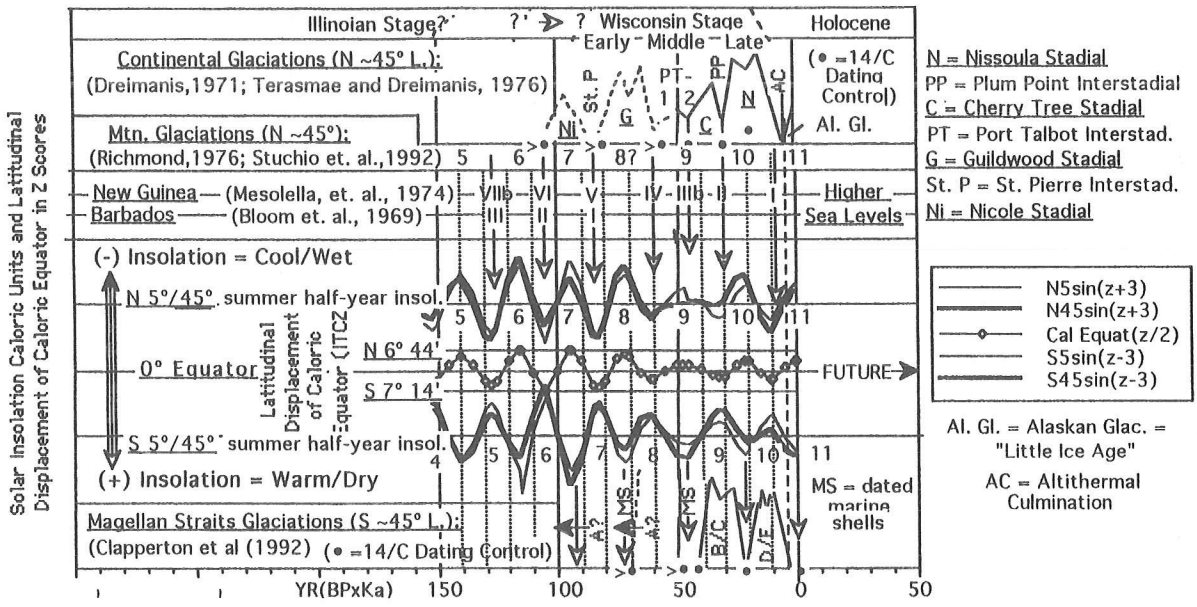

Figure 4 Correlation of Northern and SoCorrelation of Northern and Southern Hemisphere glacial records with marine chronostratigraphy, with opposing Hemispheric Presessional Trends and with Latitudinal Displacement of the Caloric Equator and Intertropical Convergence Zone (ITCZ). Note the remarkable parallelisms of the Northern Hemisphere mid-latitude glacial records, the dated sea-level records and the mid-latitude precessional trends. These correlations support the concept of glacioeustacy, but not necessarily that of inter-hemispheric climatic synchrony. This is so because the much greater volumes of N. Hemisphere ice can mask opposing melt-water trends in the interconnected southern oceans (Karlstrom 1966). Interhemispheric correlation of glaciations remain uncertain (Clapperton and others 1992). However, their B/C and C/D morainal complexes, as dated between 46,000-, 25,000-years and the present, most closely correlate with the local southern precessional trends which are displaced 10,000 years from their N. Hemisphere counterparts. The classic N. Hemisphere "Little Ice Age" is evidently absent in southern low- and middle-latitudes because of opposite precessional trends. Insolation curves after Milankovitch (1941).

Clue Search # 2—Depositional, Tree-ring, and Historical Evidence for the Phase, Subphase and Event Cycles, Numerous cut-and-fill structures and partial exposures seriously restrict the use of conventional stratigraphic criteria in identifying and correlating alluvial depositional units within and between Southwest drainage lines. Time-frequency analysis of many directly dated buried soils and associated buried trees and archaeological sites was therefore required to satisfy the critical question of parallel or random depositional histories within the region (Karlstrom and others 1976, 1988; Euler and others 1979).

As shown in Figure 5, these alluvial basal contacts (dated by radiocarbon confirmed by associated internally consistent archaeological and tree-ring derived dates) strongly cluster in phase with the Phase and Subphase Cycles—as well as with basal-contact clustering in other regions, including data sets selected by other researchers. The regional history of climate-environmental change inferred from this depositional record has been strikingly replicated by half-cycle smoothing of tree-ring evidence (Figures 6 and 7), and more recently independently by other Southwest researchers (Force and Howell, in press: Grissino-Mayer, in press)

The tree-ring thermograph record of Germany (Figure 8) and the historically dated temperature record of Iceland (Figure 9) phase remarkably well with the same Subphase Cycle; the late-postglacial warmer intervals of Europe coincide with Southwest drought intervals centered ca. AD 900, 1150, 1450 and 1700. These correlations thus strongly suggest that atmospheric circulation patterns in the North Atlantic were responding to the same tidal resonance system as that which evidently modulated circulation patterns along the southwest coast of North America (see Figure 18 below).

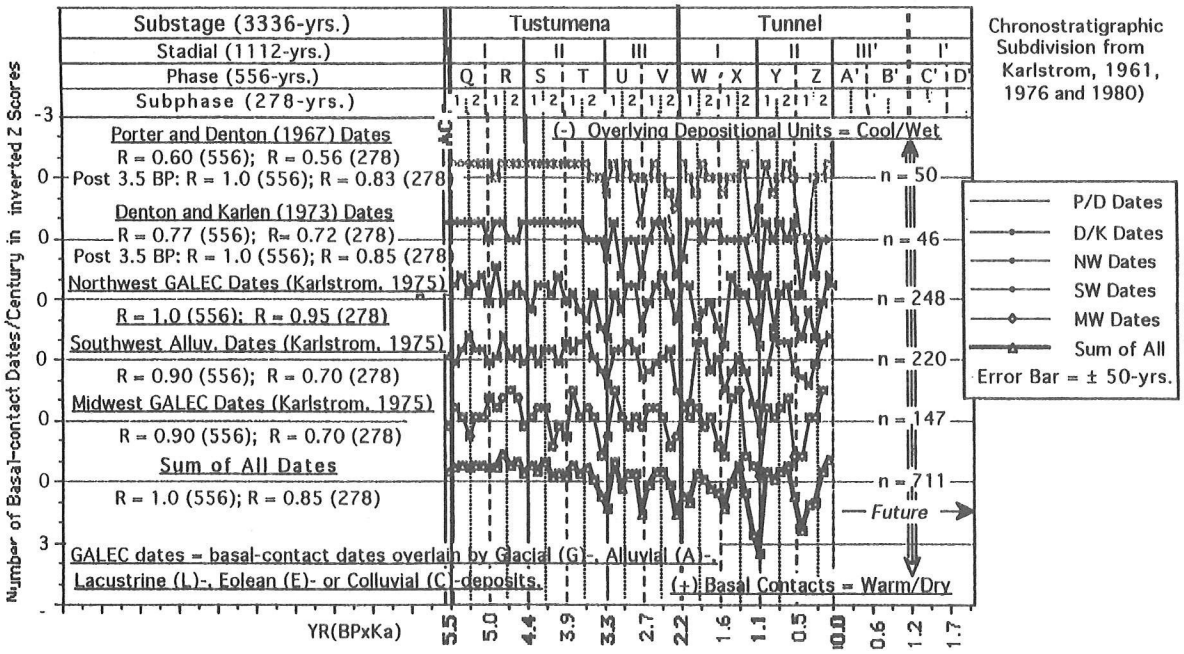

Figure 5 Summary of time-frequency analysis of basal-contact dates from North America plotted pre century on timescale of the 556-yr. phase cycle and its 2/1 (278-yr.) resonance. Summary of time-frequency analysis of basal-contact dates from North America plotted per century on timescale of the 556-yr. Phase Cycle and its 2/1 (278-yr.) resonance. The author's data is largely from Radiocarbon 1-15 and selected according to the following simple criteria: Samples of wood and organic carbon clearly described as collected from basal contacts. Many published dates are excluded because of unusually large counting errors, or because the dated materials (carbonates, bone, and humics) are more likely to be contaminated by older or younger carbon. Porter and Denton's (1967) and Denton and Karlen's (1973) independently selected glacial dates replicate the author's basal-contact analyses in confirming strong phasing with the 556-yr. Phase cycle, and lesser, but still significant, phasing with the 278-yr. Subphase Cycle. The Stratigraphic Commission (1983) defines basal-contact dates as chronostratigraphic Point Boundaries.

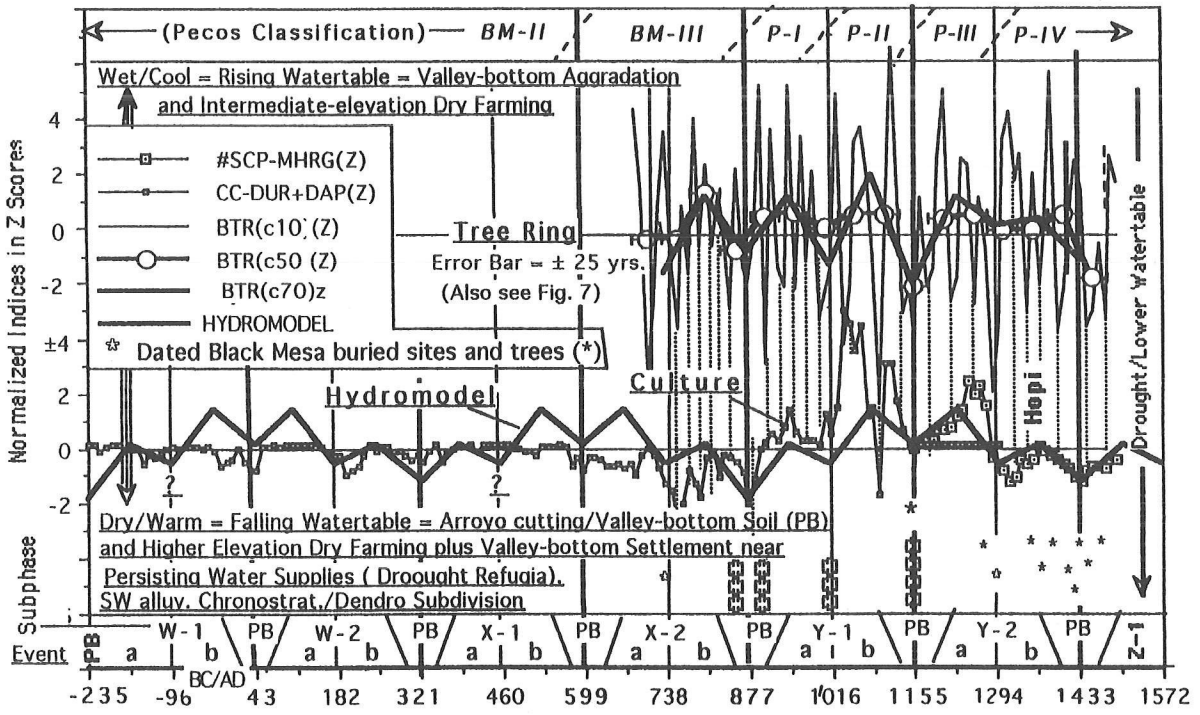

Figure 6 Colorado Plateaus hydrology. Dendroclimate and culture. Colorado Plateaus Hydrology, Dendroclimate and Culture on timescale of the 278-year Cycle and its 2/1 Event Resonance. Decadal tree-ring indices from Berry (1982); 50-yr. and half-cycle smoothing. Tree-ring- and radiocarbon-dated buried sites and trees and chronostratigraphic subdivision from Karlstrom (1976, 1988). PB=clustering of basal-contact dates. Tree-ring-dated surface sites from Euler and others (1979), Berry (1982) and Breternitz and others (1986). Note striking parallelisms between tree-ring and hydrologic records and number of dated sites (rough approximation of population size and movement). Culture designation: SCP=S. Colo. Plats. sites; MHRG=Mogollon Rim Sites; CC=Chaco Canyon sites; DUR=Durango sites; DAP=Dolores Achaeol. Project sites. To satisfy the paleoclimatic equation, higher elevation sites as potential drought indicators are subtracted from the intermediate elev. sites (SCP and CC); (+) scores=predominantly intermed.-elev. sites; (-) scores=predom. higher elev. sites.

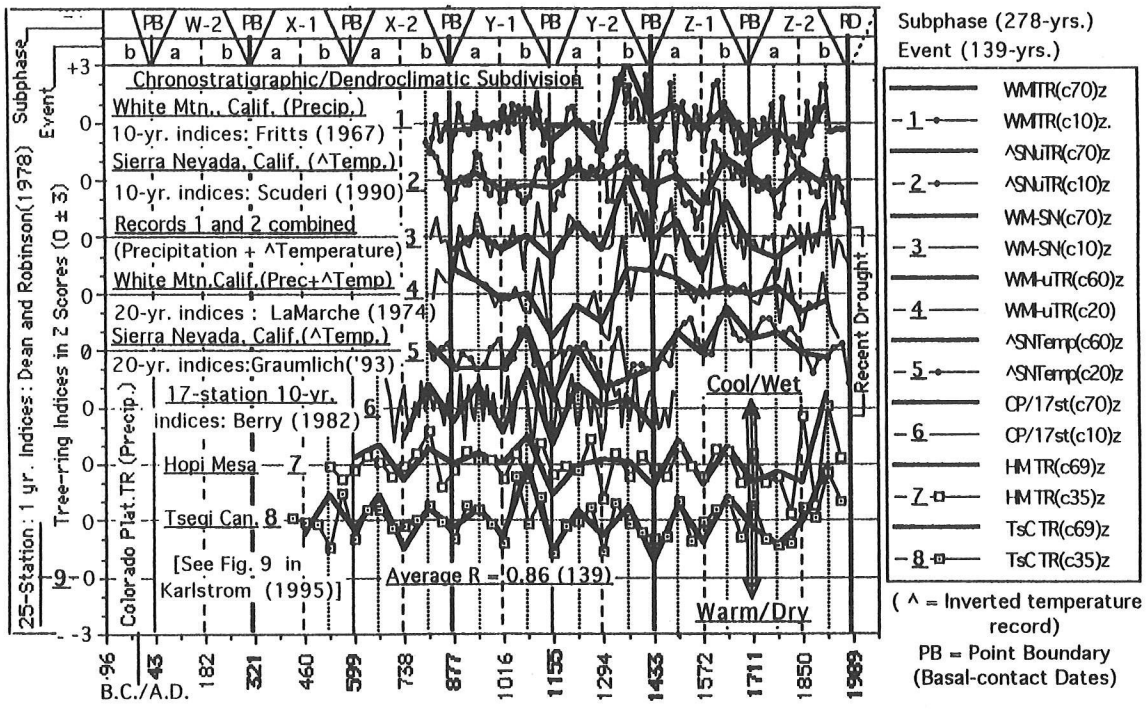

Figure 7 Southwest tree-ring records and the 139-year event cycle. Southwest Tree-ring Cycle in phase with the 2/1 (139-yr.) resonance of the 278-year Subphase Cycle. Half-cycle smoothing centered on turning points of the theoretical 2/1 resonance. Correlation of both precipitation and temperature range from 0.75 to > 0.90, or within the correlation range (< 0.60- >0.90) of published tree-ring/climate calibrations. This strongly suggests that the cycle is real, regionally robust and evidently related to changing regional atmospheric circulation patterns. Similar half-cycle analyses of other records define differing regional patterns (Karlstrom 1999) which should provide clues toward enhanced understanding of atmospheric dynamics and biologic response. Figure modified from Figure 10 in Karlstrom (1995).

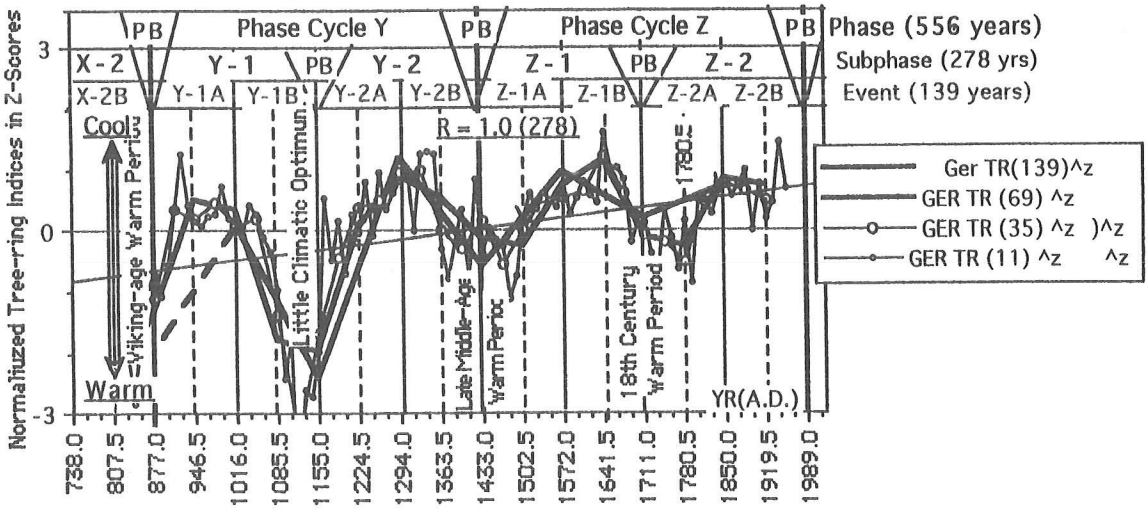

Figure 8 German tree-ring record and the 278-year subphase cycle. German tree-ring record on timescale of the 278-year Subphase Cycle and its 2/1 (139-yr.) and 4/1 110-year tree-ring indices from Ladurie (1972). Half-cycle smoothing positioned on resonance turning points. Plotted as a thermograph (inverted indices), the resulting record is strikingly similar to that derived historically for Iceland (Figure 9). Both show the same strong tendency to phase with the Subphase Cycle superposed on a general cooling trend since the 9th century. However, the abrupt trend in Iceland towards warming beginning in the 19th century is not present in Germany evidently because of a regime shift following AD 1711.

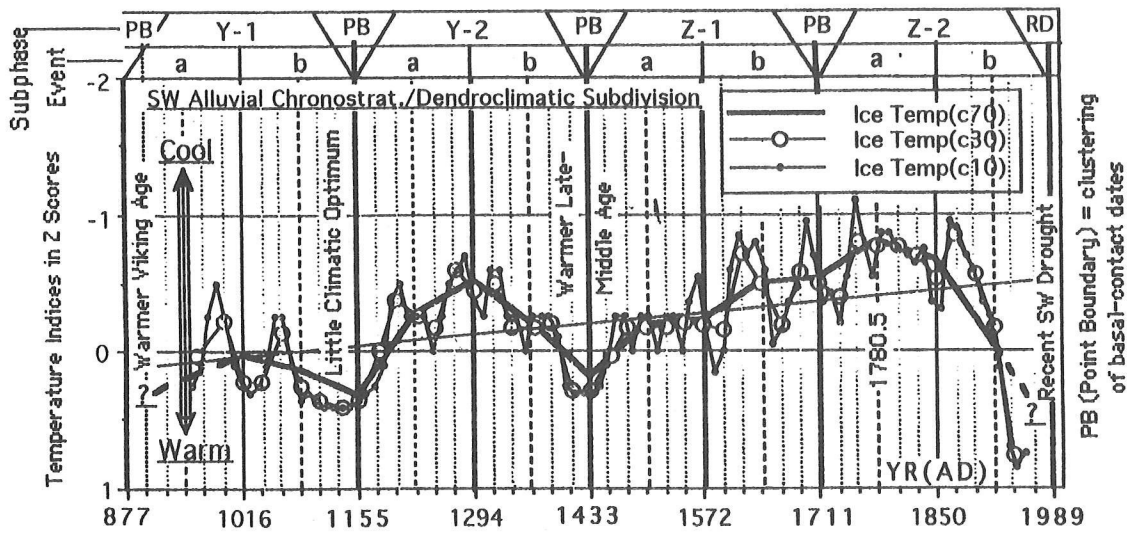

Figure 9 Iceland temperature record and the 278-year subphase cycle. Iceland temperature record on timescale of the 139-year event cycle and its 2/1 (69.5-yr.) and 6/1 (23.166-yr.) resonances. Ten-year temperature indices from Bergthorson (1969). Half-cycle smoothing as before. Note the strong tendency to oscillate in phase with the 278-year Subphase Cycle, and the lesser tendencies with the 139-year Event Cycle and its 2/1 (69.5-yr.) and 6/1 (23.17-yr.) resonances. These oscillations are superposed on a general cooling trend between the 9th and early 19th centuries, at which point there ensues a marked warming trend to present. The Medieval Warm Period (MWP), placed between AD 900 and 1300 by Lamb (1977), includes several shorter warmer intervals recorded in this and other records from Europe (see Figure 7) and variously named by other researchers. General agreement of the Iceland temperature record with SW alluvial subdivision, and the Resonance Climate Model is as remarkable as is the parallelisms with the Sunspot Cycle (Figure 10).

Clue Search #3—Volcanism as a primary or strictly a secondary factor in Climatic Change. Time-frequency analyses of radiocarbon-dated volcanic deposits and other time-series correlations indicate increased volcanic activity coincident at centennial and millennial scales with warmer/drier climatic intervals which in turn pace with the Phase and Subphase Cycles (Figure 10). The sulfuric acid indices of the Crete, Greenland ice core (interpreted as reflecting increased levels of volcanic activity,) may also correlate more directly at the decadal scale with historically recorded retreatal phases (inferred warm/dry) in the longest glacial records available from the Swiss Alps (Figure 11). These longer term correlations thus appear consistent with the historic evidence of the restrictively short cooling effects (several years at most) of ash and aerosols following major eruptions (Rampton and Self 1981). In addition, they support the dynamic concept that climate and volcanism are commonly modulated or triggered by tidal forces acting in consort on both atmosphere and lithosphere. Equally remarkable is the parallelism of the Crete acid record with both tidal-force resonances and the sunspot length record as shown in Figure 12.

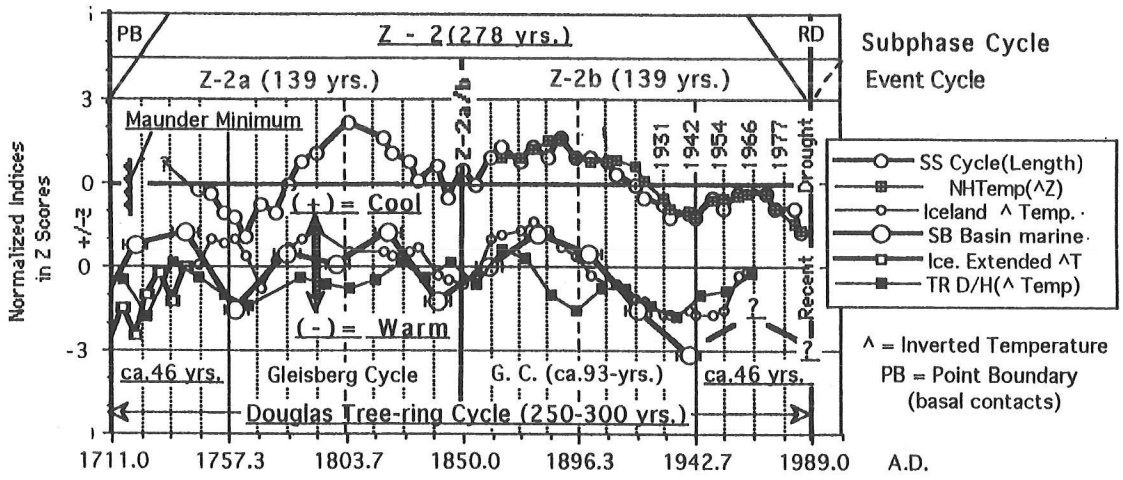

Figure 10 Sunspot length, climate records and the 139-year event cycle. Sunspot and Climate Records on timescale of the 139-year Event Cycle and its 3/1 (46.3) and 12/1 (11.5-yr.) resonances. Sunspot, hemispheric temperature and Iceland indices to 1745 from Friss-Christensen and Lassen (1991); extension of Iceland temperature record from Bergthorsen (1969); and Yap (1976). Sunspots and collated climatic records appear to be related to the Tidal Resonance Model through in-phase relations with the ca. 46-year Resonance and its double Gleissberg Sunspot Cycle. Poorer tendency for Sunspots and higher resolution climate records to oscillate in phase with the ca. 11-yr. Sunspot resonance. In the literature the Gleissberg Cycle has been variously dated between 78- and 100-yrs. The above evidence suggests it lies closer to 90 years. See Figure 12 for another parallel paleoclimatic record. From Figure 5 in Karlstrom (1996).

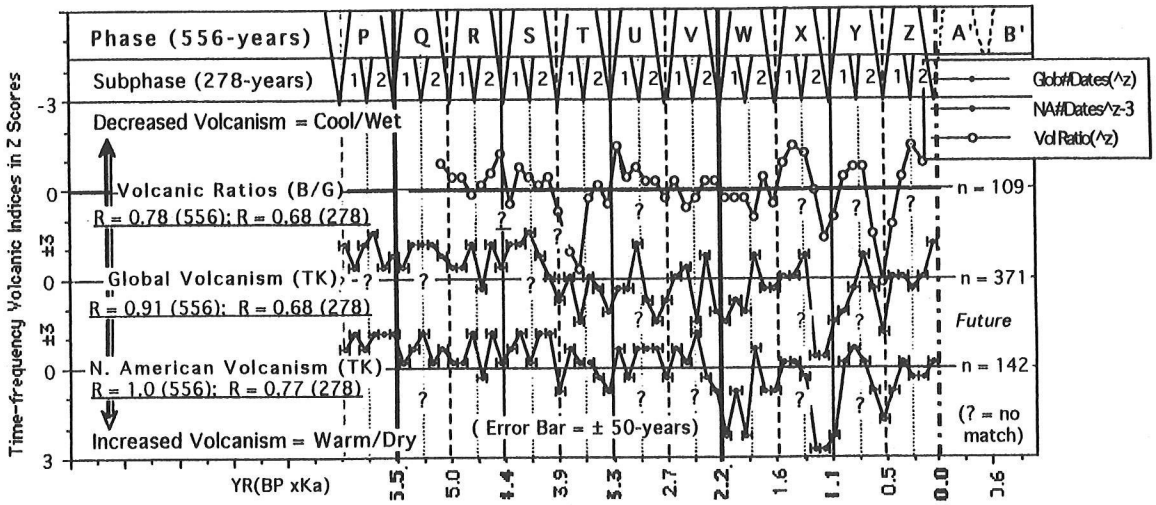

Figure 11 Volcanic time frequencies and the phase and subphase cycles. Time-frequency diagrams of global and North American Volcanic activity on timescale of the 556-year Phase Cycle and its 2/1 (278-yr.) resonance. Volcanic ratio indices from Bryson and Goodman (1980); number indices from Karlstrom (1975). Centered 100-year class intervals act as low-pass filter restricting analyses to cycles with wavelengths of more than 200 years. Note the strong tendency for clustering in phase with the Phase Cycle and the lesser, but still positive, tendencies to phase with the Subphase Cycle. The consistency of results from independently selected data sets strongly suggest that tidal resonances may play a significant role in triggering volcanic activity. However, the generally positive correlation of increased volcanism with the warm/dry epicycles minimizes the importance of transitory atmospheric cooling by volcanic ejecta and aerosols as a significant causal factor in these longer term climatic changes. Nonetheless, to predict future volcanic events solely by tidal intensity is highly uncertain because of the statistical nature of the correlation, and because the required triggering mechanism involves endogenetic threshold conditions that can vary appreciably from one volcanic center to another. Figure from Figure 6 in Karlstrom (1998).

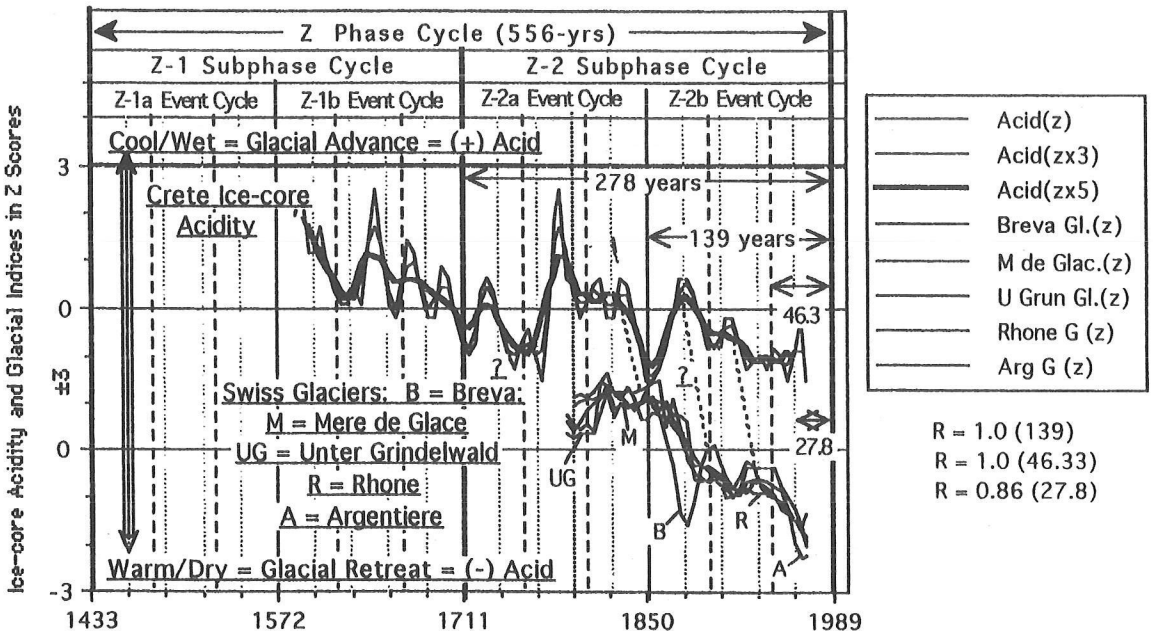

Figure 12 Greenland acidity, glacial oscillations, tidal resonances and sunspots. Crete, Greenland ice-core record of acid (volcanism), and Swiss Glaciers on timescale of the 139-year Event Cycle and its 3/1 (46.33-yr.) and 5/1 (27.8-yr.) resonances. Indices of ice-core acidity and glacial records replotted from Figures 1 and 2 in Porter (1981). Note: (1) that the interpretation of acidity as a proxy for volcanism and correlation of increased volcanic aerosols with glacial advances requires a ca. 10-year response lag (marked by dashed black lines in the figure); and (2) the remarkably clear correlation, not previously noted, of the direct phasing of Greenland Acidity with the Event Cycle and its 3/1 and 5/1 resonances, and with intervals of low acidity phasing with tree-ring-defined SW droughts (Figure 7). The Crete acidity record with its ca. 46-year phasing can now be added to Figure 10, fortifying the impression of common linkages with both tidal resonances and solar (sunspot) processes. The possible presence of the 27.8-yr. Cycle in other records requires additional half-cycle analyses after appropriate smoothing.

Clue Search #4—The ca. 11-year and 22-year Sunspot Cycles, Tidal Resonances, and possible climatic effects. Following World War I, extensive research on weather cycles resulted in cycles with so many different wavelengths that meteorologists rejected most either as products of noise or as procedural artifacts. A few cycles, however, appeared to be valid and worldwide in distribution (De Boer, 1968). These include correlatives of the single and double Hale Sunspot Cycles (ca. 11.12 and 22.24 years respectively) along with the 2/1 resonance of 5.56 years, the 4/1 resonance of 2.75 years and the 5/1 resonance of 2.22 years. Burroughs (1992) interprets the following as the best documented of the more recently defined climate cycles: ca. 2-3 year cycle, ca. 5-7 year cycle, ca. 11.1 year cycle (the equivalent of the fundamental sunspot cycle); the ca. 20-years cycle (which because of power-spectral imprecision could represent either or both of the nodal tidal-force cycle of 18.61 years and the double [Hale] Sunspot cycle of 22.24 years); the ca. 80-90 year cycle (presumably the climate equivalent of the ca. 90-year solar Gleisberg Cycle: see Figure 12) and a roughly 200-year cycle that may be the equivalent of the x 2 (180-year) cycle generated by displacement of the solar system's baricenter relative to the heliocenter.

As shown in Figure 13 the average sunspot cycle of 11.12 years is precisely the 25/1 resonance of the Subphase Cycle (with synchpoint at AD 1711) which phases very strongly with sunspot numbers—excepting the apparent abrupt phase shifts near AD 1780 and 1989. My previous correlation (Karlstrom 1998) of Sunspot number with the 24/1 resonance (11.583-yrs.) now appears less valid than that of the 25/1 resonance, although analysis of longer records is needed to verify this fine distinction.

Figures 14-17 provide examples of climatic records that appear to directly link climate with both Sunspots and Tidal Resonances. Figure 14 includes Michell and others (1979) tree-ring record of Midwest droughts and my composite (24 station) tree-ring record of the Colorado Plateaus. The Midwest record shows a very strong tendency to phase with the Hale Sunspot Cycle; the Colorado Plateaus record reflects a somewhat lesser tendency to do so. The Midwest record as first analyzed did not support the presence of the Nodal Tidal-force Cycle of 18.61 years amply evident in many Midwest climate records (Currie 1981 cf.) More refined analysis indicates, however, that this cycle is also present in the tree-ring record but masked by a phase reversal ca. AD 1780, which reversal completely canceled out its power-spectral signal (Burroughs 1992). The reversal coincides with a drought-turning point of the ca 70-year Subevent Cycle (See Figure 15 in Karlstrom 1999), which in turn is expressed in global temperatures and in the beach-ridge sequence of northern Lake Michigan(Delcourt and others 1996) and as wet/dry oscillations in China (Quan and Zhu 2002). Equally significant, the reversal is also concurrent with phase reversals in the Sunspot record (Figure 13) enhancing the impression of cause-effect relations in a complex non-linear dynamic system.

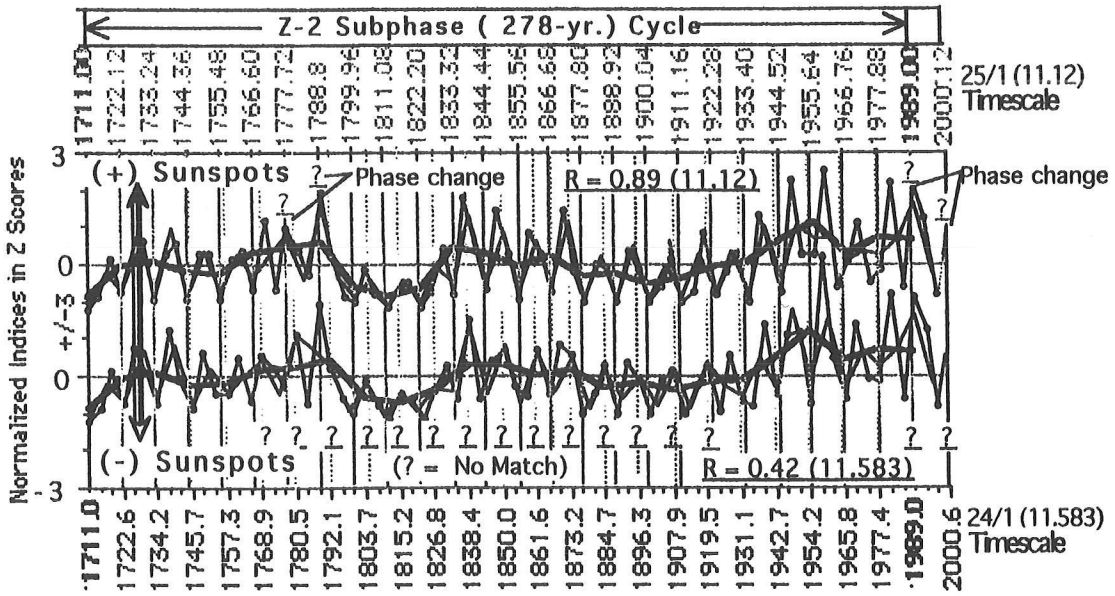

Figure 13 Sunspot numbers and the resonances of the subphase cycle. Sunspot record on timescales of the 24/1 (11.583-yr.) and 25/1 (11.12-yr.) resonances of the 278-year Subphase Cycle. Annual sunspot indices from NOAA, half-cycle smoothed by their 1/1 (ca. 11-yrs.), 2/1 (ca. 5-yr.) and 3/1 (ca. 3-yrs.) subharmonics and positioned according to their differing timescales. Note that the average solar cycle of 11.12-years strongly phases with the 25/1 resonance–except for the abrupt 180°-phase changes near 1780 and 1989. On the other hand, the 24/1 wavelength appears slightly too long as reflected in the increasing divergence in timing towards the middle of the fundamental cycle and the progressive convergence towards beginning and end. Note that at the level of detailed analysis, correlation results are highly sensitive to minor difference in cycle length.

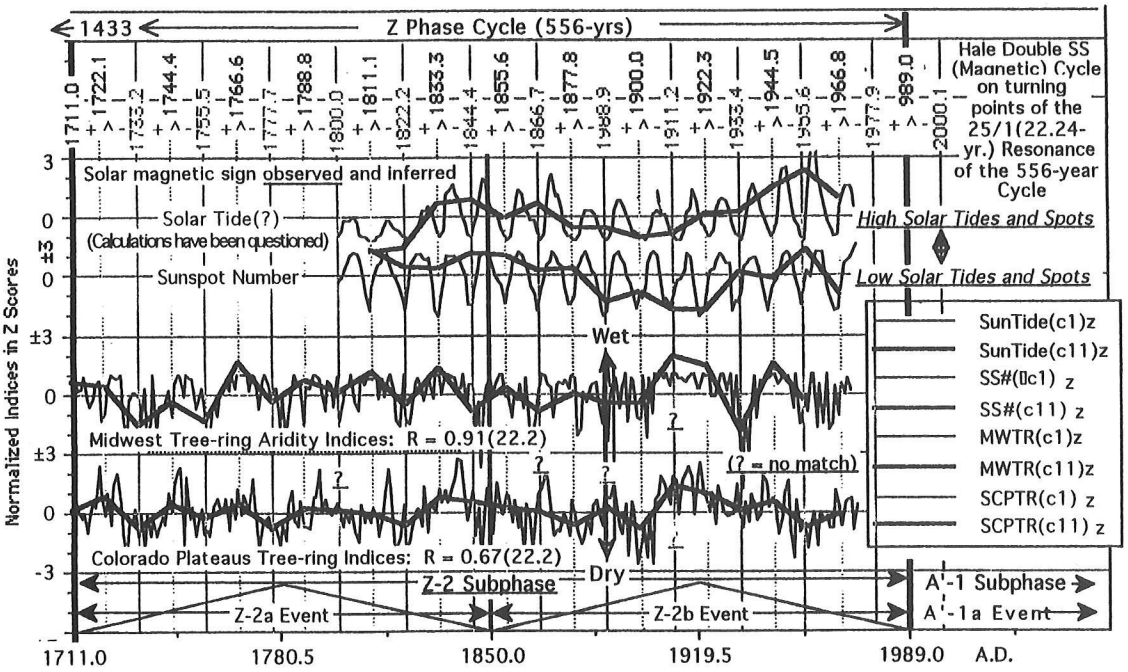

Figure 14 Tree-ring records and the 22.24-year Hale Sunspot Cycle. Solar tides, sunspots, and dendroclimatic records on timescale of the 2/1 (278-yr.), 4/1 (139-yr.) and 25/1 (22.24-yr.). Resonances of the 556-year phase cycle. Annual indices of sunspots and solar tides from Wood in Gribbin (1976); of Midwest tree-ring indices from Michell and others (1979) in Burroughs (1992); and of Colorado Plateaus tree-ring indices from Dean and Robinson (1978). Half-cycle smoothing on turning points of the 25/1 (22.24-yr.). Resonance that is in phase with the average Hale Double Sunspot (magnetic) Cycle. This, in turn, seemingly integrates solar/earth tidal phases with terrestrial climate through solar magnetic change (+ solar magnetism=generally increased earth rainfall).

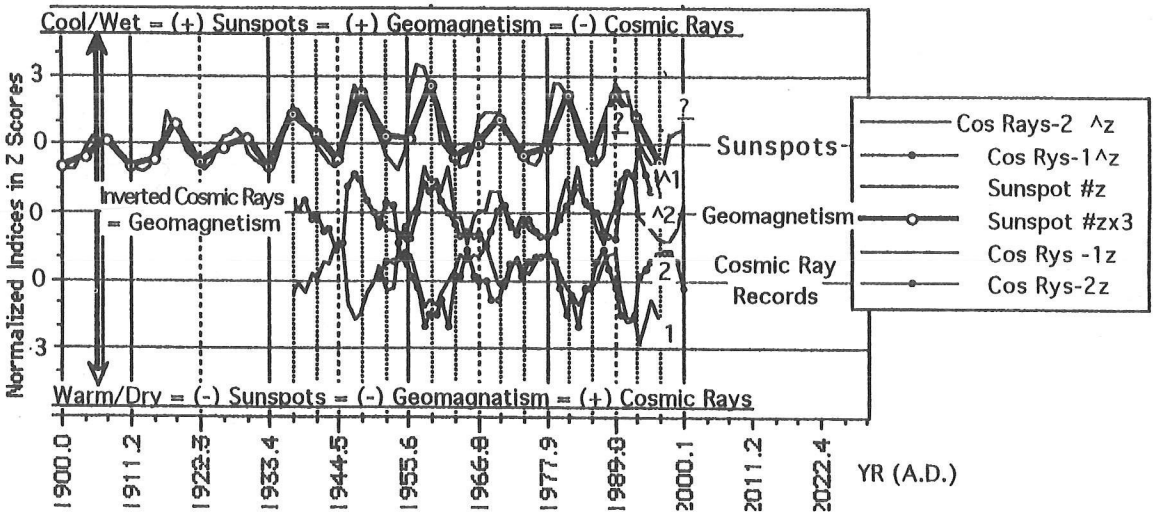

Figure 15 Cosmic rays, geomagnetism, sunspots and the 11.12-year tidal resonance. Sunspots, cosmic rays and geomagnetism on timescale of the 25/1 (11.12-yrs.). Resonance of the Subphase Cycle and its 3/1 (3.7-yrs.) subharmonic indices of suspots and two records of cosmic rays from Mercurio (2001). Note: (1) the strong negative correlation of cosmic rays with sunspot numbers, and therefore, in turn, the resulting positive correlation with the controlling variable geomagnetic field; and (2) the strong tendency for the cosmic ray records, but not the sunspots, to phase with the 3/1 resonance suggesting the superposed influence of tidal resonances on the geomagnetic field and terrestrial climate.

As shown in Figure 15, the single Sunspot Cycle is negatively correlated with Cosmic Rays and Tidal Forces but positively with Geomagnetism. Thus according to my paleoclimatic equation: Cool/Wet Climate = decreased Tidal Force = increased Sunspot numbers = increased Geomagnetism = decreased Cosmic Rays. These correlations implicate direct physical linkages between climate and solar processes evidently acting through changes in Tidal Force and Geomagnetic fields at the decadal level.

Figure 16 shows correlation between Sunspots and Langbein and Slacks (1980) U.S. and regional runoff records. Beyond expectable regional variability, the Western, Central, and Eastern records and their U.S. composite show strong phasing with the Hale Sunspot Cycle. All the records also show interrupted series of the 7.42-year subharmonic which is alternately in and out of phase with the 11.12-yr. Sunspot Cycle, thus accentuating the double Hale Cycle. The ca. 7-year cycle, however, is not evident in the Sunspot record pointing to its terrestrial genesis as a function of tidal dynamics. Significantly, this cycle is also the expected beat product of a modulating 22- and 11-year Sunspot combination (Burroughs 1992), emphasizing in turn its possible solar connection.

Figure 17 compares the runoff records of the Southwest and Northwest regions of the American West relative to the Sunspot Cycle. Whereas Southwest runoff strongly phases with the magnetic sign of the Hale Cycle (+ solar magnetism = increased runoff), Northwest runoff primarily shows opposite responses with (+) solar magnetism coinciding with intervals of decreased runoff. Whereas runoff in the eastern and central regions of the U.S. is primarily in phase with Southwest runoff, that of the Northwest is largely out of phase. This strong tendency for anti phasing evidently reflects dominating northerly atmospheric sources (the Aleutian Low) for the Northwest, whereas the rest of the country

lies largely in the path of moisture-bearing southwesterly storm tracks generated over the Pacific Ocean to the south (See Figure 18 below).

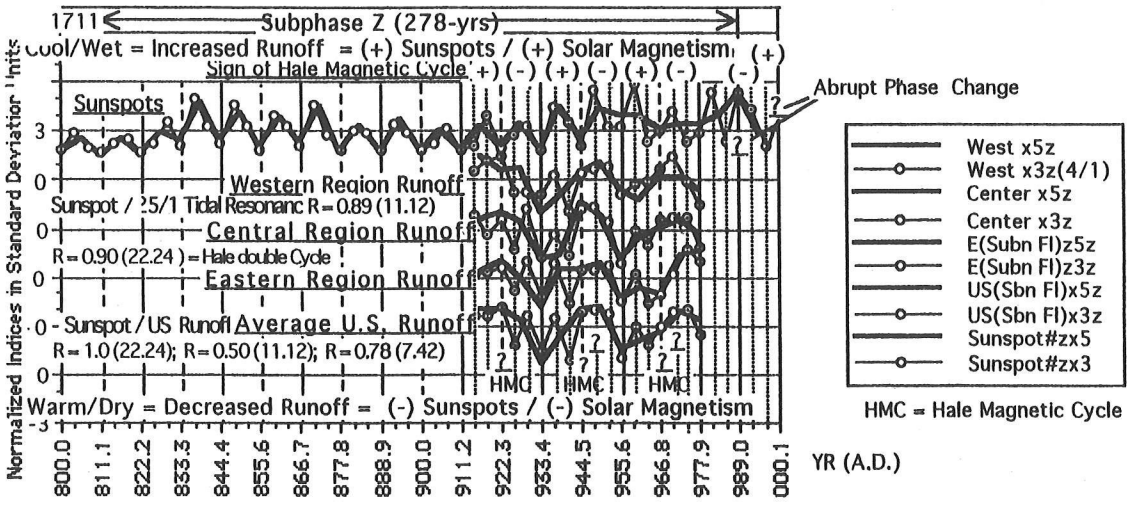

Figure 16 U.S. and regional runoff, sunspots and the 7.42-year tidal beat cycle. U.S. runoff and susnpot records on timescale of the 25/1 (11.12-yr.) resonance of the 278-year subphase cycle and its 2/1 (5.56-yr.) and 3/1 (3.71-yr.) resonances. Sunspot indices from NOAA; runoff indices from Langbein and Slack (1980). Half-cycle smoothing positioned on turning points of the 2/1 and 3/1 subharmonics of the average sunspot wavelength. Beyond expected levels of regional variabilities, note that the runoff records phase most strongly with the Hale double sunspot cycle and thus also with subharmonics of the Subphase cycle with syncpoint at 1711. Note further that all runoff records are dominated by a 7.42-year cycle which is alternately in- and out-of-phase with the 11-year cycle thus accentuating the double Hale Cycle. Significantly, the ca. 7-year cycle evidently is not part of the sunspot record suggesting that its genesis is strictly a product of resonance response within the terrestrial environment. Equally significant is the fact that a ca. 7-year cycle is the expected beat product of a modulating 22- and 11-year sunspot-cycle combination (Burroughs 1992).

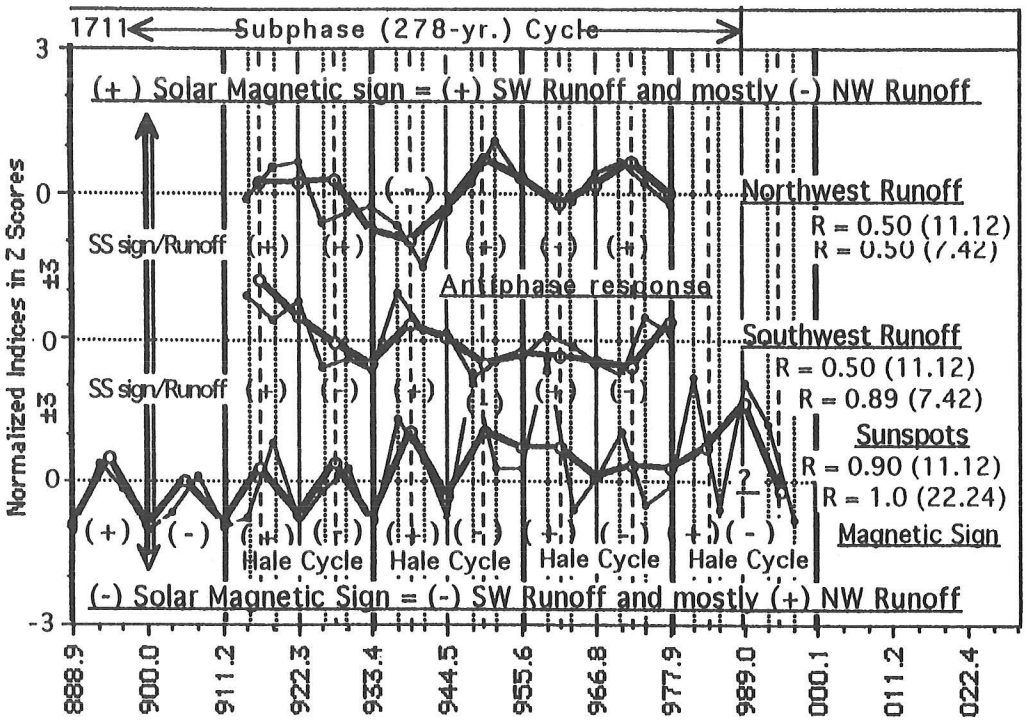

Figure 17 Sunspots and Northwest and Southwest runoff records on timescale of the 25/1 (11.12-year). Sunspots and Northwest and Southwest Runoff records on timescale of the 25/1 (11.12-yr.) resonance of the Subphase Cycle and its 2/1 (5.56-yr.) and 3/1 (3.71-yr.) resonances. Annual indices from Langbein and Slack (1982); annual sunspot indices from NOAA. Half-cycle smoothing on turning points of the 2/1 and 3/1 resonances. Note the strong tendency for Southwest flow to phase positively with the magnetic sign of the 22.24-year Hale Cycle, whereas Northwest flow tends to respond negatively

Clue Search #5—Aleutian Low Pressure, Sunspots and Climate. The Aleutian Low, and its counterpart, the Icelandic Low in the North Atlantic, dominate northern latitude atmospheric circulation which in turn steers the jet streams and the episodic excursions of polar and Arctic air southward. Thus, because of proximity, Northwest climate should most directly reflect Aleutian Low pressure changes whereas Southwest climate should primarily reflect anti phasing (see-saw) relations. As shown in Figure 18, this expectation is evidently realized. Despite strong phasing with both the single and double Sunspot Cycles, runs of the 7.42-year beat cycle in the Northwest show strong anti-phasing relative to those of the Southwest. In the Southwest, the beat cycle is in phase with the Hale Cycle, but in the Northwest it primarily oscillates out of phase with this cycle. Interruptions of the beat cycle in the pressure record thus occur where it is dominated by the opposing turning points of the longer Hale Cycle excepting, however, where it in turn dominates at ca AD 1977. Whether these response differences result from superposition of additional cycles, noise, non-linearity or other factors is not definable from the presented short records. These records, however, do strongly suggest general see-saw effects between separate pressure centers in the Pacific comparable to those associated with the Icelandic Low/Azores High in the Atlantic. It is perhaps significant that other researchers note AD 1977 as a regime shift in other types of climate records.

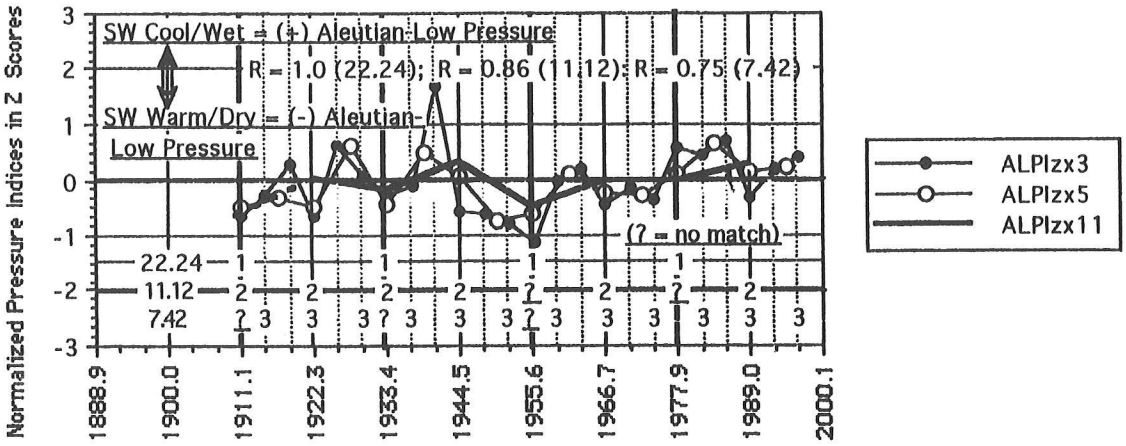

Figure 18 Aleutian low-pressure indices, sunspot cycles and the 7.4-year beat cycle. Aleutian-Low Pressure Indices on timescale of the 25/1 (11.12-yrs.). Resonance of the Subphase Cycle and its 2/1 (5.56-yr.) and 3/1 (3.71-yr.) resonances. Annual pressure indices from (Overland and others 1998) half-cycle smoothed and positioned on turning points of the 1/1, 2/1 and 3/1 resonances. Note: (1) The respectively strong to very strong phasing with the single and double sunspot cycles, strongly suggesting a direct linkage between Solar processes and Aleutian-Low pressure changes, and thus in turn with changing West Coast atmospheric circulation patterns and resulting climates; and (2) the interrupted phasing with the 7.42 beat resonance, which, in contrast to most runoff records, is in phase with the single rather than the double Hale sunspot cycle. Interruptions in the beat series generally occur at turning points where dominated by the ca. 22-year cycle except at 1977 where it dominates. The absence of the beat cycle in the sunspot record, and its antiphasing in different records reemphasize its generation in the terrestrial atmosphere and introduces compoundities in understanding its regional and/or process responses.

Summary and Conclusions

The presented data provide the following empirical clues to underlying processes and dynamics of Climatic Change:

1. Upper latitude Ice-age glaciations in both Hemispheres, along with Cosmic Rays and Geomagnetism, were evidently modulated by summer half-year insolation dominated by the ca. 40,000-year Obliquity Cycle. On the other hand, glaciations and associated climatic changes in middle to lower latitudes evidently paralleled the ca. 20,000-year Precessional Cycle characterized instead by opposing trends across the Equator;

2. The pervasive secondary oscillations recorded in most instrumental and paleoclimatic records reflect in part a complex system of globally synchronous harmonic tidal-force resonances that in the recognizably complex non-linear system of climatic change episodically undergo abrupt phase changes. These abrupt reversals result in interrupted series, or runs, of quasi-periodic cycles so typical of the climatic record. Parenthetically, these reversals (referred to as regime shifts by others) can seriously compromise the results of power-spectral analyses which assume consistent phase relations. Other limitations in defining cycles from power-spectral analyses are noted by DeBoer (1967) and by Burroughs (1992);

3. Correlation with both tidal force and sunspots implicates both tidal force and solar process as modulators for yearly, decadal and centennial climatic changes. Correlation with Cosmic Rays

and Geomagnetism strongly suggest that this integrated tidal and solar modulation involves, or directs, critical energy changes in the geomagnetic and atmospheric fields;

4. The combined data zero in on orbital perturbations of the solar system (varying both tidal force and insolation) as the operational energy system within which past climatic, volcanic and geomagnetic changes have been concurrently modulated or triggered (with occasional non-linear phase reversals) at yearly, decadal, centennial and millenial scales; and

5. The developing picture of the many natural variables underlying climatic change in effect severely restricts the validity of simply projecting average temperature trends of the past 200 or so years into the future as the sole product of man-produced "Greenhouse Gases". The temporary trend towards cooling in the instrumental temperature record between AD 1940 and 1950 and the repeated pre-Industrial Revolution oscillations between distinctly warmer and cooler climate cannot be explained by man's sporadic pollution of the atmosphere, but must instead be related to naturally induced changes in the terrestrial environment. One of the important tasks of the future is to quantitize anthropomorphic inputs versus natural inputs to the climatic changes of the past 200 years.

It is encouraging to recognize that major developments in understanding the physical world have been anticipated through empirical data long before the geophysics of underlying causal factors were fully appreciated. Three excellent examples come to mind: (1) Wegener's and Taylor's empirically derived Continental Drift Model which long anticipated developments in oceanography relating to mid-oceanic spreading centers, magnetic reversal patterns and Plate Tectonic mechanisms; (2) photogeologic interpretation of the moon suggesting volcanic episodes (subsequently described from petrologic evidence as deep Magma Oceans) during pre-Mare highland phases of lunar development (Green 1967; Karlstrom 1972). Such early lunar volcanism was essentially excluded by Urey's elegantly simple mathematical model of the moon's figure which suggested instead an exclusively cold accretionary origin and, more specific for the thesis of this paper, (3) Lord Kelvin's authoritative but premature dismissal of sunspots and solar processes as a factor in climatic change based as it was on a too simplistic energy model that could not consider subsequently identified fundamental phenomena such as solar winds, the magnetosphere, geomagnetism, cosmic rays, tidal forces, feed-back or triggering responses, fractals and non-linearity.

To be sure, much work remains in refining our understanding of underlying physical linkages as well as of the dynamics of associated atmospheric circulation patterns resulting in characteristic regional variability. Nonetheless, significant clues are now available that should provide critical focus for further research, hopefully leading to the development of more sophisticated General Circulation Models (GCM) that incorporate the critical factors of cloud cover, geomagnetism, cosmic rays and tidal forcing. along with other definable natural changes such as in atmospheric CO_2, methane, and ozone.

Acknowledgements

Extension of my more than fifty years of paleoclimatic research beyond the boundaries of my own field observations in Alaska and the Southwest is dependent on the careful reconstruction of proxy and instrumental records by researchers working in other parts of the world. My appreciation is extended to all those whose records I have selected for cyclical analysis, particularly to those early

researchers who pushed their creativity beyond then accepted limits of conventional wisdom. I accept their time series as valid. I take full responsibility for any errors that may have crept into my extended interpretations.

References

Abbot CG. 1900-1954. Annals, Smithsonian Astrophysical Observatory 1-7.

Bago EP, Butler CJ. 2000. The influence of cosmic rays on terrestrial clouds and global warming. Astronomy and Geophysics 41:18-22.

Bergthorsen P. 1969. An estimate of drift ice and temperature in Iceland in 1000 years. Jour. of Jokull 19: 94-101.

Berry CA, Hsu KJ. 2000. Geophysical, archaeological, and historical evidence support a solar-output model for climate change. PNAS 97:12433-12438.

Berry MS. 1982. Time/Space and Transition in Anasazi Prehistory. Univ. of Utah Press, Salt Lake City, 147 pp.

Bloom AL and others. 1974. Quaternary sea level fluctuations on a tectonic coast: New $^{230}Th/^{234}U$ dates from the Huon peninsula, New Guinea. Quat. Research 4: 185-205.

Breternitz DA, Robinson CK, Gross GT. 1986. Dolores Archaeological Program: Final synthetic report. U.S. Department of the Interior, Bureau of Reclamation. Denver, CO. 900 pages.

Brier GW. 1967. Rainfall and lunar tides, p. 813-816 in Fairbridge RW, The Encyclopedia of Atmospheric Science and Astrogeology, Reinhold Publishing Corp. New York.

Bryson RA, Goodman BM. 1980. Volcanic activity and climatic changes, Science, 207:1041-1044.

Burroughs WJ. 1992. Weather Cycles: Real or Imagined? Cambridge University Press, London. 201 p.

Chuey JM, Rea DK, Pisias NG. 1987. Late Pleistocene Paleoclimatology of the central Equatorial Pacific: A quantitative record of eolian and carbonate deposition. Quat. Research 38:323-33.

Clapperton CM, Sudgen DE, Kaufman DS, McCulloch RD. 1995. The last glaciation in central Magellan Strait, southernmost Chile. Quat. Research 44:133-148.

Clough HW. 1905. Synchronous variations in solar and terrestrial phenomena: Astrophys. J. 22:42.

Currie RG. 1981. Evidence for 18.6 -year signal in temperature and drought conditions in North America since AD 1800. Journal of Geophysical Research, v. 86. p. 11.055-11.064.

Currie RG. 1982. Evidence for 18.6-year term in air pressure in Japan and geophysical implications. Royal Astronomical Society Geophysical Journal, v. 69, p. 321-327.

_____1984a. On bistable phasing of 18.6 year induced flood in India: Geophysical Research Letters, v. 11, p. 50-53.

_____1984b. Evidence for 18.6 year lunar nodal drought in western North America during the past millennium. Journal of Geophysical Research, v. 89, p. 1295-1308.

_____1984c. Periodic (18.6 year) and cyclic (11-year) induced drought and flood in western North America. Journal of Geophysical Research, v 89, n. D5, p. 7215-7230.

_____1987. Examples and implications of 18.6- and 11-yr terms in world weather records. Chap. 22, p. 378-408 In Rampino, M. R., Sanders, J. E., Newman, W. S.; and Konigsson, L. K., eds. Climate: History, periodicity, and predictability: International Symposium held in Barnard College, Colunbia Univerisity, New York, New York. 21-23 May 1984 (R. W. Fairbridge Festschrift) New York, NY, Van Nostrand Reinhold Publishing Corp. 588p.

_____1992, Deterministic signals in height of sea level world-wide. In Smith, C. R. eal. (eds) Maximum Entropy and Bayesian Methods: Dordrecht, the Netherlandsk Klumer Academic Press, pp. 403-621.

_____1994, Luni-solar 18.6- and 10-11-year solar cycle signals in H. H. Lamb's dust veil index: International Journal of Climatology v. 14, p. 215-226.

_____1995, Variance contribution of Mn and Sc signals to Nile River data over a 30.8-year bandwidth. p. 29-38 in Finkl, C. W., Jr., ed, Holocene cycles: Climate, sea levels and sedimentation, A Jubilee Volume in celebration of the 80th birthday of Rhodes W. Fairbridge: Journal of Coastal Research Special Issue No. 17, 402 p.

Currie RB, Fairbridge RW. 1985, Periodic 18.6-year and cyclic 11-year induced drought and flood in north-eastern China, and some global implications: Quaternary Science Reviews, v. 4, no. 2 p 109-134.

Currie RB, Wyatt T, O'Brien DP. 1993. Deterministic signals in European fish catches, wine harvests, sea level, and further experiments; International Journal of Climatology, v. 8, p. 255-281.

Dean JS, Robinson W J. 1978. Expanded tree-ring chronologies for the Southwest United States. Chronology Series III, Laboratory of Tree-ring Research. Univ. of Arizona, Tucson, 5

De Boer HJ. 1967. Meteorological Cycles, p. 564-571, in Rhodes Fairbridge, ed., The encyclopedia of atmospheric sciences and astrogeology, Reinhold Publishing Corp. New York.

Delcourt PA, Petty WH, Delcourt HR. 1996. Late-Holocene formation of Lake Michigan beach ridges correlated with a 70-year oscillation in global climate. Quat. Research 45: 321-326

Denton GH, Karlen W. 1973. Late Pleistocene climatic variations–their pattern and possible causes. Quat. Research 3:155-205

Dreimanis A. 1971. The last ice age in the eastern Great Lakes region, North America, in Ters, M. editor, Etudes Sur le Quatinaire dans le, monde: Paris Proc. 8th INQUA Congress, 1:69-75

Douglas AE. 1919, 1928, 1936. Climatic cycles and tree growth, Carngie Instit. Wash. Publ. 289 I,II,III)

Epstein S, Yapp CI. 1976. Climatic implications of the D/H ratio of hydrogen in C/H groups in tree cellulose. Earth Planet. Sci. Letters 30:252-266.

Euler RC, Gumerman GJ, Karlstrom TNV, Dean JS, Hevly RH. 1979. The Colorado Plateaus: cultural dynamics and paleoenvironment. Science 205: 1089-1101

Fairbridge RW. 1967. Ice-age Theory, p. 462-474 in Fairbridge, R. W., The Encyclopedia of Atmospheric Sciences and Astrogeology: Reinhold Publishing Corp. New York, NY.

_____1990, Solar and lunar cycles embedded in the El Nino periodicity's. Cycles, v. 41 (2) 66-72.

Force EL, Howell W. In press. Holocene depositional history and Anasazi occupation of McElma Canyon, Southwestern Colorado, Arizona State Museum Archaeological Series

Friis-Christensen E, Lassen K. 1991, Length of solar cycle: An indicator of solar activity closely associated with climate. Science 254:698-700

Fritts HC. 1963. Tree-ring Analysis (Dendroclimatology). Pages 1008-1026 in The Encyclopedia of Atmospheric Sciences and Astrogeology. Rhodes W. Fairbridge, editor. Reinhold Publishing Corp. New York

Graumlisch LJ. 1992. A 1000-year record of climatic variability in the Sierra Nevada, California: Handout. Am. Quat. Assoc. 12th Biennial Meeting, Aug. 24-26. Univ. of Calif., Davis

Green J. 1967. Moon-Lunar Geology p.623-629 in Fairbridge R. W., Editer, The Encyclopaedia of Atmospheric Sciences and Astrogeology. Reinhold Publishing Corp.

Grissino-Mayer HD. In press. A 2129-Year Annual Record of Drought for Northwestern New Mexico, U.S. A. Tree-Rings, Environment and Humanity;. J. S. Dean,, D., Mako and T. W. Swetman, editors. Proceedings of the International Conference, Tucson, Arizona, 17-21, May, 1994. Radiocarbon,

Karabanov EB, Prokopenko AA, Williams DF, Colman SM. 1998. Evidence from Lake Baikal for Siberian Glaciation during Oxygen-isotope Substage 5d. Quat. Research 50:46-55

Karlstrom TNV. 1955. Late Pleistocene and recent glacial chronology of Southcentral Alaska: Geol. Soc. of America Bull. 66:1581-1582

_____1956. The problem of the cochrane in late Pleistocene chronology. U.S. Geol. Survey Bull. 1021J: 303-333.

_____1961. The glacial history of Alaska: Its bearing on paleoclimatic theory. Annals New York Academy of Science 95(l): 290-340

_____1964. Quaternary geology of the Kenai Lowland and glacial history of the Cook Inlet Region, Alaska. U.S. Geological Survey Professional Paper 443: 69 pp.

_____1966. Quaternary glacial record of the North Pacific Region and worldwide climatic change, pp. 153-182, in Pleistocene and Post-pleistocene climatic variations in the Pacific Area. D. J. Blumenstock, editor, Bishop Museum Press, Honolulu

_____1968. Regional setting and Geology, p 20-54 in Thor N. V. Karlstrom and George E. Ball, editors, The Kodiak Island Refugium: Its Geology, Flora, Fauna and History. The Boreal Institute, Univ. of Alberta, Ryerson Press.

_____1974. Geologic Map of the Schickard Quadrangle of the Moon, Geologic Atlas of the Moon, Schickard Quadrangle I-823 (LAC 110). Published by the U.S. Geological Survey, Washington D. C. Prepared in Cooperation with the National Aeronautics and Space Administration and the USAF Aeronautics Chart and Information Center.

_____1988. Alluvial chronology and hydrologic change of Black Mesa and nearby Regions. Pages 45-91 in The Anasazi in a Changing Environment. George J. Gumerman, editor. School of American Research Advance Seminar Book, Cambridge Univ. Press, London

_____1995. A 139-year dendroclimatic cycle, cultural/environmental history, Sunspots and longer term cycles. Pages 137-159 in Proceedings of the Eleventh Annual Pacific Climate (PACLIM) Workshop. C. M. Isaacs and V. I. Tharp, editors. April 19-22, 1994, Interagency Ecological Program. Technical Report 40, California Department of Water Resources,

_____1998. Addendum II: Paleoclimate and the Solar Insolation/Tidal Resonance Model. pp 65-93 in Proceedings of the Fourteenth Annual Pacific Climate (PACLIM) Workshop.Raymond Wilson and Vera. L. Tharp, Editors, April 6-9, 1997. Interagency Ecological Program. Technical Report 57, California Department of Water Resources.

_____1999. Southwest climate and the Quasi-bienial Oscillation, the El Nino-Southern Oscillation, and the Arctic Oscillation and Tidal Resonance, in Proceedings of the Sixteenth Annual Climate (PACLIM) Workshop, West G. J. and L. Buffaloe editors. May 2000. Interagency Ecological Program. Technical Report 67, California Department of Water Resources.

Karlstrom TNV, Gumerman GJ, Euler RC. 1976. Paleoenvironmental and cultural correlates in the Black Mesa Region, pp 149-161 in Papers on the Archaeology of Black Mesa, Arizona,. G. J. Gumerman and E. C. Euler, editors. Southern Illinois University Press, Carbondale.

Keeling CD, Whorf TP. 1997. Possible forcing of global temperature by the ocean tides; U.S. Academy of Sciences Proceedings, v. 94, no.16, p. 8321-8328. \

Ladure EL. 1971. Times for Feast and Times of Famine,: A History of Climate Since the Year 1000. New York, Doubleday.

Langbein WB, Slack JR. 1982. Yearly variations in runoff and frequency of dry years for the conterminous United States, 1911-79. U.S. Geological Survey Open-File Report 82-751.

_____1989. Variations in the national water supply 1979 update, Water resources Review, January 67, 1980, p 18. Lamarche, Jr., V. C., 1974. Paleoclimatic inferences from long tree-ring records. Science 183: 1043-1048.

Lamb HH. 1977. Climate: present, past and future 2, Climate History and the Future, Methuen, London.

Martinson DG, Pisias NG, Hays JD, Imbrie J, Moore Jr. TC, Shackleton NJ. 1987. Age dating and the orbital theory of the ice ages: development of a high-resolution 0 to 300,000-year chronostratigraphy. Quat. Research 27: 1-29.

Mercurio E. 2001. The effects of galactic cosmic rays on weather and climate on multiple time scales, p 35-56 in Proceedings of the Seventeenth Annual Pacific Climate (PACLIM) Workshop, West GW and Buf-

faloe L, eds. Interagency Ecological Program. Technical Report 67. California Department of Water Resources.

Mesolella KJ. 1969. The astronomical theory of climatic change, Barbados data. Jour. Geology 2:250-274

Michel JM, Stockton CW, Meko DM. 1979. Evidence of a 22-year rhythm of drought in Western United States related to the Hale solar cycle since the 17th century. In Solar-Terrestrial Influence on Weather and Climate. Ed. B.M. MacCormac and T.A. Selga. D. Reide Publication Co.

Milankovitch M. 1941. Canon of insolation and the ice-age problem. Translated from German by Israel Program for Scientific Translation, Jerusalem. Available from U.S. Department of Commerce, Springfield, Virginia

Overland JE, Adams JA, Bond NA. 1998. Decadal variability of the Aleutian Low and its relation to high latitude circulation. Jour. of Climate 12(5):1542-1548

Pandolfi LJ, Kalil EK, Doose PR, Levine LH, Libby LM. 1980. Climate periods in trees and a sea sediment core. Radiocarbon 22:740-745

Pettersson O. 1912. The connection between hydrographical and meteorological phenomena: Royal Meteorological Society Quarterly Journal, 39:175-191

_____1914a. Climatic variations in historic and prehistoric time: Svenska Hydrogr. Biol. Kommissiones Skrifter, No. 5, 25p

_____1914b. On the occurrence of lunar periods in solar activity and the climate of the Earth. A Study in Geophysics and Cosmic Physics: Svenska hydrogr. Biol. Kommissiones Skrifter, No. 5

_____1915. Long Periodical variations of the tide-generating force: Council Permanente International pour l'Exploration d la Mer (Copenhagen). Pub. Circ. No. 65, p.2-23.

_____1921. Etude sur les mouvements internes dans la mer et dans l'air: Svenska Hydrog. Biol. Kommissiones Skrifter, Haft VI (Goteborg).

_____1923. Innere Bewegnung in den Zwischenschichten des Meeres und der Atmosphere: Roy. Soc. Scient. Uppsala Nova Acta (IV), v. 6, no. 2

_____1930. The tidal force. A study in geophysics: Geografiska Annaler, v. 18, p 261-322.

Porter SC. 1981. Recent glacial variations and volcanic eruptions. Nature (London) 291:139-142

Porter SC. 1986. Pattern and forcing of Northern Hemisphere and glacial variation during the last millennia. Quat Res. 26:27-48

Porter SC, Denton GH. 1967. Chronology of the Neoglacial in the North America Caudil era. Amer. Jour. of Science. 165:177-210.

Qian W, Zhu Y. 2002. Little Ice Age climate near Beijing, China, inferred from historic and stalagmite records. Quat. Research. 57:109-119.

Rampino MR, Self S. 1981. Historic Eruptions of Tamboro (1815), Krakatau (1883) and Agung (1963), their stratospheric aerosols and climatic impact: Quat Research 18:127-143

Richmond GM. 1976. Pleistocene stratigraphy and chronology in the mountains of western Wyoming. Pages 353-379 in Quaternary Stratigraphy of North America., W. C. Mahany, editor. Dowden, Hutchinson and Ross Inc., Stroudsburg, Pa.

Sanders JE. 1995. Astronomical forcing functions: From Hutton to Milankovitch and beyond: Northeastern Geology and Environmental Science, v. 17, no. 3 p. 306-345.

Scuderi LA. 1987. Glacial variations in the Sierra Nevada, California as related to a 1200-year tree-ring chronology. Quat. Research 27: 220-231.

Street FA, Grove AT. 1979. Global maps of lake-level fluctuations since 30,000 yr B.P., Quat. Research 12: 83-118.

Sturchio NC, Pierce KL, Murrell MT, Sorey ML. 1994. Uranium- series ages of travertine and timing of the last glaciation in the northern Yellowstone Area, Wyoming-Montana, Quat. Research, 42:265-277.

Stuiver M, Grootes PM, Braziunas TF. The GISP Delta 18/0 Climate Record of the Past 16500 Years and the Role of the Sun, Ocean and Volcanoes. Quat. Research 44:341

Stuiver M, Braziunas TF, Grootes PM, Zielinski GA. Is there Evidence for Solar Forcing of Climate in the GISP2 Oxygen Isotope Record ? Quat. Research 48:259-268

Terasmae J, Dreimanis A. 1976. Quaternary Stratigraphy of Southern Ontario. Pages 51-63 in Quaternary Stratigraphy of North America. W. C. Mahany, editor. Dowden, Hutchinson and Ross Inc., Stroudsberg, Pa.

Vernekar AD. 1972. Long period global variations of incoming solar radiation, Meteorological Monographs 12 Whole monograph: 19 pp + 170 unnumbered pages.

Willet H. 1961. The pattern of solar climatic relationships, Ann N. Y. Acad. Sci., 95: 80-106

_____1962, The relationship of total atmospheric ozone to the sunspot cycle. J. Geophys. Res., 67

Wood FJ. 1978. The strategic role of perigean spring tides in nautical history and North American coastal flooding 1635-1978: Washington D. C., U.S. Department of Commerce National Oceanic and Atmospheric Administration. U.S. Government Printing Office, Stock no. 003-017-00420-1, 538 p.

_____1985, Tidal Dynamics, Coastal Flooding and Cycles of Gravitational Force: Dordrecht, the Netherlands. D. Reidel Publishing Company, 712 p.

Non-Precipitation Variability of the Western United States Snowpack

Mark Losleben

Abstract

Snowpack is crucial to water supplies in the western U.S. and it integrates the full range of climatic factors that effect snow accumulation. Changing climate may alter annual snowpack in many locations due to changing accumulation and ablation rates, the result of changing synoptic circulation patterns (differing air masses). Ablation depends upon the combination of many factors, including temperature, relative humidity, wind, cloud cover, solar inputs, and radiative balances. Many of these factors behave in a linear manner, but in combination they become chaotic in nature, thus the value of an index that integrates them. Precipitation is easily enough measured and independently evaluated on its own, but variability resulting from many of the other factors is more elusive. This study introduces a snowpack index (SI) as a way to evaluate the role of snowpack influencing factors beyond simply precipitation. Effectively, the SI is a measure of the winter precipitation that is sequestered in the snowpack. This paper examines the trends and variability of snowpack and its influencing components, precipitation, non-precipitation snowpack (SI) components, temperature, and elevation, for the western U.S. as a whole and by mountainous region for the past two decades (1979-1999).

Introduction

This paper examines changes in non-precipitation factors which impact the sequestration of winter precipitation in the form of snowpack in the mountainous western United States. Because winter precipitation will only be available in the spring and summer if it is sequestered in the snowpack (or captured in reservoirs), it is important to know if these non-precipitation variability factors are changing. The consistent global warming since the late 1970s has the potential to alter these factors, altering the ablation/accumulation balance. It is important to eliminate the effect of precipitation variability to accurately make such an assessment. Thus, this study uses the snowpack index (SI) which controls for precipitation variability. As an additional tool, plots of the SI as a function of temperature control for temperature variability as well, yielding a graphical picture of snowpack influencing factors independent of both precipitation and temperature. These factors include amount of solar radiation, cloud cover and type, night-time (long wave) radiation balance, relative humidity, wind speed and turbulence, and reflect synoptic conditions and air mass types.

Data

Snowpack snow water equivalent (SWE), precipitation (PPT), temperature data, and site elevations were obtained from the Natural Resources Conservation Service (NCRS) SnoTel database. SnoTel sites were used exclusively in this study because SWE, precipitation, and temperature are all measured at the same location. It is important for SWE and precipitation measurements to be co-located for accurate SI computation, as both variables are very heterogeneous over short distances. Table 1 lists

the number of stations used for April 1 data for the west as a whole and for each region. First of the month values were used from January through June for the years 1979-1999, the study period. Precipitation values are cumulative from October 1, and average SWE and PPT are the 1971-2000 mean. Cumulative temperature, used in this study, is the average maximum, minimum, or mean temperature from October 1 to the given date. Cumulative temperature more closely matches the snowpack exposure than other temperature summations.

Table 1 Number of stations used for April 1 data for the west as a whole and for each region

	Number of sites			
Region	*Total*	*SI Index*	*SWE*	*PPT*
West U.S.	621	555	614	610
Arizona (AZ)/New Mexico (NM)	25	22	25	25
New Mexico/Colorado (CO)	43	41	43	43
Colorado	61	57	61	61
Utah	70	67	70	70
Idaho (ID)/Montana (MT)	224	200	221	214
Oregon (OR)/Washington (WA)	116	97	116	116
California (CA)	28	26	28	28
Wyoming (WY)	23	19	23	23

Analysis

The snowpack index (SI) is the percent of average snowpack divided by the percent of average cumulative precipitation on any given date. An SI of 1.0 indicates there are no changes in non-precipitation snowpack development factors. Values of less than one indicate an increase in these factors that ablate snowpack, and values greater than one an increase in these factors that accumulate snowpack (independent of precipitation). To further clarify, an index value of one indicates non-precipitation factors on snowpack development are unchanging. This is true even if the actual snowpack is higher or lower than average on any year. An index value of less than one indicates that less of the winter precipitation is being stored in the snowpack, and a value greater than one indicates more is stored. Thus, the SI is a standardized index, normalizing for precipitation variability, and integrates the remaining variability factors, such as temperature, cloudiness, wind, relative humidity, solar and radiative effects.

In addition to analysis of the west as a whole, SWE, precipitation, and SI analysis was done for the four quadrants of the western U.S., separated at 40° north latitude and 112° west longitude. Then, eight smaller regions, roughly corresponding to mountain ranges, were used. Five of these roughly correspond to the spatial patterns identified by Cayan (1996) based on April 1 SWE rotated principal components analysis. Cayan's regions were named Idaho, California, New Mexico, Oregon, and Colorado in descending order of variance. The corresponding regions in this paper are ID/MT, CA,

NM/CO, OR/WA, and CO, respectively. This work also has AZ/NM (southern Arizona/New Mexico), Utah, and Wyoming regions, because they are spatially separate groups of mountain stations with reasonable statistical depth. The CA (California) region is not representative of the entire state, because only SnoTel stations were used, and these form a tight cluster of stations near the Nevada border at the bend in the state line (39°N 120°W). Although there are many excellent snow reporting sites in California, only SnoTel stations were used because of their co-located SWE and precipitation measurements.

The SI was also computed for different elevations and temperatures.

Results and Discussion

Full Western U.S.

Bi-linear saddle surface trend analysis shows an SI gradient from northeastern Montana (SI>1) to southern California and New Mexico (SI<1) (Figure 1a). Similar analysis shows minimum temperatures (Figure 1b) to be strongly longitude dependent (warmer to the west). The maximum (Figure 1c) and mean (Figure 1d) temperatures are coldest in northeast Montana, and increase toward southern California, where they are warmest.

Annual trends for April 1 data were significant for both cumulative maximum (0.15°C/year at 100% level) and minimum (-0.261°C/year (98.7% level) temperatures. This indicates the range of cumulative temperature is increasing with time, counter to global and many regional trends. It may be that the higher, remote locations are not experiencing the same temperature trends of the lower lands where many of the other temperature records originate. Increasing max-min temperature ranges could be from a decrease in both day and nighttime cloudiness. However, since precipitation is not declining (see later) in these areas, perhaps the storms are shorter and more intense (increasing hydrologic cycling?).

The SI trend was -0.007, but not significant at the 85% level. Similarly, SWE and cumulative precipitation trends were not significant.

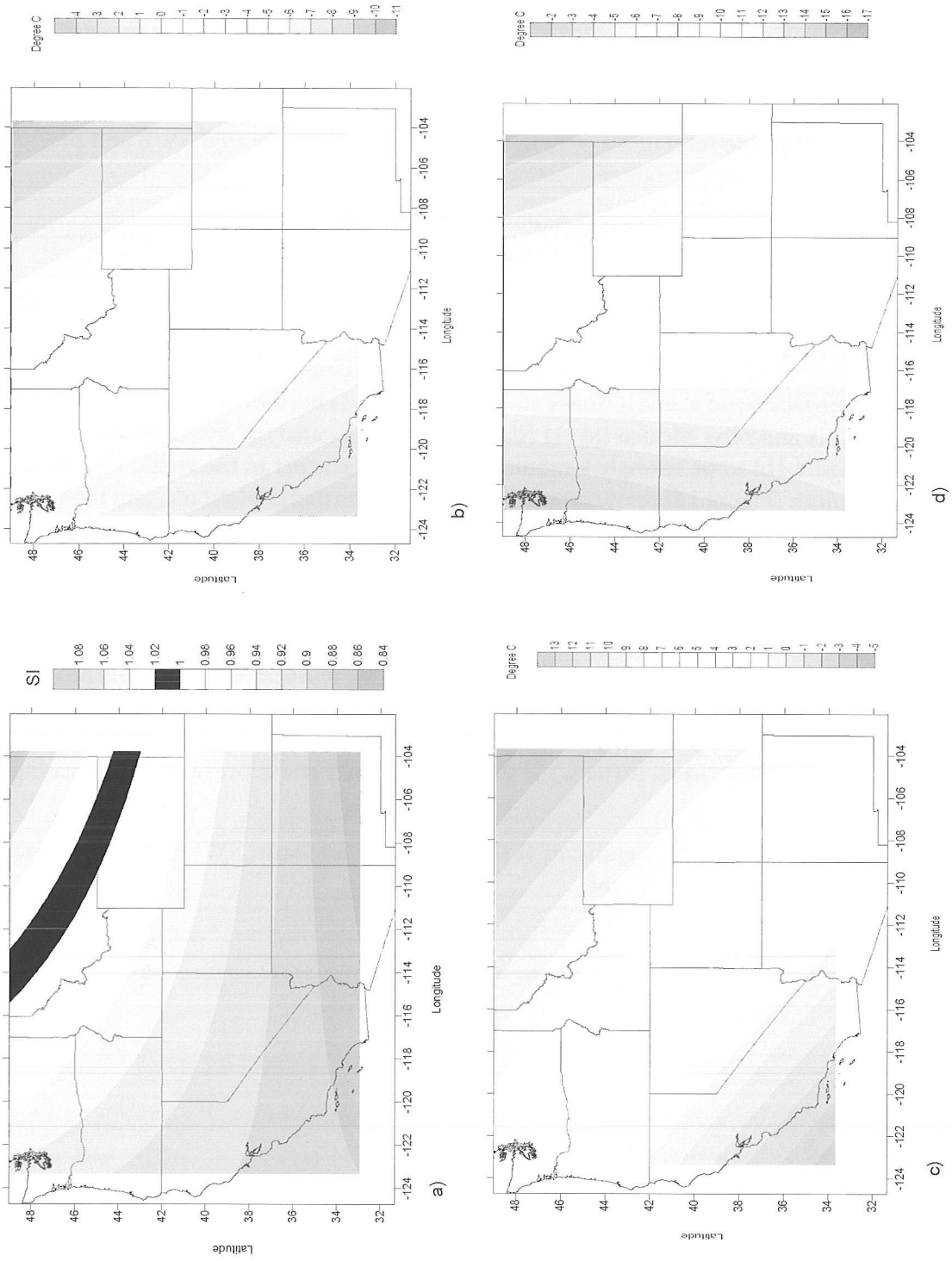

Figure 1 Surface Trend Analysis of April 1 conditions. (a) SI are highest in the upper left with the SI=1 contour across west Montana and NE Wyoming. They trend to the lowest values in the south. (b), (c), (d) are the surface trends for cumulative mean, maximum, and minimum temperatures, respectively. The 0°C maximum contour is roughly in the same place as the SI=1 contour.

The spatial distribution of SI (Figure 2) shows values >1 in the interior regions, and lower values at regions closer to the Pacific Ocean. The Arizona and New Mexico values > 1 are most likely statistical artifacts due to low sample size in the earlier years. This supposition is consistent with regional analysis which shows the values to be lower than one in the 1990s. Also, the areas of SI>=1 west of longitude 118°W, are without station data, therefore suspect of being artifacts.

Figure 3a shows a tendency for SI to be lower at low elevations and higher at upper elevations. Below about 1300 meters, there are more SI values less than 1, and the frequency of values greater than 1 increases at higher elevations. This relationship is consistent with more maritime mountain ranges dominating the signal at lower elevations. The snowpack is more vulnerable to slight temperature fluctuations in regions where the mean temperature is close to the melting point. This is the case in more maritime regions compared to interior, continental areas where maximum temperatures stay well below zero centigrade most of the winter. Figure 3a shows little time evolution of the SI, consistent with the finding that there is no significant trend with time. SWE (Figure 3b) and total winter precipitation (Figure 3c) are highest in the middle and low elevations, reflecting the increased moisture supply in the mountains closest to the Pacific Ocean compared to the higher and drier ranges of the interior west. There may also be a slight trend toward increasing SWE and precipitation at the low to middle elevations.

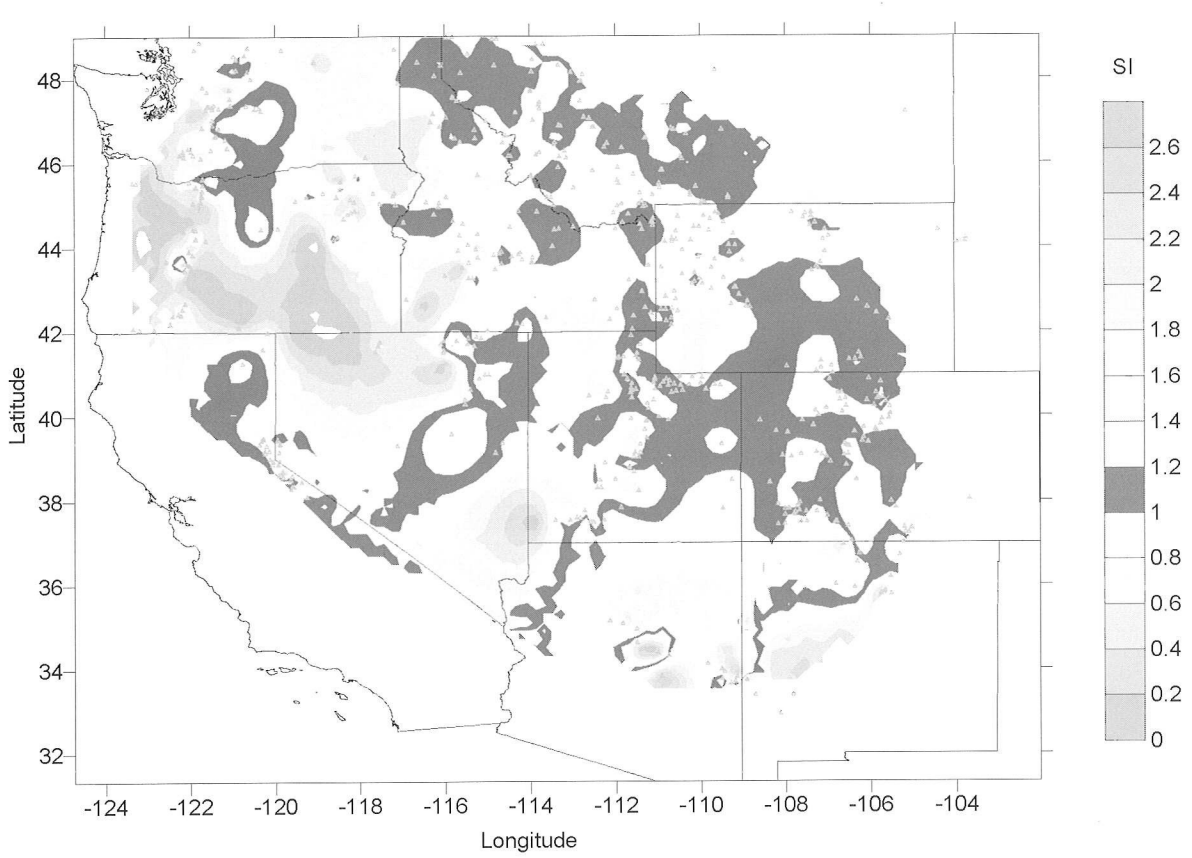

Figure 2 Location of the SnoTel sites used in this study (small triangles) and contours of the April 1 SI. SI values of one or greater are more prevalent in the interior western U.S.

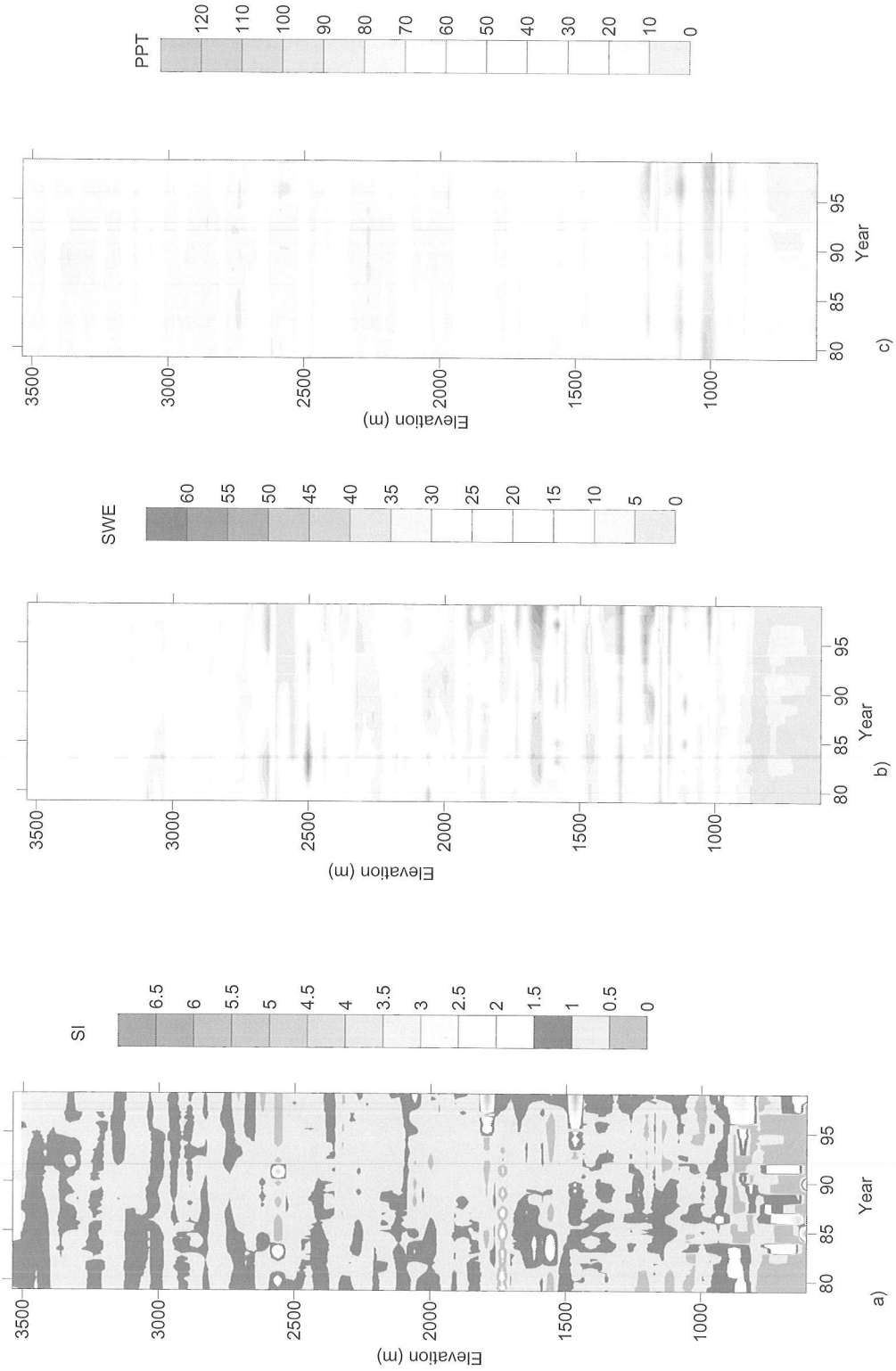

Figure 3 Elevation versus time distributions of SI (a), SWE (b), and cumulative precipitation (c) on April 1. In all cases, there is more elevational variability than temporal.

Temperature dependence on elevation and time is shown in Figures 4 a-c. The correlations of temperature and elevation are significant at the 0.0000 level for mean, maximum, and minimum temperatures. Possible temporal trends of possible cooling at elevations of 1750-2800 meters, and slight warming above 3000 and below 1500 meters, particularly for minimum temperatures, are suggested.

Figures 5 a-c show the relationship of SI to time and cumulative winter temperature (Oct 1 - Apr 1). These figures show SI temporal variability at any given temperature. In effect, we are controlling for temperature with such a plot, and the SI controls for precipitation. The result exposes snowpack sequestration factors independent of both precipitation and temperature variability. An overall decline in SI is particularly noticeable in the mean temperature plot, below -15°C and above 5°C. There is also a band of increased SI, often greater than 1, near 0°C for mean and minimum and around 8°C for maximum temperatures. The decline at the coldest temperatures may suggest increased clear skies and windiness, often following storms in continental areas at least. Both factors can increase ablation. The band of increasing SI mentioned above could reflect temperatures during a snowstorm (increased cloudiness and decreased wind). The depressing effect of cloud and wind (and other factors) on ablation is apparent since the SI is precipitation invariant. By this same course, factors decreasing ablation are seen to dominate at 0°C and those that increase ablation at less than -15°C.

Western U.S. Monthly Results

Figure 6 shows the percent of average SWE, precipitation, and SI by month. The mean 1979-99 precipitation is about average for every month, but mean SWE declines from January to June, the decline in Jan-Mar being quite small compared to May and June. This is reflected in the SI values of less than one in every month. This decline in the amount of moisture sequestered in the snowpack is the result of less snowfall, not less precipitation.

Correlations of SWE to mean SWE and precipitation to mean precipitation (Figure 7) show that average conditions are most likely to exist on April 1 for SWE and May 1 and June 1 for precipitation, and that SWE is more variable than precipitation.

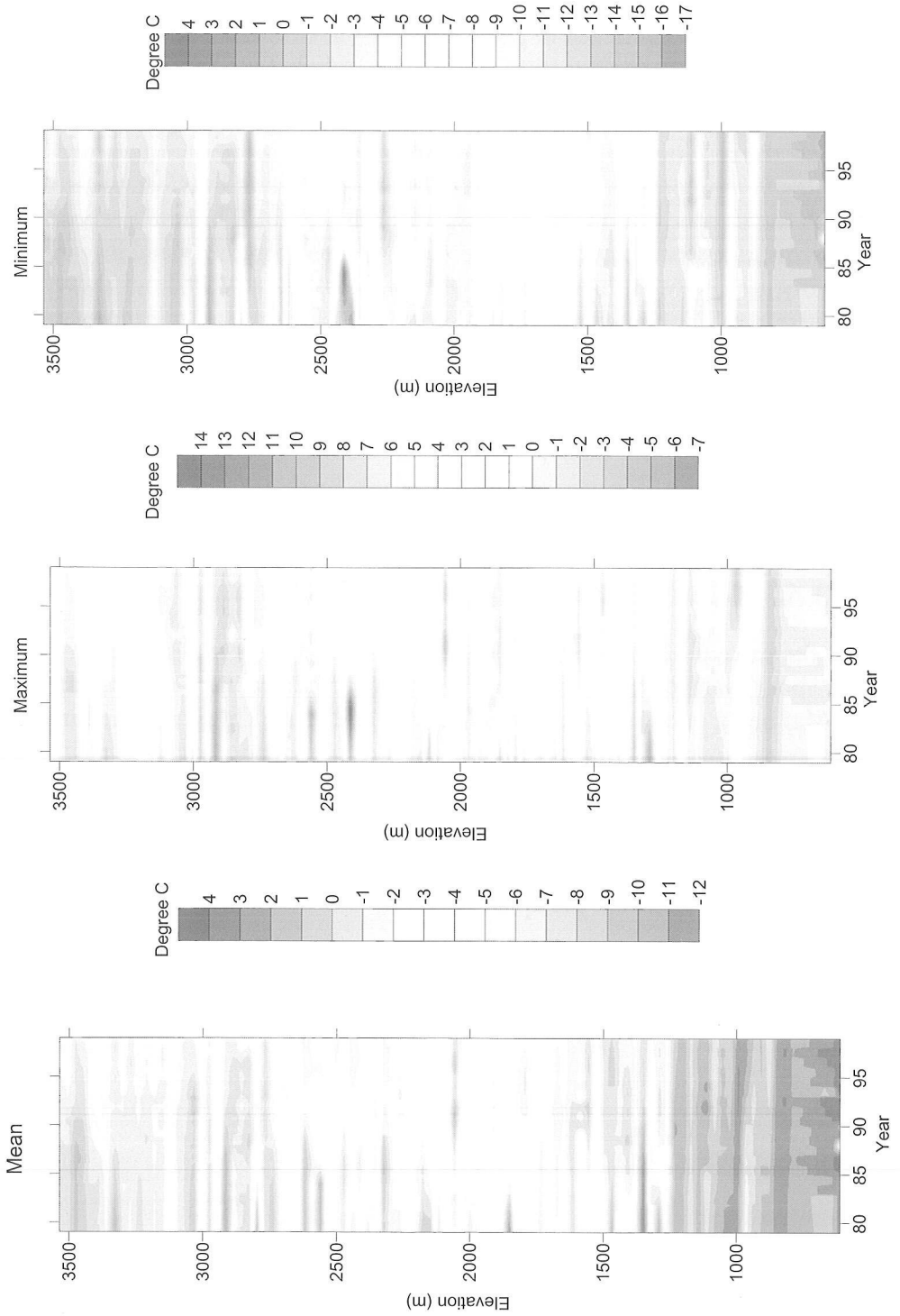

Figure 4 April 1 cumulative temperature distribution as a function of elevation and time: mean, maximum, and minimum (a), (b), and (c) respectively. All temperatures are significantly correlated with elevation (100% level), but not with time. This figure suggests temperature are increasing at lower elevations and are decreasing at higher elevations.

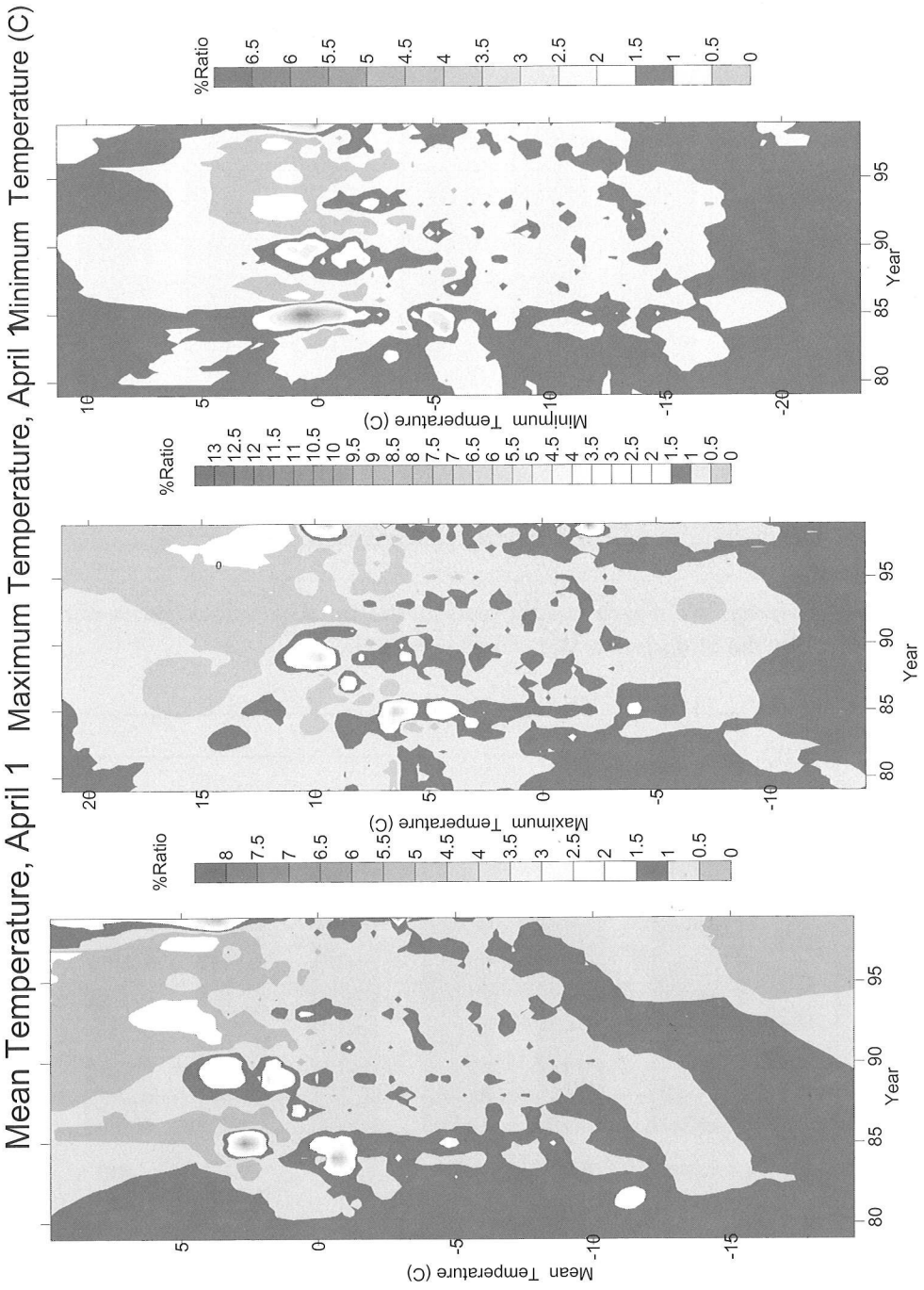

Figure 5 April 1 SI distribution as a function of cumulative temperature (mean, maximum, minimum (a), (b), (c) respectively) and time. Reading across horizontally eliminates temperature variability and the SI eliminates precipitation variability, allowing inspection of snowpack factors other than these two major ones. Such factors include relative humidity, wind, solar radiation, long wave radiation flux, and cloud cover. There is a band of maximum SI values. This is around zero mean and minimum, and 8° C for maximum temperature.

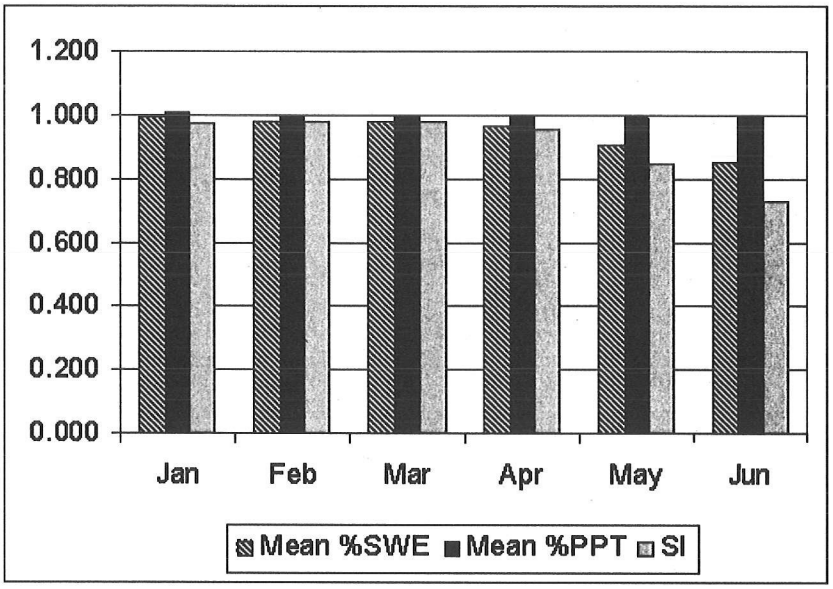

Figure 6 Conditions on the first of each month, Jan-Jun. Precipitation values remain normal all months, but the SWE and especially the SI decline as the winter progresses.

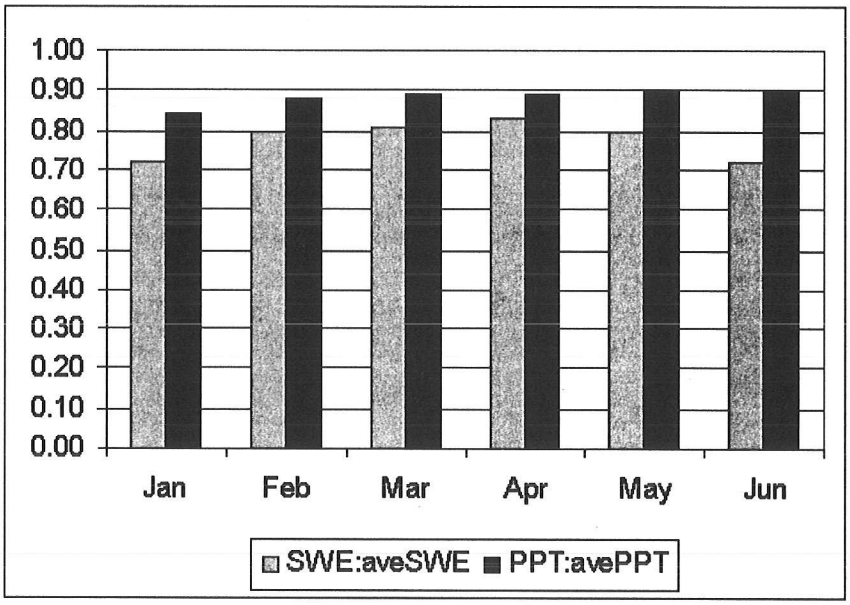

Figure 7 Monthly correlations of SWE and cumulative winter precipitation with their respective average values. Snowpack correlations are lower than precipitation correlations suggesting greater variability in snowpack than precipitation.

Western U.S. ENSO Results

Figure 8 shows the percentage of SWE, precipitation, and SI by ENSO phase. Most striking is that La Niña is the only ENSO phase to positively affect the SI (greater than one). This is due to an increase

in SWE, not precipitation. Analysis by quadrant (Figure 9) shows this to be entirely a Pacific northwest contribution. Figure 9 also shows the northwest is most variable and the northeast region the least, by ENSO phase.

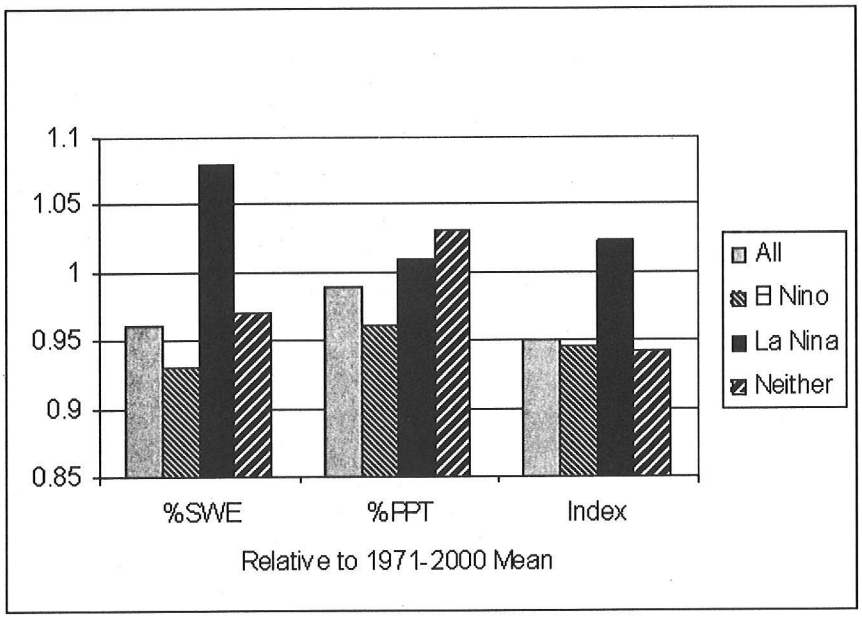

Figure 8 April 1 conditions by ENSO phase. SWE and SI are vary more by ENSO phase than precipitation, and are lower in all phases except during La Niña when they exceed normal levels (they are greater than one). Cumulative precipitation is also greater than average (normal) during La Niña and neither (neutral) ENSO phases.

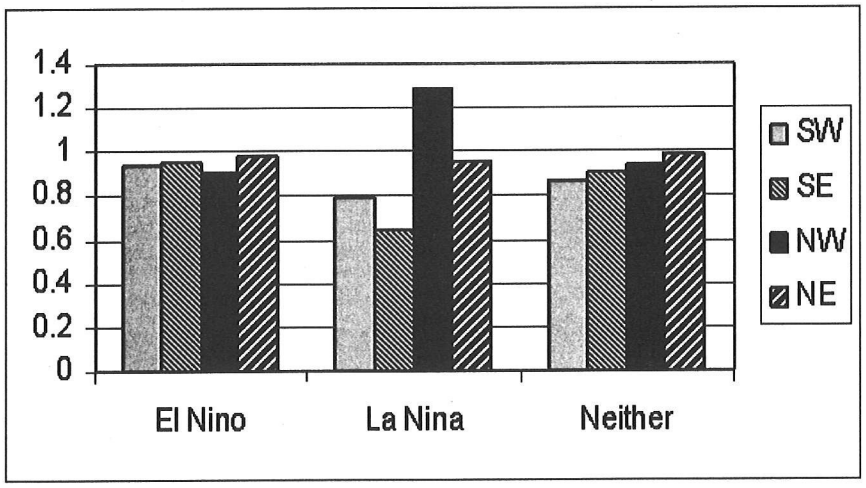

Figure 9 April 1 SI is declining (<1) during all ENSO phases in all quadrants of the western U.S. except in the northwest during La Niña.

Results by Quadrant

SWE, precipitation, and SI were analyzed in the four quadrants of the western U.S., separated at 40°north latitude and 112° west longitude.

Figure 10 shows the variability of SWE, precipitation, and the SI by quadrant. SWE and SI variability were greatest in the northwest, consistent with the SI results of Figure 9, but precipitation variability was greatest in the southwest. The least variability of all three factors was found in the northeast quadrant.

Figure 11 shows 1979-1999 precipitation to be greater than average (1971-2000) in both southern quadrants and less than average in both northern ones. The relative proportion of winter moisture (1979-1999) sequestered in the snowpack, however, is less than average (1971-2000) in all quadrants; the greatest decrease is in the southeast, and least in the northeast ones. This is not because of a decline in winter moisture, since the southwest has received 103% of average, and the southwest 104% for the comparable period. In these regions there has been an increase in precipitation, but a decrease in the relative amount that fell as snow, resulting in the low SI values. The northeast quadrant appears to have the least change in SWE, precipitation, and SI. This may reflect its position relative to large scale (synoptic) circulation, being more removed (north) from the boundary of shifting jet stream tracks, than the other three quadrants. So, although the northeast appears to be the least changeable in the past two decades, all quadrants show decline in the relative proportion of winter precipitation sequestered in their snowpack.

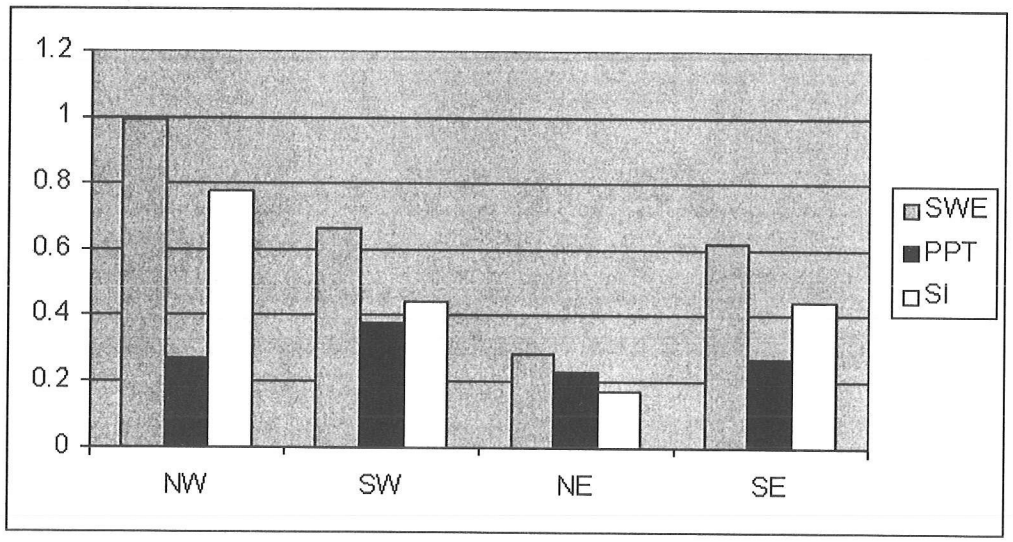

Figure 10 Variability (standard deviation) of April 1 SWE, cumulative precipitation, and the SI. Precipitation is least variable in all quadrants, and SWE is most variable. The northeast is the least variable quadrant, and the northwest the most. Variability in the south is virtually the same in the east and west quadrants.

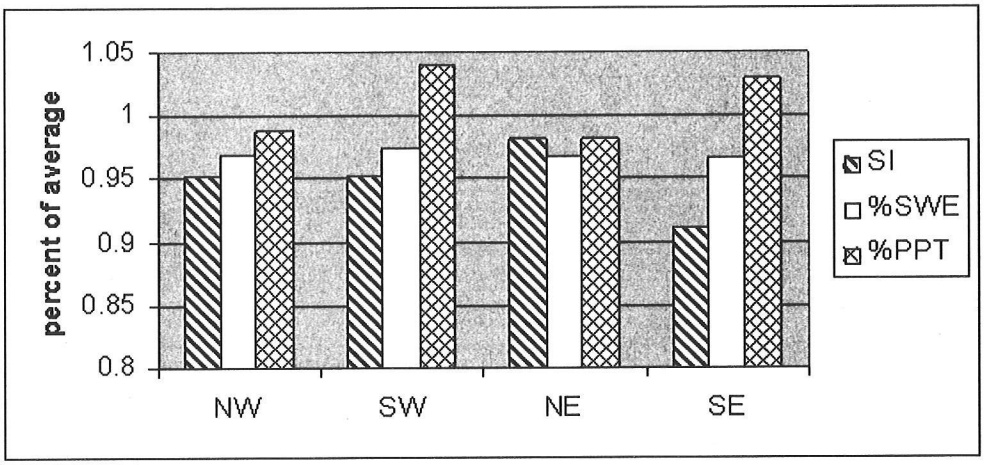

Figure 11 SI, SWE, and cumulative precipitation on April 1 in each of the western U.S. quadrants. Precipitation is above average in both southern quadrants, but all other parameters are below average in all the quadrants.

Results by Region

Analysis of the eight regions (Figure 12) suggests the strongest temporal trends are in southern AZ/NM and northern NM/southern CO, where the SI declines strongly over time at all elevations. Much of this decline is from SI values of greater than one to less than one. Colorado and Utah also show similar, but weaker, trends at middle to lower elevations. The SI in the ID/MT (Idaho/Montana) area is relatively stable over time, but SI less than 1 is more frequent than SI greater than 1. The SI in the OR/WA (Oregon/Washington) area is also fairly stable with time, but the SI may be increasing at elevations above 1600 meters. The Wyoming (central and eastern) SI values are less than one below 2400 meters, and declining below 2600 meters. The SI is greater than one between 2600 and 2800 meters, and also above about 2950 meters, and increasing at all elevations above 2600 meters. In the California group (clustered about 39°N 120°W) the SI is increasing at all elevations, and greater than one at most heights, particularly between 1950 and 2400 meters. Note that this is not spatially representative of California, but it is the strongest signal of winter precipitation sequestration in snowpack at any of the eight areas and also a region of high absolute snowpack, representing significant amounts of water.

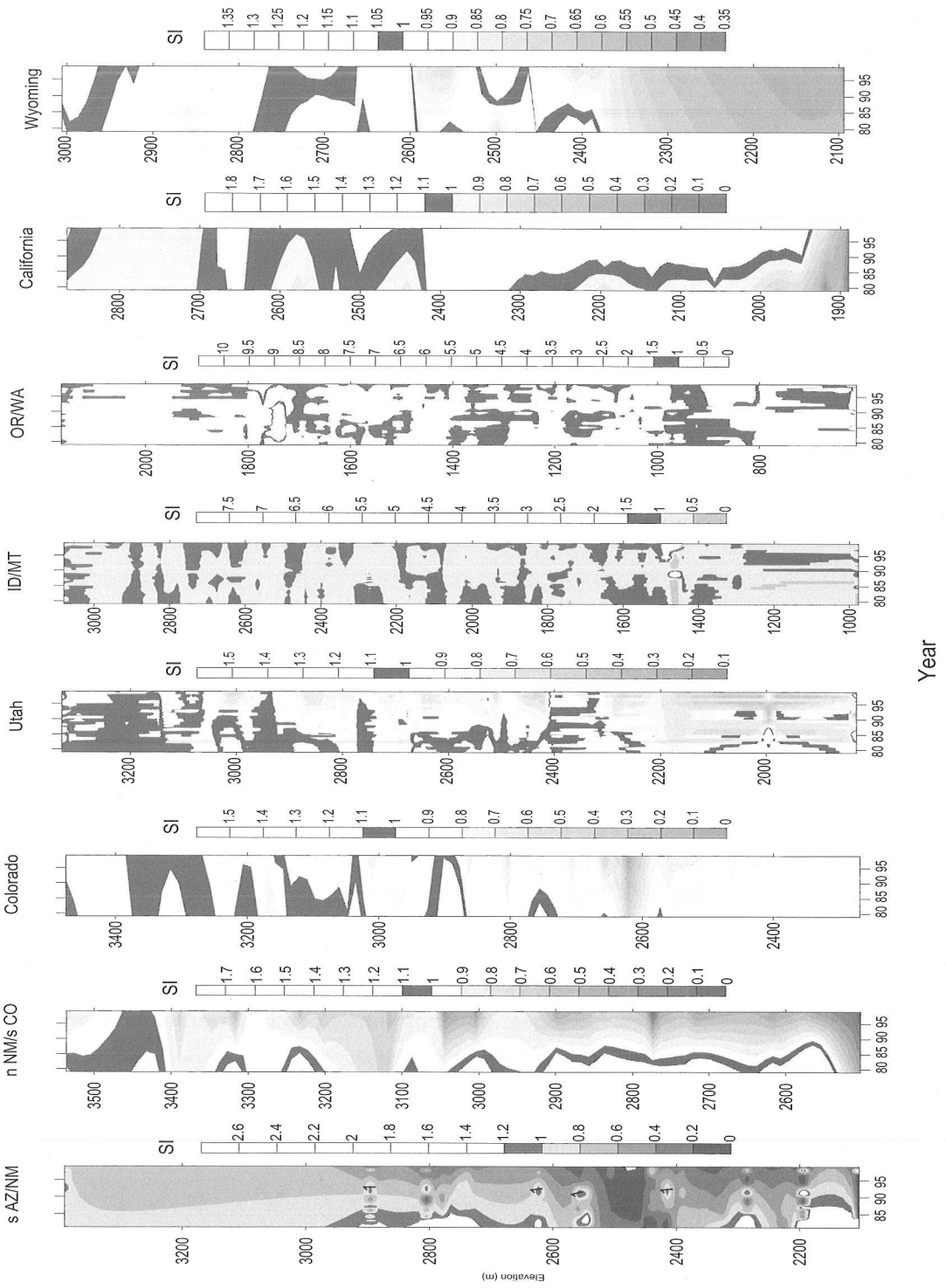

Figure 12 Depiction of the April 1 SI by elevation and time in eight regions of the western U.S. In general, the SI values are least changing (SI=1) at higher elevations, and in the earlier years. Southern regions show the largest change, and this is at all elevations. Northern regions show the least change, and possibly even an increase (SI>1) in the higher elevations of Oregon/Washington.

Summary

The SI provides a way to eliminate precipitation variability when looking at the factors effecting the sequestration of winter precipitation in snowpack. The study results suggest that winter precipitation sequestered in western U.S. mountain snowpacks is declining, and this is not due to reduced precipitation, nor is it evenly distributed by elevation or region. Often the decline is greater at lower elevations, and in the southern portion of the western U.S.

Reference

Cayan D. 1996. Interannual climate variability and snowpack in the western United States. Journal of Climate 9:928-948.

Is Streamflow Increasing in the Conterminous United States?

Gregory J. McCabe and David M. Wolock

Abstract

Ranks of annual streamflow statistics (i.e., annual minimum, median, and maximum daily streamflow) for 400 streams in the conterminous United States measured during 1941-1999 are examined for changes. Results indicate a noticeable increase in the number of sites with high-rank annual minimum, median and maximum daily streamflow events after 1970. Significant increases in the number of sites with high-rank monthly minimum, median, and maximum daily streamflow also were found for all months except April. These results suggest an increase in the magnitude of minimum, median, and to a lesser extent maximum daily streamflow events since 1970. In addition, this increase appears as a step change rather than as a gradual trend and coincides with an increase in precipitation.

Introduction

A potential consequence of climatic change is an intensified hydrologic cycle, which some have speculated will result in increased precipitation and an increased frequency of floods (Milly and others 2002). Recent studies have identified trends in various streamflow statistics and have produced contradictory results. Lettenmaier and others (1994) examined trends in annual and monthly streamflow across the conterminous United States (U.S.) and found positive trends for a large proportion of the streams analyzed. Lins and Slack (1999) also analyzed streamflow in the conterminous U.S. and found that most of the statistically significant positive trends in streamflow were for low and moderate streamflows. They found only a few positive trends in high streamflow events. Douglas and others (2000) found similar results for a study of trends in flood and low flows in the U.S. In contrast, Groisman and others (2001) found increases in large streamflow events in the conterminous U.S., particularly in the eastern U.S. They attributed the increases in large streamflow events in the eastern U.S. to increases in the frequency of heavy precipitation events. They indicate that in the western U.S. a reduction in snow cover extent has complicated the relation between heavy precipitation and streamflow.

The results of previous research indicate significant differences with regard to changes in large streamflow events. Many of these studies used trend analysis which assumes that there is a monotonic trend in the data. In addition, trend analysis has been found to be sensitive to outliers, sequences of extreme events, and to differences in time periods analyzed (Wahl 1998). Some of the differences between the results of previous studies may be due to differences in the time periods examined or due to the assumption of a monotonic trend in the data.

In this study annual streamflow statistics for 400 streams in the conterminous U.S. are examined to clarify both the temporal and spatial variability of annual streamflow statistics in the conterminous U.S.

Data and Methods

In this study, monthly and annual minimum, median, and maximum daily streamflow statistics for 400 watersheds in the conterminous United States (U.S.) measured during 1941-1999 were examined. The time series of statistics were replaced by time series of ranks (from lowest to highest) and the number of sites with high-rank (highest 10% of ranks) streamflow events were examined for each year. The watersheds were chosen from the Hydroclimatic Data Network (HCDN) (Slack and Landwher 1992). HCDN sites are relatively free of anthropogenic influences and streamflow measured at these sites is considered to be natural. The watersheds chosen represent a wide range of physiographic regions across the conterminous U.S.

Changes in Streamflow Statistics

Analysis of ranked (from lowest to highest) streamflow statistics (monthly and annual minimum, median, and maximum daily streamflow) indicate that the number of sites with the highest 10% of these streamflow statistics have increased during the 1941 to 1999 period (Figure 1). The change in the number of sites with these high-rank streamflow events appears to be a step change after 1970.

Spatial Distribution of Significant Changes in Streamflow

Student t-tests also were used to identify sites with significant differences in the mean rank of monthly and annual daily streamflow statistics between the 1941-1970 and the 1971-1999 periods. Consistent with the examination of changes in the number of sites with high-ranked streamflow statistics, there is a large number of sites with significant (at a 95% confidence level) differences in mean monthly and annual minimum and median daily streamflow ranks, and fewer sites with significant changes in mean monthly and annual daily maximum streamflow ranks (Figure 2). The sites with significant increases in streamflow statistics are primarily located in the eastern U.S.

Climate Driving Processes

The increase in the number of sites with high-rank minimum, median, and maximum daily streamflow is related to a change in climatic conditions. Monthly temperature and precipitation data for the 344 climate divisions of the conterminous U.S. used as inputs to a monthly water balance model produce changes in high-rank simulated streamflow that are similar to those found in the measured data (Figure 3; Karl and Riebsame 1984; Karl and others 1986). Increases in precipitation since 1970 account for a large part of the increase in streamflow statistics.

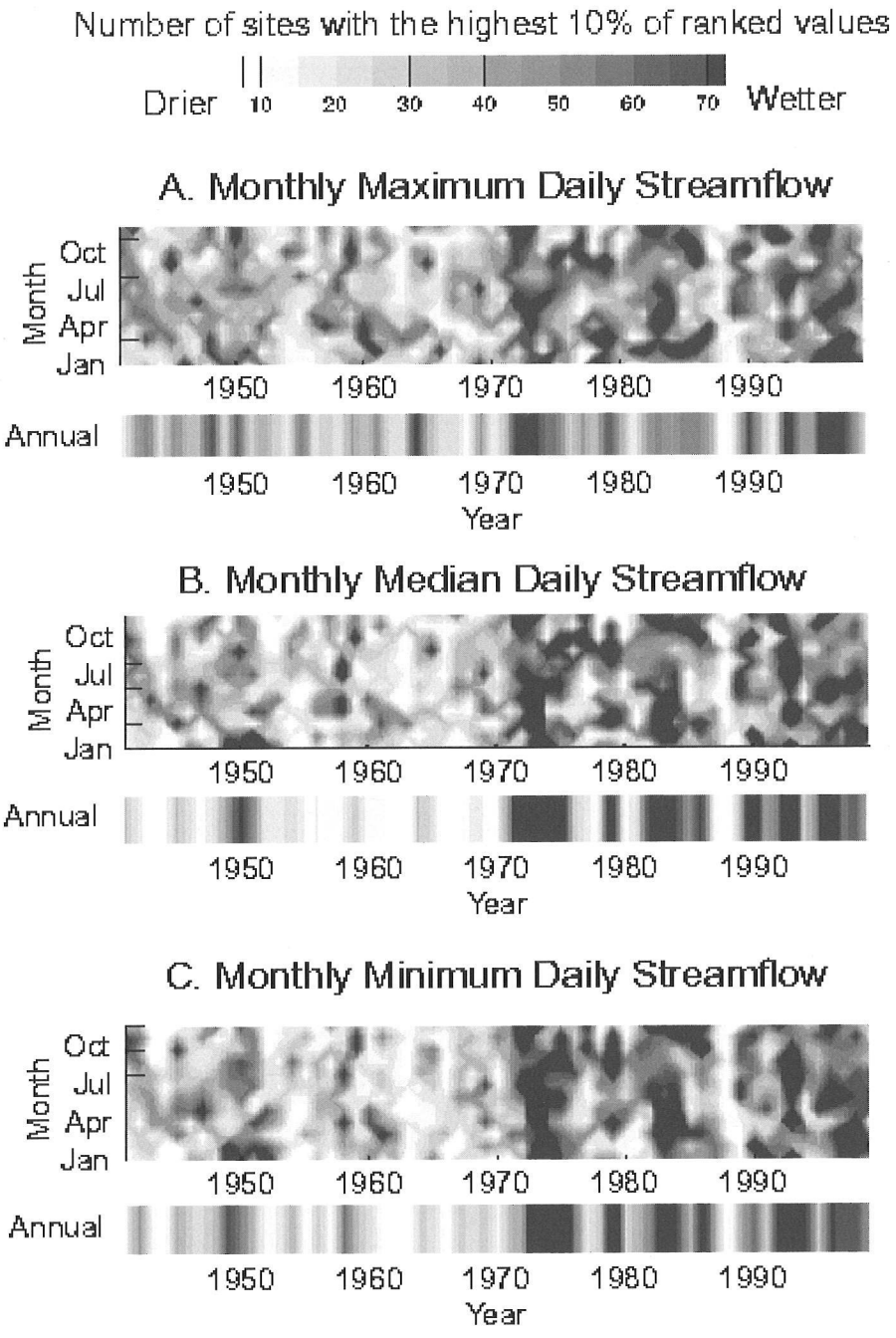

Figure 1 Number of sites with the highest 10% of monthly and annual ranked (A) maximum, (B) median, and (C) minimum daily streamflow.

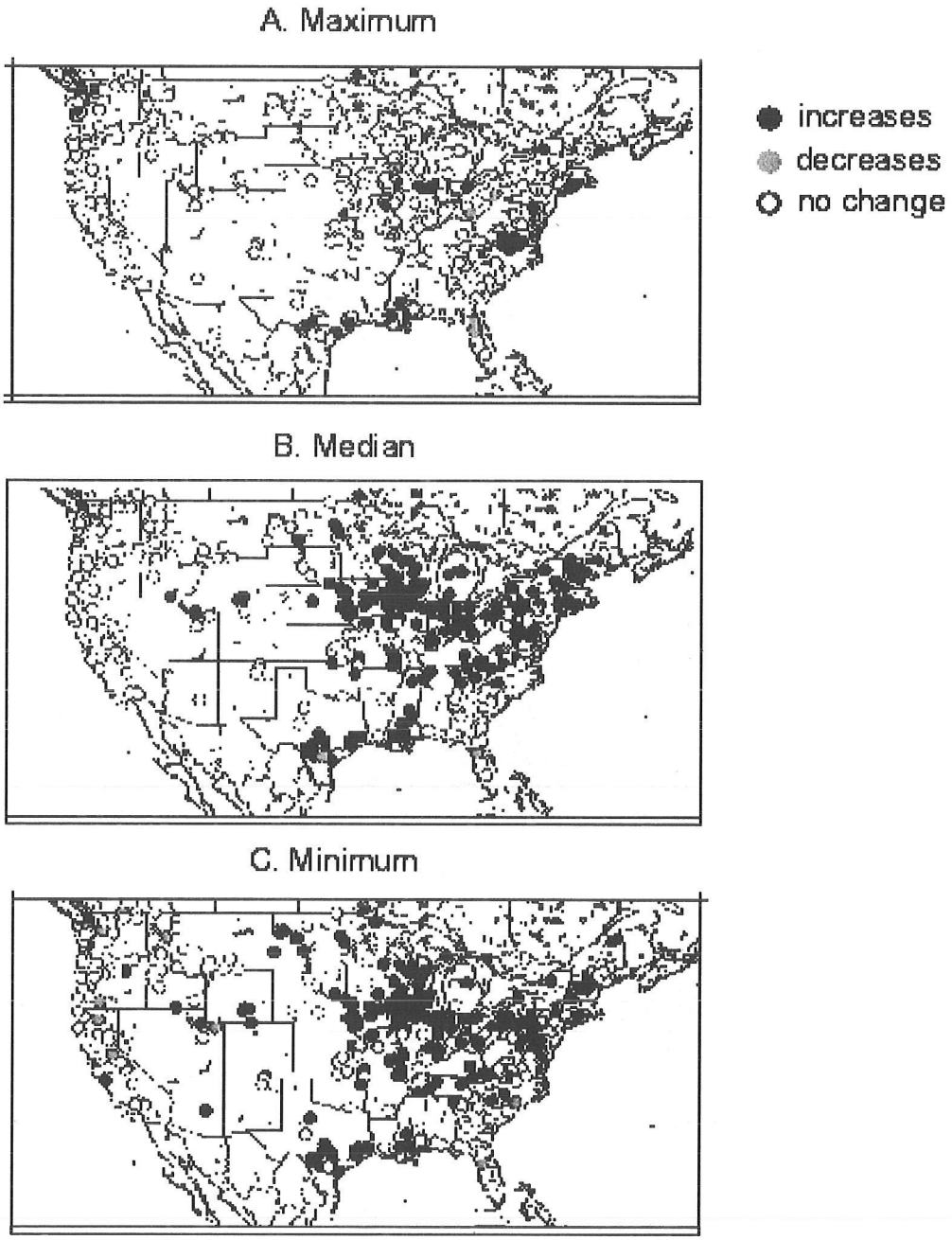

Figure 2 Sites with significant (at a 95% confidence level) increases (black dots) and decreases (C) minimum daily streamflow after 1970. White dots indicate sites with non-significant changes in streamflow.

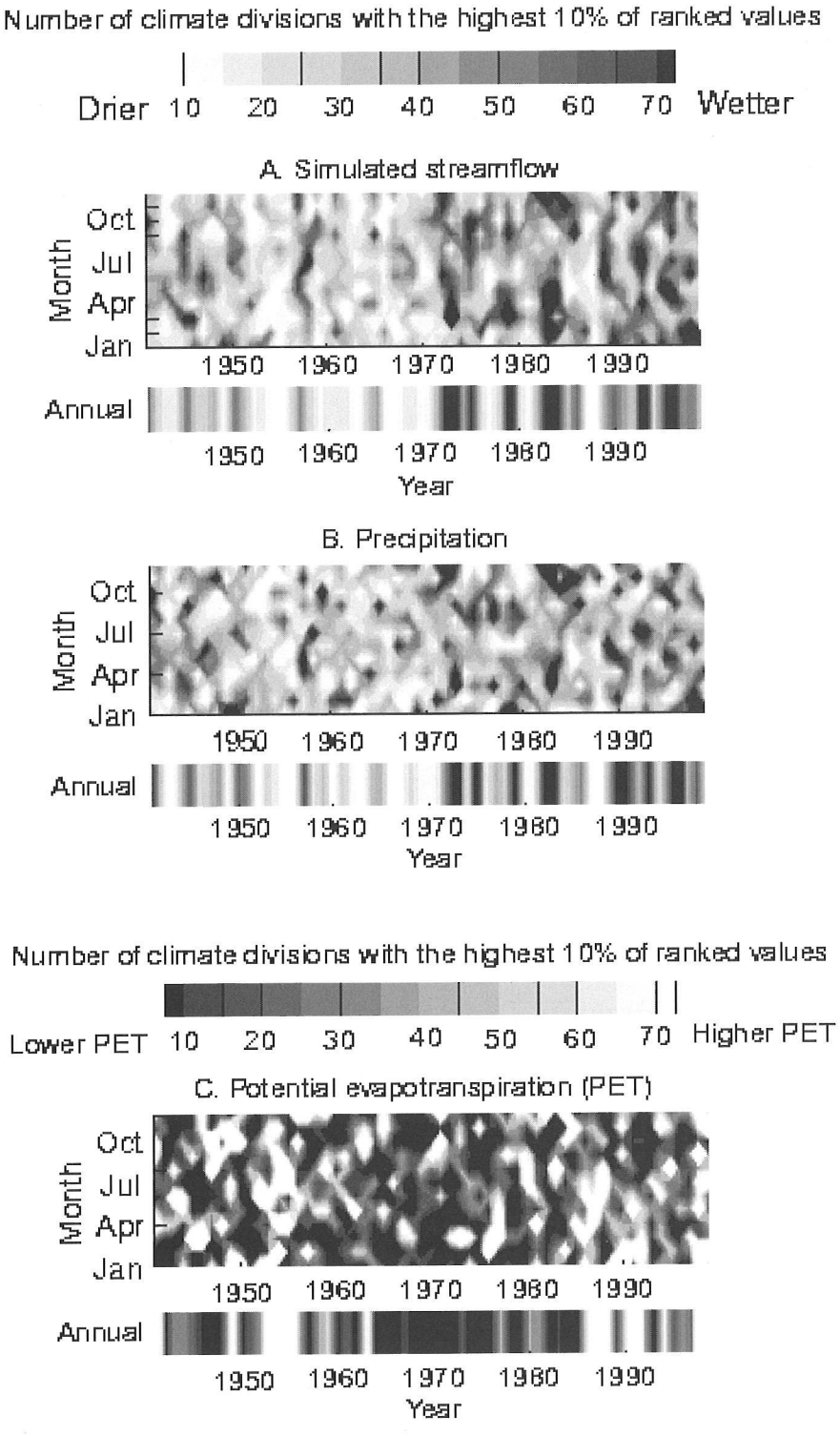

Figure 3 Number of climate divisions with the highest 10% monthly and annual ranked values of (A) simulated streamflow, (B) measured precipitation, and (C) simulated potential evapotranspiration

Summary

The temporal variability of annual statistics (i.e., minimum, median, and maximum) of daily streamflow for 400 streams in the conterminous U.S. was examined for the 1941-1999 period. Results indicate that almost half of the sites examined indicate increases in annual minimum and median daily streamflow statistics, whereas only a few sites (~10%) indicate increases in annual maximum daily streamflow. Only a few sites showed decreases in any of the streamflow statistics. The increases in annual streamflow statistics primarily occurred for sites in the eastern U.S. and occurred as a step increase around 1970 rather than as a gradual increasing trend. The step increase in streamflow appears to be related to a step increase in precipitation.

References

Douglas EM, Vogel RM, Kroll CN. 2000. Trends in floods in the United States; impact of spatial correlation. Journal of Hydrology 240:90-105.

Groisman PY, Knight RW, Karl TR. 2001. Heavy precipitation and high streamflow in the contiguous United States: trends in the 20th century. Bulletin of the American Meteorological Society 82:219-246.

Karl TR, Riebsame WE. 1984. The identification of 10- to 20-year temperature fluctuations and precipitation flictuations in the contiguous United States. Journal of climate and Applied Meteorology 23:950-966.

Karl TR, Williams CN, Young PJ, Wendland WH. 1986. A model to estimate the time of observation bias associated with monthy mean maximum, minimum, and mean temperatures for the United States. Journal of Climate and Applied Meteorology 25:145-160.

Lettenmaier DP, Wood EF, Wallis JR. 1994. Hydro-climatological trends in the continental United States, 1948-1988. Journal of Climate 7:586-607.

Lins HF, Slack JR. 1998. Streamflow trends in the United States. Geophysical Research Letters 26:227-230.

Milly PCD, Wetherald RT, Delworth TL, Dunne KA. 2002. Increasing risk of great floods in a changing climate. Nature 415:514-517.

Slack JR, Landwher JM. 1992. Hydro-climatic data network: a US Geological Survey streamflow data set for the United States for the study of climate variations, 1874-1988. US Geological Survey Open-File Report 92-129.

Wahl KL. 1998. Sensitivity of non-parametric trend analyses to multi-year extremes. Pages 157-160 in Proceedings of the Western Snow Conference, Snowbird, Utah.

The Effects of Galactic Cosmic Rays on Weather and Climate on Multiple Time Scales

Ed Mercurio

This article is an update of the article published in the proceedings of the Seventeenth Annual Pacific Climate Workshop, March 2001. A longer, more detailed version is available on my website: http://www.hartnell.cc.ca.us/faculty/mercurio/

In this article, I show that galactic cosmic rays (GCRs) may be a primary climatic forcing agent on many time scales up to and including glacial-interglacial. Levels of GCRs are inversely related to the small changes in solar radiation that have long been considered the primary agent in climatic forcing and help explain the effects of solar related climatic periodicities already established. When solar radiation is low, GCR levels are high, and both of these result in increased cooling. The magnitude of the effects of GCRs on cooling through increasing cloud cover and cloud albedo, however, is much greater and increases in levels of GCRs could be the primary cause of global cooling (Svensmark 1998; Landscheidt 1998).

GCRs are the only particles hitting the earth with enough energy to penetrate the stratosphere and troposphere. They are modulated by the sun's and earth's magnetic fields. GCRs are a major determinant of levels of ionization in the troposphere. The ionization of the lower atmosphere by GCRs is the meteorological variable subject to the largest solar cycle modulation (Svensmark 1998). Levels of ionization are a major determinant of relative humidities, levels of condensation, levels of cloudiness and cloud albedo, which, in turn, are major determinants of temperatures, levels of surface moisture and levels of equability. More GCRs would result in clouds with greater numbers of condensation nuclei, which would likely produce less precipitation. GCRs may also increase storm intensities (vorticity area index) (Herman and Goldberg 1978; Tinsley and Dean 1991).

Levels of global cloudiness were observed to increase between 3% and 4% from solar maximum to solar minimum over an~11 year cycle period studied (Svensmark 1998). This is because the solar magnetic field is lower at solar minimum, allowing more GCRs to reach the earth. A strong correlation is present only in low cloudiness (2 miles or lower), which is the type that would increase cooling (Bailunas and Soon 2000). Bago and Butler (2000) found that there was only a significant degree of correlation to levels of low cloudiness in the tropics.

In my investigation of the possible role of GCRs in the determination of weather and climate, I made the following observations and conclusions:

1. ~11 year solar cycles alternate between parallel (-) and antiparallel (+), and consistently greater levels of GCRs reach the earth over most of the duration of antiparallel cycles (Figure 1). This results in~22 year meteorological cycles including such effects as major droughts on the western Great Plains and variations in precipitation from cyclonic storms in the westerlies in areas like Southern California. A curve of Los Angeles yearly precipitation totals shows an approximately 22 year cycle with generally progressively increasing totals during antiparallel cycles and generally progressively decreasing totals during parallel cycles (Figure 2). This

results in a pattern in which wettest years often occur around antiparallel to parallel solar maxima and the driest years often occur around parallel to antiparallel solar maxima.

2. A curve of annual GCR intensities over the last four solar cycles shows higher GCR levels at sunspot maxima of longer ~11 year cycles (Figure 1). Solar maximum could be the time when the greatest variations in GCR levels occur and this could be an important factor in periods of cooling, especially on century and millennial time scales.

3. Levels of GCRs appear to have a relationship to the state of the polar vortex and the state of the polar vortex is related to the state of the El Niño Southern Oscillation (ENSO). Higher levels of GCRs appear to be associated with a stronger, colder polar vortex. Some indications of a ~22 year periodicity in winter stratospheric temperatures can be seen in Figure 3. A stronger, colder polar vortex is generally associated with ENSO-Cold Event conditions and a warmer, weaker polar vortex with ENSO-Warm Event conditions. Some indications of this can be also be seen in Figure 3. An exception to this is ENSO-Warm Events associated with large, sulfurous volcanic eruptions.

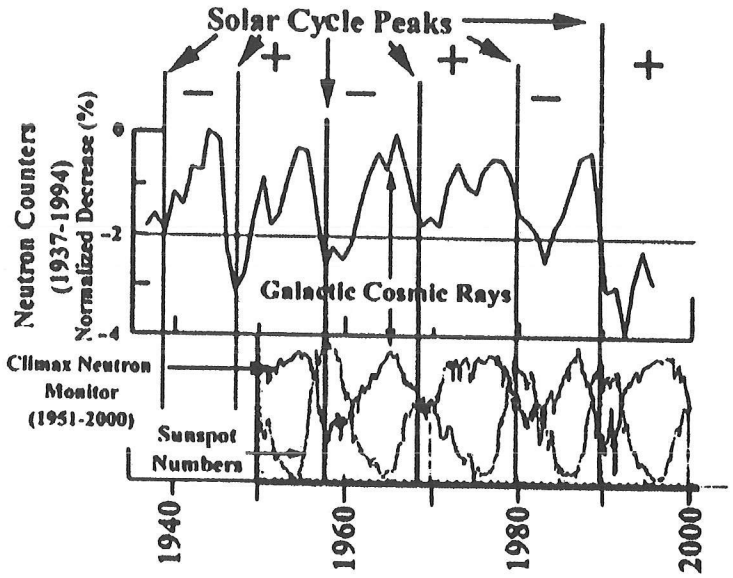

Figure 1 The top curve is the annual mean variation in cosmic ray flux as measured by ionization chambers from 1937 to 1994 (adapted from Svensmark 1998). The bottom curves are neutron flux, which is a proxy for galactic cosmic ray flux, from the neutron monitor in Climax, Colorado from 1951 to 2000 and sunspot number (adapted from University of Chicago/LASR GIF image). Note the differences in the shapes of the curves of GCRs in antiparallel (+) and parallel (-) solar cycles and the differences in GCR levels at solar maxima.

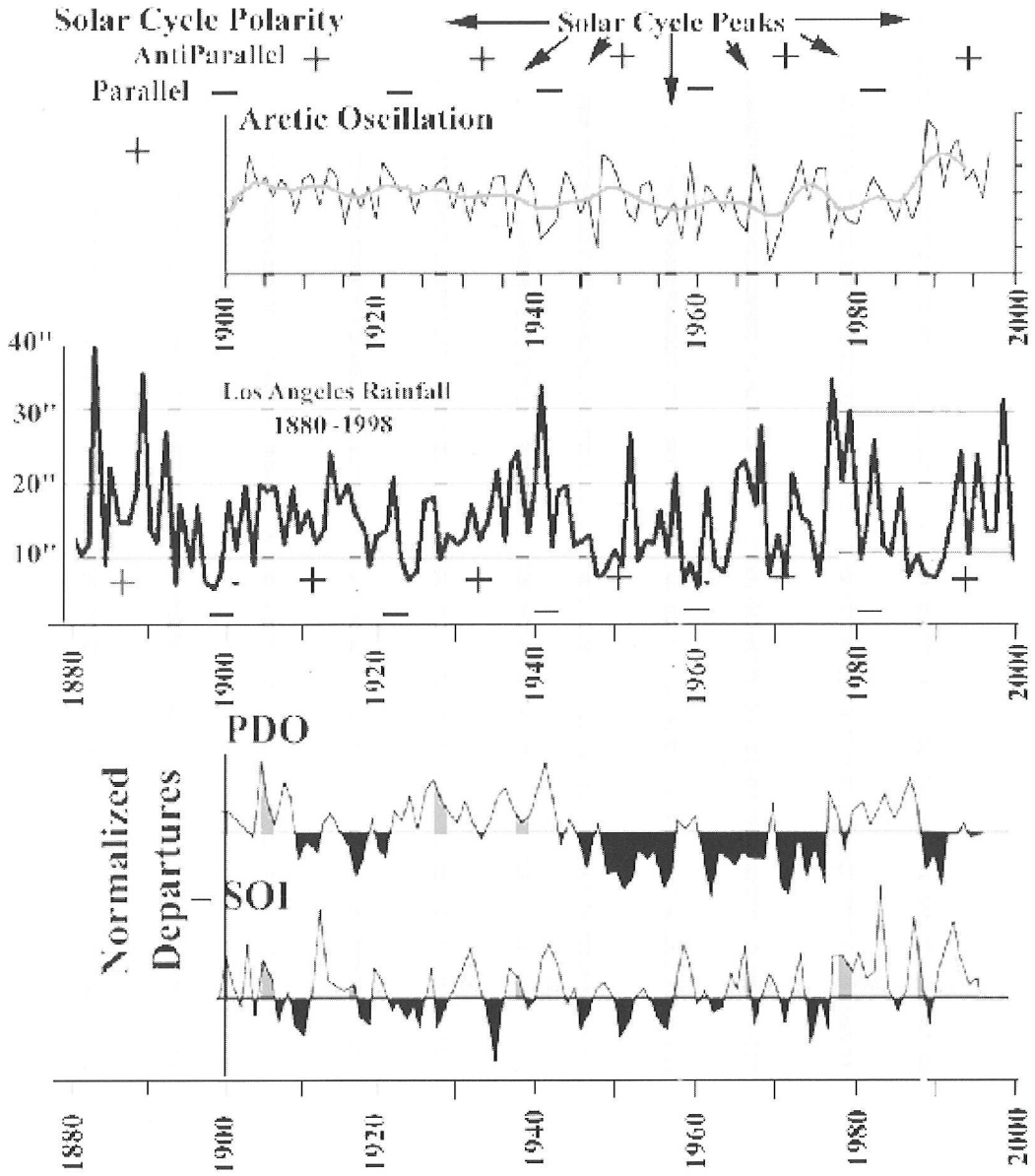

Figure 2 The top curve is the Arctic Oscillation Index with average values (adapted from Kerr 1999). More positive conditions indicative of a stronger, colder polar vortex are up in direction. The upper middle curve is July to June yearly U.S. Weather Bureau precipitation totals for Los Angeles civic center. The bottom curves are the Pacific Decadal Oscillation (PDO) and Southern Oscillation Index (SOI) (adapted from Mantua and others 1997). In the SOI curve, values indicative of ENSO-Warm Event conditions are above the line and values indicative of ENSO-Cold Event conditions are below the line and in the PDO curve, warmer sea surface temperatures are above the line and colder sea surface temperatures below the line. Note the general relationship between antiparallel (+) solar cycles and a more positive average Arctic Oscillation, progressively increasing Los Angeles precipitation totals, more positive (ENSO-Cold Event) SOI conditions and to a certain degree, more negative (colder) PDO conditions and the opposite for parallel (-) solar cycles. Also note the general relationship between ENSO-Warm Event conditions and higher Los Angeles precipitation totals.

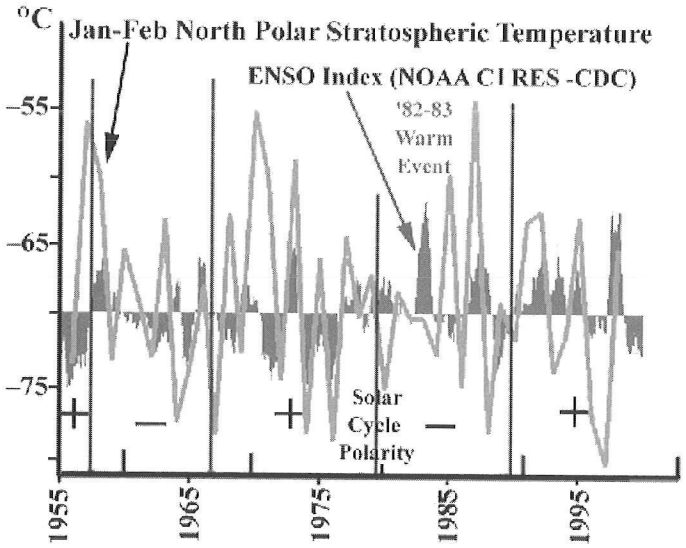

Figure 3 Comparison of January-February north polar stratospheric temperatures (adapted from Labizke and Van Loon 1999) and multivariate ENSO index (adapted from a NOAA- CIRES-Climate Diagnostic Center graphic). Note the relationship between higher temperatures and ENSO-Warm Event conditions and lower temperatures and ENSO- Cold Event conditions and ENSO-Warm Event anomalies that occur following large sulfurous volcanic eruptions such as El Chichon in 1982, Mount Pinatubo in 1991 and Mount Agung in 1963. (Unsmoothed data appears to show a closer relationship but is harder to visualize in a graphic and up to date sources were unavailable).

Over multidecadal and longer time periods, higher levels of GCRs are associated with a colder, more oscillating (frequent El Niños) tropical Pacific and lower levels with a warmer, more stable tropical Pacific. These effects, however, are also observable in the ~22 year solar cycle and many correlations of climate to ~22 year cycles, including droughts on the western Great Plains, are related to an increase in ENSO-Cold Event conditions that develop over the duration of antiparallel solar cycles.

Effects on ENSO appear to occur through effects on the strength of the Trade Winds, which are directly related to the strength of the polar vortex (Stricherz 1999; Chanin 1993). The Arctic Oscillation index is a measure of the variations in the strength of the polar vortex and some evidence for ~11 and ~22 year cycles can be seen in long term records (Figure 2).

The effect of GCRs on the polar vortex may occur in the following way:

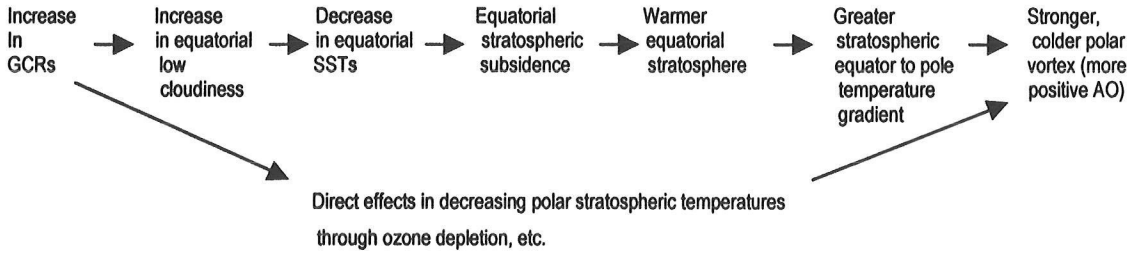

4. There appears to be a relationship between solar coronal hole area and the strength of the Arctic Oscillation. Areal extents of solar coronal holes change over solar cycles and are directly related to levels of GCRs and therefore directly related to levels of global cloudiness and inversely related to global temperatures (Soon and others 2000). There is a better correlation between solar coronal hole area specifically between solar latitudes 50° north to 50° south and the state of the Arctic Oscillation with greater coronal hole area correlated to a more positive state of the Arctic Oscillation (colder, stronger polar vortex) (Figure 4).

5. One effect of anthropogenic gasses that could contribute to global warming is to cool the stratosphere, either directly or indirectly, and in this way contribute to a more positive Arctic Oscillation. This may be a cause of recent highly positive levels in the Arctic Oscillation (Figure 2, Figure 4) as well as the Antarctic Oscillation.

6. There could be a relationship between GCRs and the Quasibiennial Oscillation (QBO), an oscillation of equatorial stratospheric winds. There is a quasibiennial oscillation in solar coronal hole area between solar latitudes 50° north to 50° south and the corresponding quasibiennial fluctuations in GCRs could somehow be involved in the origin of the QBO. The relationship of the temperature of the polar vortex to phase of the QBO changes over the ~11 year solar cycle. The reason for this could be because the quasibiennial oscillation in solar coronal hole area between solar latitudes 50° north to 50° south is slightly shorter than the QBO. If the variation in GCR levels corresponding to coronal hole area affects the temperature of the polar vortex, the interplay of the two cycles could result in the changing temperature relationship over the solar cycle in the following way:

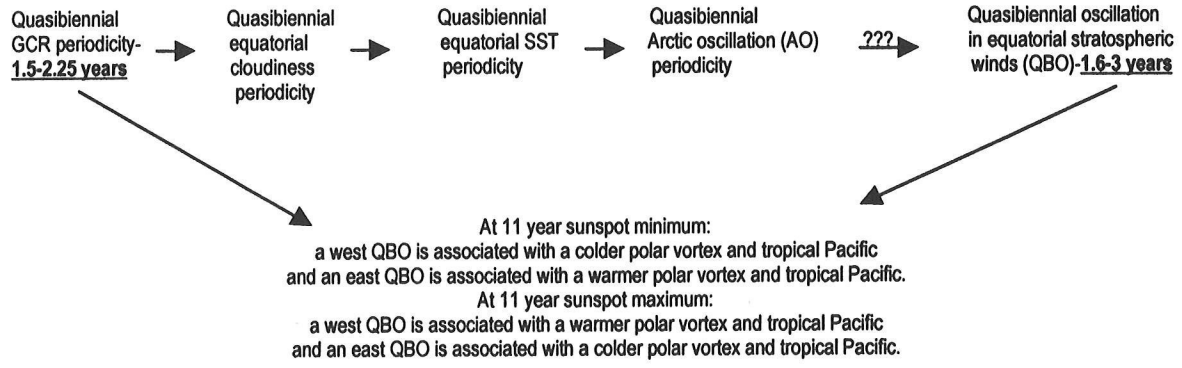

The periods of greater GCRs on the quasibiennial time scale may be most often associated with the west phase of the QBO. A strong polar vortex is three times more likely when the QBO is westerly and a weak polar vortex is twice as likely when the QBO is easterly (Baldwin and Dunkerton 2001). Also, the west phase of the QBO is longer in duration around solar minimum when there are more GCRs on the ~11 year solar cycle timescale. Data in Kane (1997) indicates that ENSO-Warm Events other than those associated with large, sulfurous volcanic eruptions often tend to be associated with every other easterly phase of the QBO. This is at least partly because ENSO-Warm Events often tend to be associated with a change from a strong to a weak polar vortex, as is the following. ~63% of ENSO-Warm Events have occurred during the descending phase of the sunspot cycle (Kane 1997). This is close to the

time of the shift in sunspot cycle polarity. It also appears that more ENSO-Warm Events may have occurred during the descending phase of parallel cycles (less GCRs) following the shift from antiparallel (more GCRs).

7. The shortest cyclic effects on climate of GCRs are on approximately weekly and monthly time scales and these may be the cause of reports of periodicities in weather phenomena on these time scales as reported in Glanz (1999). These effects arise because of variations in solar magnetism produced during the rotation of the sun. The sun has a 27 day rotation period and four magnetic sectors with boundaries equidistant from each other. Solar magnetic sector boundaries (heliospheric current sheet crossings) rotate past the earth approximately every 7 days. The increase in solar magnetic strength at these boundaries diminishes the levels of GCRs hitting the earth at the times of passage (Tinsley and others 1989). These decreases in levels of GCRs are called Forbush decreases and have been correlated with decreases in cloudiness (Veretenenko and Pudovkin 1995) and decreases in the vorticity area index (Herman and Goldberg 1978; Tinsley and Dean 1991). There are variations in solar sector structure. One sector boundary will often differ from the others in strength leading to a monthly periodicity. This could be a factor in the origin of the intraseasonal oscillations with periods usually ranging from 30 to 60 days that strongly modulate global weather.

8. Carbon 14 and Beryllium 10 records indicate that GCR levels may be the major determinant of climate variation in longer solar cycles. The most observable of these cycles are those of around 70 to 90 years in length (~80 year cycles) (Gleissberg cycles) and those of around 2,400 years in length. These cycles appear to vary in length depending on the varying lengths of the ~11 year solar cycles within them. The following meteorological factors influenced by GCRs are seen to vary with these cycles: global temperatures, total ozone levels, ENSO frequencies and amplitudes, phase of the Pacific Decadal Oscillation (PDO), the size of the circumpolar vortex, the zonal index and the earth's rotational velocity (length of day).

   Recent records show that a shift between phases of the PDO tends to occur at the lowest and highest points of ~80 year cycles. A shift to predominance of the cool phase occurs around the lowest levels of GCRs of the cycle and a shift to predominance of the warm phase occurs around the highest levels of GCRs. This information could be useful in the prediction of these important "regime shifts" in Pacific sea surface temperatures.

   The size of the circumpolar vortex is central to predicting the strength of the Indian and African Monsoons which have a remarkable resemblance to the inverse of levels of GCRs on the ~80 year cycle. The expansion of the circumpolar vortex during last peak in GCRs around 1975 was associated with the Sahelian droughts in Africa that occurred between 1970 and 1985 and killed 1.2 million people.

   Anderson (1992c) reports that ENSO-Warm Events are around twice as common during climatic minima of ~2400 year cycles. The history of the western tropical Pacific during glacial periods is indicative of more frequent and more severe ENSO-Warm Events during the climatic minima of ~2400 year cycles (stadials) and less frequent and less severe ENSO-Warm Events during the climatic maxima of ~2400 year cycles (interstadials) (Stott and others 2002).

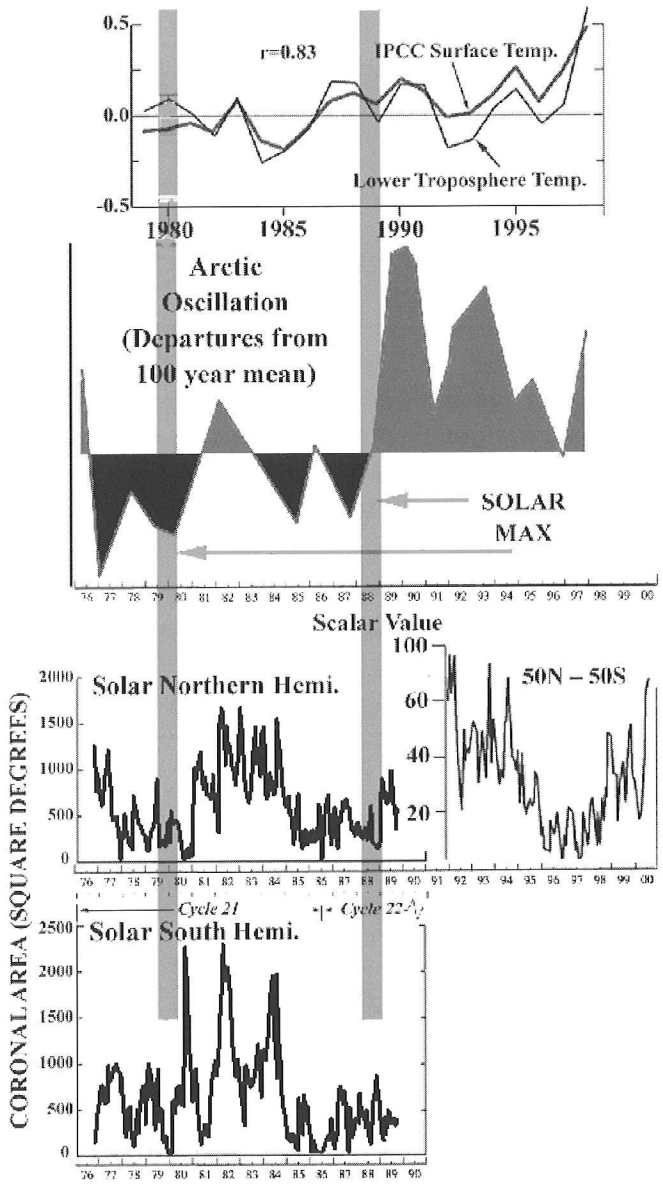

Figure 4 The upper curves are anomaly time series for observed surface and lower tropospheric temperature annual temperature data (adapted from Santer and others 2000). The upper middle curve is the Arctic Oscillation Index (adapted from Kerr 1999). The left side of the lower middle curve is solar coronal hole area in heliographic degrees between north solar hemisphere latitudes 10° to 50° (adapted from McIntosh and others 1992). The right side of the lower middle curve is solar coronal hole area in latitude correlated degrees between 50° north to 50° south solar latitudes (from K. Harvey, personal communication, 1999, derived from NSO helium 10830 data). The lowest curve is solar coronal hole area in heliographic degrees between south solar hemisphere latitudes 10° to 50° (adapted from McIntosh and others 1992). Note the relationship between total coronal hole area and Arctic Oscillation values. Note how the temperatures show an inverse relationship to the Arctic Oscillation Index with a two to three year lag time and how lower tropospheric temperatures are increasingly cooler than surface temperatures the greater the Arctic Oscillation Index and increasingly warmer than surface temperatures the smaller the Arctic Oscillation Index.

Slower rotational velocities (longer day lengths) occur at times of lower solar irradiance (Klyashtorin 1998; Courtillot and others 1982) which are times of higher levels of GCRs. This is probably due to greater meridionality at these times since the speed of rotation is directly related to the degree of zonality of the circumpolar vortex and overall strength of the westerlies. It appears that higher levels of volcanic and earthquake activity are associated with slower rotation speeds on most timescales.

9. In the longest climatic cycles that appear to be modulated by GCRs, the GCRs are modulated by geomagnetism instead of solar magnetism. These are the glacial-interglacial cycles and a ~13,000 year cycle. A direct relationship was found between the inclination of the earth with relation to external gravitational attraction and geomagnetic strength and this allowed the calculation of curves of the earth's geomagnetic history. The dynamo theory predicts that greater inclination will result in higher geomagnetism (Vanyo and Paltridge 1981). Four inclination data series are needed to calculate curves of past geomagnetism that would be induced (Figure 5, Figure 6). They are:

   a. *The inclination of the earth's orbital plane with relation to the invariable plane of the solar system.* I used a data series that had already been calculated for the last three million years by Dr. Richard A. Muller for his work on the astronomical forcing of glacial cycles. It has a ~100,000 year periodicity and a range over the last 3 million years of from ~.110° to ~2.94°. It is currently ~1.67°.

   b. *The earth's B angle.* This is the inclination of the earth's orbital plane with relation to the solar equatorial plane. I could find no existing data series for this. It was calculated by Dr. E. Myles Standish Jr. for the last three million years for this investigation. It has a ~70,000-year periodicity and a range over the last 3 million years of from ~3.25° to ~8.5°. It is currently ~7.25°.

   c. *The earth's orbital obliquity.* Data sets for this have been in existence for a long time since this was one of the three data sets used by Milankovitch in his hypothesis. I used a recent calculation of this by A. Berger available on the internet. It has a ~41,000 year periodicity and a range of from ~22.5° to ~24.5°. It is currently 23.5°.

   d. *The times of the year of the earth's maximum B angle value.* These times change because of the precessional motions of the earth. I could find no existing data set for this. This was also calculated by Dr. E. Myles Standish Jr. for the last three million years for this investigation. The time of the year of B angle values changes with the ~25,800 year cycle of precession of the earth's axis, but since the earth encounters the same angular relationship twice a year in its revolution around the sun, the cycle of angular change is actually ~13,000 years. It has a ~13,000 year cycle of times of the two times a year when maximum and minimum values occur. The maximal values currently occur in March and September.

   Curves and models were produced from this numerical data by Dr. Douglas McLain for this investigation.

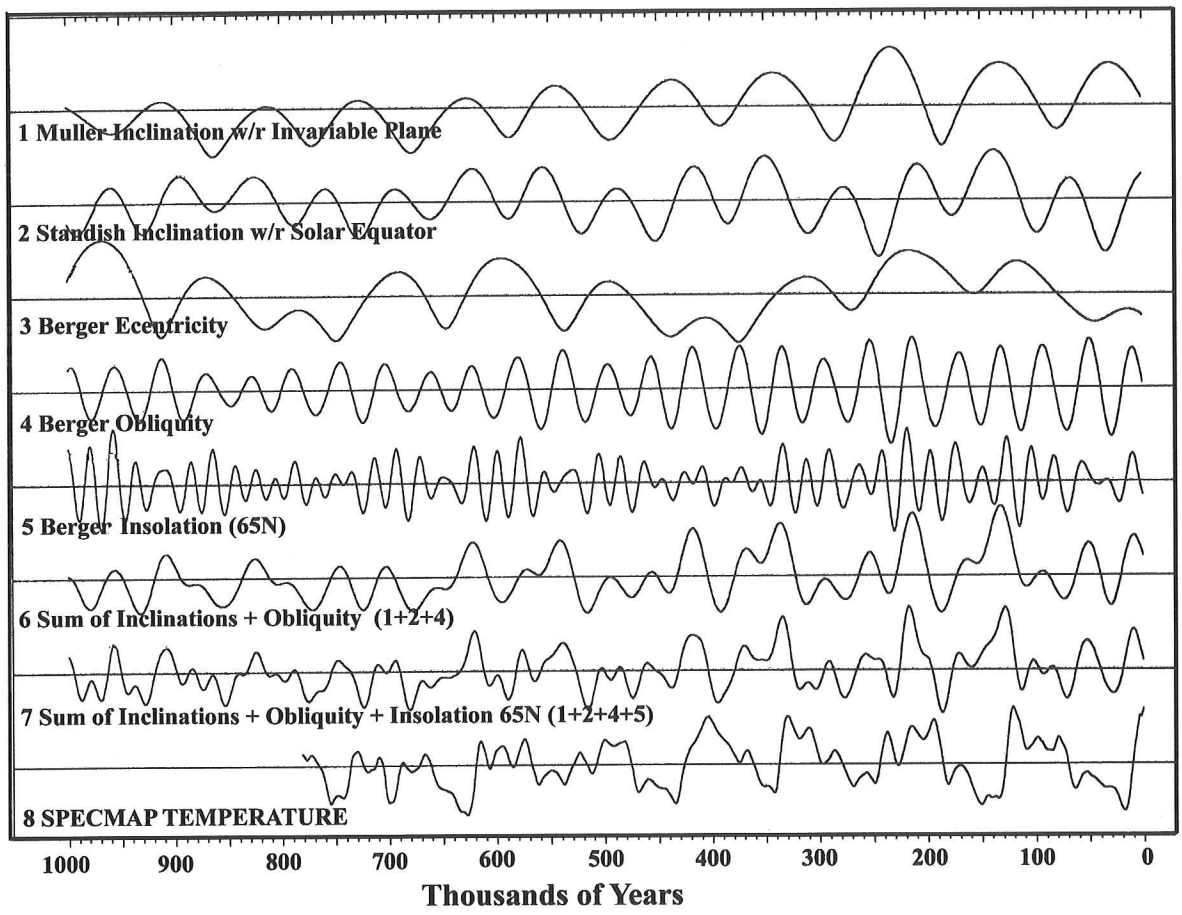

Figure 5 (1) Inclination of the earth's orbital plane with relation to the invariable plane of the solar system (by Muller, personal communication). (2) Inclination of the earth's orbital plane with relation to the equatorial plane of the sun (by Standish, for this project). (3) Orbital eccentricity of the earth (by Berger, World Data Center-A for Paleoclimatology). (4) Orbital obliquity of the earth (by Berger, World Data Center-A for Paleoclimatology). (5) June insolation at 65° north latitude (by Berger, World Data Center-A for Paleoclimatology). (6) Curve calculated from the sum of the inclination of the earth's orbital plane with relation to the invariable plane of the solar system + the inclination of the earth's orbital plane with relation to the equatorial plane of the sun + the earth's orbital obliquity. The height of this curve is hypothesized to be directly related to geomagnetic strength. (7) Curve calculated from the sum of the inclination of the earth's orbital plane with relation to the invariable plane of the solar system + the inclination of the earth's orbital plane with relation to the equatorial plane of the sun + the earth's orbital obliquity + June insolation at 65° north latitude. The height of this curve is hypothesized to be directly related to geomagnetic strength and summer northern high latitude insolation and to have the best direct relationship to paleotemperatures relating to glacial-interglacial chronology. Note the relationship of this curve to the SPECMAP curve. The highest points on this curve correlate to the starts of interglacial periods and the lowest points correlate to the starts of glacial periods and glacial periods get progressively colder until ended by one of the highest points which correlates to the start of the next interglacial. (8) SPECMAP paleotemperatures inferred from Atlantic Ocean sediment cores (by Duffy and Imbrie, World Data Center-A for Paleoclimatology).

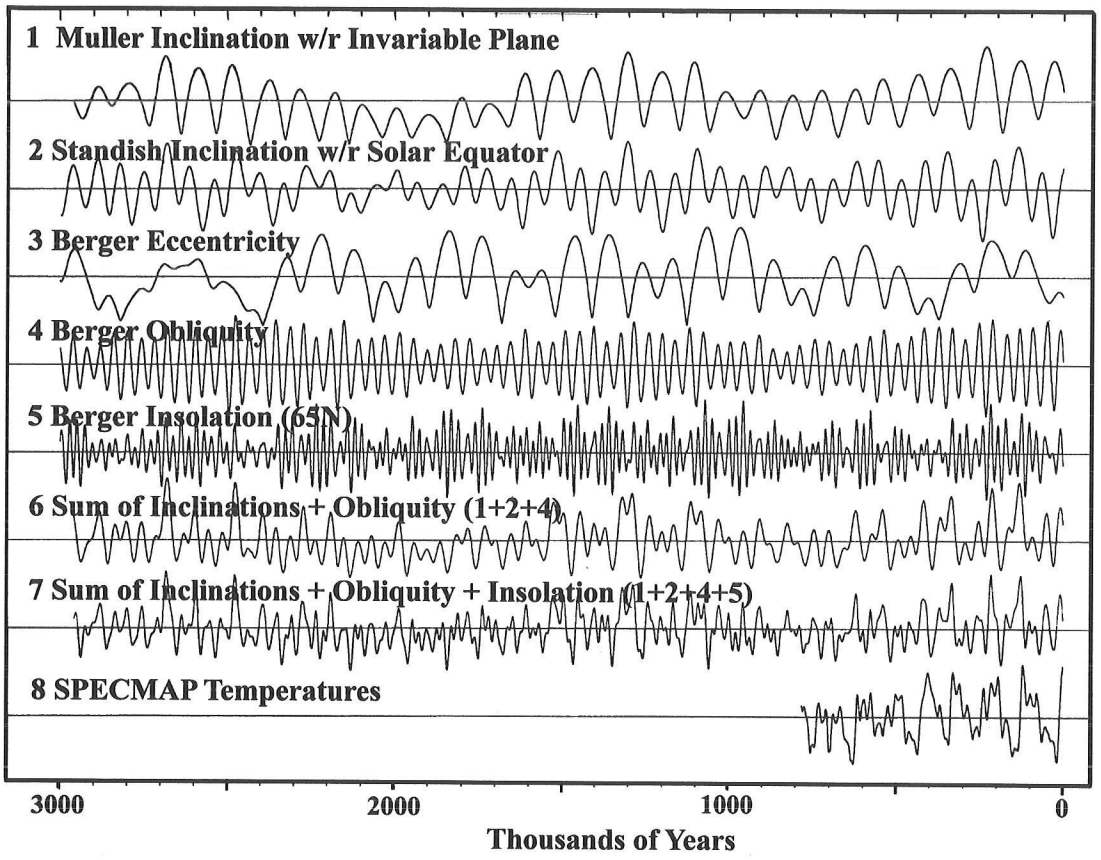

Figure 6 (1) Inclination of the earth's orbital plane with relation to the invariable plane of the solar system (by Muller, personal communication). (2) Inclination of the earth's orbital plane with relation to the equatorial plane of the sun (by Standish, for this project). (3) Orbital eccentricity of the earth (by Berger, World Data Center-A for Paleoclimatology). (4) Orbital obliquity of the earth (by Berger, World Data Center-A for Paleoclimatology). (5) June insolation at 65° north latitude (by Berger, World Data Center-A for Paleoclimatology). (6) Curve calculated from the sum of the inclination of the earth's orbital plane with relation to the invariable plane of the solar system + the inclination of the earth's orbital plane with relation to the equatorial plane of the sun + the earth's orbital obliquity. The height of this curve is hypothesized to be directly related to geomagnetic strength. (7) Curve calculated from the sum of the inclination of the earth's orbital plane with relation to the invariable plane of the solar system + the inclination of the earth's orbital plane with relation to the equatorial plane of the sun + the earth's orbital obliquity + June insolation at 65° north latitude. The height of this curve is hypothesized to be directly related to geomagnetic strength and summer northern high latitude insolation and to have the best direct relationship to paleotemperatures relating to glacial-interglacial chronology. Note the relationship of this curve to the SPECMAP curve. The highest points on this curve correlate to the starts of interglacial periods and the lowest points correlate to the starts of glacial periods and glacial periods get progressively colder until ended by one of the highest points which correlates to the start of the next interglacial. (8) SPECMAP paleotemperatures inferred from Atlantic Ocean sediment cores (by Duffy and Imbrie, World Data Center-A for Paleoclimatology).

10. The 13,000 year B angle timing cycle is the shortest of the inclination cycles and appears to have significant effects on climate. Maximal inclination, minimal GCRs and maximum warmth occur in this cycle when maximum B angles are in June and December due to the additive effect of the inclination to the obliquity of the earth's axis at these times. Minimal

inclination, maximal GCRs and maximum cold over this cycle occur when maximum B angles are in March and September when they do not add to the tilt of the earth's axis.

The effects of this ~13,000 year cycle are most easily observed during glacial periods where they often correspond to what are termed Bond Cycles. In Figure 7, the curve of B angle times shown in Figure 8 is compared to temperature changes over much of the last glacial period. Note how the June-December B angle maxima are often associated with the major warmings following colder periods and iceberg discharges into the North Atlantic termed Heinrich Events at the end of Bond Cycles. The March-September B angle maxima are often associated with colder periods not followed by rapid warmings. Since both of these are associated with colder periods, this often gives the appearance of ~6000 year cycles in the paleorecord.

The ~13,000 year cycle can also be related to events from deglaciation through the Holocene. They are: the start of deglaciation (June-December, 19-20,000 years ago), the Younger Dryas period (March-September, 12-14,000 years ago), the Altithermal period (June-December, 6-7,000 years ago) and the Little Ice Age, the coldest period since deglaciation (March-September, 1000 years ago to present).

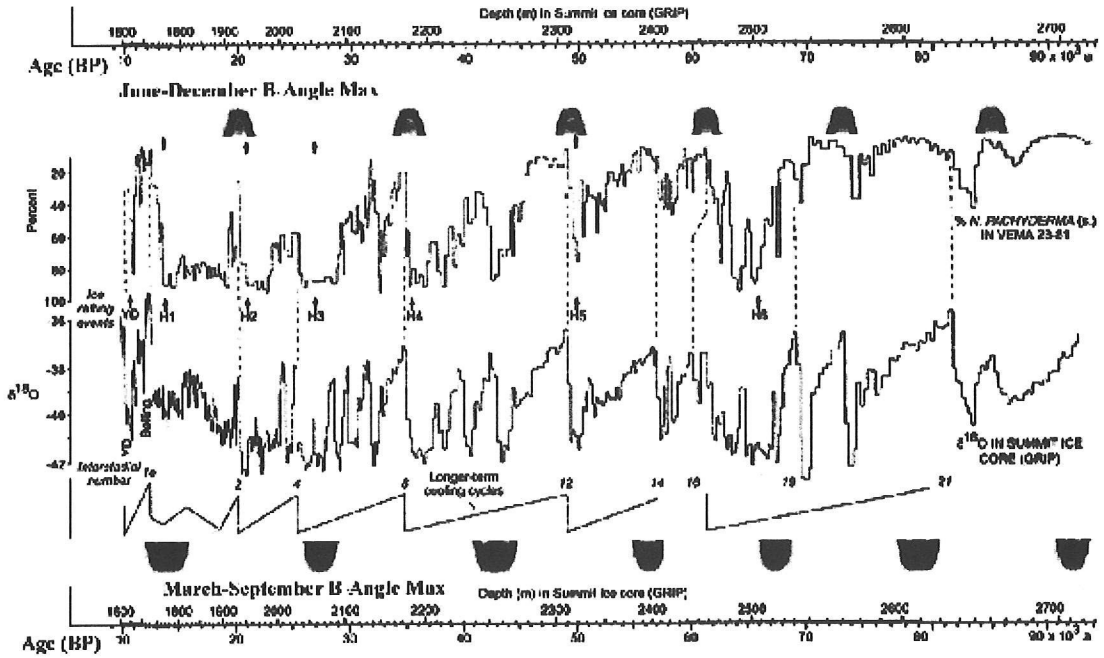

Figure 7 Comparison of times of the year of B angle maxima and minima taken from high and low points of curve 1 in Figure 13 (calculated by Dr.E. Myles Standish Jr. for this project) with the GRIP Greenland ice core temperature record as indicated by O^{18} and a deep sea core temperature record from the North Atlantic as indicated by foraminifera percentages (adapted from Bradley 1999). The bottom curve, also from Bradley 1999, shows general trends in temperatures. Note the general relationship of June-December B angle maxima to periods of rapid warming including some Heinrich events and the general relationship of March-September B angle maxima to cooing events between periods of rapid warming.

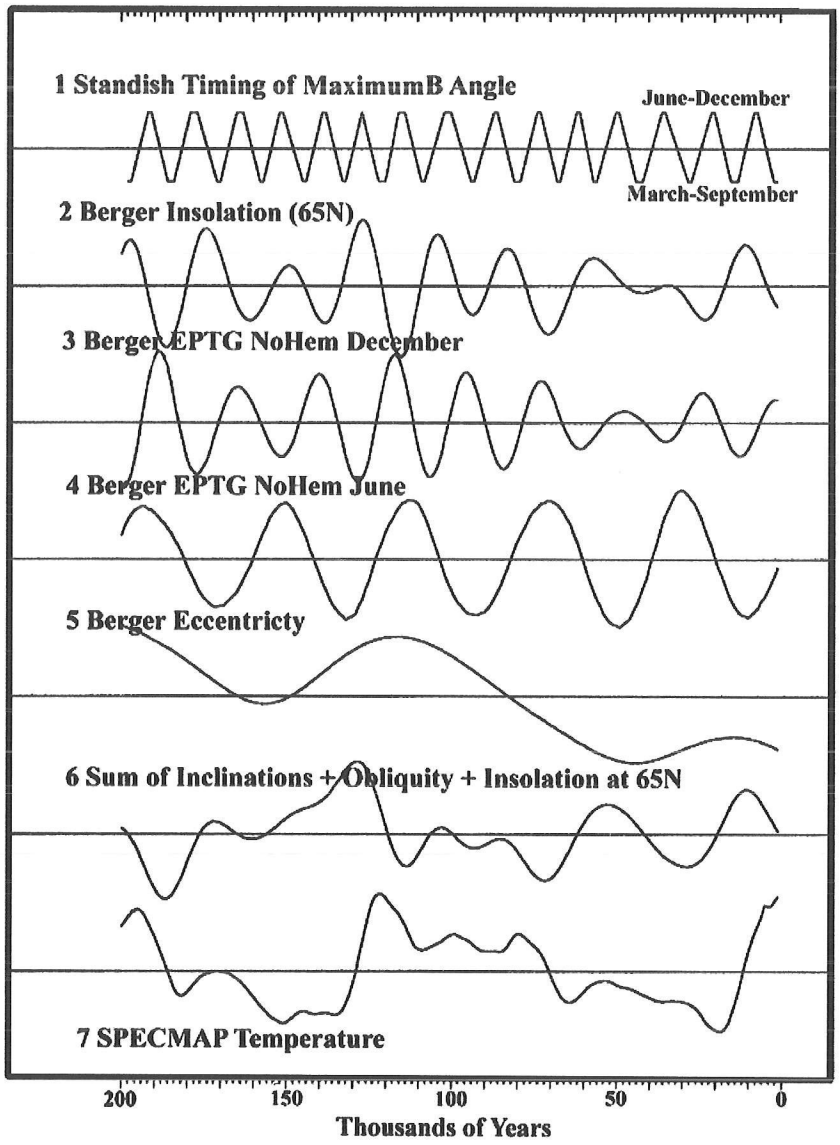

Figure 8 (1) Curve of the time of the year of the maximum B angle with June-December as top points and March-September as bottom points (by E. Myles Standish Jr. for this project). (2) June insolation at 65° north latitude (by Berger, World Data Center-A for Paleoclimatology). (3) Equator to pole temperature gradient for Northern Hemisphere in December (from data from Berger, World Data Center-A for Paleoclimatology). (4) Equator to pole temperature gradient for Northern Hemisphere in June (from data from Berger, World Data Center-A for Paleoclimatology). (5) Orbital eccentricity of the earth (by Berger, World Data Center-A for Paleoclimatology). (6) Curve calculated from the sum of the inclination of the earth's orbital plane with relation to the invariable plane of the solar system + the inclination of the earth's orbital plane with relation to the equatorial plane of the sun + the earth's orbital obliquity (see Figures 5 and 6). The height of this curve is hypothesized to be directly related to geomagnetic strength. (7) SPECMAP paleotemperatures inferred from Atlantic Ocean sediment cores (by Duffy and Imbrie, World Data Center-A for Paleoclimatology).

11. The largest variations in the inclination related motions of the earth cause the largest variations in geomagnetism which cause the largest variations in GCR levels resulting in glacial-interglacial periodicities. In my curves, inclination with relation to the invariable plane plus inclination with relation to the solar equator establishes the basic beat frequency seen in paleotemperatures of alternating ~80,000 and ~120,000 year periods (see Figures 5 and 6). This is especially observable in comparisons of times of peak interglacial warmth. This is the first explanation for the origin of this beat frequency that I know of. Adding obliquity to the above mentioned curve gives a curve that includes the ~41,000 year periodicity that is present in glacial-interglacial cycles even when the ~100,000 year periodicities are not. The ~41,000 year cycle was dominant prior to ~800,000 years ago and one possible reason for the switch to ~100,000 year cycles was the climatic effects of increasing mountain heights. Another can be seen in the curves. The values for inclination with relation to the solar equator and inclination with relation to the invariable plane were less immediately prior to this time and at other times possibly allowing obliquity to be play a more dominant role (see Figure 9). Adding summer insolation at 65°N further increases the similarity to the SPECMAP curve by adding precession related periodicities. Insolation fits in best at a 1/4 to 1/6 weighting. Summer high latitude insolation values are matched in time and magnitude by corresponding winter equator to pole temperature gradient values that result in similar effects on climate (See Figure 8). In the Milankovitch hypothesis, summer insolation at 65°N is usually used as the primary determinant of the timing of glacial-interglacial periodicities. Compare the similarities of the curve of summer insolation at 65°N and my curve to SPECMAP in Figure 6. Note how much better my curve fits the SPECMAP curve. The origin of glacial-interglacial periodicities by changing levels of GCRs does not have the numerous inadequacies seen in the Milankovitch hypothesis as described by Karner and Muller (2000) and others.

12. A ~412,000 year cycle is present. It is caused by changes in geomagnetism induced by the earth's orbital eccentricity. The effects of this cycle are not indicated in the inclination related curves presented here. The modulation of geomagnetism by the ~412,000 year cycle can be seen in Figures 10 and 11. The Stage 11 interglacial at around 400,000 years ago and the Holocene interglacial are considerably warmer than their inclination based curves on my figures indicate due to the highest geomagnetism induced by the lowest eccentricities of this cycle. The sea level was 15 to 20 meters higher in Stage 11 than it is today (Chappell 1998). That interglacial also lasted around 50,000 years longer than the Holocene has so far (60,000 years in all) (Howard 1997). It is likely that the Holocene will have a course similar to the stage 11 interglacial (Berger and Loutre 2002).

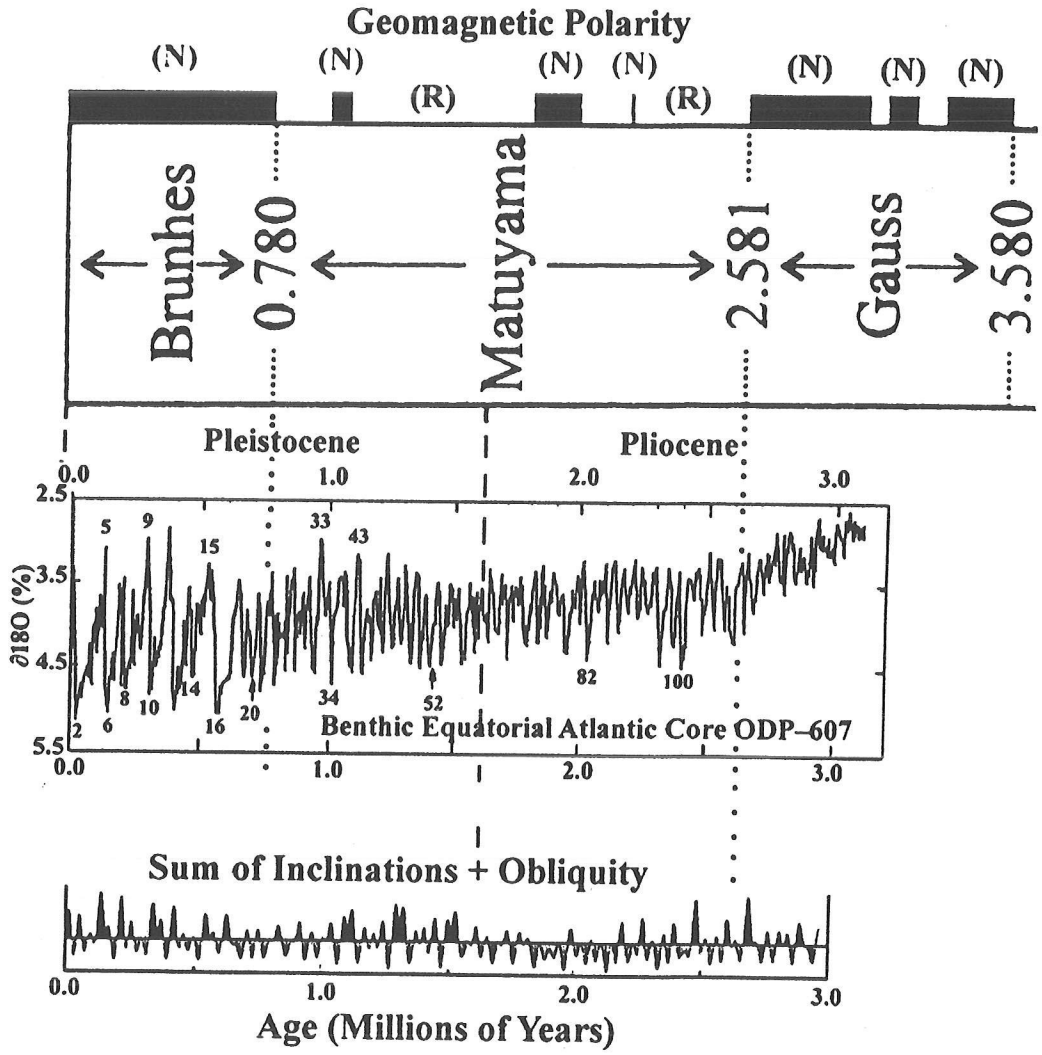

Figure 9 Comparison over 3 million years of sum of inclinations + obliquity curve, temperature records indicated by O^{18} from equatorial Atlantic deep sea core ODP-607 (adapted from Bradley 1999) and geomagnetic polarity (adapted from Merrill and others 1996). Note general relationship of greater amplitudes and more ~100,000 year glacial cycles as opposed to 40,000 year cycles in temperature variations curve with greater amplitudes in sum of inclinations + obliquity curve, especially in the last 1,200,000 years, and lower frequency of geomagnetic reversals in times of higher amplitudes in sum of inclinations + obliquity curve. Also note a relationship in more recent time of greater amplitudes and more ~100,000 year cycles with normal geomagnetic polarity (N) as opposed to reversed (R).

13. The glacials preceding these previously mentioned large interglacials are longer and colder than their curves indicate since geomagnetism appears to progressively decrease and reach its lowest point in the 412,000 cycle before rapidly rising to maximum levels (Yamazaki, and others 1995) (Figures 10 and 11). The Stage 12 glacial that preceded the Stage 11 interglacial was the coldest on record with an ice volume estimated to be 15 to 20% greater than at the peak of the last glacial period and a sea level depression of 140 meters (Chappell 1998). This is 20 meters greater than that of the last glacial which was also one of the colder ones.

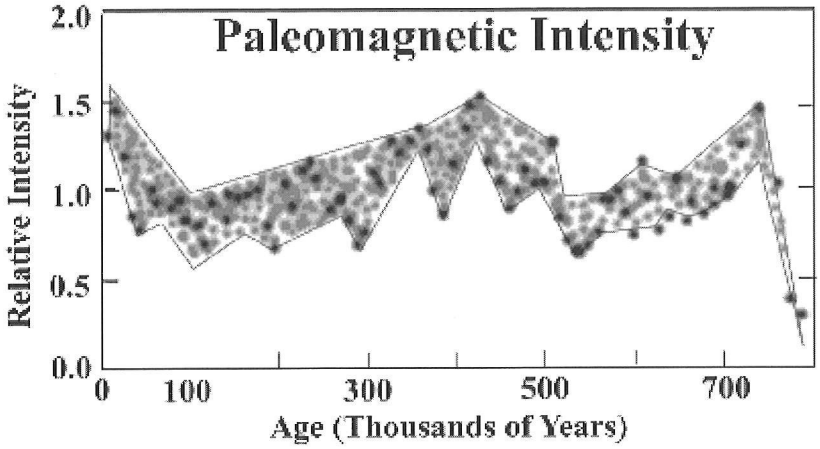

Figure 10 This is a curve of paleomagnetic intensity over the last 800,000 years that shows the effects of the ~412,000 year eccentricity cycle (adapted from Yamazaki and others 1995). Note the high points now, around 400,000 years ago and what may be around 800,000 years ago interrupted by a geomagnetic reversal. Also note the long term, progressively decreasing geomagnetism leading to the lowest values just before the fast increases around the times of maxima.

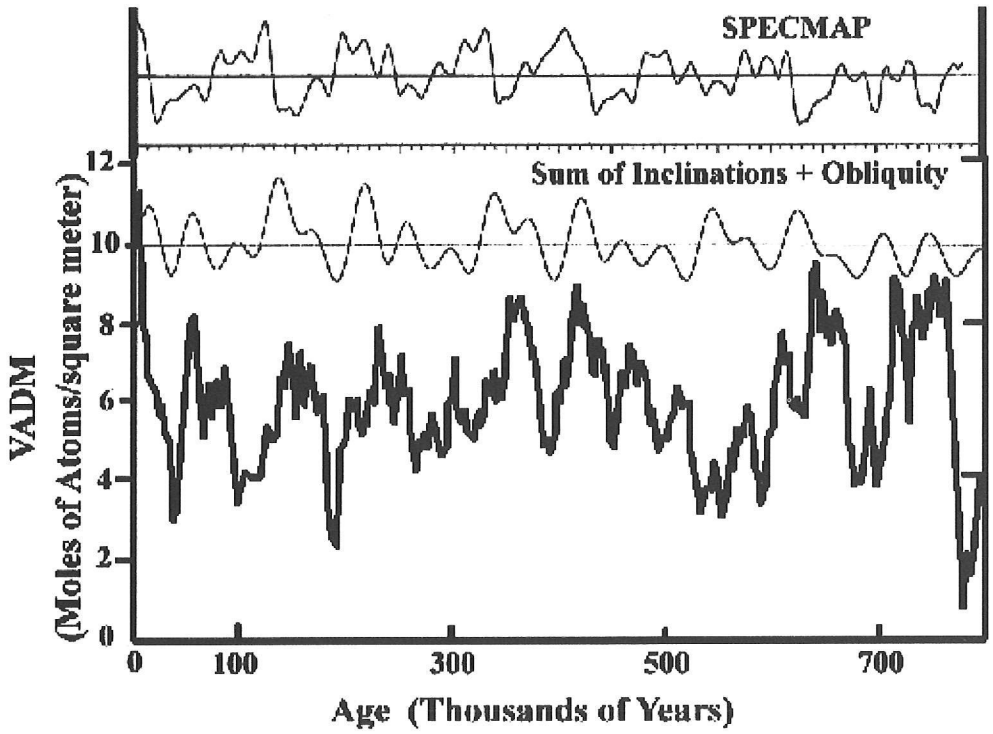

Figure 11 Comparison of 800,000 year synthetic curve of geomagnetism derived from 33 records of paleointensity (adapted from Guyodo and Valet 1999) with sum of inclinations + obliquity curve and SPECMAP curve of deep ocean core temperatures. Note general relationship of higher values on the sum of inclinations + obliquity curve with higher geomagnetism. Note how turns towards glacial or interglacial conditions generally occur in SPECMAP at minimal or maximal geomagnetic values respectively.

14. Records of paleomagnetism support the forcing of glacial-interglacial cycles by geomagnetically modulated GCR levels. Figure 11 includes an 800,000 year curve of geomagnetism, which is an integration of 33 records of relative paleointensity. The ~412,000 year cycle of geomagnetism is prominent in this curve of geomagnetism with peaks around 800,000 and 400,000 years ago and now and the beat frequency of alternating ~80,000 and ~120,000 year cycles can be observed within the last ~450,000 years. Within the last ~200,000 years, periods of glacial initiation appear to correspond to well known geomagnetic excursions. This indicates that at least one cause of geomagnetic excursions is the lowest of inclination values. Figure 12 includes a curve of geomagnetism over the last 130,000 years. It is one of the most accurate and detailed available. Note how closely it matches the curve derived from the sum of inclinations plus obliquity values alone and the similarity of both of these curves to the Vostok Antarctic surface temperatures and Beryllium 10 record. Also note the thin spikes at ~120,000 and ~15,000 to ~10,000 years ago that may indicate the presence of short duration high values that exceeded the threshold for interglacial climates. The similarities between the curves in this figure provide strong evidence for the origin of glacial-interglacial periodicity through variations in GCR intensity modulated by geomagnetism. A longer Be^{10} record going back 200,000 years presented in Sharma (2002) shows a good relationship to the sum of inclinations plus obliquity values occurring earlier than those shown in Figure 12.

15. Calculations of the increases in ionization levels at glacial maximum are consistent with modulation of glacial-interglacial periodicities by GCRs. Data from Lingenfelter and Ramaty (1970) indicate that the GCR levels at the geomagnetism of the last glacial maximum (dipole moment of 1) at sunspot minimum would be approximately 200% of today's values as measured by C^{14} at 73° latitude. Data from Volland (1995) indicate that the atmospheric ionization at tropopause levels produced by 200% of today's GCR levels would be approximately 306% of current ionization levels.

    I have not been able to find enough information at this time to be able to reliably calculate the changes in cloudiness that would result from these changes in ionization. However, the maximum estimate of the percent change in low cloudiness over the last solar cycle (~4%) was approximately one-third of the percent change in GCR levels (~12%) and approximately one fifth of the percent change in ionization at tropopause levels (~20%) over the same period and these relationships can be used to obtain some very rough estimates. Rough extrapolations from the changes in GCR levels as compared to cloudiness at the above mentioned conditions over the last solar cycle give an increase in low cloudiness of around 33% at glacial maximum at a dipole moment of 1 and a decrease of around 9% at maximum Holocene geomagnetism at a dipole moment of 15.

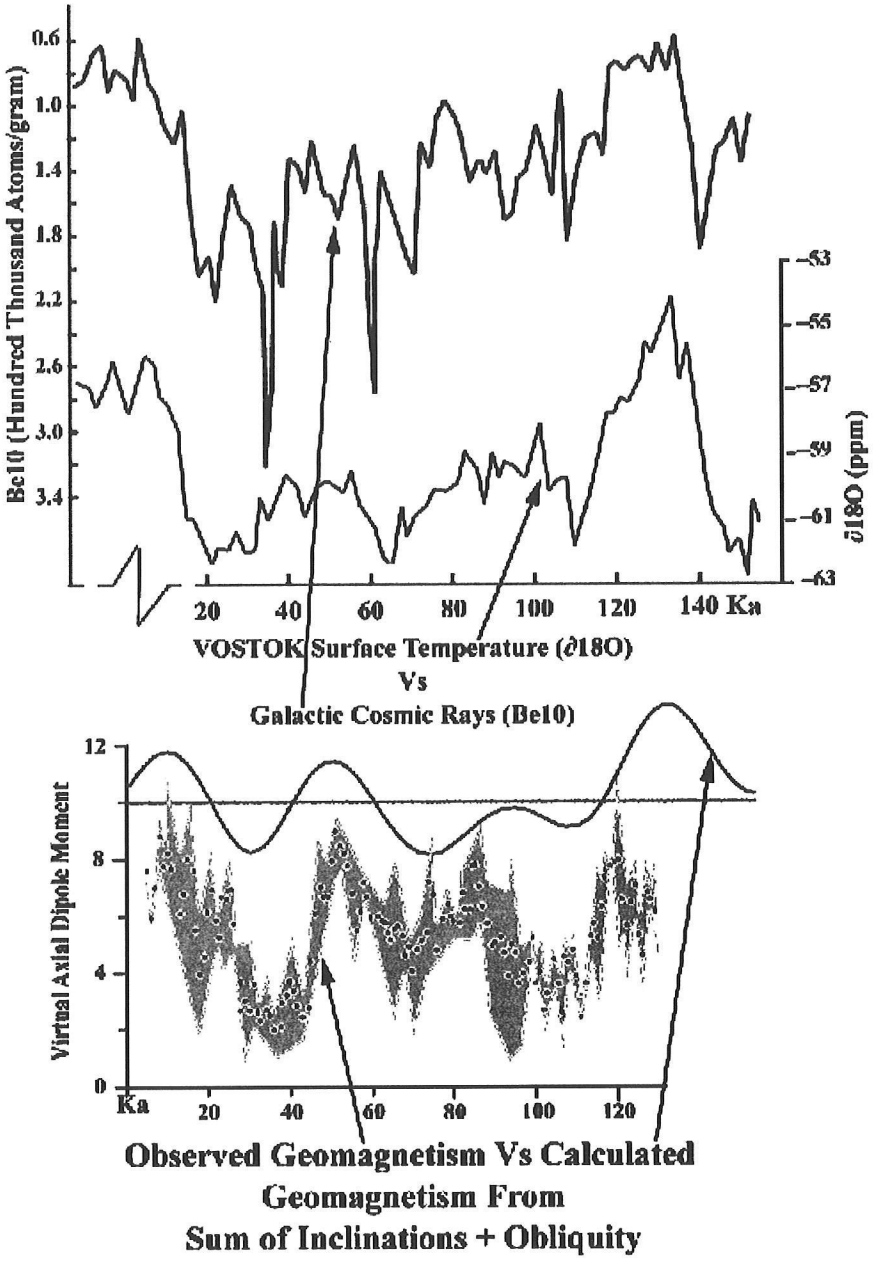

Figure 12 Comparison of observed geomagnetism obtained from four deep sea sediment cores from the Sulu Sea (Philippines) (adapted from Merrill and others 1996) with geomagnetism as indicated from the calculated sum of inclinations + obliquity curve. The geomagnetism curves are compared to temperatures as inferred from O^{18} levels from the Vostok Antarctic ice core and the Be^{10} concentration from the Vostok ice core which provides a record of galactic cosmic ray intensity (adapted from Raisbeck and others 1987). Note the inverted scale for the Be^{10} curve indicating greater galactic cosmic ray intensity in a downward direction. The sediment cores from the Sulu Sea show strong, stable magnetizations at high sedimentation rate and provide a geomagnetic history regarded as one of the most accurate available. Note the similarity between the curves providing evidence that inclinations + obliquity modulate geomagnetism, geomagnetism modulates galactic cosmic ray intensity, and galactic cosmic ray intensity modulates climate, in this case glacial-interglacial periodicity.

At today's levels of geomagnetism, (dipole moment 8) there is approximately a 12% difference in GCR levels between sunspot maximum and minimum. Theoretically, there is currently about a 20% difference in ionization at tropopause levels between sunspot maximum and minimum, but a 50% difference has been reported (Tinsley and others 1989). At a dipole moment of 1, the differences between sunspot maximum and minimum would be much greater. Data from Lingenfelter and Ramaty (1970) indicate that the range in GCR levels would be approximately 243% of today's and data from Volland (1995) indicate that the theoretical range in ionization at tropopause levels at 73° latitude would be approximately 340% of today's. This is interesting because a 60-year tree ring record from Rancho La Brea in the Los Angeles area near the end of the last glacial period shows both substantially higher precipitation totals at times and substantially greater precipitation variability than today (Templeton 1977). The ~22 year cycle is evident in this record with the wettest periods (presumably antiparallel to parallel transitions) reaching a maximum of 75 inches per year and the driest periods (presumably parallel to antiparallel transitions) reaching a minimum of 10 inches per year. The wettest periods in this record could also have occurred during strong, glacial period ENSO-Warm Events.

16. There is paleoenvironmental evidence for consistent ENSO-Cold Event conditions with frequent, severe short term oscillations to ENSO-Warm Event conditions during glacial periods and an absence of these conditions during the early Holocene when GCR levels were probably at their lowest (Kerr 1999a; Athanasios and others 2002).

17. Consistently high relative humidities, condensation and equabilities produced by the high levels of GCRs present in glacial periods helps in the understanding of what are often said to be "paradoxical glacial environments with no modern analogs." These environments have been termed "heterogeneous mosaic savannas" (Guthrie 1984). This type of environment often appears to be associated with considerable dryness but with abundant superficial moisture available from condensation during periods of low precipitation. There is, in general, evidence of less precipitation than today, but there is unusually high, year round biological productivity and unusually high numbers and diversities of species, often including species together that are characteristic of very different environments today. Even environments at the margins of continental ice sheets were mostly free of snow cover year round and had much milder winter temperatures than the same areas do today. One need only to look at the present distribution of Pleistocene relict species, and the numbers and diversities of species per area to see the connection to consistently high relative humidities, condensation and equabilities.

18. The extinctions of Pleistocene megafauna that occurred around the start of the Holocene can be best understood by looking at environmental changes produced by changes in levels of GCRs. As mentioned previously, due to the ~412,000 year geomagnetic cycle, the Holocene is unique in having the consistently highest levels of geomagnetism since those of Interglacial Stage 11 around 400,000 years ago. These consistently high levels of geomagnetism have created a Holocene environment that is unique in its climatic stability and environmental segregation and zonation. The Holocene environment is very different from those of interglacials occurring at other times in the ~412,000 cycle which were characterized by climate fluctuations as great as those seen in glacial periods (Kerr 1993). It is only during the

extreme climates of interglacials occurring during these highest periods of geomagnetism of the ~412,000 year cycle that the "heterogeneous mosaic savannas" of worldwide distribution that supported the Pleistocene megafauna largely disappeared.

The peak on the combined inclinations and obliquities curve at ~50,000 years ago during the last glacial was somewhat lower than the peak that correlates to deglaciation and was short of the interglacial threshold in the Northern Hemisphere (Figure 8). It did produce glacial to interglacial environmental changes in the Southern Hemisphere, however, which resulted in the extinction of the Pleistocene megafauna of Australia at this time and a rapid emergence and expansion of modern humans out of Africa and into most of the Old World. These migrations of humans into new areas, and the later migrations into the New World at the end of the last glacial period were much less a cause of megafaunal extinctions than a result of them.

The last major extinctions and migrations to occur before those of the last glacial- Holocene transition were the Irvingtonian which occurred between Glacial Stage 12 and Interglacial Stage 11 around 400,000 years ago. This was the last time geomagnetic conditions, and hence environmental conditions, were similar to those of the last glacial- Holocene transition.

The fact that the Holocene is unique among the three most recent interglacials negates one of the main arguments in favor of Pleistocene overkill and other hypotheses for the late Quaternary extinctions not involving major changes in environmental factors. That argument is: "the megafauna survived other interglacials, so the transition from the last glacial to Holocene interglacial environmental conditions could not have been a major factor in these extinctions."

The start of civilization coincides with the decline of the "hererogeneous mosaic savanna" and the extinction of the megafauna. This "fall from Eden" was probably a major factor in the start of agriculture. Other factors were the simplification and zonation of ecosystems and the anomalous stability of Holocene climate, both of which also made a sedentary existence in optimum areas and agriculture to augment environmental deficiencies desirable.

19. The understanding of the role of GCRs in atmospheric processes could help provide a simple unifying context that could improve the understanding and forecasting of weather and climatic change on all time scales and could also help in the understanding of major scientific problems in the earth and life sciences.

References

Athanasios K, Lynch-Stieglitz J, Marchitto TM Jr, Sachs J P. 2002. El Niño-lake pattern in ice age tropical Pacific sea surface temperature. Science 297:226-230.

Anderson RY. 1992. Solar variability captured in climatic and high-resolution Paleoclimatic records: A geological perspective. Pages 543-561 in: The Sun in Time, (Sonnet CP, Giampapa MS, Matthews MS, editors), University of Arizona.

Bago E, Butler C. 2000. The influence of cosmic rays on terrestrial clouds and global warming. Astronomy and Geophysics 41 (issue 4):18-22.

Bailunas S, Soon W. 2000. The sun also warms. Presented at the GCMI/CEI Cooler Heads Coalition, Washington, DC, March 24, 2000, http://www.marshall.org/sunalsowarms.htm (September 22, 2000).

Berger A, Loutre MF. 2002. An exceptionally long interglacial ahead? Science 279:1287- 1288.

Bradley RS. 1999. Paleoclimatology, reconstructing climates of the Quaternary. International Geophysics Series, V. 64, Harcourt-Academic Press.

Chanin M-L. 1993. The role of the stratosphere in global change. NATO ASI Series, Volume 8, Springer-Verlag.

Chappell J. 1998. Jive talking. Nature 394:130-131.

Courtillot V, Le Mouel JL, Ducruix J. 1982. Geomagnetic secular variation as a precursor of climatic change. Nature 297:386-387.

Glanz J. 1999. Landscape changes make regional climate run hot and cold. Science 283:317-320.

Guthrie RD. 1984. Mosaics, allelochemics and nutrients: an ecological theory of Late Pleistocene megafaunal extinctions. Pages 259-298 in: Quaternary Extinctions, A Prehistoric Revolution, (Martin PS, Klein RG, editors), University of Arizona Press.

Guyodo Y, Valet J. 1999. Global changes in intensity of the Earth's magnetic field during the past 800 kyr. Nature 399:249-252.

Herman JR, Goldberg R A. 1978. Sun, weather and climate. National Aeronautics and Space Administration.

Howard W. 1997. A warm future in the past. Nature 388:418-419.

Kane RP. 1997. Quasi-biennial and quasi-triennial oscillations in geomagnetic activity indices. Annales Geophysicae 15:1581-1594.

Karner DB, Muller RA. 2000. A causality problem for Milankovitch. Science, 288:2143-2144.

Kerr R. 1993. Even warm climates get the shivers. Science 261:292.

Kerr RA. 1999. A new force in high-latitude climate. Science 284:241-242.

Kerr RA.1999a. El Niño grew strong as cultures were born. Science 283:467-468.

Klyashtorin LB. 1998. Long term climate change and main commercial fish production in the Atlantic and Pacific. Fisheries Research. 37:115-125.

Landscheidt T. 1998. Solar activity: a dominant factor in climate dynamics. http://www.microtech.com.au/daly.solar.htm. (Dec. 18, 1998).

Lingenfelter RE, Ramaty R. 1970. Astrophysical and geophysical variations in C14 production. Pages 513-535 in: Nobel Symposium 12; Radiocarbon variations and absolute chronology, (Olsson IU, editor), John Wiley & Sons, Inc.

Mantua NJ, Hare SR, Zhang Y, Wallace JM, Francis RC. 1997. A Pacific interdecadal climate oscillation with impacts on salmon production. Bulletin of the American Meteorological Society 78:1069-1079.

McIntosh PS, Thompson RJ, Willock EC. 1992. A 600-day periodicity in solar coronal holes. Nature 360:322-324.

Merrill RT, McElhinny MW, McFadden PL. 1996. The magnetic field of the Earth: paleomagnetism, the core, and the deep mantle. Academic Press.

Muller RA. 1997. Glacial cycles and astronomical forcing. Science 277:215-218.

Raisbeck GM, Yiou F, Bourles D, Lorius C, Jouzel J, Barkov NI. 1987. Evidence for two intervals of enhanced ^{10}Be deposition in Antarctic ice during the last glacial period. Nature 32:273-277.

Santer BD, Wigley TML, Gaffen DJ, Bengtsson L, Doutriaux C, Boyle JS, Esch M, Hnilo JJ, Jones PD, Miihl GA, Roeckner E, Taylor KE, Wehner MF. 2000. Interpreting differential temperature trends at the surface and in the lower troposphere. Science 287:1227-1232.

Sharma M. 2002. Variations in solar magnetic activity during the last 200,000 years: is there a sun-climate connection? Earth and Planetary Science Letters 199:459-472.

Soon W, Baliunas S, Posmentier ES, Okeke P. 2000. Variations of solar coronal hole area and terrestrial lower tropospheric air temperature from 1979 to mid- 1998: astronomical forcings of change in earth's climate? New Astronomy 4:(8) 563- 579.

Stott L, Poulsen C, Lund S, Thunell R. 2002. Super ENSO and global climate oscillations at millennial time scales. Science 297:222-226.

Stricherz V. 1999. UW scientists say Arctic oscillation might carry evidence of global warming, News and Events, University of Washington 1-3.

Svensmark H. 1998. Influence of cosmic rays on Earth's climate, http://www.millengroup.com/repository/global/CREC.html (Feb. 15, 2000).

Templeton B. 1977. Comparative precipitation values in Los Angeles, 1877-1966 and approximately 15,000 years B.P. California Geology.

Tinsley B, Brown GM. Sherrer, PH. 1989. Solar variability influences on weather and climate: possible connections through cosmic ray fluxes and storm intensification. Journal of Geophysical Research 94:14,783-14,792.

Tinsley BA, Dean GW. 1991. Apparent tropospheric response to MeV-GeV particle flux variations: a connection via the solar wind, atmospheric electricity and cloud microphysics. Journal of Geophysical Research 96:22283.

Vanyo JP, Paltridge GW. 1981. A model for energy dissipation at the mantle- core boundary. Geophysical J. Royal. Astronomical Society, 66:677-690.

Veretenenko SV, Pudovkin MI. 1995. The galactic cosmic ray Forbush decrease effects on total cloudiness variations. Geomagnetism and Aeronomy 34:No.4, 463-468.

Volland H. (Editor). 1995. Handbook of Atmospheric Electrodynamics, Vol. 1. CRC Press.

Yamazaki T, Ioka N, Eguchi N. 1995. Relative paleointensity of the geomagnetic field during the Brunhes Chron, Earth and Planetary Science Letters. 136:525-540.

Suggested Research on the Effect of Climate Change on California Water Resources

Maurice Roos

Abstract

Quite significant changes in climate are being projected for the latter part of this century due to global warming. The changes would be the result of increases in greenhouse gases from human activities, such as carbon dioxide, methane, and other trace gases. These potential changes are expected to affect many of our water resources systems. Some of the more important changes would be temperature increases which would raise temperate zone snow levels and change the pattern of runoff from mountain watersheds, thereby affecting reservoir operation. Other consequences would be sea level rise which could adversely affect the Sacramento-San Joaquin River Delta, source of major water exports for the State; possibly larger floods and more extreme precipitation events; and changes in the water requirements of crops.

By and large, reservoirs and water delivery systems and operating rules have been developed from historical hydrology on the assumption that the past is a good guide to the future. With global warming, that assumption may not be valid. This paper will briefly look at the major factors affecting water resources systems and go on to suggest eleven priority items of research. The emphasis will be on items important in California and other western states.

In view of these forecasts of a significant change in future climate, with the author's knowledge of the existing water resources system in California, an analysis of potential effects and a list of higher priority research items has been developed. In summary, the list is as follows, and will be explained in more detail subsequently in the paper:

- Monitoring of hydrologically important variables
- Test operation of the Central Valley Project and State Water Project system with modified runoff
- Modeling of future precipitation
- Update depth-duration-frequency rainfall data
- Evaluate the Golden Gate Tide Gage datum
- Catalog sea level trends along the coast, in San Francisco Bay and the Delta
- Check for recent changes in evapotranspiration
- Estimate future changes in evapotranspiration and crop water use.
- Evaluate effect on major multipurpose flood control reservoirs
- Water temperature modeling in major reservoir/river systems
- Effect of climate change on regions adjoining California, such as the Colorado River and the Pacific Northwest

Possible Changes Affecting Water Resources Systems

Most of the forecasted climate changes by year 2100, the end of the century, due to the increase in greenhouse gases have been developed by the Intergovernmental Panel on Climate Change (IPCC). The IPCC was jointly established in 1988 by the World Meteorological Organization and the United Nations Environment Programme to study climate change. The IPCC has issued several reports since 1990 outlining possible global warming and the effects as a result of increased amounts of carbon dioxide, methane, and other trace gases originating from human activities.

A good assessment of the state of research on the potential consequences of climate change on water resources in the United States, including what is known and what is not known, is the report of the National Water Assessment Group for the U.S. Global Change Research Program (Gleick and Adams 2000).

The most recent IPCC Working Group I Summary Report, in its third assessment (IPCC 2001), projects a 1990 to 2100 average surface temperature increase of around 3°C, with a range of 1.4 to 5.8 degrees. The different scenarios cover a wide range of assumptions about the rate of future increases in greenhouse gases and the amount of temperature forcing in the climate system. The increase in global temperature during the 20th century was estimated to be about 0.6°C, much of which occurred by 1940, and a recent significant increase after 1980 which is believed to be primarily of human origin. Because of warmer temperatures, some increase in global evaporation and therefore precipitation is projected for the 21st century, more likely at higher latitudes. For hydrology and water resources, precipitation is the most important variable; rainfall changes in specific California regions cannot be well defined by the current general circulation climate models of the atmosphere.

Sea level (IPCC 2001) is projected to rise around 0.5 meter (1.6 feet) by 2100, with a range of 0.1 to 0.9 meters (0.3 to 2.9 feet). The rate during the 20th century appears to have been around 0.2 meters (0.7 feet) with a range of 0.1 to 0.25 meters (0.3 to 0.8 feet). The 0.2 meter figure is consistent with the historical trend at the Golden Gate tide station, although it is possible that tectonic movement, or settlement, has influenced the stages there.

There is a general expectation that a warmer climate would lead to more intense precipitation events, thereby causing somewhat bigger floods and more intense convective storms, thereby affecting the rainfall statistics used for storm drainage design. The IPCC report rates prediction confidence in more intense precipitation events as "very likely, over many areas".

The increase in carbon dioxide, from the current 370 ppm to perhaps 600 or 700 ppm, is expected to be beneficial to plant growth on many food crops, provided the water supply is adequate. Higher carbon dioxide concentrations in the air could partly offset the higher water use (evapotranspiration) resulting from warmer temperatures.

All of these projected changes, as well as some not yet identified, are likely to affect the hydrologic cycle and the water resources of California.

Water Supply Related Research

Probably the most significant change, which is judged fairly certain in the next 100 years, is a change in temperate zone mountain runoff patterns. Even if precipitation remains the same, the rise in temperatures means less snow, less snow covered area, and winter rain to higher elevations. The higher snow levels during storms, about 450 meters (1500 feet) under the 3 degree median projection, would

produce more winter runoff. Less spring snowmelt would make it more difficult to refill winter reservoir flood control space during late spring and early summer of many years, thus reducing the amount of water deliverable during the dry season. Lower early summer reservoir levels also would adversely affect lake recreation and hydroelectric power production, with possible late season temperature problems for downstream fisheries.

It is possible, if precipitation increases and the mountains are high enough, for the volume of April through July snowmelt to increase. In California, this could happen in the higher elevation southern Sierra, where about 70% of the historical April 1 snow zone area would remain with a 450 meter (1500 feet) rise (Figure 1). In the northern Sierra, however, the same rise in snow levels would reduce estimated snow covered area by over 70%, so a reduction in spring snowmelt is virtually certain. In fact, there has been such a trend during the last 50 years.

Monitoring of Hydrologically Important Variables

The first research need is good hydrometeorologic monitoring. Regular, consistent and sustained measurements of hydrologically important variables are essential to track what is happening and to verify model predictions. This means continuing measurements of variables such as precipitation and other climate data, snowpack, streamflow, and ocean and Delta tide levels. Emphasis should be in the locations where significant change is expected, for example the mountain snow zone. The National Weather Service, in its reorganized Climate Services Division, is developing a climate reference network of 250 high-grade weather stations to be a national benchmark for long term climate monitoring. That would be a good start, but only 5 to 7 of these are likely to be located in California. Scripps Institution of Oceanography, in cooperation with the Yosemite National Park and others, has recently installed a number of new snow measurement and meteorological instruments in the park, with high hopes that these will be operating for the long term. But more thought should be given to several networks along gradients from east to west and north to south, and across climate zones.

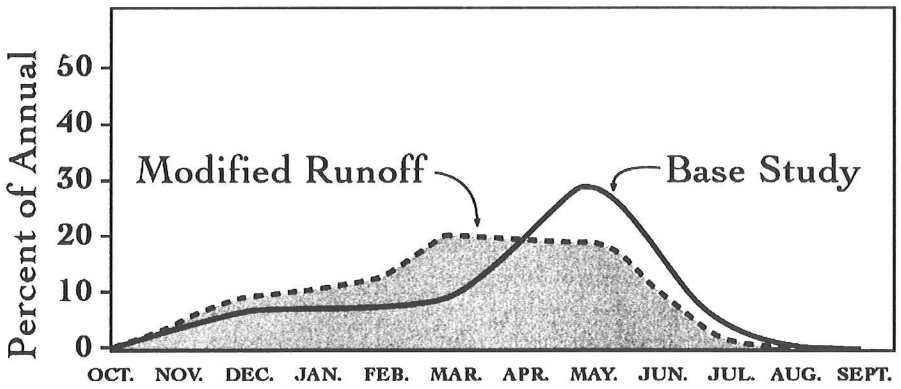

Figure 1 Comparison of historical and modified runoff from a mid-Sierra snow runoff watershed, assuming 3°C warming

Test Operation of the Central Valley Project — State Water Project System

These two big water projects furnish about 30% of California net water demand for agricultural and urban use. The major reservoirs of these two projects are located on watersheds (Trinity, Sacramento, Feather, and American) likely to see large shifts in runoff patterns as a result of rising snow levels. At

least 50 years of monthly hydrology are suggested as a minimum length for comparisons. Currently many studies are made with the 1922-1994 historical period of 72 years. This longer period includes simulation during the two major 6-year historical droughts, 1928-1934 and 1987-1992. The operation model of choice would be the CALSIM model jointly developed by the Department of Water Resources and the U.S. Bureau of Reclamation.

The test evaluations would logically proceed in two stages: (1) a simplified run involving approximate adjustments to major project reservoir inflows with the changes anticipated with global warming, and (2) more detailed studies involving all major facilities, including local and upstream power reservoirs. Initial studies should focus on the assumption of precipitation similar to the historical amounts, except warmer. Later studies could try some of the projected precipitation scenarios derived from a new generation of atmospheric general circulation models (GCMs).

Modeling Future Precipitation

Future precipitation is probably the most important variable influencing water resources and water supply. It is also the most difficult to predict at the regional and watershed levels. It should be no surprise that research should continue into modeling likely future precipitation in enough detail in time and space to feed into individual watershed runoff models. We need to support the University of California and National Laboratory experts in analyzing results of newer GCM modeling by the modeling centers of the world as they apply to California and other western states, especially in simulating historical precipitation and predicting future precipitation. And feedback from these expert researchers to the GCM modelers should be encouraged.

Depth-Duration-Frequency Rainfall Data

Support of the processing and dissemination of up-to-date rainfall depth-duration-frequency data is important to incorporate extreme events of recent years and as more of these extreme events are expected in future years. These data are some of the most valuable rainfall statistics, widely used by engineers and designers for storm drains, culverts, roofs and host of works (see the example in Figure 2). These are the curves, for example, which show that a 1-in-25-year storm can produce 2 inches (50 mm) in 2 hours at a particular place. Continual updating will gradually incorporate expected storm intensity increases as a result of climate change so that structures built with their guidance will not be out of date with less protection than intended.

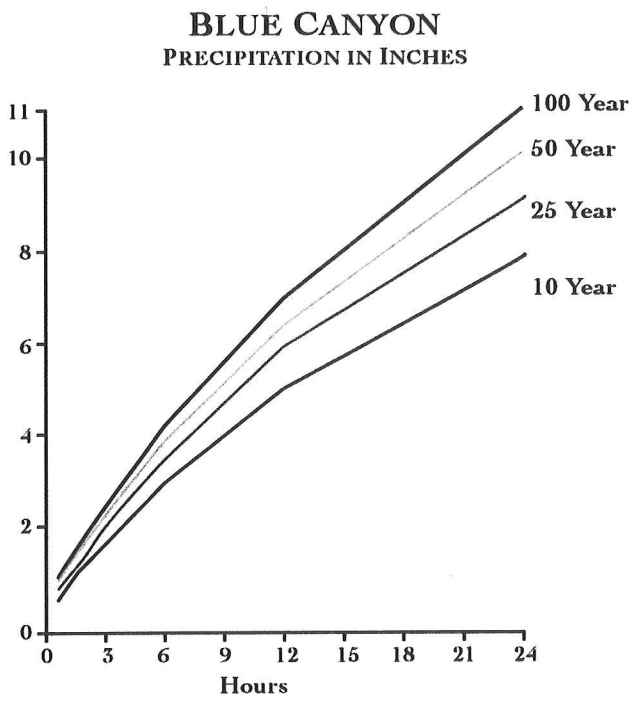

Figure 2 Chart of depth-duration-frequency statistics for Blue Canyon

Sea Level Rise

California is not generally as vulnerable to sea level rise as some of the eastern and southern states, which have lower shorelines. Since California is tectonically active, it is the combined effect of geological change, rising or falling land, and global sea level rise that matters. But there are areas, such as San Francisco Bay and the Sacramento-San Joaquin River Delta, which are vulnerable. Major water projects have been built to convey water from areas of plenty to the drier central and southern portions of the State. The tidewater region of the Delta is the hub of major water transfer; water quality there can be affected by salinity intrusion from the Pacific Ocean via San Francisco Bay.

Reservoirs in the north provide water storage and flood control. Water is then released downstream to meet Delta and fishery needs and to be exported by large pumps in the southwestern corner of the Delta. During low flow months additional water is released to repel ocean salinity incursion in the western Delta as a hydraulic barrier to preserve suitable fresh water quality within the estuary and for export. Much of the land within the Delta is below sea level protected by levees, many of which are on weak peat soil foundation.

Rising ocean levels could affect water transfer across the Delta from north to south by decreasing the stability of Delta levees. The second factor is more salinity intrusion, which would gradually degrade the quality of export supplies or require more precious fresh water releases from upstream reservoirs to repel ocean salinity.

Evaluate the Golden Gate Tide Gage Datum

Since the Golden Gate tide gage is the key reference for so many sea level determinations (i.e., the central California coast, the Bay, and the Delta), it is essential that an accurate determination of its

vertical stability be made, checking for long term vertical movement of the datum. Tools may now be available by use of highly precise space geodetic techniques, which can measure very small changes in vertical elevation. The gage has shown an apparent rising sea level trend of about 0.2 meters (0.7 feet) per century over the past 80 years, but we can't be sure if this is real or due to settlement of the pier or tectonic movements in the underlying rock. The measurements should proceed in three stages: (1) compare previous precise leveling where the Golden Gate gage can be compared to nearby benchmarks on solid rock; (2) investigate whether the GPS system can be used for a precise determination of the Golden Gate tide gage datum and its changes, if any, over time and how long a record would be needed to give confidence of a measurement which could be less than 2 mm (.007 feet) per year; and (3) perform the measurements of actual tide gage datum over a period of time, probably years. The National Geodetic Survey does this kind of work.

Catalog Sea Level Trends Along the Coast

The objective of this proposed study would be to catalog all available tide station data along the California coast, in San Francisco Bay and in the Delta. Long term data is needed, at least 20 years and preferably 50 years, to look for apparent trends in annual sea level. Presumably an average of San Francisco at the Golden Gate and San Diego can be used to represent global sea level rise. Departures from that could be due to tectonic activity or possibly some other effect such as oil and gas extraction, or perhaps consolidation of deep sediments (as in the Delta, for example). The catalog would establish a useful base to guide government and developers in the coastal zone. The San Francisco Bay Conservation and Development Commission (1988) and the California Coastal Commission (2001) have both made some studies of this matter.

Changes in Water Requirements

There are at least two factors which could change water use by vegetation. As a general rule, warmer temperatures mean more evapotranspiration. But higher carbon dioxide levels tend to reduce water consumption, at least in laboratory tests. Most observers expect the net change to be somewhat higher water requirements but not as high as would otherwise be expected from temperature change considerations.

Recent Changes in Evapotranspiration

Since carbon dioxide concentrations have increased about 17% over the past 40 years (Keeling and Whorf 2001), one wonders whether there is any noticeable effect on evapotranspiration, especially the measured reference ET of grass. During the 1960s there were a number of well measured grass lysimeter plots in various locations in California, measuring directly, by weight changes, the water consumption of grass. The University of California, in cooperation with the Department of Water Resources, should reinstall or reoperate former lysimeters at Davis and Five Points (on the San Joaquin Valley west side). Since there is variation from year to year and day to day, depending on weather conditions, it will probably take 3 to 5 years, perhaps 10 years, to see if there is a noticeably change from the measurements 40 years ago. It is possible that higher carbon dioxide is a factor in the continuing improvement in crop yields.

Estimate Change in ET and Crop Water Requirements

Knowledgeable experts in plant water consumption at the University of California and the Agriculture Extension Service and land and water use analysts in State and federal government should estimate likely future ET rates for major crops. To do this, they will need to obtain reasonable median projections of weather in 2050 and 2100 from the GCM climate modelers. This would be primarily temperatures, both average and maximum and minimum, in our dry summer climate, but could include projections of monthly rainfall changes if significant, and should include projected carbon dioxide levels. One would expect that higher water consumption because of increased temperatures will only be partly offset by carbon dioxide based reductions. The result would be slightly higher water requirements, probably varying somewhat by crop type. A complicating factor is possible shifts in the growing season of annual crops. For example, because of less frost risk, tomatoes might be planted earlier when the sun angle is not as high.

Other Items of Research

There are several other item of potential research which don't fit into the previous headings. These are discussed below.

Conduct a Systematic Review and Evaluation of the Effect of Global Warming on Major Multipurpose Flood Control Reservoirs

In a warmer world, some increase in the intensity of major precipitation events could be expected because saturated warmer air can hold more water vapor than cooler air. More intense precipitation would generate larger floods. Another factor on streams draining high mountain areas is that many storms now produce a mix of rain with snow on the higher parts of the watershed. A warmer climate means a greater proportion of storm precipitation is likely to be rain, producing more direct rain runoff.

Currently reserved flood control space in major multipurpose reservoirs during the winter may not be adequate for the larger storms. As a result, the degree of protection would gradually shrink. Additional flood control space or downstream channel capacity is likely to be expensive on our major rivers.

As GCM models are developed and improved, their precipitation results should be analyzed to see if there is a consistent trend for more intense storms and precipitation events in California. The model precipitation can then be entered into watershed runoff models to assess the higher risk. A careful analysis of historical trends during the last 30 years or so may be useful too.

Water Temperature Modeling in Rivers

Warmer air and less snowmelt will make it more difficult to maintain rivers cold enough for cold-water fish, including anadromous fish like salmon. This could create difficult problems for some salmon, such as the winter run, where fish spend the warm season in the streams. There may be similar problems for juvenile steelhead too. On most California rivers large foothill reservoirs provide some temperature control for downstream reaches.

There are some existing models of water temperature in reservoirs and downstream rivers. These models may need improvement as the job of maintaining suitable temperatures becomes more difficult. Analysis of selected foothill reservoirs and rivers is suggested to see what a different pattern

of inflow and higher temperatures would do. Some new temperature modeling is anticipated as part of the Oroville power plant relicensing during the next several years. A logical extension would be to apply the new Lake Oroville and Feather River temperature models under a changed climate and runoff regime.

Effect of Climate Change in Other Regions

The Colorado River, which drains a huge area of the American Southwest, is a very important component of California water supply, especially in the south. Earlier studies (Nash and Gleick 1993) have indicated a high probability of a change to less runoff. Since the Colorado River is already fully subscribed, if not oversubscribed, a reduction in average runoff could affect California's water supply as well as that of the other Colorado River Basin states. Hydroelectric power too could be affected, especially generation at Glen Canyon and Hoover dams due to change in reservoir levels.

California's long-term entitlements to Colorado River water are 4.4 million acre-feet (5.4 billion cubic meters) per year. In recent years, California's net diversions have been as much as 5.2 million acre-feet and the State is being forced to reduce its diversions as water demands in the other states build toward use of their entitlements. Climate change in the watershed could exacerbate the water supply situation. It is also possible that a wetter scenario could improve Colorado River runoff, even to the point of generating more flood problems on the lower river.

California depends on the Pacific Northwest, including the Columbia River system, for about 10% of its electric energy supply. As we saw during 2001, when Columbia River runoff was down, there is an impact on California's electric power supply and reliability. In conclusion, the effects of climate change, especially precipitation, in the adjoining Pacific Northwest and Colorado River watershed would have an impact on California-on electricity for both regions and on water supply for the Colorado.

It is anticipated that new research and studies on runoff and water supply in both of these regions will be forthcoming by interested regional parties. It is recommended that the California Energy Commission and the Department of Water Resources monitor results of these studies as they are completed and try to assess what they might mean for California water supply and electric energy imports.

Summary

The preceding are 11 areas of research on the effect of global warming on water resources systems in California that the author feels should have priority. There are many more items which could be added. In a report on potential water resources research ideas for a globally warmer world prepared by the author for the California Energy Commission Public Interest Energy Research (PIER) program, some 35 items were identified. However, completion of the work suggested herein would be an excellent start in adapting to a potentially different climate.

References

California Coastal Commission. 2001. Overview of sea level rise and some implications for Coastal California. CCC, San Francisco, CA.

California Department of Water Resources. 1998. Bulletin No. 160-98: California water plan update. DWR, Sacramento, CA.

Gleick PH, Adams D, Briane. 2000. Water; the potential consequences of climate variability and change for the water resources of the United States. Pacific Institute, Oakland, CA.

Keeling CD, Whorf TP. 2001. Chart showing monthly average carbon dioxide concentration, Mauna Loa Observatory, Hawaii. Scripps Institution of Oceanography, La Jolla, CA.

Intergovernmental Panel on Climate Change. 2001. Summary for policy makers, third assessment report, a report of Working Group I on the IPCC web site. 20pp.

Knowles N, Cayan D. 2001. Global climate change: potential effects on the Sacramento/San Joaquin Watershed and the San Francisco Estuary. Scripps Institution of Oceanography, La Jolla, CA.

Nash L, Gleick P. 1993. The Colorado River and climatic change, prepared for the Environmental Protection Agency by Pacific Institute for Studies in Development, Environment, and Security, Oakland, CA.

Roos M. 2002. The effects of global climate change on California water resources, a chapter of the PIER Climate Change Research Plan, Calif. Energy Commission, Sacramento, CA.

San Francisco Bay Conservation and Development Commission. 1988. Sea level rise: prediction and implications for San Francisco Bay, prepared by Moffatt and Nichol, Engineers. SFBC & DC, San Francisco, CA.

A Holocene Record From Medicine Lake, Siskiyou County, California: Preliminary Diatom, Pollen, Geochemical, and Sedimentological Data

Scott W. Starratt, John A. Barron, Tara Kneeshaw, R. Larry Phillips, James L. Bischoff, Jacob B. Lowenstern, and James A. Wanket

Abstract

Medicine Lake is a small (165 ha), relatively shallow (average 7.3 m), medium altitude (2036 m) lake located within the summit caldera of Medicine Lake volcano, a dormant Quaternary shield volcano located in the Cascade Range about 50 km northeast of Mount Shasta. During the fall of 1999 and 2000, high-resolution bathymetry, seismic reflection, and sediment cores were collected from the lake. B100NC-1 (water depth 12.6 m; length 226 cm) was the longest core collected and was chosen for a multi-proxy study of Holocene climate variability in northern California. Twenty-six samples were analyzed for physical properties, sediment grain size (sand/mud ratio), diatoms, pollen, and total organic carbon (TOC). Using both ^{14}C (AMS) dating and tephrochronology, the sediments at the bottom of the core were estimated to have been deposited about 11,400 cal yr BP, thus yielding an estimated average sedimentation rate of about 20.66 cm/1,000 yr. The lowermost part of the core (11,400 to 10,300 cal yr BP) records the transition from glacial to interglacial conditions. During the period from about 11,000 to 5,500 cal yr BP, Medicine Lake consisted of two small, steep-sided lakes or one lake with two steep-sided basins connected by a shallow shelf. During this time, both the pollen (*Abies/Artemisia* ratio) and the diatom (*Cyclotella/Navicula* ratio) records indicate that the effective moisture increased, leading to a deeper lake. Over the past 5,500 calendar years, the pollen record shows that the effective moisture continued to increase, but the diatom record indicates fluctuations in the level of the lake. The change in the pattern of lake level from one of increased deepening prior to about 6,000 cal yr BP to a pattern of variable depths may be related to changes in the morphology of the Medicine Lake caldera associated with the movement of magma and the eruption of the Medicine Lake Glass Flow about 5,000 calendar years ago. Changes in basin morphology caused Medicine Lake to flood the shallow shelf which surrounds the deeper part of the lake. During this period, the *Cyclotella/Navicula* ratio and the percent abundance of *Isoetes* vary, suggesting that the level of the lake fluctuated, resulting in changes in the shelf area available for colonization by benthic diatoms and *Isoetes*. These fluctuations are not typical of the small number of low-elevation Holocene lake records in the region, and probably reflect hydrologic conditions unique to Medicine Lake.

Introduction

Geologic History

The Medicine Lake volcano is a large Pleistocene and Holocene shield volcano located about 50 km northeast of Mount Shasta. The volcano began erupting about 500,000 years ago (Donnelly-Nolan and Ramsey 2001). At least 17 eruptions have occurred during the past 12,900 calendar years. The

composition of these lavas ranges from basalt to rhyolite, with those of silicic composition dominating the last 5,000 calendar years. Depending on their location, these eruptions affected the morphology of the Medicine Lake caldera, provided a source for some of the tephra layers found in lake sediments, and may have indirectly affected lake level through influences on groundwater flow. About 5,000 calendar years ago (Lowenstern, unpublished data), the dacite of the Medicine Lake Glass Flow erupted on the floor of the caldera. Between about 3,300 and 800 calendar years ago, seven eruptions of varying composition took place.

Anderson (1941) was the first to study the region in some detail. In addition to discussing the eruptive history of the volcano, he briefly presents the evidence for glacial activity and the presence of lacustrine sediments that pre-date the present lake. Evidence for the Last Glacial Maximum at Medicine Lake volcano extends down to an elevation of at least 1,890 m (Donnelly-Nolan, in press). Ice accumulated in the caldera and flowed out to the southeast through the lowest point on the caldera rim. The suggestion that there was ice as thick as 150 m on the volcano is supported by mapping (Anderson 1941; Donnelly-Nolan and Nolan 1986) and fluid inclusion studies (Barger 2001).

Medicine Lake occupies a portion of the summit caldera (Figure 1) of Medicine Lake volcano. Anderson (1941) noted both geomorphological and sedimentological evidence for higher lake levels during the Quaternary. He suggested that at one time, the basin to the northeast, Arnica Sink, appears to have been connected to Medicine Lake. Anderson (1941) further suggested that the Medicine Lake Glass Flow may have dammed the drainage that connected Arnica Sink and Medicine Lake in the late Quaternary. His evidence for past higher lake levels includes abandoned shorelines north of the lake and diatomaceous deposits to the south.

Hydrocast Profiles

Medicine Lake is a small (165 ha), relatively shallow (average 7.3 m), medium altitude (2036 m) lake. In September 1992, temperature, specific conductance, dissolved oxygen, and pH data were collected at Medicine Lake using a multiparameter probe (Schneider and McFarland 1996). These data were collected as part of a hydrologic monitoring program related to potential geothermal resource development.

The lake exhibits a strong seasonal thermocline, indicating that the present lake is either a warm monomictic or dimictic lake. The strength, duration, and timing of seasonal overturn may vary depending on the date of lake thaw, which presently ranges from late May to July. Surface temperature in September 1992 was about 15° C, and approached 4° C at 25 m. The thermocline occurred between about 12 m and 15 m. The dissolved oxygen profiles indicate an orthograde oligotrophic lake in which the oxygen concentrations are controlled by wind mixing with saturation at or near 100%. The highest levels of oxygen (10 mg/L) were recorded between 12 and 17 m. Specific conductance is uniform (20 μS/cm) between profiles with the exception of the profile measured in the shallowest part of the lake (90 μS/cm). The pH values were neutral to slightly acidic reflecting the increased concentration of humic acids in deeper parts of the lake.

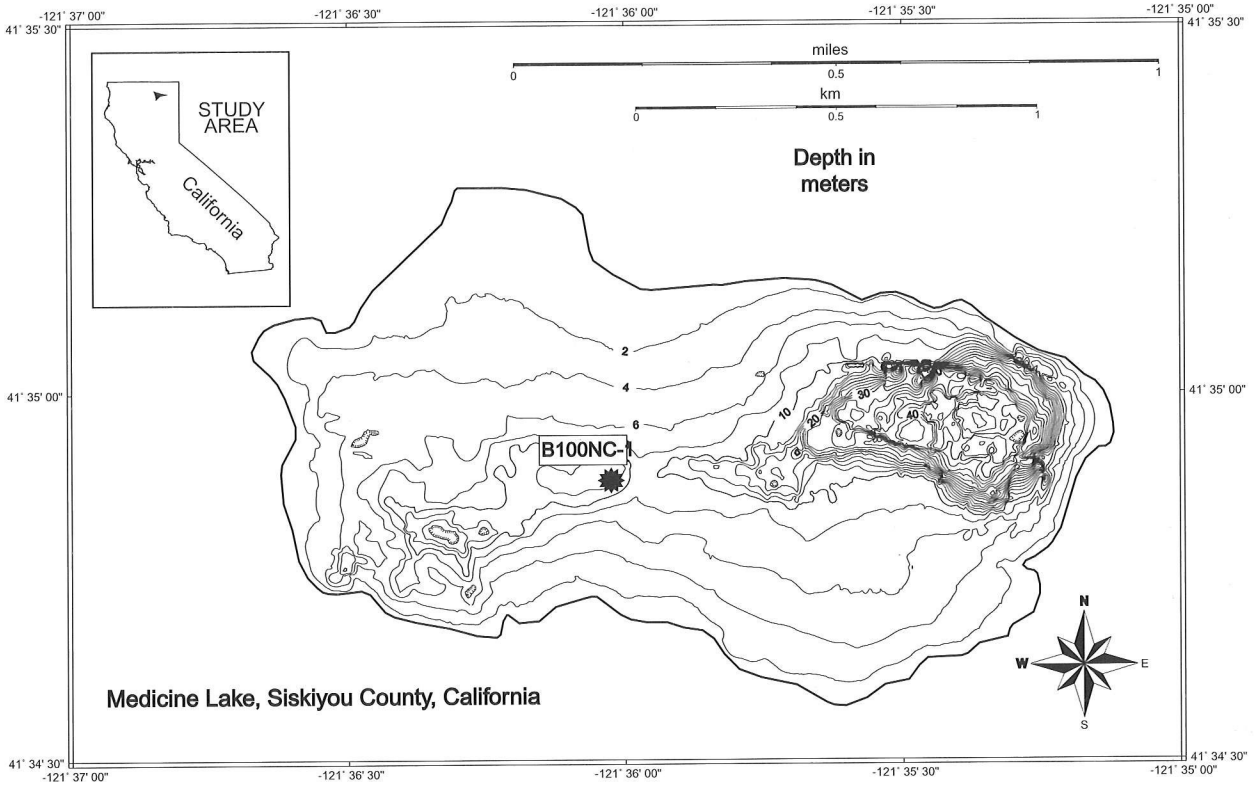

Figure 1 Map showing the location of Medicine Lake. The lake is located in eastern Siskiyou County, CA, about 50 km northeast of Mount Shasta (modified from Childs and others 2000).

Modern Climate and Vegetation

Medicine Lake lies within a semi-arid winter rainfall climate. More than 75% of the annual precipitation falls during the period of October through March. Large variations in temperature occur both diurnally and seasonally. Warm summer temperatures and low precipitation, coupled with high evapotranspiration, lead to a low effective moisture for the region. During the summer, orographic and convection processes cause sporadic late afternoon thunderstorms. Occasionally, during the late spring and summer, day-long storms descend over Medicine Lake volcano (Donnelly-Nolan, personal communication).

The modern forest surrounding Medicine Lake is dominated by Lodgepole pine (*Pinus contorta*). Other pine species in the area include Ponderosa (*P. ponderosa*), Jeffrey (*P. jeffreyi*), sugar (*P. lambertiana*), and western white (*P. monticola*). Red (*Abies magnifica*) and white (*A. concolor*) fir are found at higher elevations and on shaded north-facing slopes. Incense cedar (*Calocedrus decurrens*) and western juniper (*Juniperus occidentalis*) are present in small numbers on dry slopes and at lower elevations. *Artemisia tridentata* is common in open areas at lower elevations throughout the Modoc Plateau. Oaks are represented by the huckleberry oak (*Quercus vaccinifolia*). Several species of grass and bracken fern (*Pteridium* sp.) are common in forest clearings.

Methods

In September 2000 core B100NC-1 (226 cm long; 12.6 m depth) was collected from the shallower western basin of Medicine Lake using a Vibracore system (Figure 2). Density was measured at intervals of 1 cm before the core was split. Paired samples were collected for paleontological (26) and inorganic geochemical (25) analyses. Sampling intervals were determined by variations in the stratigraphy of the core. Additional samples were taken for dating (AMS ^{14}C and tephra analyses), grain size, and total organic carbon (TOC) analyses.

Three samples containing fibrous root(?) material were dated at the CAMS facility at Lawrence Livermore National Laboratory using AMS ^{14}C. Seven tephra samples from discrete layers were analyzed using the JEOL electron microprobe at the U.S. Geological Survey (Menlo Park). Four of the samples were correlated with identified tephras.

Samples for diatom analyses were processed using H_2O_2, HCl, HNO_3, and $Na_4O_7P_2$ and permanently mounted using Naphrax. A total of 300 frustules were enumerated at magnifications of 500X to 1,000X. Pollen samples were prepared using standard techniques, which include digestion in HCl, KOH, HF, HNO_3, $C_4H_6O_3$, and H_2SO_4. Residues were mounted in silicone oil and a minimum of 300 non-aquatic pollen grains were counted at 400X. Due to the high proportion (80-90%) of *Pinus* (pine) pollen in all samples, counts were extended to include at least 100 non-*Pinus* grains.

Twenty-five samples were acid leached and the leachate was analyzed for geochemistry using the ICP-MS facility at the U.S. Geological Survey (Menlo Park). In addition, 177 samples were analyzed for sediment grain size. Samples were disaggregated and sieved using a 63 μm screen. A Columetrics Incorporated coulometer was also used to analyze 66 samples for TOC content.

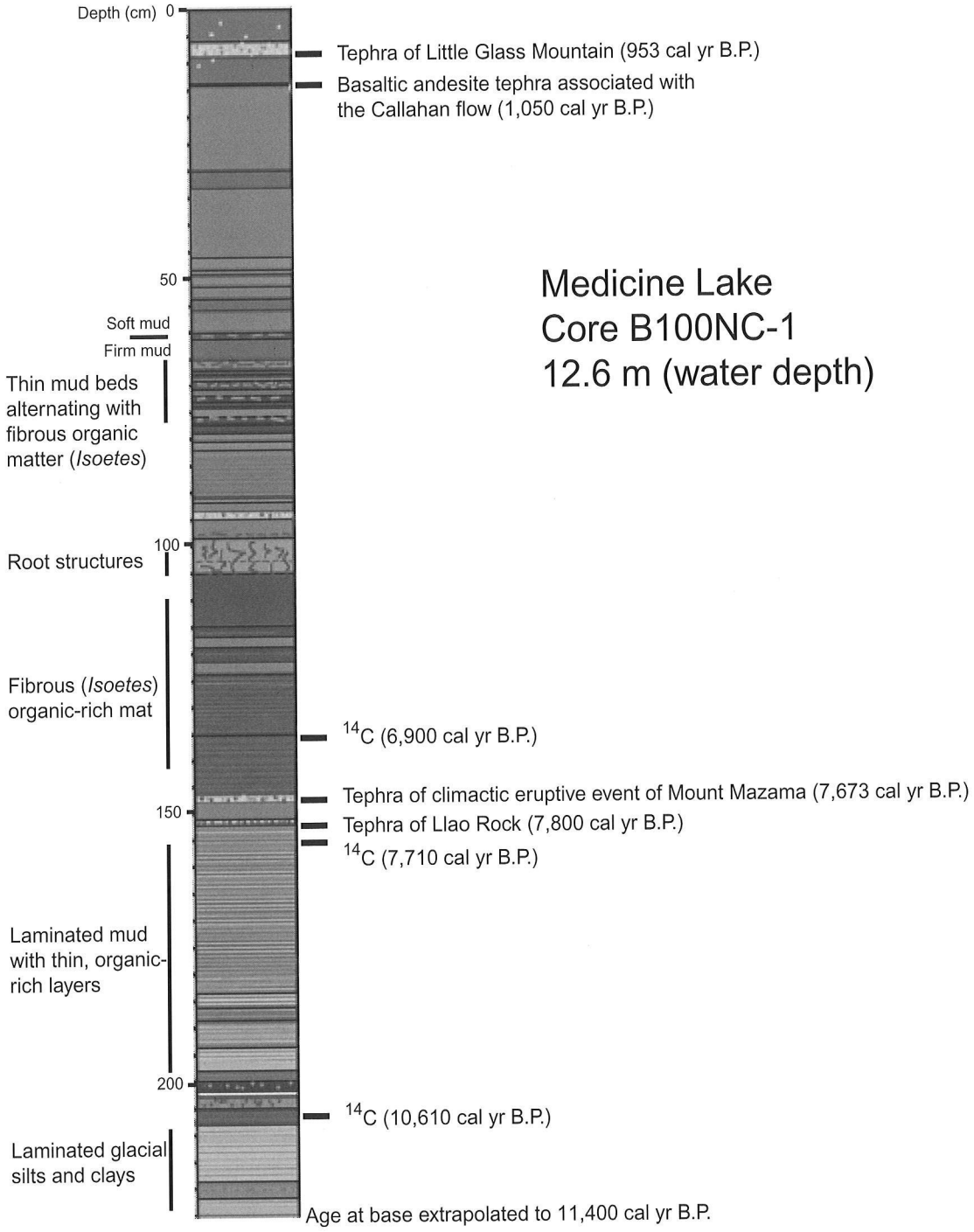

Figure 2 Generalized stratigraphic column for Core B100NC-1. Dates from geochemical correlation with ash beds of known age and AMS ^{14}C dates. See Childs and others (2000) for a detailed description of symbols used in stratigraphic column.

Results

Stratigraphy

The sand fraction records the deposition of varying amounts of fine-grained mud clasts, diatoms, seeds, disseminated tephra, along with seven discrete tephra layers (Figure 2). The organic material in some of the laminated intervals is comprised of the aquatic macrophyte *Isoetes* (quillwort). The tephra layers contain between 17 and 68% sand-size sediment. The sediments at the bottom of the core are estimated to be about 11,400 calendar years old. The earliest laminated interval, approximately 11,400 to 10,600 cal yr BP consists of silt and clay which contains diatoms, seeds, and fine-grained disseminated tephra. Two unidentified tephra layers were deposited between 10,500 and 10,250 cal yr BP The sequence from 10,250 to 8,300 cal yr BP consists primarily of laminated mud with thin, organic-rich layers. Between 10,250 and 8,300 cal yr BP, the sand fraction is composed mainly of rare diatoms, seeds, and abundant fine-grained mud clasts (fecal pellets?). The laminated interval between 8,300 and 7,780 cal yr BP is similar in composition, with abundant mud clasts and the remains of *Isoetes*. Two tephra beds at the top of the laminated sequence have been identified as the products of two closely spaced eruptive events at Mount Mazama. The laminated sequence deposited from 7,540 to 6,090 cal yr BP consists of fibrous organic-rich mud. The sand fraction contains abundant mud clasts and diatoms with thick mats of *Isoetes* present from about 7,200 to 6,090 cal yr BP. The sediments deposited between 6,090 and 4,590 cal yr BP are laminated and the sand fraction contains abundant diatoms and mud clasts, as well as rare disseminated tephra. The laminated interval deposited between 4,590 and 3,380 cal yr BP contains abundant *Isoetes* remains, mud clasts, and diatoms. The consistency of the sediment changes from firm to soft mud about 3,380 calendar years ago. A change to poorly-defined bedding occurs gradually between 3,380 and 1,680 cal yr BP with the sand fraction consisting of disseminated tephra, mud clasts, diatoms, and rare tubes (root casts?). Sand-size sediments deposited over the last 1,680 calendar years are dominated by mixed black and white pumice clasts, with distinct tephra layers deposited at about 1,050 and 953 cal yr BP.

Age Model

Three AMS ^{14}C dates were calibrated using CALIB 4.3 (Stuiver and others, 1998). These dates (10,610 cal yr BP; 7,710 cal yr BP; 6,900 cal yr BP) constrain the age of the lower part of the core (Figures 2 and 3). Four of the tephra samples can be correlated with tephras of known age. These include two from Mount Mazama (Llao Rock; 7,800 cal yr BP, climatic eruptive event of Mount Mazama; 7,673 cal yr BP [Bacon, personal communication]) and two from local volcanic centers (basaltic andesite tephra associated with the Callahan flow; 1,050 cal yr BP, tephra of Little Glass Mountain; 953 cal yr BP). All ages discussed in this paper are in cal yr BP. The three AMS ^{14}C and four tephra dates were used to construct the age model for Medicine Lake. Based on these ages, the sediment accumulation rate is approximately 20.66 cm/1,000 yr (Figure 3).

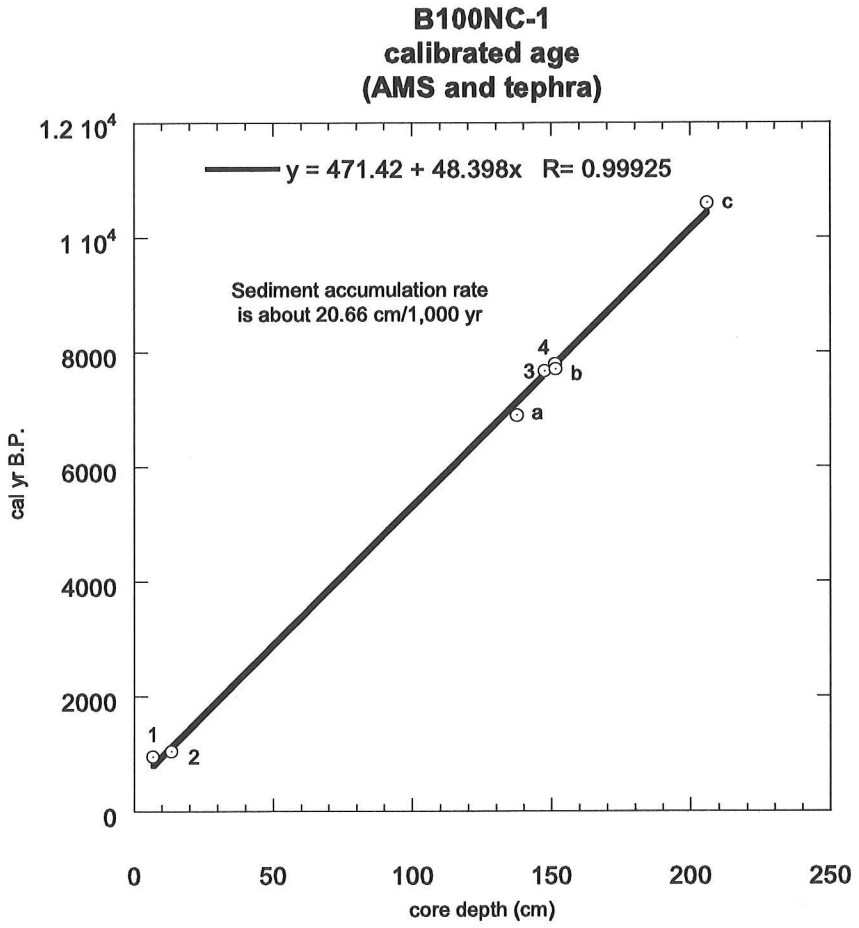

Figure 3 Age model for Core B100NC-1 based on three AMS ^{14}C dates and correlation to two ash beds of known age. Control points: (1) tephra of Little Glass Mountain (953 yr BP), (2) basaltic andesite tephra associated with the Callahan flow (1,050 yr BP), (3) tephra of climactic eruptive event of Mount Mazama (7,673 yr BP), (4) tephra of Llao Rock (7,800 yr BP), (a) ^{14}C 6,900 yr BP, (b) ^{14}C 7,710 yr BP, and (c) ^{14}C 10,610 yr BP. Tephra control points are from unpublished analyses by J.B. Lowenstern.

Physical Properties

With the exception of two density peaks which correspond to tephra layers, the density gradually decreases from 11,400 to approximately 5,500 cal yr BP (Figure 4). This decrease in density represents the dilution of glacially derived sediments by fine-grained organic matter. Over the last 5,500 calendar years, the density increased slightly. The lowest density intervals between 8,000 and 6,000, and 4,000 and 3,500 cal yr BP corresponded to intervals in which the sediment is rich in fibrous organic material.

Grain Size

The percentage of the sediment that is comprised of mud (<63 μm) ranges from 60% to nearly 100% (Figure 4). Peaks in the abundance of sand (63 μm to 2 mm) are comprised of airfall tephra deposits.

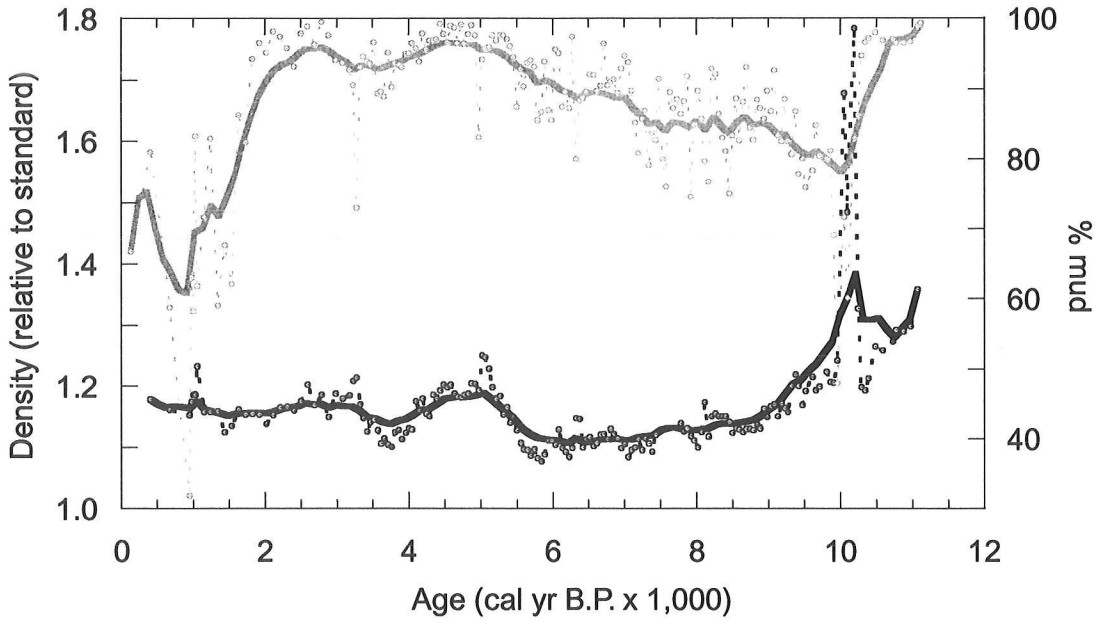

Figure 4 Record of variation in density (relative to density calibration standard) (black curve) and percent of mud in sediment (gray curve). Curves are smoothed using the Stineman function which incorporates + 10% of the data range.

Between 11,400 and 10,400 cal yr BP, the mud component decreased from 98 to 80%, as silt and clay derived from local glacial activity were replaced by coarser grained detrital sediment. The mud content slowly increased from 80 to 95% between 10,300 and 5,500 cal yr BP, as the organic matter diluted the clastic input. The percentage of mud remained relatively stable until about 2,000 cal yr BP. The decrease in mud over the last 2,000 cal yr was due to a decrease in organic matter and the presence of two tephra layers that are dominated by sand-size clasts.

Total Organic Carbon (TOC)

Organic carbon represents the dominant form of carbon in Medicine Lake sediments. Peaks of 7 to 8% TOC occur between 9,000 and 5,500 and at 4,300 and 3,300 cal yr BP (Figure 5). The sediments deposited during these time periods contain a high percentage of *Isoetes* root mat material.

Acid-leachable Geochemistry

The acid-leachable elements (Ca, Fe, K, Li, Mg, Mn, Na, Sr, Ti) of twenty-five sediment samples were analyzed using an ICP-MS. With the exception of Na and Sr, all elements demonstrate similar patterns in their abundance, with their greatest respective concentrations, as illustrated by Fe, occurring between 11,400 and 10,400 cal yr BP (Figure 6). This interval corresponds to a high abundance of glacially derived silts and clays. This high abundance is due to the relative ease with which ions can be removed from clay minerals. The concentration of most of the elements gradually decreases until about 5,500 cal yr BP. Strontium is anomalous, increasing in concentration from about 200 to 500 ppm between 11,400 and 6,000 cal yr BP. The values then decline to modern levels of less than 150 ppm.

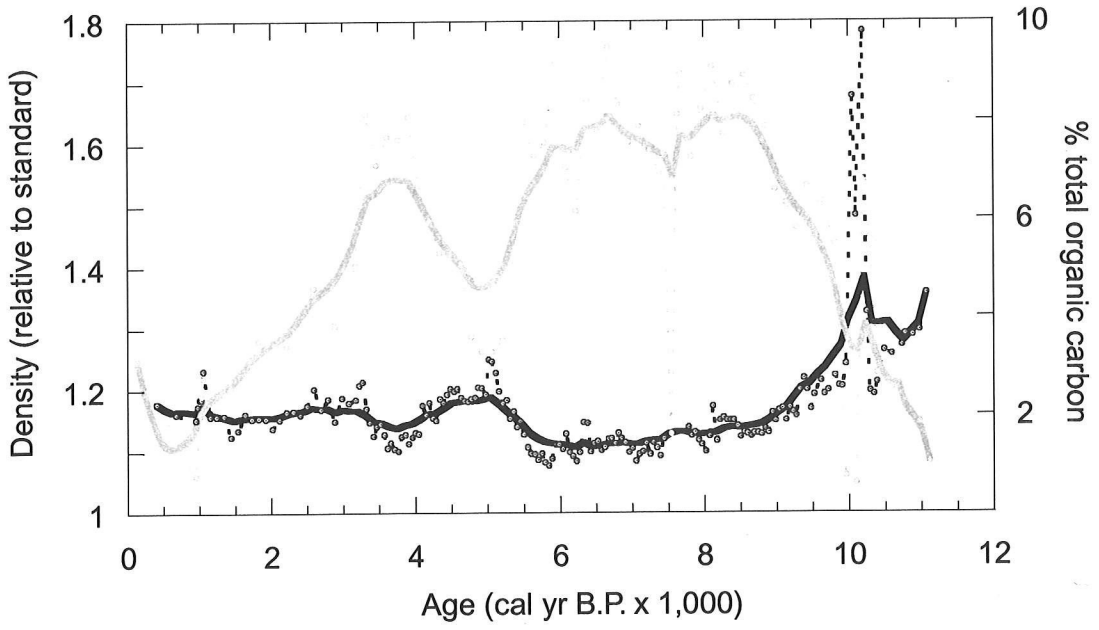

Figure 5 Record of variation in density (relative to density calibration standard) (black curve) and percent total organic carbon (TOC) (gray curve). Curves are smoothed using the Stineman function which incorporates ± 10% of the data range.

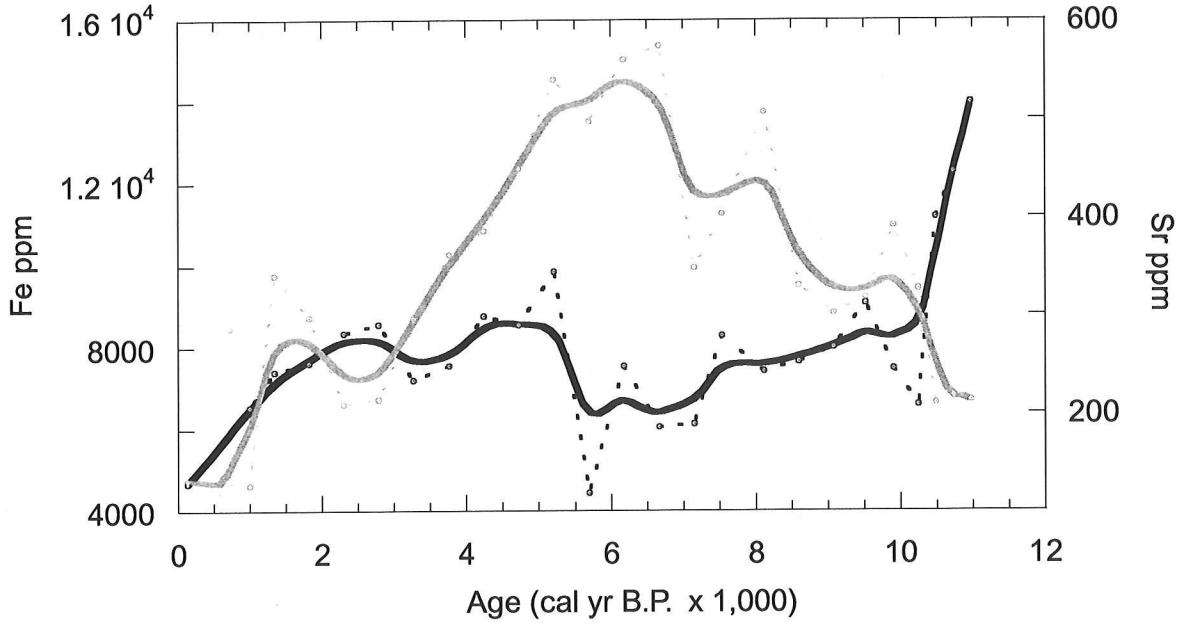

Figure 6 Record of Fe (ppm) (black curve) and Sr (ppm) (gray curve) from the acid leachable component of the sediment. Additional elements (Ca, K, Li, Mg, Mn, and Ti) have abundance variation patterns similar to that of Fe. Curves are smoothed using the Stineman function which incorporates ± 10% of the data range

Diatoms and Chrysophyte Stomatocysts

Diatoms and chrysophyte stomatocysts were extracted from surface samples collected in 1999 and 2000 and from 26 samples from core B100NC-1. More than 160 species and varieties were identified in the modern and fossil floras. These include several taxa that are probably airborne contaminants from regional late Neogene and early Quaternary diatomite deposits. A detailed analysis (including SEM) would likely yield a significantly more diverse flora. The final paleolimnological conclusions will probably hinge on the identification of the rarer taxa, as they are often the best indicators of subtle variations in environmental parameters.

The benthic flora is represented by more than 25 genera. These include both periphytic and mobile taxa. Several of the samples contain aerophilic taxa which suggests that there is as least some input of sediment from the surrounding watershed. *Navicula* is the dominant genus, both in terms of diversity and absolute abundance, and is used as a proxy for the relative amount of shallow shelf area in the lake. Planktonic taxa (*Cyclotella* spp.) are abundant in the sediments in the deeper part of the lake. Because the environmental parameters controlling the distribution of many of the taxa found in Medicine Lake are not well understood, it is difficult to make a detailed analysis of the physical and chemical changes that have taken place over the past 11,400 calendar years.

The composition of the modern flora indicates a fresh water, circum-neutral (around pH 7) to slightly alkaline, oligotrophic lake. The samples from core B100NC-1 suggest that these conditions have not changed substantially over the past 11,400 calendar years. Despite the limitations of the physical and chemical data, it is possible to construct a lake level history using the diatom flora. *Cyclotella* spp. are used as a proxy for periods when the oligotrophic lake occupied a small, steep-sided basin with little shallow shelf area. As the most abundant benthic genus, *Navicula* is used as a proxy for periods during which lake level was higher and the deep central basins were surrounded by a broad shallow shelf (less than about 5 m deep). The ratio of *Cyclotella/Navicula* is used as a proxy for lake level (presence or absence of a shallow shelf which provided habitat for the benthic diatoms). The increase in the abundance of the obligate planktonic taxa *Fragilaria*, *Staurosira*, and *Pseudostaurosira* over the last 5,000 calendar years suggests an increase in the availability of a shallow shelf environment. The *Cyclotella/Navicula* ratio (Figure 7) gradually increases from near zero at 11,400 cal yr BP to 7.5 about 6,000 cal yr BP, suggesting a gradual rise in lake level. The ratio then drops to an average of about 3 for the last 5,500 calendar years, with variations in the ratio that suggest fluctuations in the amount of shallow shelf available for colonization by benthic taxa.

Pollen

Although the Medicine Lake record is dominated by *Pinus*, variations in the secondary terrestrial and aquatic pollen types suggest changes in regional climate and site conditions. Prior to 7,000 cal yr BP, low levels of *Abies* (fir) pollen can best be explained by an inconsistent snowpack, whereas relatively high levels of *Artemisia* (sagebrush) pollen suggest an upslope displacement of sagebursh-dominated cover relative to present conditions. The presence of *Pteridium* (fern) may be due to frequent disturbance by fire. The abundance of *Isoetes* (quillwort) spores may be correlated with the area available for colonization. *Isoetes bolanderi* var. *pygmaea*, the species presently found in Medicine Lake, is generally found in shallow lakes above 1,500 m, and the spores mature in late summer.

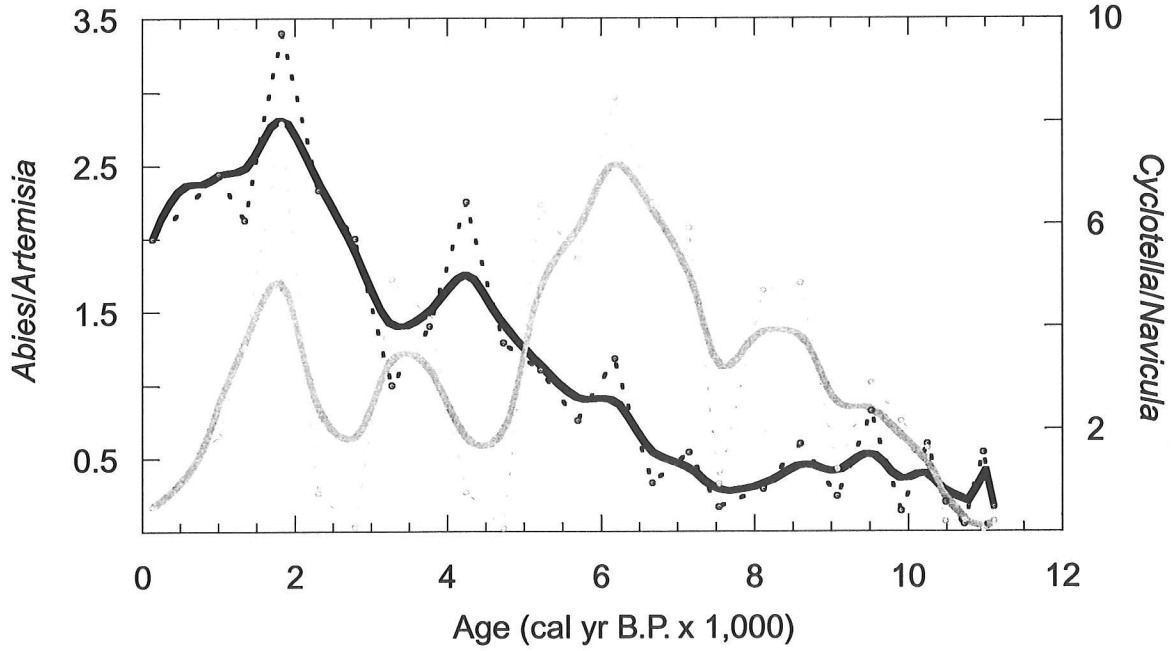

Figure 7 Record of variations in the ratios of *Abies/Artemisia* (black curve) and *Cyclotella/Navicula* (gray curve). The *Abies/Artemisia* ratio is a proxy for regional changes in effective moisture. Higher values indicate greater availability of moisture. The *Cyclotella/Navicula* ratio is a proxy for relative lake level. Higher values indicate a deeper lake with minimal shallow shelf area. Curves are smoothed using the Stineman function which incorporates ± 10% of the data range.

After 7,000 cal yr BP, the increasing importance of *Abies* and declining importance of *Artemisia* probably reflect a middle and late Holocene trend toward the establishment of a snowpack similar to present day levels. Shorter-term variations in the aquatic pollen record spanning two to four samples (1,000-2,000 years) may reflect variations in lake level over the past 7,000 calendar years. Periods of high *Isoetes* abundance coincide with an increased proportion of emergent aquatic pollen, which may be due to increased shallow shelf area.

In summary, the pollen data can be used to evaluate both the regional climate and variations in lake level. The *Abies/Artemesia* ratio is stable from 11,400 to about 7,000 cal yr BP. The ratio increases from an average of about 0.5 to 3 from 7,000 to 1,500 cal yr BP, and decreases to 2 today. The abundance of *Isoetes* follows a similar pattern with relative low numbers until about 7,000 cal yr BP, and then increasing to the present. A ratio of *Abies/Artemesia* (Figure 7-9) can be used as a proxy for effective moisture and the abundance of *Isoetes* spores (Figure 8) can be used as an indicator of lake level and available shallow shelf.

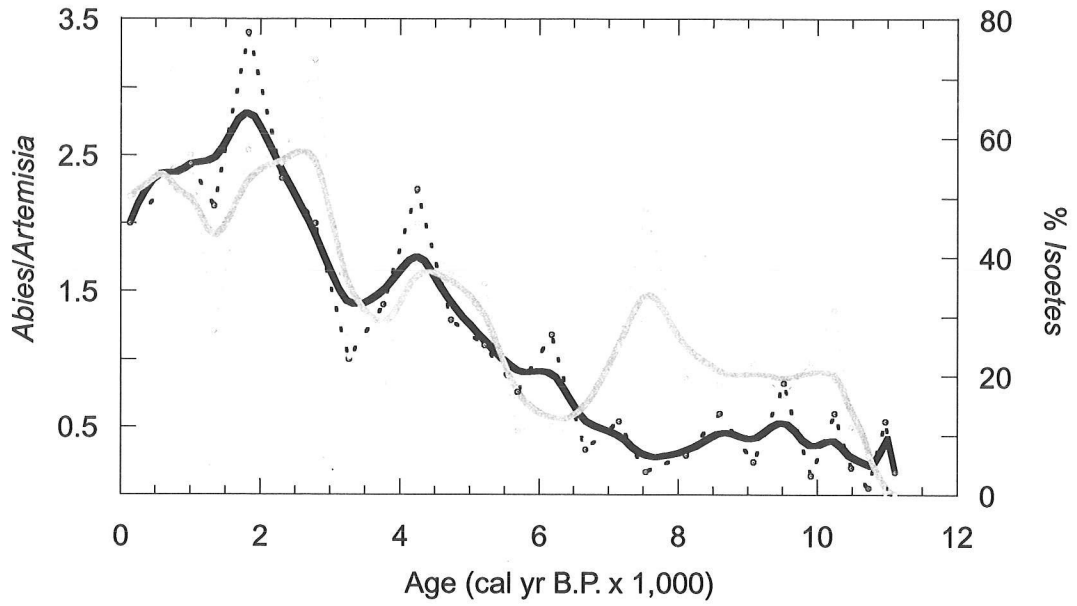

Figure 8 Record of variations in the ratio of *Abies/Artemisia* (black curve) and percent abundance of *Isoetes* (gray curve). The *Abies/Artemisia* ratio is a proxy for regional changes in effective moisture. Higher values indicate greater availability of moisture. The *Isoetes* abundance is a proxy for relative lake level. Higher values indicate a lake with greater shallow shelf area. Curves are smoothed using the Stineman function which incorporates ± 10% of the data range.

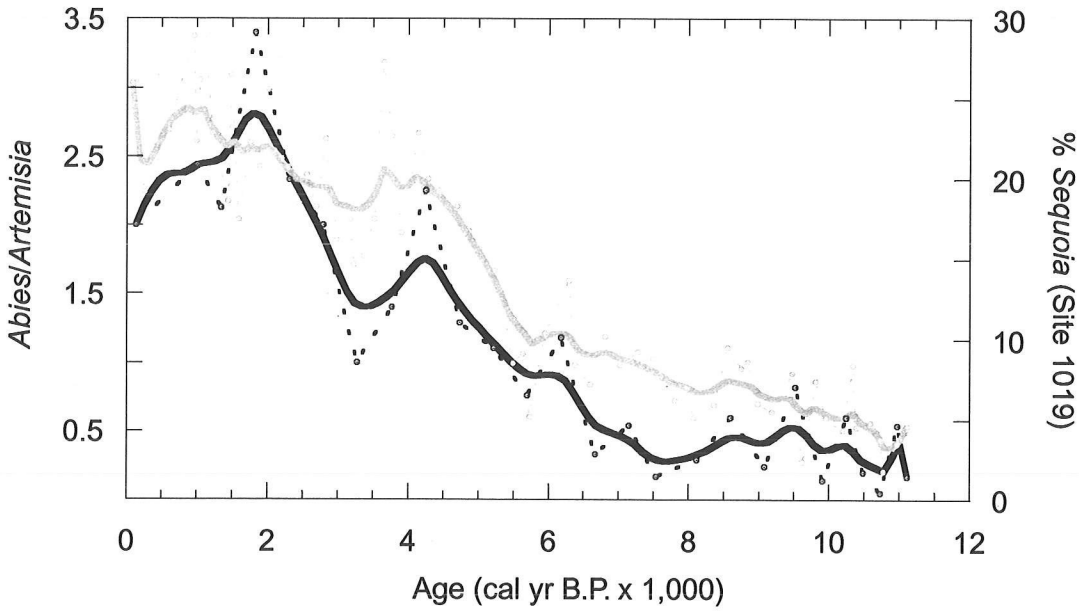

Figure 9 Record of variations in the ratio of *Abies/Artemisia* (black curve) and percent abundance of *Sequoia* (gray curve) from Ocean Drilling Program Leg 167 Site 1019. The *Abies/Artemisia* ratio is a proxy for regional changes in effective moisture. The *Sequoia* abundance record is an indicator of the effective moisture along the northern California coast. In both cases higher values indicate greater availability of moisture in their respective regions. Curves are smoothed using the Stineman function which incorporates ± 10% of the data range.

Discussion and Conclusions

The geological and paleontological data for Medicine Lake provide evidence of both the local geological processes and the regional climatic variations that affected the Medicine Lake region since the Last Glacial Maximum. Lake levels in Medicine Lake are a function of both intrinsic and extrinsic factors.

In a recent study of ODP Site 1019, off the northern California coast, Barron and others (in press) used a number of paleontological and geochemical proxies to unravel the complex Holocene climate history of the region. Over the past 11,400 calendar years, the abundance of *Sequoia* pollen increased from about 5 to more than 25% of the palynoflora (Figure 9). An increase in *Sequoia* pollen indicates a shift towards the climate of the present, with wet winters and cool, foggy summers. The *Abies/Artemesia* ratio reflects a similar trend in effective moisture. Throughout the Holocene, but particularly over the last 7,000 calendar years, the amount of precipitation in the form of both snow and rain has increased. This trend is similar to the trend found in other lakes in the western U.S. (Fritz and others 2001) which show that the middle Holocene (to about 5,500-4,500 cal yr BP) was dryer than the later part of the Holocene (Figure 10). The data from Medicine Lake suggest that during the early Holocene the basin was occupied by either two small lakes, with a surface about 10 m below the modern lake level, or that the lake was a single narrow one with two deeper basins connected by a small shallow shelf (Figure 11). For the remainder of the Holocene the surface area of the lake varied by several meters with climate-driven changes in effective moisture. The most recent evidence for these variations in lake level came with a reduction in the surface area of the lake during the droughts of the 20th century.

The ratio of *Cyclotella/Navicula*, variations in the abundance of the benthic diatom flora, and the abundance of *Isoetes* also suggest a gradual filling of one or two small, isolated basins until about 5,500 calendar years ago. The late middle and late Holocene levels of the lake exhibited changes in depth of several meters, which affected the area of shallow shelf available for colonization by *Isoetes* and benthic diatoms.

Between 2,000 and 1,500 cal yr BP an increase in the *Cyclotella/Navicula* ratio and the abundance of *Isoetes* suggest a decrease in available moisture. This interval corresponds to decreased fresh water flow into San Francisco Bay via the Sacramento and San Joaquin rivers (Starratt 2001), a brief decrease in the abundance of *Sequoia* at ODP Site 1019 (Barron and others, in press), low lake levels at Mono Lake on the east side of the Sierra Nevada (Stine 1990), and increased varve thickness in Saanich Inlet, British Columbia, which may correspond to the Roman Warm Period (Nederbragt and Thurow 2001). A more detailed analysis of short-term regional trends is not possible at this time due to the lack of high-resolution data from the available sites.

These conclusions are supported by the results of analyses from the lakes in the Klamath basin (elevation about 1,230 m) 25 km to the north. Paleontological (pollen and diatom) and archaeological data suggest the lake levels were relatively higher in the early part of the Holocene. For the last 6,000 calendar years, the lake levels in the Klamath basin appear to have fluctuated in much the same way as the lake levels at Medicine Lake (Bradbury 1991). The differences between the lakes on the Klamath basin and Medicine Lake may be due to the differences in moisture availability in low- and middle altitude lakes, changes in the morphology of the Medicine Lake volcano caldera due to magmatic movement, or some combination of these two explanations.

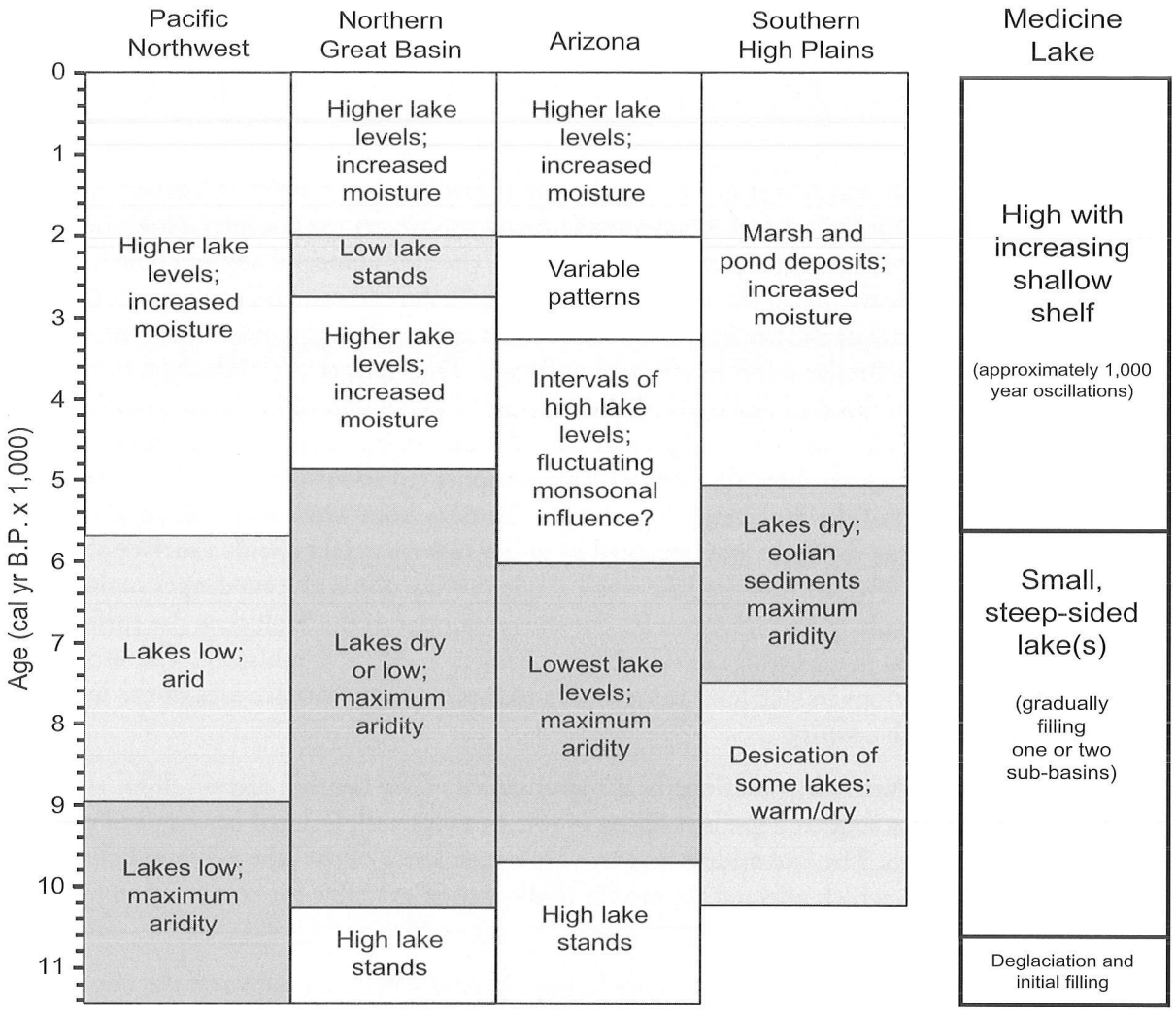

Figure 10 Paleoclimatic interpretations of selected paleolimnological records for the United States. Darker gray areas indicate periods of aridity in the Pacific Northwest, northern Great Basin, Arizona, and the southern high plains. The record at Medicine Lake indicates (1) an initial period of filling following the melting of local glacial ice, (2) a period during which two small, steep-sided lakes or one lake with two steep-sided basins connected by a small shallow shelf, and (3) a period during which the lake level increased, possibility in response to a dam created by the Medicine Lake glass flow, during which the amount of shallow shelf increased, providing increased area for colonization by benthic diatoms.

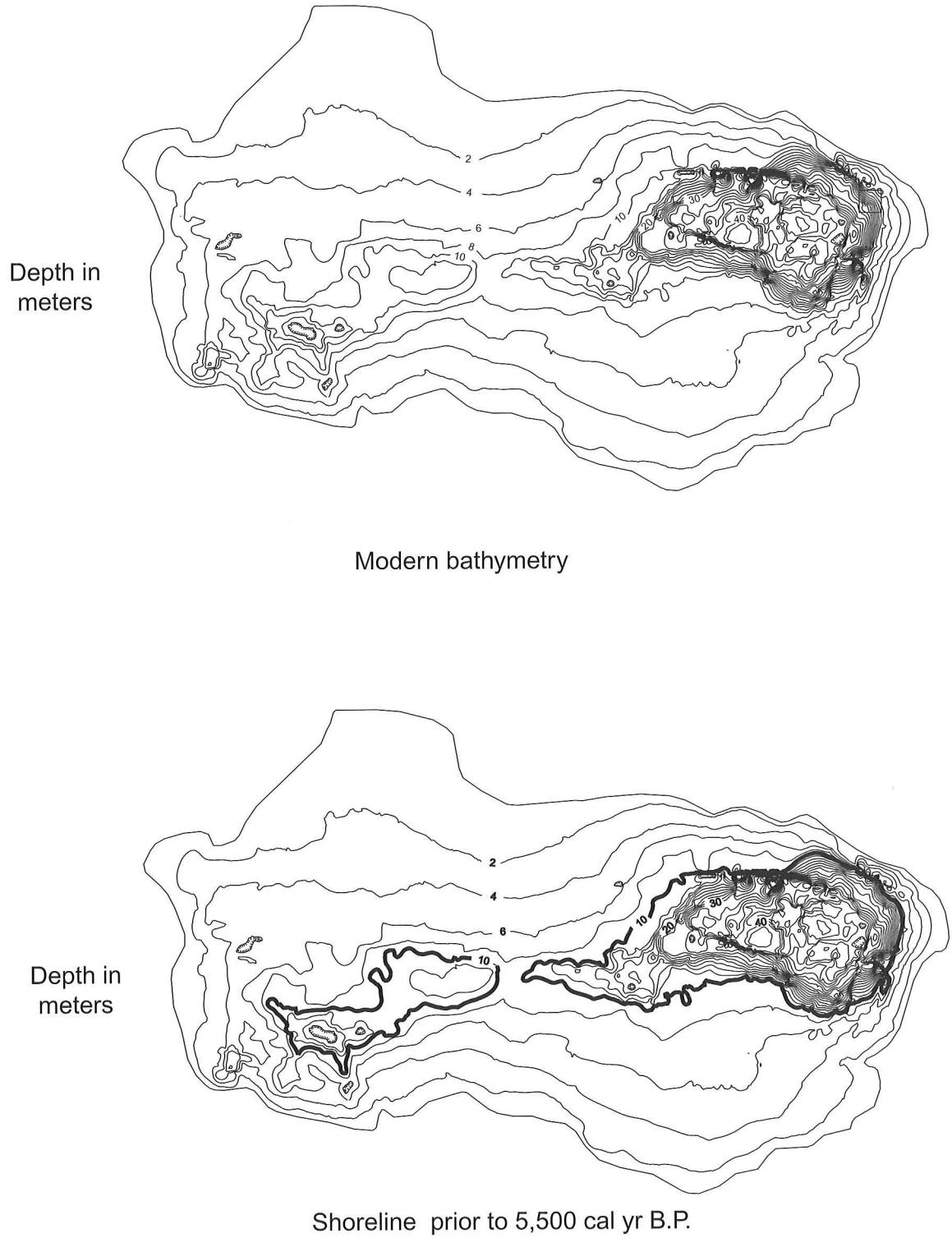

Figure 11 Comparison of modern lake boundary and a possible shoreline (bold line) for the lake at about 5,500 cal yr BP (modified from Childs and others 2000).

Acknowledgments

We thank Julie Donnelly-Nolan and Mary McGann of the USGS for their detailed reviews which not only cleaned up the grammar in the text and greatly clarified the figures, but also for reining in some of the speculative conclusions concerning the recent history of Medicine Lake volcano. Julie Donnelly-Nolan generously provided a great deal of information on the history of Medicine Lake volcano. Information on the tephra from Crater Lake and Medicine Lake volcano was provided by Charlie Bacon, Julie Donnelly-Nolan, and Manuel Nathenson and ^{14}C AMS dates were provided by Jack McGeehin, all of the USGS. This research was supported by the Earth Surface Dynamics and Volcano Hazards Programs of the USGS.

References

Anderson CA. 1941. Volcanoes of the Medicine Lake Highland, California. University of California Publications Bulletin of the Department of Geological Sciences 25:347-422.

Bargar KE. 2001. Fluid-inclusion studies of hydorthermal minerals from geothermal drill holes at Medicine Lake Volcano, northern California. California Geology 54:12-21.

Barron JA, Heusser L, Herbert T, Lyle M. in press. High-resolution climatic evolution of coastal Northern California during the past 16,000 years. Paleoceanography.

Bradbury JP. 1991. The late Cenozoic diatom stratigraphy and paleolimnology of Tule Lake, Siskiyou Co. California. Journal of Paleolimnology 6:205-55.

Childs JR, Lowenstern JB, Phillips RL, Hart P, Rytuba JJ, Barron JA, Starratt SW, Spaulding S. 2000. Bathymetric, geophysical and geologic sample data from Medicine Lake, Siskiyou County, northern California. U.S. Geological Survey Open-File Report 00-043. http://geopubs.wr.usgs.gov/open-file/of00-043/

Donnelly-Nolan JM. in press. The geologic map of Medicine Lake volcano, northern California. U.S. Geological Survey Miscellaneous Investigations Map.

Donnelly-Nolan JM, Nolan KM. 1986. Catastrophic flooding and eruption of ash-flow tuff at Medicine Lake volcano, California. Geology 14:875-8.

Donnelly-Nolan JM, Ramsey DW. 2001. Geologic mapping of Medicine Lake volcano, CA, USA. Eos, Transactions, American Geophysical Union. 82:F1318-9.

Fritz SC, Metcalfe SE, Dean W. 2001. Holocene climate patterns in the Americas inferred from paleolimnological records. In: Markgraf V, editor. Interhemispheric Climate Linkages, San Diego, Academic Press p 241-63.

Nederbragt AJ, Thurow JW. 2001. A 6000 yr varve record of Holocene climate in Saanich Inlet, British Columbia, from digital sediment colour analysis of ODP Leg 169S cores. Marine Geology 174:95-110.

Schneider RR, McFarland WD. 1996. Hydrologic data and description of a hydrologic monitoring plan for Medicine Lake volcano, California. U.S. Geological Survey Open-File Report 95-750. 17 pp.67.

Starratt SW. 2001. Diatoms as indicators of freshwater flow variation in central California. In: West, GJ, Buffaloe, LD, editors. Proceedings of the Eighteenth Annual Pacific Climate Workshop; 18-21 Mar 2001; Asilomar, California. Interagency Ecological Program for the San Francisco Estuary Technical Report 69. Sacramento (CA): California Department of Water Resources. p. 129-44.

Stine S. 1990. Late Holocene fluctuations of Mono Lake, eastern California. Palaeogeography, Palaeoclimatology, Palaeoecology 78:333-81.

Stuiver M, Reimer PJ, Bard E, Beck JW, Burr GS, Hugen KA, Kromer B, McCormac FG, van der Plicht J, Spurk M. 1998. INTCAL98 radiocarbon age calibration 24,000-0 cal BP. Radiocarbon 40:1041-83.

Overture to a Landslide—A Seasonal Moisture Prerequisite

Raymond C. Wilson

Abstract

In the San Francisco Bay region (SFBR), the threshold combinations of storm rainfall intensity and duration required to trigger shallow landslides in steep terrain were established, on a regional scale, in the late 1980s. Before even severe rainstorms can trigger landslides, however, another climatic prerequisite must be satisfied. The "antecedent condition" marks a transition in the hydrologic response of the hillslope soils from a moisture deficiency, where capillary suctions absorb most early precipitation, to a moisture surplus where a significant proportion of the precipitation drains away as stream flow. This transition must be reached before intense rainfall can produce the positive pore pressures that trigger shallow landsliding. Variations in soil moisture during the year are governed by the phase relationships and relative magnitudes of two separate climatic cycles, precipitation and evapotranspiration. In the Mediterranean climate of the SFBR, these cycles are about six months out-of-phase, leading to significant seasonal variations in soil moisture.

In place of difficult and expensive instrumental measurements of hillslope soil moisture, computing the ratio of stream runoff to rainfall (Q/R) during storms may serve as a useful proxy for the antecedent condition. Real-time data on both rainfall and runoff are already available for some small mountain watersheds. Q/R ratios were computed and analyzed for several recent seasons in two small mountain watersheds, Pescadero Creek in the Santa Cruz Mountains and San Ramon in the East Bay Hills. The Q/R ratios are very low early in the rain season, increase dramatically around the time of the winter solstice, and then drop steeply after the spring equinox. The Q/R data also appear to agree well with estimates of hillslope moisture levels computed from rainfall data and the Thornthwaite water budget model.

Prerequisites to Rainfall-Triggered Landslides

In order for heavy rainfall to trigger a debris flow or other shallow landslide, two prerequisite conditions must be satisfied: (a) *Storm rainfall*—rainfall intensity > 6 mm/hr, continuously sustained for a duration of at least several hours. The intensity/duration thresholds for debris flows are already well established in the San Francisco Bay region (SFBR) (Cannon and Ellen 1988). (b) *Antecedent moisture*—before an intense storm can produce the positive pore pressures that trigger debris flows, the hillslope materials must already contain a certain amount of moisture. This prerequisite, less well understood, forms the subject of this paper.

In his studies of debris flows in southern California, Campbell (1975, p. 20) noted the requirement of "an initial period of enough rainfall to bring the full thickness of the soil mantle to field capacity (the moisture content at which, under gravity, water will flow out as fast as it flows in)." Campbell noted further that the antecedent threshold may be more closely associated with total seasonal rainfall than

with rainfall shortly before a storm that triggered debris flows. In his study of debris flows at La Honda, south of San Francisco, Wieczorek (1987) noted a similar requirement for antecedent rainfall.

Subsequent authors have related antecedent rainfall to the soil suctions (also described as negative pore pressures) that exist in under-saturated soils. For example, after monitoring rainfall, positive pore pressures, and soil suctions on a hillslope near Berkeley, Johnson and Sitar (1987) concluded that the chance that a rainstorm would generate positive pore pressures was strongly linked to the pre-storm soil moisture conditions. Under dry conditions, high soil suctions (> 1500 mm of water) will prevent the formation of the positive hydrostatic pore pressures. Storms occurring under wet conditions with relatively low soil suctions (< 500 mm of water) were much more likely to generate positive pore pressures. Because debris flows are believed to be triggered by high positive pore pressures (e.g., Wieczorek 1987), the linkage between antecedent soil moisture and pore pressure becomes very important.

What Controls Hillslope Moisture?

To fully understand the interaction between rainfall and landslides, we must examine the seasonal variation in hillslope soil moisture in the region (Figure 1). The two largest factors affecting the moisture balance in hillslope soils are the input from precipitation and loss from evaporation and transpiration (evapotranspiration, ET). (Drainage by streams and subsurface percolation are relatively minor until the hillslope soils become saturated.) In the SFBR, precipitation nearly always falls as rain and is produced almost entirely from marine cyclonic systems from the northern Pacific Ocean. These storms are largest and most frequent in mid-winter, with only small, very infrequent showers during the summer and early autumn (Mediterranean climate).

Evapotranspiration is the combination of direct evaporation from the soil surface and transpiration through plant leaves. As described by Thornthwaite and Mather (1955), potential evapotranspiration is principally controlled by two factors, the air temperature and the length of daylight (related to photosynthesis). Both reach a maximum in summer and a minimum in winter, as does, therefore, the potential ET. (Dehydration of natural vegetation may shift the actual ET cycle, as described later.) The shifting balance of rainfall and ET during the year, between the peak precipitation in winter and the peak ET in summer, produces strong seasonal variations on hillslope soil moisture.

Following the water balance approach of Thornthwaite and Mather (1955), a moisture deficit is defined as the accumulated difference between evapotranspiration and precipitation over a period when ET exceeds the precipitation, referenced to an equilibrium moisture state. Conversely, a moisture surplus is attained when precipitation exceeds ET after the soil moisture has reached the equilibrium state. In Thornthwaite's system, this equilibrium state represents optimal moisture conditions for the growth of irrigated crops, but it also correlates closely with the so-called field capacity, described by Campbell (1975) as the maximum soil moisture that can be held against gravitational drainage. While moisture deficits may be accumulated over long periods of time, Thornthwaite assumed that any excess moisture would quickly dissipate as surface drainage, but the surplus values estimated from the water balance calculations may be of some use as a book-keeping device (see Figures 5 and 6).

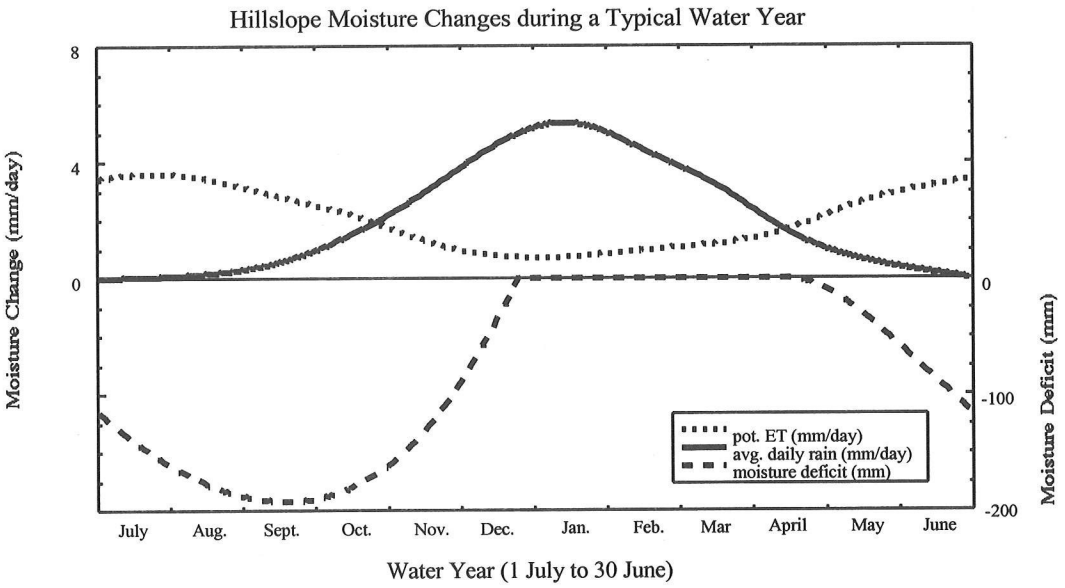

Figure 1 Plots of rainfall, potential evapotranspiration (ET), and soil moisture deficit for a site near the Pescadero watershed during a typical (mean, 1948-1998) annual cycle. The rainfall season spans the change in calendar years, so the curves are plotted in terms of the Water Year (July 1 to June 30).

During the dry months of summer and early fall (June though September), there is only scanty precipitation, but a significant loss of moisture to the atmosphere by evapotranspiration. Thus, the soils become dehydrated and, by the time rainfall resumes in mid-autumn, a substantial moisture deficit has built up. Soil suctions are strong and stream flows are very low, fed by ground water drained from bedrock (base flow). Early season rainfall is simply absorbed into the soil. Until the autumnal moisture deficit is made up, even heavy rainfall may have little effect on slope stability and landslides are very unlikely.

During the early winter, rainstorms become more frequent and evapotranspiration (ET) losses decrease, leading to a reduction in the moisture deficit. If winter rainfall is sufficient, eventually the soil moisture becomes completely restored to equilibrium (zero deficit). Once the antecedent threshold is passed, subsequent rainfall may produce a soil-moisture surplus, which is removed within a few days by stream runoff. Heavy rainfall may even create significant positive pore pressures, which reduce the frictional shear resistance of the soils, and may result in debris flows or other types of landslides. In a typical year in the SFBR, the moisture deficit is satisfied in late December, then remains at or near equilibrium until mid-April, when rainfall decreases and warmer temperatures and longer days increase ET, leading again to an increasing moisture deficit (Figure 1).

Actual Versus Potential ET: Thornthwaite's water-balance system, developed for managing agricultural irrigation, is based largely on his concept of potential evapotranspiration — the amount of moisture that the atmosphere would absorb from healthy, well-watered agricultural fields during daylight hours. However, as natural, non-irrigated hillslopes dry out, the actual ET decreases because there is less available soil moisture. Actual evapotranspiration rates can be estimated as the product of the potential ET times the ratio of the remaining soil moisture to the equilibrium moisture content (Thornthwaite and Mather 1955, p. 23). Thus, actual ET approaches the potential ET only during

mid-winter, when the hillslope soil moisture is at or near equilibrium. While potential ET peaks in mid-summer, the actual evapotranspiration rates reach a maximum during late spring (Figure 2).

A Proxy for the Antecedent Condition: It would be very important to the operation of a debris-flow warning system to establish when early seasonal rainfall approaches the antecedent moisture condition. Prior to this, even heavy rainfall is unlikely to trigger significant debris-flow activity, but once attained, the antecedent moisture condition can be maintained with even modest rainfall through the mid-winter and early spring (Figure 1) until ET increases again after the Vernal equinox. Thus, this period of high soil-moisture levels essentially defines the season during which hazardous debris-flow activity is a threat.

Direct instrumental measurements of hillslope moisture can be difficult and expensive to carry out on a regional scale, however. During the mid-1990s, USGS staff (M. Reid and S. Christian) installed a small network of tensiometers and time-domain-reflectometry (TDR) soil moisture probes on a small hillslope near La Honda, California. These instruments were monitored for several rainfall seasons and provided some intriguing results (Reid, unpublished data), but required a significant investment of labor to install, calibrate, and maintain. Eventually, it became obvious that the costs for scaling up the network to cover even a few square kilometers would be formidable.

Fortunately, a proxy may be available that would make use of real-time and historical data that are already being collected. Here, I undertake a preliminary study, based on data sets available on the Internet, to see if the ratio of stream runoff to rainfall (Q/R) from a storm, might characterize the moisture content of a small watershed. Using the USGS real-time water data network (http://waterdata.usgs.gov/ca/nwis/), runoff data (mean daily discharge) were collected from stream gages in two small, low-order watersheds, Pescadero Creek on the west slope of the Santa Cruz Mountains (USGS stream gage 11162500), and San Ramon Creek on the east slope of the East Bay Hills (USGS stream gage 11182500). Both watersheds are composed mostly of steep hillslopes and natural vegetation. Using rainfall data from the NOAA National Climate Data Center archive, compiled and re-formatted by a commercial vendor (EarthInfo, Boulder. CO), daily rainfall data for the Pescadero Creek study were selected from the rain gauge at San Gregorio (NCDC Cooperative Network Index, CA-7807) and, for the San Ramon area, from a gauge near San Leandro Reservoir (NCDC Cooperative Network Index, CA-9185).

The interactions of the rainfall and stream flow data with the estimated soil moisture in the Pescadero watershed are illustrated in Figures 3 and 4. The daily rainfall and daily mean stream flow data are directly from the rain gauge at San Gregorio and the stream gauge on Pescadero Creek. The soil moisture is calculated using a water balance model adapted from Thornthwaite and Mather (1955). Figure 3 is a plot of the three variables during the 1998 Water Year, one of the wettest years on record.

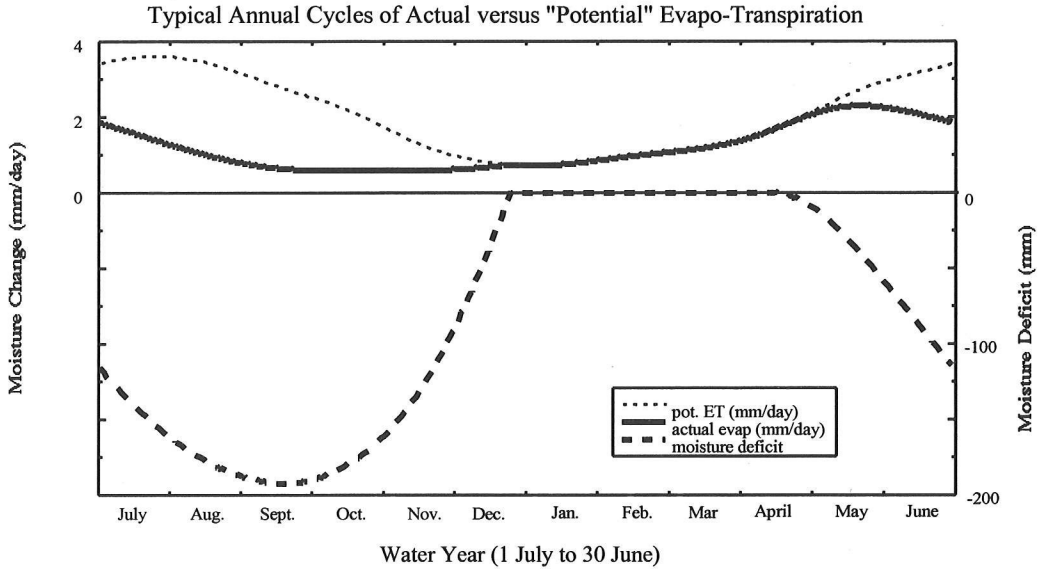

Figure 2 Plots of actual, versus potential, evapotranspiration and soil moisture deficit for typical water year depicted in Figure 1.

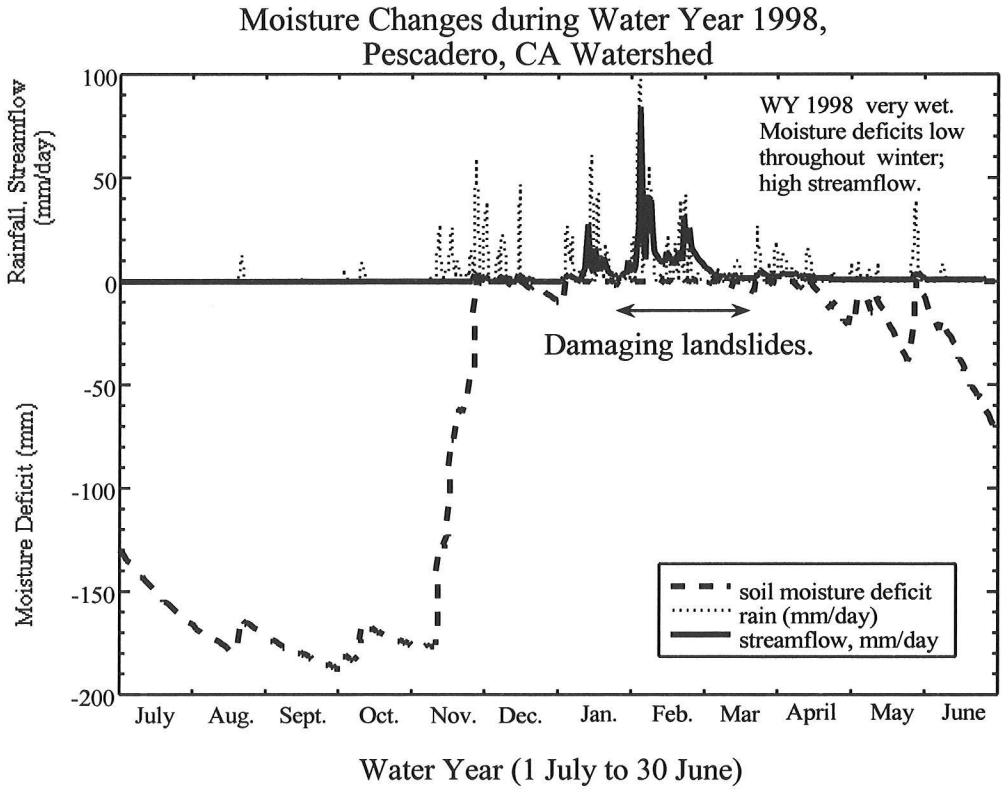

Figure 3 Plots of rainfall, stream flow, and soil moisture deficit for the Pescadero watershed during the very wet 1998 Water Year. (Daily stream flow is converted from discharge (cfs) into equivalent water depth over the watershed area, mm/day.)

The first few rainstorms in the early autumn of 1997 had virtually no effect on stream flow and only temporary effects on the soil moisture (Figure 3). Beginning in November, however, more frequent rainfall began to re-hydrate the soil and the moisture deficit decreased until reaching zero at the beginning of December. The storms in December produced detectable, but modest, amounts of stream flow, but then dropped back to base flow during a dry spell in late December. In mid-January, however, the rains returned in force and the soil moisture quickly returned to its equilibrium (zero-deficit) levels, and the stream gauge recorded substantially increased discharge from each storm episode. Ultimately, a severe storm sequence in early February produced heavy steam flow, local flooding downstream from the stream gauge, and many debris flows in the upper portion of the watershed (Jayko and others 1999). In a neighboring watershed, the hillslope moisture levels rose enough to re-activate a portion of a deep-seated landslide, damaging and destroying a number of homes (Jayko and others 1998).

Later in the spring, the rains abated somewhat, but the hillslope moisture levels stayed near equilibrium until early April, when higher ET values from the longer days and higher temperatures began to dry to soil. An unseasonable rainstorm in late May produced a brief return to wet conditions, but the stream flow response was only modest. Finally, by June, the rains had ended and high ET values quickly began to dehydrate the hillslope soils. The annual grasses wilted and turned brown, and the hillslopes returned to the dry summer portion of the annual cycle (Figure 1).

Figure 4 shows a similar plot for a different, much drier water year—WY 1994. The 1994 WY actually began with a smaller moisture deficit than WY 1998, and the October levels were about the same for both years. The beginning of the 1993 autumn rains was close to the normal schedule, but then rainfall was far less than normal in December and January, and well below normal in February and March. Even so, the soil moisture level almost reached equilibrium in late January. There were a few, modest elevations of stream discharge during moderate rainstorms in February, but the total discharge for the year was much below normal. There was no landslide activity reported in the Pescadero watershed during WY 1994.

The next step in this study was to perform a hydrograph separation analysis to distinguish the pulses of rapid storm runoff from the background base flow, assumed to represent seepage of bedrock ground water. Long-term variations in base flow were traced by plotting stream flow hydrographs for the entire rainfall season. Use of a semi-logarithmic scale allowed a more accurate portrayal of the relatively low discharges in the periods between storms, so that the base flow could be traced visually. The net storm discharge, Q, was found by subtracting the estimated base flows from the total discharge flows recorded during storm periods. Finally, as shown in Figure 5, the ratio of storm runoff (Q) to storm rainfall (R) was plotted against an estimate of the hillslope moisture content during the storm.

Figure 5 shows the interaction between soil moisture and the ratio of storm runoff to storm rainfall, Q/R. Although there is an area of somewhat ambiguous Q/R behavior in the mid-range of soil moisture values (-50 mm to +40 mm), the overall influence of the hillslope moisture over the Q/R ratio is clear. For moisture deficits deeper than -50 mm, none of the Q/R ratios exceed 0.10. For strong surplus conditions (> +50 mm), there is a clear increase in Q/R with increasing moisture surplus, albeit with a fair amount of scatter. All of the very strong discharge events, Q/R > 0.40, occur during periods of moisture surplus. The seasonal pattern of stream flow versus hillslope moisture may be seen even more clearly in Figure 6, which superimposes plots of Q/R for several years (WY1994-1998) onto a single, seasonal axis referenced to the Water Year Day the storm began.

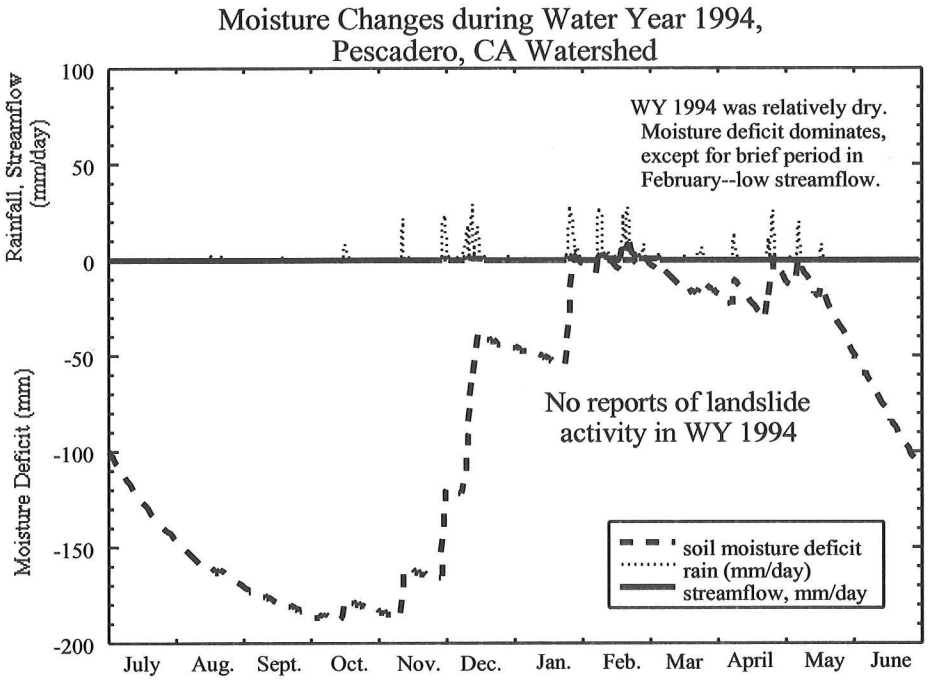

Figure 4 Plots of rainfall, stream flow, and soil moisture deficit for the Pescadero watershed during the relatively dry 1994 WY. (Same units and procedures as Figure 3.)

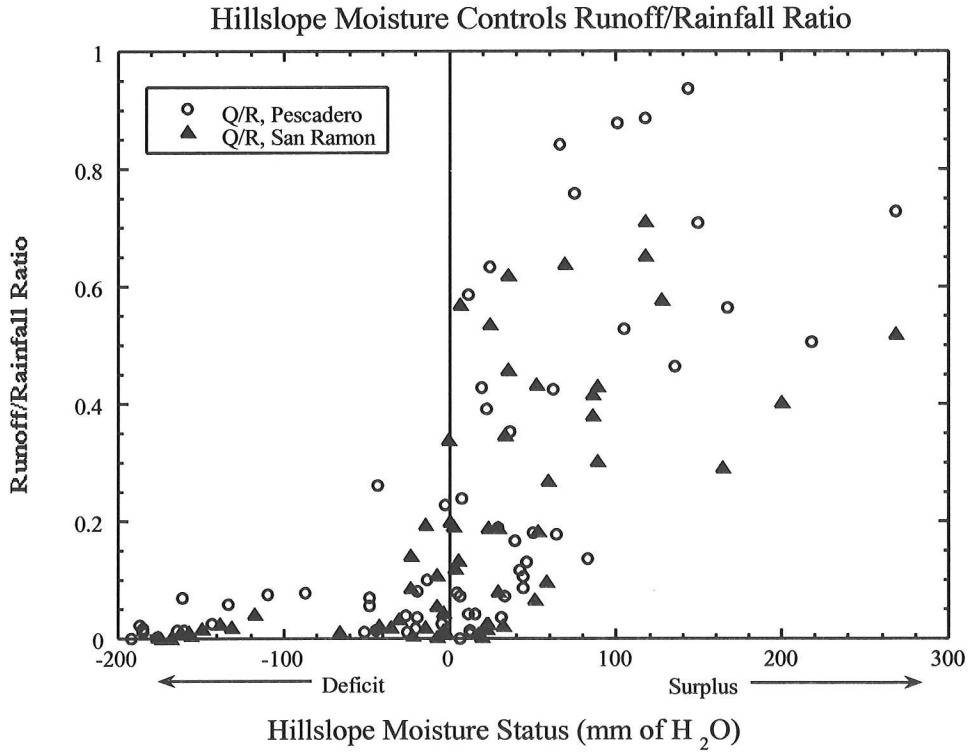

Figure 5 Plots of the runoff-to-rainfall ratio (Q/R) versus the status of the soil moisture for the San Ramon and the Pescadero watersheds during a period of five years (WY1994-WY1998).

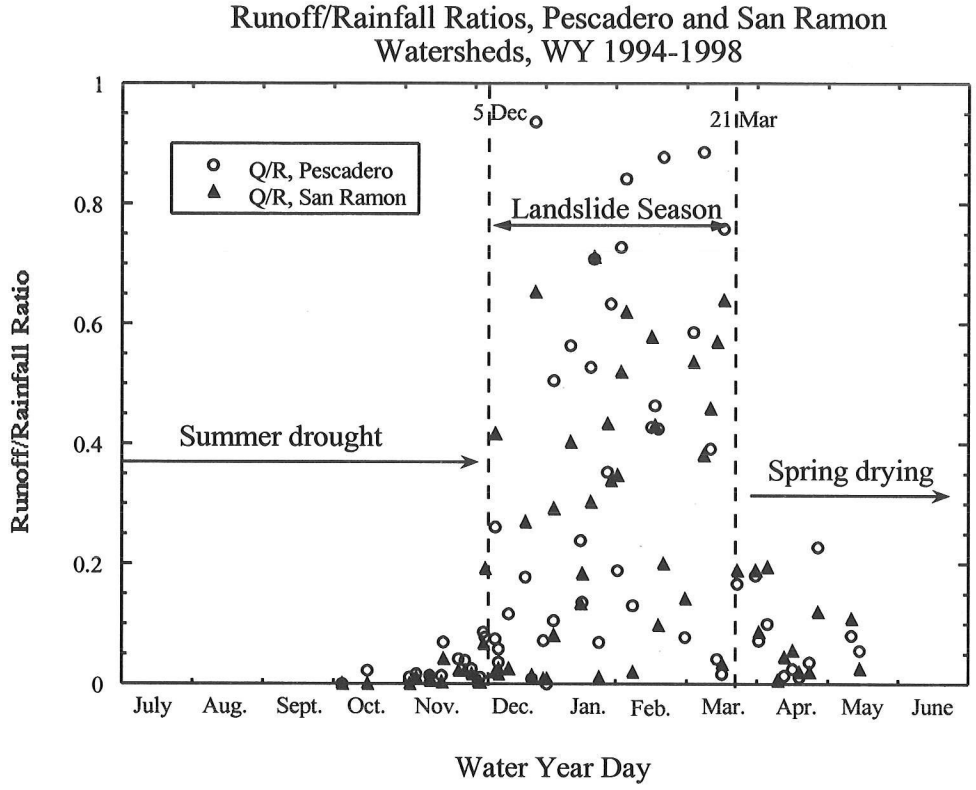

Figure 6 Plots of runoff-to-rainfall ratio (Q/R) versus the day during the Water Year (WYD) that the storm began. (San Ramon and Pescadero watersheds; WY1994-WY1998)

While the Q/R ratio is uniformly low early in the Water Year (July-October), in early December there is an abrupt transition to a widely variable Q/R state with much higher maximum values. This period of high—and highly variable—Q/R values continues through the balance of the winter (January to mid-March). After the Spring Equinox (~March 21), the upper range of Q/R declines steeply, returning to uniformly low values by late May. This timing is in general agreement with the water balance model shown in Figure 1, but the Q/R ratios appear to rise and fall more abruptly, over the space of only a few days. This may reflect the fact that the Q/R ratio is based on actual measurements of rainfall and stream flow, while the idealized ET/water-balance assumes an artificially smoothed distribution of rainfall and uniform properties for hillslope soils across the watershed.

Conclusion

In light of the great variation in Q/R during the post-antecedent winter months (Figures 5 and 6), this procedure still gives us no reliable way to forecast the stream discharge from rainfall alone. The goal of this work is not to forecast peak storm flow, however, but rather to understand the seasonal variation in the potential for landsliding and its relation to the hillslope soil moisture. For this purpose, we need only know when the soils are at or near moisture equilibrium, and a Q/R ratio exceeding a value of 0.20 appears to be a reliable indicator of this condition. Within the SFBR, the first storm of the annual rain season where Q/R crosses this threshold may be considered the date on

which the "antecedent condition" is fulfilled in that watershed. Barring extraordinarily long dry spells (> 2 weeks), the soil moisture should remain high until at least the Vernal equinox in late March.

References

Campbell RH. 1975. "Soil slips, debris flows, and rainstorms in the Santa Monica Mountains and vicinity, Southern California," USGS Professional Paper no. 851, United States Geological Survey, Washington D. C., 51 pp.

Cannon SH, Ellen SD. 1988. Rainfall that resulted in abundant debris-flow activity during the storm, in Ellen SD, Wieczorek GF eds., Landslides, floods, and marine effects of the storm of January 3-5, 1982, in the San Francisco Bay region, California: U.S. Geological Survey Professional Paper 1434, p. 27-33.

Jayko AS, Rymer MJ, Prentice CS, Wilson RC, Wells RE. 1998. Scenic Drive landslide of January-March 1998, La Honda, San Mateo County, California: U.S. Geological Survey Open-File Report 98-229, 1 plate.

Jayko AS, De Mouthe J, Lajoie KR, Ramsey DW, Godt JW. 1999. Map showing locations of damaging landslides in San Mateo County, California, resulting from 1997-98 El Niño rainstorms: U.S. Geological Survey Miscellaneous Field Studies Map MF 2325-H (available on-line at http://greenwood.cr.usgs.gov/pub/mf-maps/mf-2325-h/).

Johnson KA, Sitar N. 1987. Debris flow initiation: an investigation of mechanisms: Geotechnical Engineering Report UCB/GT/87-02: Department of Civil Engineering, University of California, Berkeley, California, 179 pp.

Thornthwaite CW, Mather JR. 1955. The water balance: Publications in climatology, v. 8, no. 1, Laboratory of Climatology, Drexel Institute of Technology, Centerton, New Jersey, 104 pp.

Wieczorek GF. 1987. Effect of rainfall intensity and duration on debris flows on central Santa Cruz Mountains, California, in Costa JE, Wieczorek GF eds., Debris flows/avalanches: processes, recognition, and mitigation: Geological Society of America, Reviews in Engineering Geology, v. 7, p. 23-104.

The 400-Year Wet-Dry Climate Cycle in Interior North America and Its Solar Connection

Zicheng Yu and Emi Ito

Several high-resolution paleoclimatic records from lakes and peatlands in the northern Great Plains (NGP) show some regular patterns of late Holocene climate changes at centennial time scales. Sites from Minnesota to Alberta (Figure 1) that show centennial wet-dry cycles, especially at ~400 years, include Elk Lake, MN (400- and 84-yr; Dean 1997); Pickerel Lake, SD (~400-yr; Dean and Schwalb 2000); Moon Lake, ND (400-yr; Laird and others 1996); Coldwater Lake, ND (137-yr; Fritz and others 2000); Rice Lake, ND (400-, 201-, 129- and 99-yr; Yu and Ito 1999); Pine Lake, AB (440-yr; Campbell and others 1998); and the Upper Pinto Fen, AB (386-yr; Yu and others unpublished). The most pronounced feature in most of these NGP records is that relatively dry periods alternate with short-lived wet periods about every 400 years. Superimposed on these wet-dry cycles, stacked time series from four sites (Rice, Moon, Coldwater, and Elk lakes) for the last 1000 years show characteristic climate patterns during the Medieval Climate Anomaly (MCA) and Little Ice Age (LIA). The MCA was represented by two dry peaks centered at 650 and 850 cal BP, while the LIA was dominated by a single drought peak around 300 cal BP (Yu and others 2002). These double Medieval droughts are likely correlated with two generations of relict tree stumps as recorded in the Great Basin of California (Stine 1994, 1998).

We attribute this dominant 400-year wet-dry cycle to solar forcing (Yu and Ito 1999, 2000). Solar activities as indicated by solar proxy of cosmogenic isotopes (^{14}C, ^{10}Be) show a fundamental periodicity at ~400 years (Stuiver and Braziunas 1989; Figures 2 and 3). Dry periods in the NGP appear to correlate with solar minima (Yu and Ito 1999). Recent climate modeling suggests that solar variation likely causes a large temperature change at regional scale through a forced shift in atmospheric variability (e.g., North Atlantic Oscillation), although global-scale temperature only shows a minor response (Shindell and others 2001). These modeling results also indicate that lands and oceans show opposite responses to solar forcing. Thus we argue that the interior of the continents is more sensitive than other land areas to small changes in solar variations, especially over a longer time scale. This response in the NGP is perhaps related to a shift in dominant modes of the atmospheric pressure fields (e.g., Pacific-North American teleconnection pattern).

Aridity could be caused by either decreased precipitation (moisture availability and atmospheric circulation support) or increased evapotranspiration (net radiation and temperature). Either of these changes could occur either during particular seasons or throughout the year. Shindell and others' (2001) modeling results suggest much greater cooling in winters over the continents, in response to Maunder Minimum of solar irradiance. Similar seasonal changes might also occur in the NGP during portions of climate cycles of late Holocene. For example, during the mid-Holocene dry prairie period, ostracode data from Elk Lake, MN, indicate colder winters and summers but very dry summers (Forester and others 1987). This combination of cold and dry conditions rather than warm and dry conditions may occur more commonly than generally assumed. If this is the case during the late Holocene in the NGP, then decreased precipitation may play a greater role in causing droughts than increased evapotranspiration. Multiple proxy approach would be useful in investigating this seasonal

nature of droughts in future studies, which would provide further test of modeled results. Paleoclimate records in continental interior would also contribute toward the detection of spatial pattern of climate changes, which may provide new insights into the cause and mechanism of climate changes (Bond and others 2001).

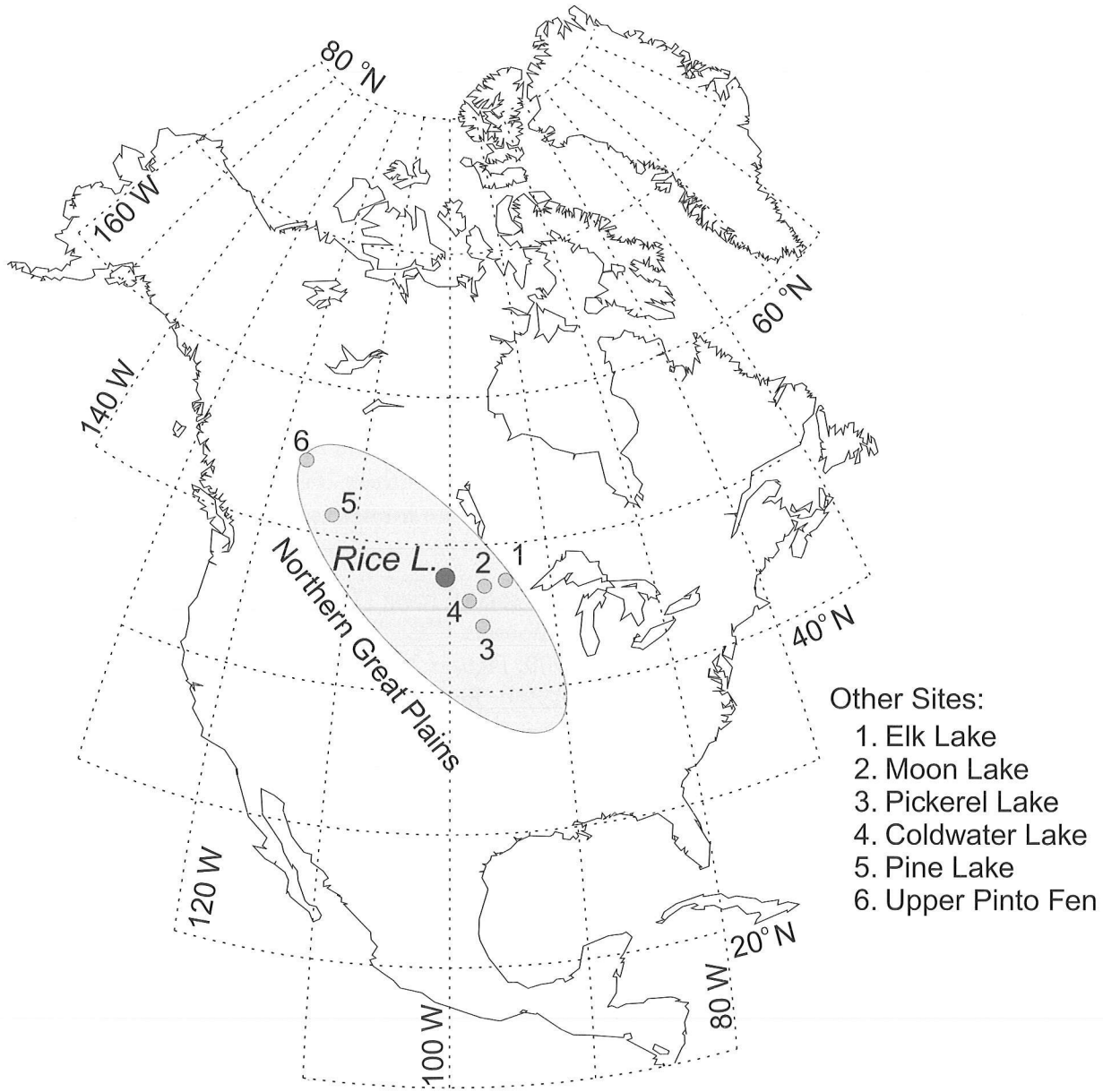

Figure 1 Map showing the location of Rice Lake, Ward County, North Dakota (Yu and Ito 1999) and other sites in the northern Great Plains of North America. (1) Elk Lake, MN (Dean 1997); (2) Moon Lake, ND (Laird and others 1996); (3) Pickerel Lake, SD (Dean and Schwalb 2000); (4) Coldwater Lake, ND (Fritz and others 2000); (5) Pine Lake, AB (Campbell and others 1998); (6) Upper Pinto Fen, AB (Z. Yu and others unpublished data).

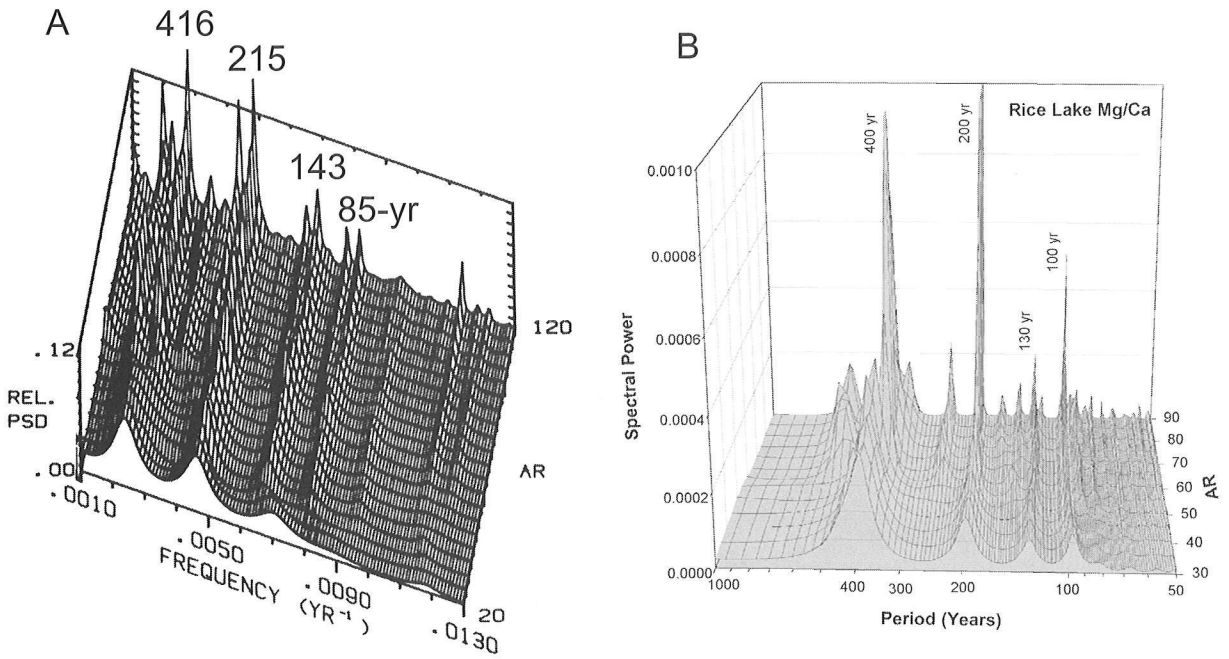

Figure 2 Similarity of spectral features of solar proxy (^{14}C time series) and climatic proxy (Mg/Ca ratios). A. Relative power spectral density (PSD) versus autoregressive (AR) order and frequency (1/yr), derived from maximum entropy method (MEM) analysis of the ^{14}C production rate. Periods (416-, 215-, 143-, and 85-yr) were converted from frequency data. From Stuiver and Braziunas (1992). B. Spectral power of Mg/Ca time series from Rice Lake. Plot shows periods (in year) and relative spectral power at different AR orders derived from MEM (Yu and Ito 1999). The dominant 400-, 200-, 130-, and 100-yr periods (as a distinct set of harmonics) persist from AR order of 30 (high confidence and low resolution) to AR order of 90 (low confidence and high resolution).

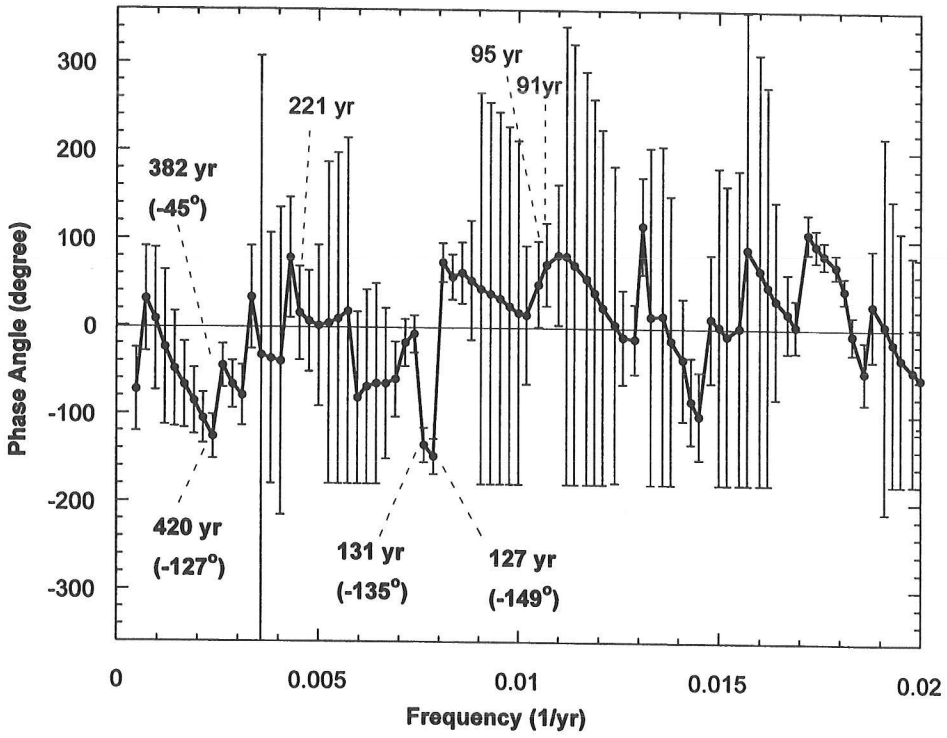

Figure 3 Phase spectrum (shown as phase angle) between Rice Lake Mg/Ca ratios and ^{14}C time series, derived from cross-spectral analysis using SPECTRUM program (Schulz and Stattegger 1997). The bold letters indicate periods (420-yr, 382-yr, 131-yr, and 127-yr) significant statistically at 80% level (coherent) with phase angle in bracket (negative values indicating the Rice series lagged behind ^{14}C series). For example, at period of 131 years Rice climatic events lag solar forcing by ~49 years (131 years * [135°/360°]). The plain letters are periods showing as peaks but below 80% significance level.

References

Bond G, Kromer B, Beer J, Muscheler R, Evans MN, Showers W, Hoffmann S, Lotti-Bond R, Hajdas I, Bonani G. 2001. Persistent solar influence on North Atlantic climate during the Holocene. Science 294:2130-2136.G.

Campbell ID, Campbell C, Apps MJ, Rutter NW, Bush AB. 1998. Late Holocene ~1500 yr climatic periodicities and their implications. Geology 26:471-473.

Dean WE. 1997. Rates, timing, and cyclicity of Holocene eolian activity in north-central United States: Evidence from varved lake sediments. Geology 25:331-334.

Dean WE, Schwalb A. 2000. Holocene environmental and climatic change in the Northern Great Plains as recorded in the geochemistry of sediments in Pickerel Lake, South Dakota Quaternary International 67:5-20.

Forester EM, Delorme LD, Bradbury JP. 1987. Mid-Holocene climate in northern Minnesota. Quaternary Research 28:263-273.

Fritz SC, Ito E, Yu ZC, Laird KR, Engstrom DR. 2000. Hydrologic variation in the northern Great Plains during the last two millennia. Quaternary Research 53:175-84.

Laird KR, Fritz SC, Maasch KA, Cumming BF. 1996. Greater drought intensity and frequency before AD 1200 in the Northern Great Plains. Nature 384:552-554.

Shindell DT, Schmidt GA, Mann ME, Rind D, Waple A. 2001. Solar forcing of regional climate change during the Maunder Minimum. Science 294:2149-2152.

Schulz M, Stattegger K. 1997. SPECTRUM: Spectral analysis of unevenly spaced paleoclimatic time series. Computers and Geosciences 23:929-945.

Stine S. 1994. Extreme and persistent droughts in California and Patagonia during medieval time. Nature 369:546-9.

_____1998. Medieval climatic anomaly in the Americas. Pages 43-67 in Water, Environment and Society in Times of Climatic Change. A.S. Issar, and N. Brown, editors. Kluwer, Dordrecht.

Stuiver M, Braziunas TF. 1989. Atmospheric ^{14}C and century-scale solar oscillations. Nature 338:405-408.

_____1992. Evidence of solar activity variations. Pages 593-605 in Climate Since A.D. 1500. R.S. Bradley, and P.D. Jones, editors. Routledge, London.

Yu ZC, Ito E. 1999. Possible solar forcing of century-scale drought frequency in the northern Great Plains. Geology 27:263-266.

_____ 2000. Historical solar variability and mid-continent drought. PAGES Newsletter 8(2):6-7.

Yu ZC, Ito E, Engstrom DR, Fritz SC. 2002. A 2100-year trace-element and stable-isotope record at decadal resolution from Rice Lake in the northern Great Plains, USA. The Holocene 12:605-617.

Abstracts[1]

Abstracts for PACLIM 2002
Asilomar Conference Grounds
Pacific Grove, California
March 3-6, 2002

Influence of ENSO on Flood Frequency Along the California Coast

E.D. Andrews[1], Ronald C. Antweiler[1], Paul J. Neiman[2], and F. Martin Ralph[2]
[1] U.S. Geological Survey/WRD, Boulder, CO
[2] NOAA/Environmental Technology Laboratory, Boulder, CO

The influence of the El Niño-Southern Oscillation (ENSO) phenomena on flooding in California coastal streams is investigated by analyzing the annual peak floods, Q_{pk}, recorded at 38 gaging stations. The state of ENSO prior to and during flooding is characterized by the multivariate ENSO index (MEI) where MEI < - 0.5 is La Niña and MEI > 0.5 is El Niño. The flood magnitude—as represented by log Q_{pk}—in all 20 streams located south of 35° N has a significant positive correlation, (r = 0.3 - 0.6) whereas in 3 of the 4 streams located north of 41° N, flood magnitude has a significant, negative correlation with increasing MEI from -2.2 to increasing +3.2. Correlations are uniformly weak and insignificant, however, when the floods are subdivided into El Niño, neutral, and La Niña periods. South of 35° N, El Niño floods are significantly larger than non-El Niño floods. The mean log Q_{pk} (El Niño) is 2-16 times the mean log Q_{pk} (non-El Niño). During an El Niño, however, the relative strength of the El Niño has, at most, a weak influence on flood magnitude. Flood exceedance probabilities for the El Niño and non-El Niño period were calculated for all gaging stations using the log-Pearson Type III distribution. For exceedance probabilities from pe = 0.50 - 0.02, the ratio of the El Niño to non-El Niño floods varies from greater than 10 near 32° N to less than 0.7 near 42° N. Latitude explains 76 to 90 percent of the observed variation in the relative magnitude of El Niño versus non-El Niño floods over the range of exceedance probabilities.

A 2000-Yr-Long Record of Climate from the Gulf of California

John A. Barron, David Bukry, and James L. Bischoff
Earth Surface Dynamics Program, USGS, Menlo Park, CA

Kasten Core BAM80-E-17 (27.920 °N, 111.610 °W, 620 m water depth), contains a high-resolution record of paleoceanographic change within the Guaymas Basin, a region of very high diatom productivity within the central Gulf of California. Published varve counts and radiocarbon studies establish a sedimentation rate of 133 cm/kyr, so that samples taken every 5 cm for study of diatoms, silicoflagellates, and ICP-AES geochemistry, yield a sample resolution of ca. 40 yr.

1. In alphabetical order by lead author.

Roughly every 200 years, intervals enriched in diatoms alternate with intervals characterized by higher terrigenous and organic carbon (TOC), suggesting solar forcing. It seems likely that these cycles result from varying diatom abundance against a relatively constant detritus input. A prolonged interval of increased diatom accumulation between ca. 1550 and 1810 AD coincides with the Little Ice Age, implying that the November-May seasonal cycle of strong northwest winds and enhanced diatom productivity was dominant over the June-September seasonal cycle of monsoon-driven climate during this period.

A prolonged interval of dramatically warmer SSTs that is marked by a two-fold increase (above normal background fluctuations) in the relative abundance of the tropical diatom *Azpeitia nodulifera* and the tropical silicoflagellates *Dictyocha perlaevis* and *Dictocha* sp. aff. *D. aculeata* occurs between ca. 900-1170 AD, corresponding to the Medieval Warm Period. In the middle of this interval (ca.1040 AD) is a brief period of enhanced diatom production and reduced numbers of tropical diatoms and silicoflagellates that coincides with the Oort sunspot minimum.

Cycles in Sediments of Santa Barbara Basin: Is there a Solar Signal?

Wolfgang H. Berger
Geosciences Research Division, Scripps Institution of Oceanography
University of California, San Diego, CA

The varve record of Santa Barbara Basin, for the last millennium, shows a number of cycles for different properties, for example, varve thickness and abundance of fish scales. These cycles (near 100 y, and whole-number fractions thereof) have been reported on previously in the literature. The question whether some of these cycles are of solar origin is considered by comparing the spectrum of sunspot cycles with spectra of varve cycles. A simple statistical device is used to produce a "diagnostic spectrum" from a regular spectrum. It allows sorting out relationships between cycles with different periods, thus giving hints as to the underlying basic period(s). Results suggest that tidal cycles may provide important forcing for the series described.

Decadal Variability in the California Current System: Patterns, Change Points, and Biological Implications

Steven Bograd[1], Roy Mendelssohn[1], Franklin B. Schwing[1], Ronald J. Lynn[2], and John A. McGowan[3]
[1] NOAA/NMFS/Pacific Fisheries Environmental Laboratory, Pacific Grove, CA
[2] NOAA/NMFS/Southwest Fisheries Science Center, La Jolla, CA
[3] Scripps Institution of Oceanography, La Jolla, CA

We explore decadal variability in hydrographic structure, circulation, and ecosystem response within the California Current System (CCS) over the period 1950-2000. In the first part of the talk, we use the 50-year CalCOFI data set to document and quantify significant changes in water column structure (deepening of the thermocline and increase in stratification) in the coastal ocean off southern California following the North Pacific climate shift of 1976-1977. These changes have combined to reduce the supply of inorganic nutrients to the upper water column, leading to large declines in zooplankton biomass and the abundances of many higher trophic level organisms. In the second part of the talk, we use state-space models to examine long-term trends, nonorthogonal

common trends, and significant climate-driven change points in a set of subsurface temperature time series representing the meridional and offshore extent of the CCS. We use global one-degree summaries from the World Ocean Database at 11 locations and 10 standard depths in the upper 200 m for the period 1950-1994. Four common trends account for most of the total variance and the important time-dependent features of the temperature series. The first common trend, essentially a weighted mean of the series, reveals a series-long warming tendency at all locations, with the greatest changes occurring at 50 m (75 m) depth for the coastal (offshore) stations. Superimposed on the long-term warming trend are a number of interannual fluctuations, most associated with El Niño and La Niña events. Weights for the second and third common trends clearly separate the study area in the offshore and meridional directions, respectively, while the fourth common trend separates the series by depth. Many of the features and change points described by the first common trend are also seen in the second common trend, but accentuated at coastal locations and mitigated offshore. In particular, the rapid warming seen around the 1976 regime shift in the first common trend appears to be an acceleration of a warming trend that began several years earlier. The third common trend, with weights greatest in the thermocline, features maxima during strong El Niño years, thus accentuating these events at southern latitudes (and in the thermocline) but neutralizing their signal north of 40°N. The depth-dependent effect of the fourth common trend reveals a gradual warming of the thermocline prior to 1983 followed by a cooling trend, leading to increased thermal stratification in the CCS. We use these results to speculate on the nature and causes of regime shifts and variable ENSO responses in the Northeast Pacific, and on their biological consequences.

Framework for Assessing the Risk of Using Remote Climate-Based Streamflow Forecasts in California Reservoir Operations

Levi Brekke and John A. Dracup
Department of Civil and Environmental Engineering, UC Berkeley, Berkeley, CA

This research investigates risks of using remote-climate-based streamflow forecasts in California reservoir operations. The term "remote-climate" means (1) geographically relative to our local region (i.e. Northern California) and (2) one- to six-month average atmospheric pressure structure or sea surface temperature conditions in the Pacific region. The framework includes climate teleconnection analyses, water resource systems operations studies, and risk assessments on using imperfect forecast information from several decision-making perspectives.

The teleconnection analyses are performed to identify the strongest associations between remote-climate variability and local hydrologic variability. Results from these analyses are used to develop a streamflow forecast model based on remote- and locally-observed variables (e.g. snowpack accumulation). The model is then used to develop historical streamflow forecast data with and without consideration of the remote-climate variables for an operations study to assess changes in (1) monthly delivery level forecasts prior to delivery year cycles and (2) monthly water allocation. The California State Department of Water Resource's model of the Central Valley Project and State Water Project, CALSIM II, is used to conduct the historical operations study. Finally, the risk assessments are performed using delivery level forecast and water allocation information from the operations study to characterize the marginal risk carried by multiple decision-makers when remote-climate data are used to influence California reservoir operations. Each assessment includes a decision model

describing use of delivery level forecast information and two risk assessments: a business-as-usual case and an alternative case where remote-climate conditions are considered.

Preliminary results will be presented on the teleconnection analyses and on the business-as-usual risk assessment for the San Joaquin Valley row crop farmers. Special considerations for other decision-making perspectives will also be discussed, including those for agricultural producers, municipal water distributors, and state/federal water resource system managers.

Late Holocene Climate Change and Mesoamerican Prehistory: A Highland-Lowland Comparison

Roger Byrne
Department of Geography, University of California at Berkeley, CA

Until recently most prehistorians rejected the thesis that climate change was an important factor in Mesoamerican prehistory. This negative point of view was in part at least a reaction against the early environmentalist views of Huntington and others. However, during the past 20 years or so the situation has changed. Several investigators have suggested that late Holocene changes in climate did have an important impact on the distribution and density of prehistoric populations, especially in the Mayan lowlands.

In this paper I review some of the pollen and isotope evidence for late Holocene climate change in Mesoamerica. The evidence shows that during most of this time period rainfall trends in highland and lowland Mesoamerica were out of phase. I also suggest that these changes in climate had far reaching impacts on human populations both in the highlands and the lowlands. One important implication of the evidence is that the Maya Decline at ca. AD 900 was not due to drought but to increased precipitation.

Twentieth century climate data indicate that the highland-lowland teleconnection is also important on a decadal time scale. Possible causal mechanisms will be discussed.

Climatic Impacts on Fijian Coral Reefs During the 1990s

Richard Casey[1] and Annette Casey[2]
[1] Ocean Research International and University of San Diego
[2] Ocean Research International, San Diego, CA

Two coral reefs on the Fijian island of Vanua Levu were affected by bleaching, physical breakage, siltation, overgrowths of black and calcarious algae and sponges, high temperature shock, and salinity changes.

On January 3, 1993, Cyclone Kina hit the Fiji Islands. Two reefs were studied in detail, one off the airport near Savu Savu; and another off the Mu Mu Resort 15 kilometers east of the airport. Both transects were studied in 1992 as well, in which the only reef damage noted was the presence of coral bleaching from the ongoing El Niño. Sea pennies (large foramnifera) were present along both of these transects. Reef flats were dominated by coral hash. *Acropora* dominated the reef crests of both transects with significant amounts of *Porities*. Immediately after the hurricane, *Acropora* was found to

be planed off the reef crests and deposited on the reef flats with silt and sand covering some of them. The July 1993 stumps of *Acropora* and *Porities* at the reef crest were covered by masses of sponge. On the reef flats coraline algae covered much of the coral hash (mainly *Acropora*) and no sea pennies were found for the rest of the year's study. It was in July 1993 that obvious black band disease was found at the base of the inner tidal zones. The last transects taken were in 1997. We saw the reefs after a Fijian drought of 18 months had ended with a considerable storm. As a result, sediment laden streams, especially at the Airport site with road construction at the time, caused siltation which appeared to have done most of the damage to the reefs during this decadal study.

The pristine reefs of 1992 suggest that the following decade of reef destruction was an uncommon scenario of climate effects and man-made pertubation.

Tropical Tropospheric Temperature Variations Caused by ENSO and Their Influence on the Remote Tropical Climate

John C. H. Chiang[1], Adam H. Sobel[2], and Yochanan Kushnir[3]
[1] Joint Institute for the Study of the Atmosphere and Ocean, University of Washington, Seattle, WA; and Department of Geography, University of California, Berkeley, CA.
[2] Department of Applied Mathematics and Applied Physics, and Department of Earth and Environmental Sciences, Columbia University, New York, NY
[3] Lamont-Doherty Earth Observatory, Columbia University, Palisades, NY

The warming of the entire tropical troposphere to an El Niño is well established, if not well understood. This observation allows for a useful simplification of the tropical El Niño-Southern Oscillation (ENSO) teleconnection problem, through assuming that ENSO controls the interannual variability of tropical tropospheric temperatures. We examine the potential impact of this warming to tropical climate away from the ENSO region by examining the vertical adjustment of a single column model to imposed tropospheric temperature variations. The column model is set to predict the ENSO impact over Precipitation(P)>Evaporation(E), P<E, and no convection regions over a hypothetical mixed layer ocean. In both P>E and P<E regions, model precipitation and sea surface temperature (SST) responds significantly to the forcing; in general, precipitation decreases and SST increases to warmer tropospheric temperatures. However, the amplitude and phase of precipitation and SST response depends on how fast the mixed layer ocean adjusts to the forcing. We analyze the model response to understand the underlying mechanisms behind the precipitation and SST variations.

We show observational evidence that suggests our model results are applicable to SST and precipitation variability over the global tropics. Our mechanism offers a simple explanation for the large-scale spatial structure of remote tropical surface temperature response to ENSO, in particular why the southeastern tropical Atlantic and southeastern tropical Indian Ocean SST variability is not linked to ENSO. We discuss the implications of our results to ENSO teleconnections over the global tropics.

Climate Science and Services: Some Lessons from CLIMAS

Andrew C. Comrie[1], Maria Carmen Lemos[2], Malcolm K. Hughes[3], and Jonathan T. Overpeck[4]
[1] Department of Geography and Regional Development, University of Arizona, Tucson, AZ
[2] Center for Latin American Studies, University of Arizona, Tucson, AZ
[3] Laboratory of Tree-Ring Research, University of Arizona, Tucson, AZ
[4] Institute for the Study of Planet Earth, University of Arizona, Tucson, AZ

The Climate Assessment for the Southwest (CLIMAS) is one of several Regional Integrated Science and Assessment (RISA) projects established in recent years in the United States. These RISAs have begun to blur the division between climate science and society, through the production of "usable" knowledge from interaction between scientists, policymakers and the public. Climate scientists, like many other members of the science community, have typically had difficulty involving users (stakeholders) in the process of knowledge creation in efforts to gain broader support for their research enterprise. One critical aspect has been their inability to reconcile the needs of users with the state of their science. We address this issue by describing the way basic and applied climate science have been integrated with user needs in the "end-to-end" RISA model by CLIMAS. First, we discuss how the interdisciplinary CLIMAS team works with users to identify common research objectives. Next, these objectives are placed in a framework that summarizes the basic character of the research and its relation to users. We then highlight these interactions by examining specific examples of climate research sub-projects driven by users' needs. We draw from our interactions with users in different areas such as water and wildland fire management, public health, farming and ranching. Finally, we discuss lessons learned and highlight how the concept of usable science can be expanded into a critical component of the climate science enterprise with the establishment of a new national climate services program. We emphasize the need for continual and iterative interaction between the science and user communities, extending the "end-to-end" model in order to sustain science-user partnerships such as those that have been developed by CLIMAS.

Cyclic Variations in Rainfall and River Flow on the West Slope of the Sierra Madre, Mexico: Titanium as a Proxy for Influx of Volcanic Rock Debris

Walter E. Dean
U.S. Geological Survey, Denver, CO

Titanium concentrations in sediment samples from a core collected in the Gulf of California off the west coast of Mexico between the mouths of the Rio Yaqui and Rio Mayo, two of the largest rivers draining the west slope of the Sierra Madre Occidental, exhibit striking cycles over the last 200 years with an average period of about 10 years. The concentration of titanium is higher in basic volcanic rocks than in average crustal rocks, and the Sierra Madre is a very large pile of volcanic rocks. The average titanium concentration in the record (0.35%) is more than twice the average titanium concentration (0.16%) in sediments deposited over the same time interval recovered in a core taken farther offshore, and farther north, closer to the Colorado River delta. The cycles are interpreted as due to greater and lesser riverine influx of volcanic rock debris from the Sierra Madre. The titanium cycles coincide almost exactly with 10- to 12-year cycles of precipitation as reconstructed from tree rings (Fritts 1991). The cycles are more distinct in sediments deposited prior to AD 1940, which may

reflect damming of rivers during the 20th century. Could variations in rainfall and river flow on the west slope of the Sierra Madre somehow be connected with the solar sunspot cycle?

Exciting the Delayed-Action Oscillator of the Tropical Pacific Climate with Decadal Changes in the Sun's Irradiance

Michael D. Dettinger[1] and Warren B. White[2]
[1] U.S. Geological Survey, Scripps Institution of Oceanography, La Jolla, CA
[2] Scripps Institution of Oceanography, La Jolla, CA

Decadal variations of global and regional temperatures, precipitation, and other climatic conditions that parallel historical changes in the Sun's irradiance have been difficult to understand given the small amplitude of the associated radiative-forcing changes at the Earth's surface (e.g., ~ 0.5 W m^{-2}). A mechanism is proposed here whereby natural modes of the Earth's climate system are excited by these small solar-irradiance changes, yielding a near-resonant response that amplifies the Sun's influence. The delayed-action oscillator mechanism, at the root of El Niño/Southern Oscillation (ENSO) processes in the tropical Pacific Ocean basin, is a natural mode of the Earth's climate system that influences climate variability significantly and globally. Recent studies have shown that this delayed-action oscillator mechanism influences the Pacific climate variability on three principal time scales, biennial, interannual, and decadal timescales, with the latter phase locked to variations in the Sun's total irradiance.

Here we force a model of a broad band delayed-action oscillator for the Pacific basin, with relatively small periodic and quasiperiodic solar-irradiance variations, and obtain simulated tropical sea-surface temperature and zonal-wind variations that align with, and are much more energetic than expected from, the small quasiperiodic solar signals alone. We find that the freely oscillating natural modes of the global climate system resulting from the Pacific's delayed-action oscillator mechanisms can resonate with small decadal changes in the Sun's total irradiance (even when there is considerable mismatch between their respective time scales). In nature, this interaction would yield global climate variations that parallel and greatly exceed those expected from simple Stefan-Boltzmann radiative balances at the Earth's surface. Also, the excited decadal modes are closely in phase with the solar forcings, in agreement with observed upper-ocean temperature variations. Finally, temperature responses simulated with historical solar-irradiance forcings are more realistic than are corresponding simulations forced by historical insolation changes associated with fluctuating volcanic-aerosol loads in the atmosphere.

Sensitivity of California Vegtation to CO2-Induced Climate Change: A Regional Modeling Study

Noah S. Diffenbaugh, Lisa C. Sloan, Mark A. Snyder, and Jason L. Bell
Department of Earth Sciences, University of California-Santa Cruz, Santa Cruz, CA

Anthropogenic increases in atmospheric carbon dioxide (CO2) concentrations may affect vegetation distribution through at least two mechanisms: directly through CO2 fertilization, and indirectly through CO2-induced climate change. An equilibrium vegetation model (BIOME4) and a regional climate model (RegCM2) were used to test the relative sensitivity of California vegetation to the

doubling of pre-Industrial atmospheric CO2 concentrations and the potential climatic changes caused by that doubling. The kappa statistic was used to quantitatively test these sensitivities. Biomes containing deciduous trees show the greatest sensitivity to direct CO2 effects. Cool and cold forest biomes, along with temperate grassland and shrubland, show the greatest sensitivity to secondary climatic effects, and the California vegetation as a whole is statistically more sensitive to climatic effects than to direct CO2 effects. Finally, in all but one case (evergreen taiga/montane forest), individual California biomes show greater sensitivity to the two effects combined than to either of the individual effects, indicating that the two must be considered in tandem when assessing the regional impacts of anthropogenic greenhouse gas emissions.

Stratigraphic Evidence in Polar Ice of Variations in Solar Activity

Gisela A.M. Dreschhoff
Department of Physics and Astronomy University of Kansas, Lawrence, KS

The ice caps of the Earth are a working example of the mechanism of cold traps, which accumulate records of both large and small-scale atmospheric variations. Highly detailed plots of sequential chemical analyses on a core from Greenland have revealed pronounced oscillations in the concentrations of nitrate which are present in the firn. The geophysical significance of these thin nitrate-rich layers, dating from the period 1561-1991, has been examined in detail. They are shown to be the result of individual impulsive nitrate events, which are causally related to the generation of energetic particles by solar activity. This interpretation is based on the high degree of statistical correlation, together with the modeling studies of Jackman and coworkers. Furthermore, the impulsive nitrate events are reliable indicators of the occurrence of large flux solar proton events and are in good agreement with probabilities derived from cosmogenic isotopes in moon rocks.

The significance of the declining phase of the 11-year solar activity cycle has been recognized in the long-term record of individual ionization events in the polar atmosphere. It is suggested that there were five periods when large solar proton events were up to eight times more frequent than in the era of satellite observations. There is an indication of a well-defined Gleissberg (~80 yr) periodicity in large flux solar proton events, and that solar proton production was most active for the Gleissberg cycle 1580-1660 (just before the Maunder Minimum) and 1820-1910. Based on these data we may expect a significant increase in the frequency of solar proton events beginning with the next solar activity cycle. In addition, this type of oscillation appears to reflect changes in solar activity, which have occurred in the past 1000 to 3000 years with implications for the climate of the Earth.

A Review of Climate Change and Marine Mammals—Patterns, Hypotheses, and Questions

Karin A. Forney
Southwest Fisheries Science Center, National Marine Fisheries Service, Santa Cruz, CA

Potential effects of climate change on marine organisms are complex and the subject of myriad studies spanning broad taxonomic groups. Marine mammals encompass about 120 species grouped into 20 distinct families spanning five orders with diverse life histories. Although mechanisms of physical-biological coupling linking oceanography and marine mammals are still poorly understood,

hypotheses about potential effects of climate change on marine mammals have been formulated based on studies combining population or distribution data with oceanographic measures at varying time scales. Highly mobile cetacean species are likely to respond to climate change primarily by changing their distributions as the location of productive foraging areas or suitable breeding habitat shifts. Some of the expected shifts may mirror patterns documented on seasonal and interannual time scales for regions where temperate and tropical waters mix, such as the California Current System. Ultimately, such shifts may cause changes in the relative abundances of individual species as oceanographic conditions change the amount of suitable habitat or prey for each species. Studies of local abundance and distribution of marine mammals have revealed such fundamental shifts in community assemblage at interannual scales, spanning El Niño and La Niña events. Greater effects of climate change are expected for species that depend on the presence of specific oceanographic conditions for critical aspects of their life history. For example, arctic species, which are tightly linked to sea-ice extent, may be particularly sensitive to climatic change. Further, many baleen whales forage seasonally at high latitudes, building up fat reserves that sustain them through extensive migrations to and from their breeding grounds, where they may not feed. A change in the timing and availability of prey resources can thus have profound effects on the population growth rates of such whales. Other marine mammal species that may be particularly vulnerable to climate change are those with geographically restricted distributions, such as the endangered vaquita, a small porpoise that is found only in the northernmost regions of the Gulf of California.

Looking for Recent Climatic Trends and Patterns in California's Central Sierra

Gary J. Freeman
Pacific Gas & Electric Company, San Francisco, CA

Pacific Gas & Electric Company's (PG&E) water management team has historically assumed that future years, as groups of three or more successive years, were subject to the same levels of climatic randomness as characterized the past 25-50 years. There is increasing ongoing analysis to indicate that this may not always be the best assumption for future planning.

With approximately 40% of its long term average annual hydroelectric generation derived from aquifer outflow, typical historic practice at PG&E, with regard to forecasting future seasonal runoff beyond the current year, has focused almost entirely on analyzing the current baseflow trend for the volcanic watersheds in northern California, such as in the Pit and McCloud river watersheds. Historic climate randomness is then assumed for future seasonal precipitation and a multi-year baseflow forecast for a number of years forward is made for these northern watersheds. For watersheds overlaying the central Sierra granites, the baseflow effect of prior years is minimal and the season-to-season randomness associated with historic seasonal precipitation has with past multi-year runoff forecasts been assumed. No attempt has previously been made to utilize historic climate oscillation and trends as possible input to predict overall likelihood for precipitation in successive groups of upcoming years.

Relatively recent analysis, however, cautiously suggests that there may be approximately 14-16 year short precipitation cycles and possibly longer term cycle and trend movements, which, while not necessarily helpful for defining wetness or dryness in the following year, may possibly provide helpful insight to better anticipate wetness for successive groups of years in terms of three or more years as a

group. The apparent non-random subtle reflections of climatic cycling and trending was first noticed from the natural multi-year smoothing that accompanies decadal baseflow trends and cycles of the large northern California volcanic springs that continuously contribute water as diminishing echoes of past wetness. A portion of the water, which is now emerging from underground storage to become surface runoff, came from seasonal precipitation that occurred many decades in the past.

In this paper, an array of monthly and seasonal groupings of historic precipitation, snowpack and runoff are analyzed to reveal subtle signs of climatic oscillation and trending. While no attempt is made here to forecast future cycles of wetness based on observations of historic data, or being able to define the wetness for any given 1-2 years specifically, there may be potential for anticipating future wetness in terms of using successive groups of 3 or more years.

Seasonal Predictability of Precipitation: Frequency of Daily Precipitation Extremes over the Contiguous United States

Alexander Gershunov and Dan Cayan
Scripps Institution of Oceanography, La Jolla, CA

We explore statistical and hybrid dynamical-statistical seasonal predictability of precipitation in the contiguous United States for all seasons. Although total seasonal precipitation and frequencies of less-than-extreme daily precipitation events are more predictable, we focus on frequencies of daily precipitation above the seasonal 90th percentile (P90). Frequency of such heavy daily precipitation is shown to be predictable due to ENSO as well as to non-ENSO forcing. Diagnostic analysis suggests that ENSO and decadal variability in the north Pacific, including possible trends, are among the main predictors of U.S. hydroclimate in general and P90 in particular.

Specification skill achieved by a statistical model based on contemporaneous SST forcing with and without an explicit dynamical atmosphere is compared and contrasted. Statistical models relating the SST forcing patterns directly to observed station precipitation are shown to perform consistently better in all seasons than hybrid models where the SST forcing is first translated to atmospheric circulation via three separate general circulation models (GCMs) and the dynamically computed circulation anomalies are statistically related to observed precipitation. Skill is summarized for all seasons, but in detail for January-March, when we show that predictable patterns are spatially robust regardless of the approach used. Much of this predictability is due to ENSO. However, we also find that non-ENSO-related predictability is significant, especially for the extreme southwest, and that this is due mostly to non-ENSO interannual and decadal variability in the North Pacific SST forcing.

Prognostic analysis is carried out with the purely statistical approach to analyze P90 predictability based on antecedent SST forcing. Skill at various lead times will be presented and it will be shown that significant regional skill can be achieved at lead times of up to six months even in the absence of strong ENSO forcing.

History of the Atmosphere and Recent Weather Trends as an Indicator of Climate Trends

Jim Goodridge
Box 750, Mendocino CA 95460

Earth's atmosphere was apparently quite hot in the beginning and lacking in abundant oxygen that we share today. The history of the composition of the atmosphere is tied to the history of the biosphere. Oxygen abundance came to our planet after the chlorophyll producing organisms started releasing it in excess of that needed to precipitate soluble minerals from the oceans. The emergence of plants would not have started until nitrogen-fixing organisms flourished. Since the time that plants vigorously invaded the land the regulation of atmospheres carbon dioxide levels has been the function of chlorophyll.

In recent years the solar constant has been found to vary as the sunspot numbers. This relationship has permitted us to construct an index of the solar constant for the last 500 years. A 45-year running average of this index has two notable features. These are the Little Ice Age and the current era of robust rainfall variation in California. This relationship is even reflected in the growth records of bristlecone pines of the White Mountains of eastern California.

The third part of this paper deals with sea surface temperature and its influence on California's climate. The sea surface temperature reflects regional upwelling. Upwelling seems to respond to sea levels that are influenced by winds.

Use of Paleo-Climate Proxy Data to Enhance Drought Planning and Response

Stephen T. Gray[1], Stephen T. Jackson[1], and Christopher L. Fastie[2]
[1] Department of Botany, University of Wyoming, Laramie, WY
[2] Biology Department, Middlebury College, Middlebury, VT

We used a network of six tree-ring sites to provide 500-1000+ year proxy-records of regional drought in Wyoming. In turn, we are using these records to examine the potential effectiveness of the Wyoming state drought plan. Under the current policy, the state of Wyoming is preparing for droughts equaling the severity of events in the instrumental record. However, our proxy records show that the instrumental period was unusually mild, encompassing both wetter than average conditions and a time in which the duration of most dry events was relatively short. Variation in precipitation between wet and dry events was also dampened during the instrumental period. Likewise, spectral analysis reveals that the interval between dry events during the instrumental period differs from that of the previous 1000 years. In addition, the state plan calls for drought monitoring and mitigation efforts to be based on predetermined reporting regions. However, data from our network of sites show the spatial extent of drought conditions varying widely among dry events. As a result, the units (political and watershed boundaries) currently used in drought monitoring may be inadequate. While such spatial and temporal heterogeneity of extreme climatic events is well recognized within the paleo-climate community, our analysis demonstrates that state agencies must incorporate a longer-term perspective in their drought management policies.

Decadal to Centennial Variability in the California Current: Patterns from High Resolution Laminated Sediments

J. C. Herguera[1], B. Olivier-Salomé[1], M. A. Esparza-Alvarez[1], Carina Lange[2], G. Bernal[1], and S. Ramos-Sanchez[1]
[1] Centro de Investigación Científica y Educación Superior (CICESE), Ensenada, Baja California, México
[2] Universidad de Concepción,Concepción, Chile

There is an ongoing debate on the consequences and relevance of the last 40 year warming trend on the California Current's biological productivity decline. The observed decreased levels of zooplankton in its waters could be either interpreted as the expression of the natural variability of the Current, or alternatively as a sign of a change towards a new state where warmer surface waters would increase the mixed layer and the nutricline depth. This deepening would decrease the injection of nutrients into the photic zone and consequently lower the biological productivity of its surface waters. Records longer than the extraordinary CALCOFI historical time series are needed to characterize the variability of the Current. Here we present results derived from a high resolution reconstruction of sea surface properties from the southern reaches of the California Current with the goal of (1) characterizing the variability of sea surface temperatures timescales longer than the existing instrumental record and (2) to recover the decadal periodicities that modulate its physical and biogeochemical variability. Our study site, San Lazaro Basin at 25°N, is further characterized by relatively high levels of primary production, mostly a consequence of the advection of the cold and nutrient rich California Current waters and associated upwelling processes, which are responsible for the production and high export of organic matter, opaline and calcitic shells from the mixed layer, and the origin of the light laminae on the sea-floor of the San Lázaro basin. The microfaunal and geochemical indices preserved in these laminated sediments record the variations in the strength of the cooler flow of the California Current and its biological response. SST records were independently derived from planktic foraminiferal assemblages and from the alkenone unsaturation index (U^{k}_{37}) and compared with the instrumental SST record from the compilation by COADS for this southern region of the California Current. The planktic foraminifera derived SSTs capture the variability of the instrumental record fairly well and allow us to extend this reconstruction for the last few centuries. We will discuss the decadal to centennial periodicities we find in the reconstructed SSTs and its biological response captured by the biogenic opal record and discuss its implications in terms of the large scale North Pacific's surface circulation patterns.

Teleconnections in the Southern Hemisphere and Their Influence on Australian Hydrology

Hugo G. Hidalgo and John A. Dracup
Department of Civil and Environmental Engineering, University of California, Berkeley, CA

A rotated principal component analysis of 2.5ox2.5o gridded data of 700mb geopotential heights (Z700) for the Southern Hemisphere, obtained from the U.S. National Center for Environmental Prediction and the National Center for Atmospheric Research (NCEP-NCAR reanalysis) were used to produce monthly teleconnection time-series. The results showed trends in the Annular (2nd mode)

and Tropical Influence (6th mode) from 1948 to 2000 associated with an increase of the pressures in mid-latitudes and lower pressures in the tropics, suggesting increased transport from the tropics to mid-latitudes. Additionally, an exploratory analysis of the relationship between Southern Hemisphere's (SH) atmospheric/oceanic variables and streamflow variation in Australia is presented. Correlations at various lags and averaging windows of different size were used to link the teleconnection modes with monthly streamflow variables from Australia. The connections between these modes and ENSO variables are also included. It is expected that our study will show significant links between circulation and hydroclimatic variation in Australia.

Frequency-Dependent Climate Signal in Upper and Lower Forest Border Trees in the Mountains of the Great Basin

Malcolm K. Hughes and Gary Funkhouser
Laboratory of Tree-Ring Research, University of Arizona, Tucson, AZ

In the mountains of the arid and semi-arid interior western United States, it is particularly difficult to disentangle the effects on plant growth of elevation-related differences in temperature, precipitation and related variables such as the length of the growing season. LaMarche (1974a) explored the properties of tree-ring records along an ecological gradient, from lower- to upper- forest border in the Snake Range of eastern Nevada. He showed that there were positive correlations between high-frequency variations at all sites, but that the longer term trends and fluctuations at the upper forest border were negatively correlated with fluctuations at the lower forest border. Using both response function analysis and reasoning from the biology of bristlecone pine, he concluded that the negatively correlated low-frequency variations were likely related to warm-season temperature fluctuations, whereas the positively correlated high-frequency variations were related to precipitation. His response functions showed rather weak temperature responses, but he argued that the longevity of needles in bristlecone pine, from one to several decades, and the strong correlation between their length and summer temperature would place a bidecadal and longer temperature signal in the upper forest border ring series. This analysis was conducted using data for the period ad 1480 to 1965, from a single mountain range. LaMarche (1974b, 1974c, 1978) subsequently applied these findings to other sites in the same general region — the mountains in and bordering the Great Basin of the western United States.

Here we examine the same issues for four mountain ranges spread across the region, from the Sierra Nevada of California to Pearl Peak in northeastern Nevada, and much longer time spans, from one thousand to several thousand years. It had already been shown (LaMarche and others 1984) that there was a change in the character of the tree-ring record at high elevation in this species, with an unprecedented long upward trend continuing to the late 20th century. Although the causes of this trend are still being debated, it is clear that it is not possible to derive a useful direct calibration of the upper forest border chronologies against instrumental temperature records. Graybill and Idso (1993) showed that, prior to approximately AD 1850, the decadal and longer fluctuations in ring-width series at upper forest border in the Great Basin do indeed track summer temperature rather well, consistent with LaMarche's (1974) suggestion. They did this by comparing the mean of a set of these chronologies with a well-calibrated and verified April-September temperature reconstruction produced from maximum latewood density in a completely independent network of trees back to AD 1600 (Briffa and others 1992). As the problem of the recent century-long trend is not marked in

the case of the lower forest border chronologies, it has been possible to develop calibrations with satisfactory cross-validation for the precipitation signal at lower forest border (Hughes and Graumlich 1996; Hughes and Funkhouser 1998). These results, and other comparisons with records such as reconstructed lake levels (Stine 1994), also confirm that there is low-frequency (at least century-scale) precipitation information in the lower-forest-border chronologies. We will investigate the relationships between fluctuations in various frequency bands in the chronologies from upper- and lower-forest border.

Reference List

Briffa KR, Jones PD, Schweingruber FH. Journal of Climate 5, 735 (1992).

Graybill DA, Idso SB. Global Biogeochemical Cycles 7, 81 (1993).

Hughes MK, Funkhouser G. The Impacts of Climate Variability on Forests. Beniston M, Innes JL, editors. (Springer, Berlin, 1998), pp. 99-107.

Hughes MK, Graumlich LJ. Climatic variations and forcing mechanisms of the last 2000 years. Bradley RS, Jones PD, Jouzel J, editors. (Springer Verlag, Berlin, 1996), pp. 109-124.

LaMarche Jr, VC. Tree-Ring Bulletin 34, 1 (1974).

_____Science 183, 1043 (1974).

_____Nature 276, 334 (1978).

_____Stockton CW. Tree-Ring Bulletin 34, 21 (1974).

_____Graybill DA, Fritts HC, Rose MR. Science 225, 1019 (1984).

Stine S. Nature 269, 546 (1994).

A Lagrangian Trans-Pacific Drift Index, 1967-1998

W. James Ingraham, Jr.
Alaska Fisheries Science Center, NMFS, NOAA, Seattle, WA

In search of a new index of North Pacific Ocean circulation with the Ocean Surface Current Simulator (OSCURS) has led to the computation of 3-year trans-Pacific Lagrangian drift trajectories starting every 2.5° of latitude between 32.5° N and 45° N, along 155° E on the first of each month from 1967-1998. Nominal drift starting between 38°-42° N travels across the North Pacific Ocean constrained between 35°N and 50°N and takes about 2 years to reach the U.S. Pacific Coast where it branches northward to Kodiak, Alaska, or southward to Hawaii after the third year. Seasonal, interannual, and decadal time scales of variability are demonstrated with computer animations and discussed.

The OSCURS model is updated monthly with the new sea level atmospheric pressure fields by the Pacific Fisheries Environmental Lab (PFEL), NOAA, National Marine Fisheries Service, Pacific Grove, CA and is available to the public on http://las.pfeg.noaa.gov/las_oscurs .

Hydrologic Controls on Proxy Climate Records in Northern Great Plains Lakes

Emi Ito[1], Zicheng Yu[2], Daniel R. Engstrom[3], Sherilyn C. Fritz[4], Alison J. Smith[5] and Joseph J. Donovan[6]

[1] Limnological Research Center, University of Minnesota, Minneapolis, MN

[2] Earth and Environmental Sciences, Lehigh University, Bethlehem, PA

[3] St. Croix Watershed Research Station, Science Museum, Marine On St. Croix, MN

[4] Department of Geosciences, University of Nebraska, Lincoln, NE

[5] Department of Geology, Kent State University, Kent, OH

[6] Department of Geology and Geography, West Virginia University, Morgantown, WV

In the northern Great Plains (NGP) of North America, three dominant air masses vie for dominance throughout the course of a year. The effective moisture (P-ET) of the NGP decreases from 0 cm near its eastern edge, to -60 cm in the western Dakotas and eastern Montana, increasing to -30 cm toward its western edge. The seasonal temperature variation can exceed 50 °C. The lakes in the glaciated regions of NGP are groundwater supported and are typically found in sandy outwash plains, tunnel valleys, and kettle holes. Thus clusters of lakes and wetlands are connected by shallow aquifer system(s) leading to complex hydrochemical and isotopic responses to climate change. We discuss two case studies that illustrate these complexities.

During the mid-Holocene, two extended droughts were recorded in the sediment from Elk Lake, Grant Co., MN (deepest in a chain of lakes), centered at 5385 and 5220 cal yr BP. A drop in lake level of 14.9 m below 1994 level at ca. 5385 cal yr BP is inferred based on *Heterocypris fretensis* occurrence and higher $\delta^{18}O$, $\delta^{13}C$, and Mg/Ca values. The later drought at 5221 cal yr BP is marked by a shift to lower rather than higher $\delta^{18}O$ values and an increased abundance of the saline ostracode species *Limnocythere staplini*. That such a seemingly contradictory response can occur during severe droughts has been verified by a study of the effect of 20th century drought on the same chain of lakes based on Elk Lake sediment and historical air photos. Drought caused a 4.0 m to 5.1 m hydraulic head decline in these lakes between 1923 and 1938; all but three lakes either dried completely or declined to < 1.7m depth. The geochemistry of *Candona rawsoni* shells showed that Mg/Ca increased during drought, indicating increasing salinity as lake levels declined, corroborated by shifts to more salinity-tolerant ostracodes. However, $\delta^{18}O$ decreased during the same period as was observed for the 5220 cal yr BP drought. A numerical model of transient groundwater response to simulated drought showed that lake water level declines rapidly in the first 15 years of drought, in agreement with those inferred from air-photo lake strandlines. The unexpected finding of decreased shell $\delta^{18}O$ during drought is attributed to the absence of water in shallow wetlands that seep back into deeper lakes (during non-drought years) and to the dominance of snow-melt-derived recharge reaching Elk Lake.

Similarly, fossil ostracode shell $\delta^{18}O$ values at Rice Lake, Ward Co., ND, were found to correlate poorly with Mg/Ca. The 1998 and 2001 samplings of 13 lakes and associated upgradient wetlands in the Rice Lake chain indicated that the total dissolved solids (TDS) content of the lakes increased

down the hydrologic gradient. Conservative solutes, such as Na^+, Cl^-, and SO_4^{2-}, showed an increase with TDS while Mg/Ca increased with TDS until TDS •10,000 ppm. However, the $\delta^{18}O$ values of the lakes were found to be nearly constant (-6 ‰ VSMOW) whereas the $\delta^{18}O$ values of waters discharging from several local shallow groundwater were about -17 ‰, suggesting recharge mainly from late autumn rain or spring snowmelt. During wet years, Rice Lake probably receives, in addition to low-$\delta^{18}O$ groundwater, evaporatively evolved high-$\delta^{18}O$ water from one upland lake and several large wetlands.

There may very well be a seasonal bias in the ostracode shell data, with their $\delta^{18}O$ values strongly influenced by groundwater reflecting the $\delta^{18}O$ value of snow pack, and the Mg/Ca values largely a record of salinity controlled primarily by summer evaporation.

Climate of the Last Two Centuries: Constraints from the Instrumental Data and Paleoproxies

Alexey Kaplan
LDEO of Columbia University

Release 1c of the Comprehensive Ocean Atmosphere Data Set produced last year pushes compilations of marine observations from ship reports back to 1800. The 19th century exhibits dramatic changes in the marine data availability, from on the order of 1000 reports per year in the first two decades to a quarter of million reports per year at the close of the century. We apply the reduced space objective analysis technique to reconstruct near-global fields of sea surface temperature, sea level pressure, and surface winds with spatial resolution of 4 degrees and monthly temporal resolution for the 19th and 20th centuries. The quality of reconstructions changes significantly with the amount of available data. The reconstructions are compared with the climate variability inferred from land station measurements and with historical chronologies of prominent climatic events, like El Niño. Instrumental reconstructions are intercompared with the networks of paleoclimatic proxies. We discuss differences between the trends and dominant covariance patterns derived from the paleo and instrumental data for the 19th vs 20th centuries and attempt to distinguish between data problems and the violation of the assumption of stationarity for means and covariances that is intrinsic for the reconstruction technique.

The Empirical Search for Clues to Process and Dynamics of Climatic Change

Thor Karlstrom
U.S. Geological Survey (retired), Seattle, WA

In the absence of a generally accepted theory of past climatic change, paleoclimatic research necessarily concentrates on the empirical evidence of past climates in the search for clues relating to underlying process and dynamics. Early analysis of radiometrically, varve- and tree-ring- dated time series (Karlstrom 1955, 1956, 196l and 1972 cf.) suggested correlation of: (l) longer term ice-age trends with latitudinal changing solar insolation (the Milankovitch Climate Hypothesis);
(2) superposed shorter fluctuations modulated by globally synchronous changes in tidal forces generated by orbital relations between Sun, Moon, and Earth (The Pettersson Climate Hypothesis)

and (3) of associated processes such as volcanism (atmospheric dust and aerosols), geomagnetism and sunspots (intrinsic or geometrically induced changes in the solar constant).

Paleoclimatologists with few exceptions now accept the geometric Solar Insolation Climate Hypothesis for the Ice Ages. Most assume, however, that the waxing and waning of the larger Pleistocene terrestrial ice sheets of the northern Hemisphere determined parallel glacial and climatic changes in the Southern Hemisphere. Within the last ten years an increasing number of paleoclimatologists have turned their attention to the pervasive patterns of yearly, decadal, centennial and millennial oscillations in their paleoclimatic and instrumental time series. Relative few, however, have analyzed the possible phasing of these oscillations with solar or lunar perturbations (For exceptions, however, see, among others, Berry and Hsu 2001; Burroughs 1992; Currie and others 1981-1990; Fairbrdge 1968; Frissen-Christensen and Lassen 1991; Michell and others 1979; Keeling and Whorf 1997; Wood 1985; Sanders 1995) A major breakthrough relating to correlation of geometric solar perturbations with geomagnetism, cosmic rays, and climate (primarily precipitation) at scales ranging from the decadal sunspots to the millennial solar-insolation trends is most recently summarized in Mercurico (2001).

The purpose of this poster is to provide time-series correlation that strongly suggest cause-and-effect relations between solar/lunar perturbations and climate, volcanism, cosmic rays and solar/earth magnetism. The presented correlations focus in on definable orbital perturbations of the solar system (varying both gravity and insolation) as the operational energy system within which past climatic, volcanic and geomagnetic changes have been concurrently modulated (evidently with occasional nonlinear phase reversals) at yearly, decadal, centennial and millennial scales. The harmonic interrelations of climatic oscillations and abrupt phase reversals are characteristic of a complex noisy nonlinear system which can dramatically amplify the effects of impinging minor external periodicities or quasi-periodicities. Much work remains in further defining and understanding the operational physical linkages (physics) as well as the underlying dynamics leading to atmospheric circulation-pattern changes and evident regional variability.

According to the Solar Insolation/Tidal Resonance Climate Model, a significant, most likely dominant, part of the climatic changes of the past 100 or so years resulted from natural rather than anthropological (Industrial Revolution) factors.

The Inorganic Carbon Cycle in Subtropical Oceanic Gyres Seen in Time-Series Measurements of Surface Water near Bermuda and Hawaii

Charles D. Keeling
Scripps Institution of Oceanography, La Jolla, CA

The reservoir of dissolved inorganic carbon (DIC) in ocean water is large compared with amounts entering and leaving the surface of the oceans, but in a few locations time-series measurements have been made precisely enough in near-surface water to deduce seasonal and longer-term net air-sea exchange fluxes of CO_2. The inclusion of measurements of the $^{13}C/^{12}C$ isotopic ratio of DIC, and of alkalinity coupled with temperature, and salinity, have further provided evidence of how rapidly inorganic carbon is assimilated and remineralized within the oceans. The carbon dioxide program at the Scripps Institution of Oceanography, although focused largely on time-series measurements of atmospheric CO_2, has acquired time series for 18 years near Bermuda and 12 years near Hawaii. From

these data, a comparison of the carbon cycle can be made for two distinctly different anticyclonic subtropical gyres, the Atlantic gyre having a mixed layer that strongly varies in depth with the seasons and the Pacific gyre only a slightly varying mixed layer depth. Furthermore, the data for both gyres over the full records show a persistent increase in DIC and an even more distinct shift in the $^{13}C/^{12}C$ ratio of DIC, demonstrating that both gyres are chemical sinks for atmospheric CO_2.

Characterization of Drought in California Using the New Multivariate Drought Index

John Keyantash and John A. Dracup
Department of Civil and Environmental Engineering, University of California, Berkeley, CA

A new drought index has been developed that conjunctively considers the meteorologic, hydrologic, and agricultural aspects of drought. The Multivariate Drought Index (MDI) is based on principal components analysis (PCA) of monthly climate divisional data for six hydrologic variables: precipitation, evaporation, streamflow, reservoir storage, soil moisture, and snowpack (where appropriate). The variable set was analyzed 16 different ways to determine the best overall description of drought, as judged against the Palmer Drought Severity Index (PDSI) over the approximate period of 1970-2000 in three California climate divisions: the North Coast, San Joaquin, and South Coast Drainages. Additionally, the MDI was compared with the satellite-based Vegetation Condition Index (VCI) over the 1985-1997 period. The MDI is found to closely match the PDSI spatially and temporally, but its computational procedure is both simpler and more mathematically objective than that of the PDSI.

Cyclic Climate Change and Forecasts for Major Pacific Commercial Fish Stock Fluctuations

Leonid B. Klyashtorin
Federal Institute for Fisheries and Oceanography (VNIRO)
107140 Moscow, Russia

Instrumental time series of Global temperature anomaly (dT); Atmospheric Circulation Index (ACI); Pacific regional climatic indices (ALPI, NPI, PDO) for the last 150 years, and reconstructed air surface temperatures for the last 1500 years by Greenland Ice cores were subjected to Spectral analysis. The results suggest a general 55-60 year periodicity. Similar periodicity was revealed from analyses of sardine and anchovy outburst reconstructions for the California upwelling region for the last 1600 years. Catch statistics were analysed for major Pacific commercial species: Japanese, Californian and Peruvian sardine; Pacific herring; Pacific salmon; Alaska pollock; Chilean jack mackerel; Peruvian anchovy and some others. These also demonstrate approximately 60-year cyclic fluctuations. A stochastic model of cyclic 55-65 year fluctuations of climate and Pacific fish production intended to forecast it up to 30 years ahead has been developed for fisheries management purposes.

The Influence of Climate on Lower Food Web Production in Northern San Francisco Bay

Peggy W. Lehman
Environmental Services Office, Department of Water Resources, Sacramento, CA

Numerous studies have demonstrated the strong influence of the 1977 climate regime shift in the eastern Pacific on lower food web production in northern San Francisco Bay estuary since the 1970s. The climate shift was associated with a region wide shift in phytoplankton species composition from pennate to centric diatoms and a decrease in chlorophyll *a* biomass. These changes coincided with a shift in the percentage distribution of biomass among phytoplankton species groups. Changes in the quality and quantity of the phytoplankton biomass subsequently affected both micro and macro zooplankton production. In all studies there was a direct link between climate indices, water quality conditions and biological production. Initially the climate shift appeared to be a function of a single long-term climate shift, but detailed analyses of interannual variation suggested the long-term change was really caused by long-term change in the frequency and duration of water-year type.

Recent Changes in Snowpack Conducive Factors in the Mountainous Western United States

Mark Losleben
Mountain Research Station, INSTAAR, University of Colorado

Factors that determine whether winter precipitation is sequestered in the form of snowpack are many and varied, but a simple index may integrate these for evaluation of change over time. This index, the SCF (snowpack conducive factor), separates changes in precipitation from those factors that determine sequestration of winter precipitation in the form of snowpack, or not. This is an important distinction, climatologically, because of the hydrological and ecological ramifications during spring and summer. The SCF is the ratio of the percent of average snow water equivalent to the percent of average total cumulative precipitation, on any given date. The study area is much of the mountainous western United States, and the period is 1981-2000.

Changes in the SCF raise the question of the role of global warming on western snowpack formation, and what can be expected in the future. This study period is completely within the virtually unambiguous rise in global temperatures, and the positive phase of the Pacific Decadal Oscillation. During this period there are five strong El Niño winters, two strong La Niñas, and ten winters that are neither (weak ENSO phase winters are omitted). The results are presented in temporal, spatial, and ENSO phase contexts.

Climate Variability and Plant Migrations

Mark E. Lyford[1], Stephen T. Jackson[1], and Julio L. Betancourt[2]
[1] Department of Botany, University of Wyoming, Laramie, WY
[2] USGS Desert Research Lab, Tucson, AZ

Climate change has long been recognized as a primary cause of plant distribution changes through both range expansions and contractions. The specific role of climate variability in dictating migrations, however, is often poorly addressed. Past climate change initiated widespread natural plant migrations, but climate variability over centennial and millennial timescales may have served as a pacing mechanism of species advances. Pulses in plant migrations at scales of 10^1 to 10^3 years are likely linked to climate fluctuations at similar timescales, including oscillations associated with ENSO, Pacific Decadal Variability, and apparent millennial-scale variations in the Pacific Ocean complex. The effect of climate variability is also species dependent; particular changes in the climate system may prompt migration of some species but halt or postpone others. Climate variability may also help explain the rapid migration rates of species observed following deglaciation. Short pulses of suitable climate may permit the establishment of small satellite populations well in advance of the advancing core population. Persistence of these satellite populations through unsuitable climatic conditions would provide seed sources for further expansion under a return to favorable climatic conditions. Understanding climatic conditions that determine individual species responses will help refine our interpretations of past climate changes based on past species migrations. In addition, more comprehensive knowledge of the nature of climate variability and plant migrations will aid in estimation of future natural plant migrations under a changing global climate, as well as the expansion of non-native species.

Patterns in 20th Century Pacific Climate and Marine Ecosystems: Will Improved Predictability Lead to Improved Fishery Management?

Nathan Mantua
University of Washington, JISAO, Seattle, WA

Over the past few decades a wealth of evidence has pointed to important connections between multi-decadal climate changes coherent with North Pacific ecosystem changes. The period from the late 1970s through the mid-1990s, for example, saw sustained high productivity for most Pacific salmon at the northern end of their range coinciding with sustained low productivity for Pacific salmon at the southern end of their range. It is now recognized that this "north-south inverse production pattern" for Pacific salmon played out over much of the 20th century in response to Pacific climate changes: over multiple decades associated with the Pacific Decadal Oscillation, and from year-to-year associated with the El Niño Southern Oscillation. There is likewise abundant evidence for climate impacts on many other North Pacific marine species from the California Current north to the Bering Sea.

The growing recognition of climate influences has undoubtedly aided our understanding of variations in Pacific marine ecosystems. In contrast, understanding and predicting ecosystem changes at the time-space scales important to fishery management decisions remains a major challenge. Based on the results of a case study aimed at developing a model for predicting the abundance of Oregon coho

salmon, I will speculate on answers to the following two questions: (1) Is it likely that an improved understanding of past variations in marine ecosystems will lead to improved predictions of future ecosystem changes? (2) Would improved fishery forecasts yield improved fishery management?

Changes in Streamflow Statistics in the Conterminous United States

Gregory J. McCabe[1] and David M. Wolock[2]
[1] U.S. Geological Survey, Denver, CO
[2] U.S. Geological Survey, Lawrence, KS

A potential consequence of climatic change is an intensified hydrologic cycle, which some have speculated will result in an increased frequency of floods. Recent studies have identified trends in various streamflow statistics and have produced contradictory results. Because trend statistics can be sensitive to outliers, sequences of extreme events, and to differences in the time periods analyzed, a new approach was used in this study to identify changes in streamflow. In this study, annual minimum, median, and maximum streamflow data for 405 watersheds in the conterminous United States (U.S.) measured during 1941-2000 were examined for changes by ranking the annual minimum, median, and maximum streamflow data from lowest to highest. The original data time series were replaced by the time series of ranks. Analyses of the rank time series indicated a noticeable increase in the frequency of high-rank annual minimum and especially annual median streamflow events after 1970 for the 405 watersheds analyzed. No changes in the frequency of high-rank annual maximum streamflow were detected. These results suggest an increase in the magnitude of annual minimum and median streamflow events for recent decades compared to earlier decades, and this change appears to have been a step change rather than a gradual trend. An evaluation of climate data for the conterminous U.S. suggests that the increased magnitude of annual minimum and median streamflow events after 1970 coincides with changes in precipitation during the same time period.

Climate and Oceanic Biology-Introduction

John McGowan
Scripps Institution of Oceanography

The background for this special session is the observation that the earth's atmosphere and oceans are warmer now than at any time since reliable instrumental measurements began. We can expect the warming to continue. A great deal of effort is being devoted to understanding the physics of the warming and in picking apart the details of the carbon cycle. But it is the consequences of such climatic variability to the biology of the oceans that concerns a rather small group of biologists and this, after all, is or should be of major importance. This research is a new kind of ecology. Most biologists are unprepared for study on the time/space scales of the phenomenon, but somehow we must find our way.

This session is an attempt to gather together those biological oceanographers concerned about the consequences of change, to report on the status of their research and to determine if there is common ground among us.

San Joaquin River Flow Reconstructed to AD 901 from Tree Rings

David M. Meko[1], Ramzi Touchan[1], Malcolm K. Hughes[1], and Anthony C. Caprio[2]
[1] Laboratory of Tree-Ring Research, The University of Arizona, Tucson, AZ
[2] Sequoia and Kings Canyon National Parks, Three Rivers, CA

The San Joaquin river receives much of its runoff from the Sierra Nevada, where previous paleoclimatic evidence suggests the occurrence some 600+ years ago of droughts more severe than any in the instrumental record. The annual flow of the San Joaquin River is reconstructed from a newly assembled network of tree-ring data to quantify flow variations during those droughts and infer the associated spatial moisture patterns. The reconstruction, which accounts for 63% of the flow variance in the 1901-1989 calibration, supports the existence of a severe multi-decadal drought near AD 1300, but suggests that 100-year means of San Joaquin flow have stayed within about ±10% of the long-term mean since AD 900. Individual tree-ring records in the south show an unmatched reduction in growth near AD 1200-1300. The associated reduction in San Joaquin flow was probably small because of a strong gradient toward much wetter than normal conditions to the north in the Sacramento River drainage.

The Effects of Galactic Cosmic Rays on Weather and Climate on Multiple Time Scales

Ed Mercurio
Natural Sciences, Hartnell College, Salinas, CA

In this poster, evidence is presented that galactic cosmic rays (GCRs) are a major forcing agent on weather and climate on multiple time scales ranging from weekly through glacial-interglacial. Known effects of GCRs are used to explain phenomena and observations in the fields of meteorology, climatology, paleoclimatology and paleoecology. Evidence is presented that primary effects of increases in levels of GCRs are increases in the amounts of low clouds-especially over the tropics, increases in the albedo of low clouds and decreases of the temperature of and increases of the strength of the stratospheric polar vortex. This has widespread effects on atmospheric circulation including the El Niño Southern Oscillation (ENSO). Other effects of increases in levels of GCRs include increases in relative humidities and surface condensation, possible decreases in average amounts of precipitation, and increases in storm intensities (vorticity area index). Secondary effects arising from these include decreases in surface temperatures, increases in equabilities and, over the long term, a colder, more oscillating (more frequent ENSO-warm events) tropical Pacific and increases in levels of glaciation. Levels of GCRs in the earth's atmosphere are inversely related to the strengths of the solar magnetic and geomagnetic fields that modulate them. Variations in solar magnetic field structure are used to explain the origin of approximately weekly, monthly, quasibiennial, decadal, bidecadal, multidecadal and millennial scale climatic cycles. Changes in geomagnetism are used to explain glacial-interglacial and ~13,000 year cycles. The sum of the earth's obliquity, inclination of the orbital plane with relation to the invariable plane of the solar system and inclination of the orbital plane with relation to the plane of the solar equator is used to calculate a hypothetical curve of geomagnetism that would result over the last three million years. Higher geomagnetism and lower levels of GCRs are attributed to a greater sum of these factors. The effects of a ~412,000 year geomagnetic cycle

modulated by the earth's orbital eccentricity are also considered. The curve obtained is compared to glacial-interglacial chronologies derived from ice core and deep sea core records. Effects of extended periods of very high levels of GCRs are used to explain glacial climates. The cycle of the changing time of the year of the earth's maximum B angle (the maximum angle of inclination of the earth's orbital plane with relation to the solar equatorial plane) is used to calculate the hypothetical 13,000 year cycle of geomagnetism which is used to explain the origin of climate cycles of around this length. Effects of GCRs are used to explain characteristics of prehistoric biological communities and their variations with glacial-interglacial chronology, the uniqueness of the Holocene, causes of quaternary megafaunal extinctions and effects of resulting climates, environments and their changes on human prehistory. Predictable levels of GCRs in the future are used to predict future changes in climate.

Dynamic Similarities in North Pacific-North American Climate Variations

Tom Murphree[1], Frank Schwing[2], Bruce Ford[1], and Paula Hildebrand[1]
[1] Naval Postgraduate School, Monterey, CA
[2] Pacific Fisheries Environmental Lab, Pacific Grove, CA

The North Pacific-North American (NPNA) region undergoes a wide range of climate variations, including intraseasonal to decadal events. These events may have major impacts on basin to local scales. Sorting out the mechanisms that create these events and their interactions with each other is a complex problem. However, applying dynamic similarity concepts can make the problem much simpler. In our studies we have found several major similarities in the processes that operate over a wide range of time and space scales. The similarities in atmospheric teleconnections, air-sea forcing, and the development of upper ocean anomalies are especially pronounced. We present several examples of these processes and their impacts on the NPNA at intraseasonal, interannual, and decadal scales. We also examine how climate variations in the NPNA are linked to those occurring in Asia and the North Atlantic, and how these linkages vary seasonally.

Solar and Ocean-Related Signals of Climate in the Tropics: Evidence from Lake Turkana, East Africa

P. Ng'ang'a[1], T.C. Johnson[2], and M.D. Dettinger[3]
[1] Department of Biology and Earth Sciences, Texas A&M University-Commerce, Commerce, TX
[2] Large Lakes Observatory, University of Minnesota, Duluth, MN
[3] USGS, Scripps Institution of Oceanography, La Jolla, CA

Century- to millenial-scale variations in the $\delta^{13}C$, $\delta^{15}N$, %C, and %N in the organic matter are observed in Lake Turkana sediments. These variations seem to represent past changes in lake level in response to changes in precipitation and probably are related to solar activity, changes in sea-surface temperature and instabilities in ocean circulation. Specifically, variations in the $\delta^{13}C$ of the organic matter in Lake Turkana sediments have periodicities established in the radiocarbon record of 400-yr (Suess cycle) and 84-yr (Gleissberg cycle) cycles related to solar periodicities. The %C and %N of the organic matter have periodicities of 628-yr and 518-yr. These cycles are proxies of precipitation and are similar to cycles observed in ocean sediments at the end of glacial terminations I, II, and IV, and

thus probably are related to changes in sea surface temperatures and instabilities in ocean circulation. Less robust 47- to 53-year cycles in the $\delta^{13}C$, $\delta^{15}N$, and nitrogen content might be related to the 44-yr "Double Hale" cycle (4 x Sunspot cycle). The interaction of solar, atmosphere, and ocean-related phenomena and their effects on climate are most pronounced on a decadal-scale as evidenced by the presence of high-frequency periodicities in the paleo-record representing these phenomena.

Solar Irradiance Variations from UV to Infrared

Judit M. Pap
Goddard Earth Science and Technology Center,
University of Maryland, Baltimore County/NASA Goddard Space Flight Center

The Sun's radiative output has been monitored at various wavelengths and integrated over the entire solar spectrum — hence total irradiance — for almost three consecutive solar cycles. These multi-decade long space measurements of total solar and spectral irradiance established conclusively that the Sun's radiative output varies on time scales from minutes to the 11-year solar cycle and these variations are associated with the Sun's magnetic activity. Since the Sun's radiative output establishes the Earth's thermal environment, knowing the source and nature of its variability is essential to understanding and predicting the interactions in the Sun-Earth system. Recent studies indicate that long-term variations in total solar irradiance, which may be larger than observed over the last solar cycles, may contribute to climate changes from decades to millennia. It has also been shown that variations in the UV irradiance influence the stratospheric ozone and may indirectly influence circulation and climate in the troposphere. In this talk we will summarize the results of the multi-decade long irradiance measurements and will discuss the various mechanisms causing irradiance variations.

Solar Effect on North American Hydroclimatology Through Pacific Sea-Surface Temperatures and Atmospheric Vorticity

Charles A. Perry
U.S. Geological Survey, Lawrence, KS

Significant correlations exist between total solar irradiance (SI) and measured hydroclimatologic characteristics in North America. These characteristics include annual regional precipitation, annual glacier-mass change, mean annual lake levels, and annual river flow. A physical mechanism is proposed to account for these correlations that begins with the absorption of varying amounts of solar energy into the tropical Pacific Ocean Warm Pool, creating ocean-temperature anomalies. The ocean-temperature anomalies then are transported over time by ocean currents to the North Pacific where the warmer or colder than normal water initiates the development of ridges or troughs in the upper atmosphere. Upper atmospheric ridges or troughs in the North Pacific have a distinct effect on the formation of lower atmospheric low-pressure or high-pressure systems over North America. Low-pressure systems produce precipitation, and their intensity and frequency determine the regional hydrologic response.

In this study evidence for the mechanism for the solar/climate correlation is examined step by step. A 50-year sequence of Lean's annual SI is first correlated with sea-surface temperatures (SSTs) just

northeast of the Philippine Islands in the area 130 to 140° E and 20 to 30° N (Area 1). Next, the SSTs in Area 1 are correlated with SSTs in the eastern North Pacific Ocean at 150° W and 50° N (Area 2). Then the SSTs in Area 2 are correlated with the vorticity of the upper atmosphere, which provides a measure of upper atmospheric ridging or troughing above Area 2. Subsequently, the upper atmospheric vorticity over Area 2 is correlated with the lower atmospheric vorticity over central North America near 92° W and 41° N (Area 3). Finally, the lower atmospheric vorticity in Area 3 is correlated with a standardized flow index for six major rivers in Iowa, which is significantly correlated with the original annual SI variations now lagged 4 to 5 years.

Variations in the correlations among the individual steps indicate that the solar/climate mechanism is complex and has a time element (lag) that is not constant. The Pacific Decadal Oscillation (PDO) phase seems to have some effect on the lag time between various steps of the mechanism with the cool, eastern Pacific phase creating shorter lag times. When the average SST of the North Pacific Ocean (20 to 55° N and 130° E to 110° W) is considered, there appears to be a direct relation between SI and average SST.

High Resolution Stable Isotope Record in Holocene Lake Cahuilla Tufa: Evidence of Paleoclimatic Change and/or Episodic Colorado River Delta Switching?

Richard A. Peters[1], Hongchun Li[2], H. Paul Buchheim[1], and Lowell D. Stott[2]
[1] Department of Natural Sciences, Loma Linda University, Loma Linda CA
[2] Department of Earth Sciences, University of Southern California, Los Angeles CA

The level of ancient Lake Cahuilla in the Salton Basin depends on the balance of Colorado River inflow, and local evaporation and precipitation. The inflow of the Colorado River into the Salton Basin has been strongly tied to episodic switching of the Colorado River delta between the Gulf of California and the Salton Trough. These events are initiated by overbank flooding of the Colorado River, and result in rapid filling and/or freshening of Lake Cahuilla. $\delta^{18}O$ and $\delta^{13}C$ isotopic analysis of 153 samples obtained from a 60-cm thick slice of tufa collected from the ancient shoreline of Lake Cahuilla yields trends that suggest frequent changes in its hydrologic balance. The $\delta^{18}O$ values range from -7.8" to -2.4" (PDB), and $\delta^{13}C$ values range from 1" to 3.6" (PDB). The calculated water-$\delta^{18}O$ values equilibrated with the tufa were much heavier than those of Colorado River water and local meteoric water, indicating the tufa was deposited in a saline closed-basin lake. This is further supported by a good $\delta^{18}O$-$\delta^{13}C$ covariance, and carbonate mineralogy of the tufa and fossil shells found in the tufa. There are about 27 strong depletions of the $\delta^{18}O$ signal in the record. If the record is continuous, these have durations on decadal to century scales. According to the radiocarbon dates of Smith and Turner (1975), who analyzed a tufa slice from the same location, we estimate that the chronology of the tufa is from 17,000 to 7,000 years BP. Using this chronology we are able to reconstruct lake level fluctuations of Lake Cahuilla. If these fluctuations can be tied exclusively to precipitation changes in the Colorado drainage basin, it will be possible to reconstruct the paleoclimate of the basin. Alternatively, these fluctuations could be influenced by changes in inflow volume associated with switching of the Colorado River delta, thus obscuring the paleoclimatic signal. Currently, we have only analyzed one fourth of 608 collected samples. Further analyses will allow us to obtain higher resolution records.

The Colorado River drainage system covers an area of 629,760 km^2 and its water serves nearly 25 million people of the United States. Variations in its discharge strongly influence water and power supply, agriculture and ecological systems, and flooding disaster of the downstream states including California, Nevada and Arizona. Understanding forcing mechanisms of variations in the regional precipitation is an important task. Precipitation in this region is sensitive to the variability of westerly jet stream and monsoon strength from the Gulf of Mexico and northeastern Pacific. Our study results could provide detailed information for examining the relative contributions of the Pacific winter storm and the summer monsoonal storm to the Colorado drainage basin. The comparison of our record with other paleoclimate records in the western U.S. may enable us to understand the regional climate response to changes in forcing factors such as orbital forcing, jet stream shift and ocean circulation.

Changes in Biological Productivity in the Pacific Ocean Due to Anthropogenic Forcing

David W. Pierce[1], Tim P. Barnett[1], Mathew Maltrud[2], and Joanne Lysne[3]
[1] Scripps Institution of Oceanography, La Jolla, CA
[2] Los Alamos National Lab, Los Alamos, NM
[3] National Center for Atmospheric Research, Boulder, CO

Much work has been devoted to examining the expected changes in the physical environment arising from projected anthropogenic forcing. The question of how these physical changes will affect ocean productivity is an important one that seems to have been little examined. We present the results of a pair of ocean ecosystem models driven with changes in the environment expected due to anthropogenic forcing. The first model is a simplified one that calculates changes in nitrogen, phytoplankton, and zooplankton given externally specified changes in ocean temperature, mixed layer depth, and cloudiness as predicted by a coupled ocean-atmosphere model for the year 2090. The second model is considerably more complex, and includes iron and sulfur cycling, better parameterizations of nutrient recycling, and the full effects of horizontal advection by ocean currents. The simplified model predicts that productivity will decrease in the central North Pacific, while productivity in the California Current System will increase. Comparing the results of the complex model to the simplified model sheds light on the validity and robustness of this prediction, and points to areas where this work can be usefully extended in the future.

Teleconnective Controls on Yellowstone Riverflow During the Past Three Centuries

Michael F.J. Pisaric and Lisa J. Graumlich
The Big Sky Institute, Montana State University, Bozeman, MT

Water resources throughout the western United States are coming under increasing pressure from growing populations, agriculture and shifting climatic conditions. As water needs continue to grow, there is increasing need to understand the natural variability within these systems and the overlying controls on them. Climatically sensitive tree-rings can provide annually resolved records of climate

and climate-related time series extending back centuries to millennia, allowing 20th century trends to be examined in a long-term context.

Using drought-sensitive Douglas-fir (*Pseudotsuga menziesii*) trees from southwestern Montana, we reconstructed annual volume of flow for the Upper Yellowstone River. While our tree-ring based reconstruction reasonably modeled 20th century flows it failed to capture extreme flows during the instrumental period, especially high flows. Because climate in the western United States is sensitive to conditions in the Pacific basin, we developed a second model incorporating two measures of Pacific climate variability, specifically the PDO and SOI. We focused on tree-ring based circulation indices that made use of climatically sensitive tree-ring records from the southwestern United States because climate in the southwest tends to be in anti-phase with the northern Rockies and the Pacific Northwest (PNW): that is, severe drought in the southwest is correlated with anomalously high precipitation in the northern Rockies and vice versa. By including variability related to the Pacific basin, we improved the ability of our model to reconstruct flows during years of anomalously high precipitation in the northern Rockies and PNW.

Our reconstruction suggests that flows during the 1930s were the lowest during the past three centuries. However, overall 20th century flows have been higher than most periods in the reconstruction. For example, average flows during the 1990s represented the 2nd highest decadal average during the reconstruction and contained back to back 100 year floods in 1996 (4.04 x 10^9 m^3/year) and 1997 (4.61 x 10^9 m^3/year). The lowest reconstructed annual flow occurred in 1816 with annual volume of flow of 1.66 x 10^9 m^3/year.

Weather and Climate Conditions for "PACLIM Year" PY2002

Kelly Redmond
Western Regional Climate Center, Desert Research Institute, Reno NV

Vestiges of La Niña remained for a fourth consecutive year as simultaneously a potential El Niño struggled to take shape at meeting time. For the second consecutive year the monsoon arrived very early, and for the second consecutive year the total precipitation was below average in Arizona and New Mexico, challenging a recently developed rule of thumb. After one of the driest winters in its history, the Pacific Northwest redeemed its rainy reputation with a return to somber soggy stratus status. Based on early behavior, much of the West appeared to be heading toward a similarly wet cold season, but as the calendar odometer rolled over, precipitation rates began to lag behind long term averages, particularly in the southern and eastern portions of this 11-state region. Drought was largely alleviated in the Cascades/Sierra chains, but continued and even intensified in Wyoming and especially Montana. Some locations here recorded their driest second half of a calendar year on record, and both valleys and mountains failed to secure desired moisture. The Rio Grande, with already very low reservoirs in its lower reaches, faced the driest conditions relative to average for major western rivers. Once again nearly the entire West was above average in temperature, especially in the northern Rockies, continuing a trend that has persisted over recent years. Portions of the interior West and some coastal stations were near or below average in temperature. As February waned, the biggest questions seemed to revolve around whether El Niño, mild or wild, would venture back onto the Pacific stage. Ocean temperatures in the eastern Pacific remained generally lower than average at higher latitudes also, adding to speculation whether the Pacific Decadal Oscillation had again reversed sign.

Central Valley Precipitation Based on 400 Years of Blue Oak Records

Kelly Redmond[1], Dave Stahle[2], Matt Therrell[2], Mike Dettinger[3, 4], and Dan Cayan [4, 3]
[1] Western Regional Climate Center/Desert Research Institute
[2] University of Arkansas
[3] U.S. Geological Survey
[4] Scripps Institution of Oceanography

The Sacramento-San Joaquin River systems in the Central Valley are crucial to the California economy. Interests with a significant stake in how this system is managed span the range from agriculture, municipal, flood control, water resources, fish and wildlife, navigation, marine and estuary, ecological restoration, and several others. Effective management of these water resources requires knowledge of the climate behavior that drives the entire system. The growth rate of California blue oak has been shown to be highly correlated with winter precipitation. These trees grow mainly in an elevation band extending between a few hundred and to about a thousand meters. They thus neatly outline the entire combined basin. Furthermore many of them live to 300-400 years, and as much as 500, years. They have been used to reconstruct salinity in San Francisco Bay for several hundred years. Here we use a dozen chronologies more or less uniformly distributed at lower elevations (but above the flood plain) to perform pattern analysis and examine temporal properties. The full set covers 1711-1992, and various subsets cover periods from 1586-1996. The earliest individual chronolology starts in 1519. A pattern analysis has been performed, and the first EOF (55 percent variance) closely tracks the overall variations of 20th century precipitation in the Central Valley. The second and third EOFs describe north-south (Sacramento vs San Joaquin) and east-west (coastal vs Sierra mountain) variations, respectively. Of interest is whether temporal variability exists on the several-decade scale (similar to the Pacific Decadal Oscillation, PDO). Spectra do not show prominent peaks at these frequencies. Significant ENSO-scale variability is noted, especially in the north-south component at 2.5-4 year scales. Significant variability is seen at 6-8 year time scales, and to a slightly lesser extent at 14-17 years. Multi-year drought and wet episodes are seen during the 20th century, many with typical durations of 6-8 years. These have considerable societal impact and are thus of great interest to water managers. This behavior remains robust in longer reconstructions starting anywhere from 190 to 420 years ago.

Will WY 2002 Be Wet Enough to Avoid Drought?

Maurice Roos
California Department of Water Resources, Sacramento, CA

Water year 2001 (October 2000 through September 2001) was dry in northern California with statewide runoff only about half average. It was driest in the northeastern region of the State. For most users, reservoir storage from previous good years helped take some of the slack, but, as the water year ended, storage was about 10% under average and over 20% behind the previous year. There was much concern that a second dry year would plunge California into drought.

This paper will look at the major parameters of water supply for the current water year 2002—precipitation, snowpack, runoff, and storage. From information on hand in late February slightly over

midway through the season, an attempt will be made to assess whether we have had enough rain and snow to prevent drought, at least for another year.

The current water year started slowly with less than average precipitation during October. But, in contrast with several previous years, both November and December produced well above average precipitation in northern California. January started with rain but then shifted to a drier pattern. We do not yet know whether the spring rains will be sufficient to cause runoff for the year to be above average. But there is enough snowpack in the mountains to preclude a critical dry runoff year; in fact runoff exceeding the dismal amounts of 2001 seems assured as of this writing.

Suggested Research on the Effect of Climate Change on California Water Resources

Maurice Roos
California Department of Water Resources, Sacramento, CA

Rather large changes in climate are being forecasted for the latter part of this century due to global warming as a result of the increase in greenhouse gases. Potential changes which could especially affect water resources systems are: changing mountain area runoff patterns from higher elevation snow levels on mountain watersheds, sea level rise which might adversely affect the Sacramento San Joaquin Delta source of major water exports for the State, possibly larger floods and extreme precipitation events, and changes in the water requirements of crops.

By and large, our reservoir and water delivery systems and operating rules have been developed from historical hydrology on the assumption that the past is a good guide to the future. With global warming that assumption may not be valid.

In view of these forecasts of global warming, based on the author's knowledge of California resources, a list of higher priority suggested research items has been developed to study the effect of warming on water resource systems. In summary, the list is as follows, and will be explained in more detail in the presentation:

1. Monitoring of hydrologically important variables
2. Modeling of future precipitation
3. Testing operation of the CVP-SWP system with modified runoff
4. Updating depth-duration-frequency rainfall data
5. Evaluate Golden Gate tide gage datum
6. Catalog sea level trends along the coast, in the bay and the delta
7. Check for recent changes in evapotranspiration
8. Estimate future changes in evapotranspiration and crop water use
9. Evaluate effect on major multipurpose flood control reservoirs
10. Water temperature modeling in major reservoir/river systems
11. Effect of climate change on regions adjoining California

Extreme Paleofloods In Northern and Southern California: Evidence for a Matching Pattern

Arndt Schimmelmann[1], Carina B. Lange[2], David Drake[3], and Christopher K. Sommerfield[4]
[1] Department of Geological Sciences, Indiana University, Bloomington, IN
[2] Depto. Oceanografía, Universidad de Concepción, Concepción, Chile
[3] Drake Marine Consulting, Ben Lomond, CA
[4] College of Marine Studies, University of Delaware, Lewes, DE

Every few hundred years the culmination of regional precipitation and extreme runoff in California produces extraordinary flooding that dramatically increases riverine transport of fine-grained terrigenous sediment toward California's offshore basins and continental shelf. In the Santa Barbara Basin the most massive gray, clay-rich flood deposits of the past two millennia were dated via varve-counting to ca. AD 1605, 1418, and 440. Off the Eel River in Northern California, clay-rich deposits on the continental shelf have been linked to extreme or frequent flooding. Radiocarbon-based dating of prominent prehistoric flood beds off the Eel River points towards ca. AD 1400-1600 and 450. Although the radiocarbon dates have an uncertainty of at least ±100 years, the similarity of flood ages from Northern and Southern California suggests a matching pattern.

The short instrumental record of California indicates that flood occurrence in North Coast and South Coast hydrologic regions is generally not synchronous. The matching pattern in the longer sediment records suggests, however, that rare flood-producing atmospheric circulation anomalies may occasionally be of sufficient duration and spatial extent to impact both regions. We hypothesize that at times of large-scale climatic changes, such as associated with the Little Ice Age, the storm-track pattern impacting California was altered and occasionally resulted in severe runoff events that affected Northern and Southern California within time windows of several years to decades.

Decadal Regime Shifts: Physical Mechanisms and Ecosystem Consequences

Franklin B. Schwing[1], Tom Murphree[2], Steven J. Bograd[1], and Phaedra Green-Jessen[1,3]
[1] Pacific Fisheries Environmental Laboratory, Pacific Grove, CA
[2] Naval Postgraduate School, Monterey, CA
[3] JIMAR, Honolulu, HI

The global atmosphere and ocean interact and vary on interannual scales due to the tropical climate phenomenon El Niño-Southern Oscillation (ENSO). Through processes related to ENSO, the north Pacific experiences large perturbations in its physical state, which are often manifested as ecosystem changes. The atmosphere and oceans also fluctuate on multidecadal scales, commonly called climate regime shifts. The changes that oceans and their ecosystems undergo during regime shifts may be a rough proxy of how these systems have responded to past climate variability, and will respond to future change. Regime shifts are a fundamental and important natural scale of climate variability, similar in magnitude to EN anomalies. Moreover, they appear to be amplified at higher latitudes, specifically in the extratropical northeast Pacific (EN anomalies are greater in the tropics), and have been associated with significant changes in fishery resources and their socio-economic consequences.

For example, the collapse of the California sardine fishery in the early 1940s, documented in popular literature by John Steinbeck, is believed to have occurred in association with a regime shift toward cooler ocean conditions.

The most recent regime shift occurred in late 1998 during the rapid transition away from EN conditions in the tropics. As with many oceanic changes, reports of shifts in living marine resources first drew attention to this period as a regime shift. Atmospheric and oceanic conditions in the Pacific since late 1998 have resembled a classic La Niña pattern. Strong atmospheric pressure over the north Pacific has led to vigorous anticyclonic wind stress, including anomalously strong upwelling-favorable winds along the North American west coast and stronger than normal trade winds. A horseshoe-shaped region of cooler than normal upper ocean temperature extends along the axis of the north Pacific trade winds from the western equatorial Pacific to Baja California, and along the North American west coast into the Gulf of Alaska. Surface atmospheric anomalies are part of atmospheric teleconnections, principally emanating out of east Asia. These are likely important mechanisms for the development and maintenance of upper ocean anomalies, through their influence on surface atmospheric processes. Distinct atmospheric teleconnections from the tropical Pacific, east Asia, and the Arctic may interact to drive the physical state of the north Pacific.

A number of major biological changes in the Pacific coincided with the rapid evolution toward this new physical state. These occurred at many trophic levels, from primary producers to top predators. Most of the recent ecological changes are consistent with those identified with historical cooler conditions in the northeast Pacific. At a minimum, we have learned that marine ecosystems can respond to environmental change in a surprisingly swift and dramatic way.

Spatial Patterns of U.S. Winter Temperature Since 1600 AD

Louis A. Scuderi
Department of Earth and Planetary Sciences, University of New Mexico, Albuquerque, NM

Winter temperature reconstructions derived from western United States tree-rings indicate that since 1600 AD the North American mid-latitudes have experienced significant decadal winter warming and cooling trends closely coupled to low-frequency variability with a period of ~120-years. Evidence of this periodicity has also been found in glacial and $\delta^{18}O$ records.

During the positive phase of this cycle the western portion of North America warms while the eastern portion cools. This pattern appears to be associated with anomalous SST gradients over the central and eastern Pacific Ocean which alter long wave circulation both above and downstream of the SST anomaly. Tree ring evidence from a number of sites suggests that this pattern may have been in existence in the western United States for the past 2000 years.

Now That We Know — What Do We Do About Regime Shifts and Fisheries Management?

Gary D. Sharp
Center for Climate/Ocean Resources Study, Monterey, CA

After several generations, fisheries science is growing into its role in the System Sciences. Rather than focusing only on the predator-prey relationship of fishermen and fish, the science has expanded to include the temporal and spatial changes in physical forcing, and ecological responses at many levels, rather than only commercial catches. While decadal and century scale patterns of climate-driven ocean variability and fisheries responses have been debated for over a century, it is only within the recent two decades that it has begun to dominate the thinking of many fisheries scientists, particularly fisheries oceanographers and fisheries ecologists.

Given the broad recognition of various dipolar climate indices—SOI, ENSO, PDO, AO, and NAO—it is time to consider the management implications, particularly in those higher latitude and eastern boundary current fisheries that appear to provide such clear evidence of two interactive, opportunistic faunas, each of which thrives for particular portions of the two extreme climate regimes. Aspects of conventional population modeling used in fisheries management are clearly obsolete. The need to provide regular and complete environmental monitoring, in conjunction with fuller reporting of catches, their locations and complete compositions, is more than obvious under the new concepts of how to manage such fisheries environments. The basic tenet of equilibrium can be retired, and, in its place, a more real time assessment of both species distributions and abundances can provide more useful information than only that required for better management of living resources. Some species can be used as bioindicators. These and general geophysical indicators, described elsewhere in this year's PACLIM, (c.f. Klyashtorin, Langscheidt, Peterson, and others) thus offer insights about present and future global climate.

Estimating Climate and Unsaturated Zone Moisture Flux for The Past 24,000 Years At The Nevada Test Site

Saxon E. Sharpe[1], Michael H. Young[2], Clay A. Cooper[1], and Julianne J. Miller[2]
[1] Desert Research Institute, Reno, NV
[2] Desert Research Institute, Las Vegas, NV

Understanding the rate and direction of liquid water movement in the valley fill sediments at the Nevada Test Site (NTS) is important for performance assessment calculations and long-term monitoring of radionuclide transport at the Area 5 radioactive waste management site. Net liquid water movement is influenced by many factors, but the precipitation and evapotranspiration rates, soil hydraulic properties, and relationship to surface drainage are among the most important. The direction of the hydraulic gradient within the upper 50 to 70 meters at Area 5 indicates that net liquid water movement is upward, toward the land surface. Previous estimates of upward flux of liquid water at the site have resulted in a wide range of values: from 0.001 to 0.41 mm/yr. These estimates assumed that precipitation rates were equal to modern for the last 10,000-30,000 years. Moreover, laboratory-measured unsaturated hydraulic conductivity data were not available.

Goals of this work were to generate past climate parameters (temperature and precipitation) for the NTS for the last 24,000 years, and to use these estimates in a multiphase flow simulator to constrain the estimates of upward flux. Climate states were estimated for the last 24,000 years based on the ostracode record in sediment cores from Owens Lake, California. Ostracodes are microscopic bivalved crustaceans that are particularly sensitive to changes in hydrology. The present and past hydrology of Owens Lake is closely linked to climate because the Owens Lake climate signal is dominated by Sierran snowpack and summer evaporation. Hence, the Owens Lake record can be considered a proxy for persistence and strength of the polar front and high and low pressure systems. Evaporation was incorporated into the simulator by fixing the relative humidity at the upper (land surface) boundary to a value representative of the dry conditions of southern Nevada. Laboratory hydraulic conductivity values were obtained from laboratory tests on Area 5 sediments to improve material characterization. Liquid water and vapor transport were then simulated for 24,000 years through the upper 250 m of unconsolidated sediment. Results of these simulations suggest that the rate of liquid water movement in the upper 20 m of the unsaturated zone is ~0.06 mm/yr toward the land surface. The velocity of the gas phase (air and water vapor) is downward at ~0.009 mm/yr. These estimates are within the range of values estimated by previous investigators.

Causes of Climate Changes Since 1850

Fred Singer
University of Virginia, Arlington VA

Global temperatures have risen in the past 150 years but the cause or causes are still disputed. It is necessary to examine the record in greater detail: Global climate warmed from about 1850 to 1940, then cooled until 1975, and warmed suddenly during 1976-1978. Surface stations show continued warming since then while atmospheric temperatures measured by satellites and balloon-borne radiosondes do not show a perceptible warming trend. Proxy data likewise show no recent warming.

(1) Is the pre-1940 warming anthropogenic (as claimed by Wigley)?

(2) Is the 1940-1975 cooling caused by sulfate aerosols (IPCC)?

(3) Is post-1979 warming supported by sea-ice shrinking, deep-ocean warming, shrinking of glaciers, and caused by greenhouse gases (IPCC)?

We argue that PDO and/or solar variability can account for the observed changes and present some evidence that PDO may itself be caused/triggered by changes in solar activity.

Application of Marine Bird Research to The Study of North Pacific Ecosystem Dynamics

William J. Sydeman and K. David Hyrenbach
PRBO/Marine Science Division, Stinson Beach, California

Marine birds are some of the most conspicuous and abundant upper trophic-level predators in coastal ecosystems. As secondary and tertiary consumers, shifts in seabird population distribution, abundance, demography and food habits can complement traditional oceanographic research by

providing an integrated picture of change in difficult to study lower trophic-level organisms, and in the physics supporting ocean productivity and prey aggregation. Examples of recent findings from colony-based, at-sea, and telemetry studies of seabird ecology will be provided. In particular, we will describe long-term changes in marine ecosystems and food web structure and seabird responses to the purported 1977, 1989, and 1999 regime shifts in the California Current System. Moreover, we will evaluate the relative effects of recent ENSO events on seabirds in relation to lower frequency ocean climate variability. Finally, we will describe an international network of marine bird research programs that has been established to assess basin-wide spatial and temporal variability in large marine ecosystems over much of the North Pacific Ocean.

Comparison of Biological Responses to ENSO and the Climatic Shift of 1976

Paul E. Smith and H. Geoffrey Moser
Fisheries Division NOAA/NMFS Southwest Fisheries Science Center, La Jolla, California

The environment has proved to be more effective in controlling fish and fishery populations than the usual population models would allow. In the 50-year time series of CalCOFI, we have seen the sardine recover from extremely low levels with the reversal occurring in the middle seventies. The mackerel population also underwent a massive increase at that time. We have used the usual environmental descriptors and 12 fish and fishery stocks from all the water masses juxtaposed in the CalCOFI sample area to display the wide range of responses to ENSO and the climatic shift of 1976. Other large changes in population are also examined in context of the time series of environmental change. We illustrate a time series which uses long term "instantaneous surplus production rate" instead of catch or biomass time series. This expands the work on the great anchovy and sardine fisheries to species that have not yet been fished.

Evaluation of the Impacts of Future Climate Change on California Using a Regional Climate Model

Mark A. Snyder, Jason L. Bell, and Lisa C. Sloan
Department of Earth Sciences, University of California, Santa Cruz, Santa Cruz, CA

Atmospheric pCO_2 is expected to double within this century, resulting in changes to the climate system. The effects of these changes have been evaluated primarily using global climate models (GCM) and statistical downscaling techniques. The inherent limitations of coarse resolution GCMs make it necessary to use models capable of higher resolutions. This study incorporates ensembles of experiments with a high resolution regional climate model (RCM) over a climatically sensitive region. The model was run for three scenarios, a preindustrial case with 280 ppm CO_2 (1x), a modern day case with 365 ppm CO_2, and a future case with 560 ppm CO_2 (2x) on the climate of California. The model output was subdivided by hydrologic regions, defined by the California Department of Water Resources, and then analyzed. The model performs well in simulating the mean modern day climate, but underestimates the variability. The RCM output for the 1x and 2x cases was analyzed to determine differences, the significance of the results, and the amount of variability. Statistically significant temperature increases of up to 3.8 °C occur on an annual average basis throughout the

state. Precipitation increases by 23% over the northern half of the state, while precipitation in the southern half shows no change. Annual average snow accumulation decreases everywhere in the state by up to 120 mm water equivalent.

A Holocene Record From Medicine Lake, Siskiyou County, California: Preliminary Diatom, Pollen, Geochemical, and Sedimentological Data

Scott W. Starratt[1, 2], John A. Barron[1], James L. Bischoff[1], Tara Kneeshaw[1], R. Larry Phillips[1], and James A. Wanket[2]

[1] U.S. Geological Survey, Menlo Park, CA

[2] Department of Geography, University of California, Berkeley, CA

Medicine Lake is a small (1.65 km^2), relatively shallow (average 7.3 m), medium altitude (2036 m) lake located within the summit caldera of Medicine Lake volcano, a dormant Quaternary shield volcano located in the Cascade Range about 50 km northeast of Mount Shasta. During the fall of 1999 and 2000, high-resolution bathymetry, seismic reflection, and sediment cores were collected from the lake. B100NC-1 (water depth 12.6 m; length 226 cm) was the longest core collected and was chosen for a multi-proxy study of Holocene climate variability in northern California. Twenty-six samples were analyzed for physical properties, sediment grain size (sand/mud ratio), diatoms, pollen, and sediment geochemistry (total organic carbon, Ca, Fe, K, Li, Mg, Mn, Na, Sr, and Ti). The Holocene sedimentation rate of approximately 21 cm/1,000 yr was determined using both ^{14}C (AMS) dating and tephrochronology.

The lowermost part of the core (226 cm - ~200 cm)represents the transition from glacial to interglacial conditions. During the period from about 11,000-7,200 cal yr BP, lake level fluctuated between deeper oligotrophic conditions with a diatom flora dominated by *Cyclotella* spp. and shallower intervals with a diverse benthic flora. The earliest part of this interval (226 cm - 210 cm) is almost devoid of *Cyclotella* and may represent an amictic lake. The relative low abundance (10-15%) of *Abies* (fir) pollen and relative high abundance (30-40%) of *Artemesia* (sagebrush) suggest drier than present-day conditions. At the beginning of this interval, Fe, K, and Ti are at their highest levels in the core, indicating the presence of glacial muds derived from the surrounding intermediate volcanic rocks. From about 7,200 cal yr BP to the present, conditions have fluctuated between higher lake levels (three intervals) dominated by *Cyclotella* and a reduced number and diversity of benthic taxa, and lower lake levels (two intervals) during which *Cyclotella* fall to levels of less than 10% of the flora. Relative values of *Abies* and *Pinus* (pine) are higher during high lake levels and the aquatic taxa (primarily *Isoetes* [quillwort]) increase in significance at lower lake levels. The abundance of Fe, K, and Ti is low during high stands and high during low stands, possibly reflecting variations in the mode of sediment input to the system. In contrast, values for total organic carbon are lower during low stands and higher during high stands. These cycles are not typical of the small number of continental Holocene records in the region, and may, in part, reflect hydrologic conditions unique to Medicine Lake volcano.

Isolation of Climatic Causes of Historical Runoff-Timing Changes In Western North America

Iris T. Stewart[1], Daniel R. Cayan[1, 2], and Michael D. Dettinger[2, 1]
[1] Scripps Institution of Oceanography, La Jolla, CA
[2] U.S. Geological Survey, San Diego, CA

Although projected near-future precipitation and temperature changes over western North America are subject to much debate, they are generally projected to cause widespread reductions in snowpack accumulation and snowmelt-derived streamflow. These changes would have important consequences for water resource supply and management, especially for the western United States where the largest contribution to annual streamflow from mid- and high-altitude basins is from the spring snowmelt runoff pulse. Establishing the dependence of streamflow timing on climate indicators and their changes is important both for assessing potential changes in streamflow runoff under different climate change scenarios and for monitoring seasonally-integrated current and future climate changes.

Regionally coherent fluctuations and trends in the timings of both (1) the start of the snowmelt runoff pulse and (2) the center of mass for flow (center time) towards earlier in the water year are found in much of western North America during the past 50 years, using a new data set combining U.S. (HCDN) and Canadian streamflow records. The great regional coherency of the observed timing variations suggests continental- and regional-scale climatic forcings, that are superimposed upon basin-scale processes. Changes in streamflow timing show strong positive correlations with gridded monthly temperature anomalies, and inverse correlations with both annual flow-volume and precipitation anomalies. Removing these dependencies on temperature and precipitation reduces the variance in the center timings by 40-70%. Although the residual variance shows mild large-scale coherence, large residual variances are concentrated in California and coastal Washington. Widespread negative correlations between center timing and both the PNA and PDO indices are present throughout the study area, especially in the interior northwestern parts of the contiguous U.S., in Canada, and in Alaska. For the same region, positive correlations between the SOI and center timing are found.

Thus, regionally coherent variations in streamflow timing in western North America reflect variations of both temperature and precipitation. In addition, solid links exist between the regionally coherent changes in streamflow timing and important Pacific climate indices. Notably, though, observed trends in runoff timing are most closely associated with recent warming trends across western North America.

Climate Trends In the Pacific Northwest In the Last 100 Years

George H. Taylor
Oregon Climate Service, Oregon State University, Corvallis, OR

The last century has seen significant changes in climate in the Pacific Northwest. Precipitation, snowfall, temperatures, growing season, and other climate parameters have shown evidence of strong short- and long-term variation. The influence of rapid population growth, especially in the last 50 years, has raised concerns about possible data contamination due to Urban Heat Island influences.

To assess climate trends in this region, data from long-term rural stations (mostly HCN stations) were analyzed. Annual and seasonal precipitation, annual and seasonal mean temperatures, high and low extreme temperatures, snowfall, and growing season were examined. Correlations with multi-decadal variations (including PDO) were made. The influence of ENSO and other large-scale climate phenomena was assessed.

Northern Hemisphere Circulation Variability for the 20th Century

Zbigniew T. Ustrnul
Institute of Meteorology and Water Management, Cracow, Poland
(Temporarily: Department of Geography and Regional Development, University of Arizona, Tucson, AZ)

The study contains characteristics of the temporal differentiation of the atmospheric circulation in the Northern Hemisphere for the 20th century. Analysis was done on the basis of daily circulation types, which were specified for each grid with the resolution of 5° latitude and longitude of the hemisphere between 15° and 85° N. Classification was created on the basis of the predominating air advection which is the main element of the whole system and undergoes further analysis. Advection was determined according to the geostrophic wind vector for grids. Detailed temporal analysis was estimated on the basis of a few circulation indices: zonal (W), meridional (S) and non-advective (A).

The highest westerly circulation is observed over central parts of the Pacific and Atlantic oceans, the meridional index exhibits considerable differentiation in the subtropical areas, while the non-advective index reaches the lowest values over oceans and south-central Asia. Temporal variability of circulation conditions in the 20th century did not change considerably but they were naturally oscillating at a low frequency. That conclusion seems obvious if we look at the large territory of the entire hemisphere. It does not mean that rather high variability can not be observed in smaller areas including some particular points. In some areas especially, the W index shows high variability, such as the last 15 years over Europe. Specific examples are provided for western North America.

Global Average Upper Ocean Temperature Response to Changing Solar Irradiance: Exciting Earth's Internal Decadal Mode

Warren B. White and Michael D. Dettinger
Scripps Institution of Oceanography
University of California, San Diego, La Jolla, CA

Global-average upper ocean temperatures anomalies of ±0.05 °C fluctuate in fixed phase with decadal signals in the Sun's total irradiance of 0.5 Watts m-2 over the past 100 years (White and others 1997), but its amplitude is 2 to 3 times that expected from the Stefan-Boltzmann radiation balance (White and others 1998). Thus, some positive feedback appears to be operating to increase the sensitivity of the ocean's upper layer temperature to changes in the Sun's total irradiance. Examining global patterns of upper ocean temperature on decadal period scales finds a particular global decadal mode operating in phase with the decadal signal in the Sun's total irradiance. Yet, this global decadal mode is similar to that of the global standing mode of the El Niño-Southern Oscillation (ENSO), the latter associated with a global-average upper ocean temperature anomalies of ±0.05 °C, independent of changing solar

irradiance (White and others 2000). This suggests that the observed internal decadal mode in Earth's ocean-atmosphere-terrestrial system is excited by the decadal signal in the Sun's irradiance. To understand the thermodynamics of this association, we conduct a global-average upper ocean heat budget utilizing upper ocean temperatures from the SIO reanalysis and air-sea heat and momentum fluxes from the COADS reanalysis, finding the source of decadal global warming to be the reduction in trade wind intensity across the tropics, decreasing the global average latent heat flux out of the ocean. We demonstrate that this reduction in trade wind intensity in the Pacific Ocean is governed by a delayed action oscillator mechanism in the ocean-atmosphere system differing little from that used to explain the ENSO (Graham and White 1998). We operate an intermediate coupled model of this delayed action oscillator, normally driven by white noise, by superimposing the Stefan-Boltzmann upper ocean temperature response to decadal changes in the Sun's irradiance. We find the latter, with weak amplitude of ±0.02 °C and non-random phase, able to excite a decadal signal in this delayed action oscillator, yielding a damped resonance response of ±0.06 °C, with dissipation provided by long-wave radiation to space.

Overture to a Landslide—A Seasonal Moisture Prerequisite

Raymond C. Wilson
U.S. Geological Survey, Menlo Park, CA

Severe rainstorms may trigger abundant debris flows and other shallow landslides in steep terrain. In the San Francisco Bay region (SFBR) of California, the critical combinations of storm rainfall intensity and duration required to trigger debris flows are now fairly well established. There is, however, another climatic prerequisite for landsliding—the so-called "antecedent condition," that sufficient moisture must already exist in hillslope materials before landslides can be triggered, even by severe storms. At the antecedent condition, the hydrologic behavior of the hillslope is transformed from a moisture deficiency where additional water is absorbed by capillarity and clay rehydration, to a moisture surplus where added water creates positive pore pressures and rapid drainage. Variations in soil moisture during the year are governed by the phase relationships and relative magnitudes of two separate climatic cycles—precipitation and evapotranspiration. In the SFBR's Mediterranean climate, these cycles are about six months out-of-phase, leading to significant seasonal variations in soil moisture.

Forecasting of landslides and floods in the SFBR could be improved by a reliable, observation-based system for tracking the replenishing of hillslope moisture during the early part of the rainfall season, using observational data on rainfall and runoff as a proxy. To that end, I have examined several years of daily rainfall and runoff data from several small, upland watersheds in the SFBR, including the Pescadero Creek watershed, an area with relatively frequent landslides and debris flows. The storm runoff/rainfall ratio, very low in early winter, increases dramatically when the antecedent condition is passed, a few weeks after the winter solstice, then begins to drop again after the spring equinox. This timing appears to be controlled by the near-coincidence of minimum evapotranspiration and maximum rainfall frequency in mid-winter, and is only mildly influenced by variations in soil type or thickness. Mid-season dry spells create only minor deficits on hillslope moisture (< 20 mm for 25 days), which may be made up quickly by subsequent rainfall.

Western Colorado Snowpack Reconstructed From Tree Rings

Connie A. Woodhouse
NOAA Paleoclimatology Program, National Geophysical Data Center, Boulder, CO

Snowpack is the major source of surface water supplies in Colorado. An understanding of the variability and expected range of extremes in snowpack is important for water resource management and planning. Instrumental snowpack records are limited in length (a very few approach 70 years) and do not provide a long-term perspective on natural variability in seasonal snowpack. These limited length records are also inadequate for assessing how multidecadal large-scale climate fluctuations impact regional snowpack. Paleoclimatic proxy data has been used to extend climate records back in time and tree rings have been used successfully to reconstruct hydroclimatic variables such as precipitation, drought, and streamflow. To date, tree rings have not been used to reconstruct snowpack, although this possibility has been explored. Reconstructions have likely not been generated because of the short temporal overlap between snow measurements and available tree-ring chronologies. New collections of tree-ring chronologies in western Colorado now provide an adequate period of overlap for the calibration and verification of tree-ring models of snowpack, and for snowpack reconstructions in the Colorado River headwaters region.

In this study, a reconstruction of April 1 snow water equivalent (SWE) is generated for a region that includes the Gunnison River basin and the southern headwaters of the main stem of the Colorado River. A stepwise regression process produced a model with four chronologies as predictor variables that explains 63% of the variance in the instrumental record. The reconstruction extends from 1569 to 1999 and is evaluated with regard to variability, frequency and distribution of extreme values and persistent events over the past 431 years. Although the mean and variability of SWE in the 20th century is similar to that over the full record, the distribution of extreme SWE years (years with values greater or less than one standard deviation from the mean) in the 20th century is not representative of the past centuries. In particular, the 20th century contains a period notable for few dry extremes between 1909 and the 1960s. Overall, the 20th century contains the lowest percent of extreme dry years when compared to other centuries (13% compared to 21% in the 18th century or 22% of the 31 years in the 16th century). Evaluation of persistent dry periods shows a higher frequency of three to seven year dry periods in the 16th, 17th, and first half of the 18th centuries than in the 19th and 20th centuries, although the most severe 3-year drought occurred in the 19th century. Other analyses suggest fluctuations in variance over time and may provide clues about the circulation mechanisms that influence snowpack in the Gunnison region.

The 400-Year Wet-Dry Climate Cycle In Interior North America and Its Solar Connection

Zicheng Yu[1] and Emi Ito[2]
[1] Department of Earth and Environmental Sciences, Lehigh University, Bethlehem, PA
[2] Limnological Research Center, University of Minnesota, Minneapolis, MN

Several high-resolution paleoclimatic records from lakes and peatlands in the northern Great Plains (NGP) show some regular patterns of late Holocene climate changes at centennial time scales. Sites from Minnesota to Alberta that show centennial wet-dry cycles, especially at ~400 years, include Elk

Lake, MN (400- and 84-yr; Dean 1997); Pickerel Lake, SD (~400-yr; Dean and Schwalb 2000); Moon Lake, ND (400-yr; Laird and others 1996); Coldwater Lake, ND (137-yr; Fritz and others 2000); Rice Lake, ND (400-, 201-, 129- and 99-yr; Yu and Ito 1999); Pine Lake, AB (440-yr; Campbell and others 1998); and the Upper Pinto Fen, AB (386-yr; Yu and others unpublished). The most pronounced feature in most of these NGP records is that relatively dry periods alternate with short-lived wet periods about every 400 years. Superimposed on these wet-dry cycles, stacked time series from four sites (Rice, Moon, Coldwater and Elk lakes) for the last 1000 years show characteristic climate patterns during the Medieval Climate Anomaly (MCA) and Little Ice Age (LIA). The MCA was represented by two dry peaks centered at 650 and 850 cal BP, while the LIA was dominated by a single drought peak around 300 cal BP. These double Medieval droughts are likely correlated with two generations of relict tree stumps as recorded in the Great Basin of California (Stine 1994, 1998).

We attribute this dominant 400-year wet-dry cycle to solar forcing. Solar activities as indicated by solar proxy of cosmogenic isotopes (^{14}C, ^{10}Be) show a fundamental periodicity at ~400 years (Stuiver and Braziunas 1989). Dry periods in the NGP appear to correlate with solar minima. Recent climate modeling suggests that solar variation likely causes a large temperature change at regional scale through a forced shift in atmospheric variability (e.g., North Atlantic Oscillation), although global-scale temperature only shows a minor response (Shindell and others 2001). These modeling results also indicate that lands and oceans show opposite responses to solar forcing. Thus we argue that the interior of the continents is more sensitive than other land areas to small changes in solar variations, especially over a longer time scale. This response in the NGP is perhaps related to a shift in dominant modes of the atmospheric pressure fields (e.g., Pacific-North American teleconnection pattern).

Aridity could be caused by either decreased precipitation (moisture availability and atmospheric circulation support) or increased evapotranspiration (net radiation and temperature). Either of these changes could occur either during particular seasons or throughout the year. Shindell and others (2001) modeling results suggest much greater cooling in winters over the continents, in response to Maunder Minimum of solar irradiance. Similar seasonal changes might also occur in the NGP during portions of climate cycles of the late Holocene. For example, during the mid-Holocene dry prairie period, ostracode data from Elk Lake, MN indicate colder winters and summers but very dry summers (Forester and others 1987). This combination of cold and dry conditions rather than warm and dry conditions may occur more commonly than generally assumed. If this is the case during the late Holocene in the NGP, then decreased precipitation may play a greater role in causing droughts than increased evapotranspiration. Multiple proxy approach would be useful in investigating this seasonal nature of droughts in future studies, which would provide further test of modeled results. Paleoclimate records in the continental interior would also contribute toward the detection of spatial pattern of climate changes, which may provide new insights into the cause and mechanism of climate changes (Bond and others 2001).

References:

Bond G and others. 2001. Science 294: 2130-2136.

Campbell ID and others. 1998. Geology 26:471-473.

Dean WE. 1997. Geology 25:331-334.

Dean WE, Schwalb A. 2000. Quaternary International 67:5-20.

Forester RM and others. 1987. Quaternary Research 28:263-273.

Fritz SC and others. 2000. Quaternary Research 53:175-184.

Laird KR and others 1996. Nature 384:552-554.

Shindell DT and others 2001. Science 294:2149-2152.

Stine S. 1994. Nature 369:546-549.

_____ 1998. In A.S. Issar and N. Brown (eds.) Water, Environment and Society in Times of Climate Changes. 43-67.

Stuiver M, Braziunas TF. 1989. Nature 338:405-408.

Yu ZC, Ito E. 1999. Geology 27:263-266.

Appendix A: Agenda

Nineteenth Annual PACLIM Workshop
Asilomar State Conference Grounds
Pacific Grove, California
March 3–6, 2002

PACLIM is a multidisciplinary workshop that broadly addresses the climatic phenomena occurring in the eastern Pacific and western America. Its purpose is to understand climate effects in this region by bring together specialists from diverse fields including physical, social, and biological sciences. Time scales addressed range from weather to paleoclimate.

Our primary theme sessions this year address climatic influences on oceanic biology and solar influences on climate. John McGowan (Scripps Institution of Oceanography), and Gary Sharp (Monterey) and Charles Perry (USGS), respectively, organized and attracted a fine collection of talks and posters on these two themes. As always, the remainder of PACLIM will be dedicated to a wide range of climate-related topics.

The atmosphere of the Workshop is intentionally informal, and room and board are provided for many of the participants. The Workshop is organized by representatives from several organizations, but historically it has been spearheaded by U.S. Geological Survey scientists. Held annually, the Workshop has benefited from funding and other forms of support from several agencies (public and private). This year's PACLIM is sponsored by:

The CALFED Bay-Delta Science Program:	Samuel N. Luoma
The U.S. Geological Survey Water Resources Division:	Bill Kirby
The NOAA Office of Global Programs:	Roger Pulwarty and Harvey Hill
The State of California Department of Water Resources:	Zach Hymanson
The U.S. Naval Postgraduate School:	Tom Murphree

Agenda

Sunday Evening, March 3

Current Events and Abrupt Changes
Moderator: Mike Dettinger

Registration, etc.

6:00–7:00 pm	Dinner
7:00–7:10 pm	Opening Comments Mike Dettinger (USGS) and Janice Tompson (LBCC)
7:10–7:35 pm	*Weather and Climate Conditions for "PACLIM Year" PY2002* Kelly Redmond (WRCC)
7:35–8:00 pm	*Will WY 2002 Be Wet Enough to Avoid Drought?* Maury Roos (California DWR)
8:00–9:00 pm	*Abrupt Climate Change During the Past 100,000 Years: Is the Sun the Pacemaker?* Jeff Severinghaus (Scripps Institution of Oceanography)
9:00 pm on	Socializing

Monday Morning, March 4

7:30–8:30 am	Breakfast
	Special Session: Climate and Marine Biology **Moderator: John McGowan**
8:30–8:40 am	Introductory Remarks John McGowan (Scripps Institution of Oceanography)
8:40–9:10 am	*Decadal Variability in the California Current System: Patterns, Change Points, and Biological Implications* Steven Bograd (PFEL), R. Mendelssohn, F.B. Schwing, R.J.Lynn, and J.A. McGowan
9:10–9:40 am	*Comparison of Biological Responses to ENSO and the Climatic Shift of 1976* Paul Smith and H.G. Moser (Southwest Fisheries Center)
9:40–10:10 am	*Decadal Regime Shifts: Physical Mechanisms and Ecosystem Consequences* Frank Schwing (PFEL), T. Murphree, S.J. Bograd, and P. Green-Jessen
10:10–10:30 am	Break
10:30–11:00 am	*Patterns in 20th Century Pacific Climate and Marine Ecosystems: Will Improved Predictability Lead to Improved Fisheries Management?* Nate Mantua (JISAO, Univ. Washington)
11:00–11:30 am	*The Inorganic Carbon Cycle in Subtropical Oceanic Gyers* Dave Keeling (SIO)
11:30–12:00 pm	*A Review of Climate Change and Marine Mammals: Patterns, Hypotheses, and Questions* Karin Forney (Southwest Fisheries Center)
12:00–1:00 pm	Lunch
1:00–1:30 pm	*Application of Marine Bird Research to the Study of North Pacific Ecosystem Dynamics* William J Sydeman and K. David Hyrenbach (PRBO)
1:30–2:00 pm	*Changes in Biological Productivity in the Pacific Ocean Due to Anthropogenic Forcing* Dave Pierce (SIO), T.B. Barnett, M. Maltrud, and J. Lysne

Monday Afternoon, March 4

Modern Climate and Its Effects
Moderator: Connie Millar

2:00–2:30 pm	*Climate of the Last Two Centuries: Constraints from the Instrumental Data and Paleoproxies* Alexey Kaplan (Lamont-Dougherty Geophysical Observatory)
2:30–3:00 pm	*Dynamic Similarities in North Pacific-North American Climate Variations* Tom Murphree (Naval Postgraduate School), F. Schwing, B. Ford, and P. Hildebrand
3:00–3:30 pm	Break
3:30–4:00 pm	*Tropical Tropospheric Temperature Variations Caused by ENSO and Their Influence on the Remote Tropical Climate* John Chiang (JISAO), A.H. Sobel, and Y.Kushnir
4:00–4:30 pm	*Evaluation of Impacts of Future Climate Change on California Using a Regional Climate Model* Mark Snyder, J.L. Bell, and L.C. Sloan (UCSC)
4:30–5:00 pm	*Seasonal Predictability of Precipitation: Frequency of Extremes of the U.S.* Sasha Gershunov and Dan Cayan (SIO)
5:00–5:30 pm	*Influence of ENSO on Flood Frequency Along the California Coast* Ned Andrews (USGS), R.C. Antweiler, P.J. Neiman, and F.M. Ralph
6:00–7:00 pm	Dinner

Monday Evening, March 4

Observed Solar Variability and Processes
Moderator: Charles Perry

7:00–8:00 pm	*Total Solar Irradiance Variability During Solar Cycles 21-23* Richard Wilson (Columbia Univ.)
8:00 pm on	Socializing

Tuesday Morning, March 5

7:30–8:30 am	Breakfast
	Solar Influences on Climate **Moderator: Gary Sharp/Charles Perry**
8:30–8:40 am	Introductory Remarks Gary Sharp (Monterey)
8:40–9:10 am	*Solar Irradiance Variations from UV to Infrared* Judit Pap (Goddard Space Flight Center)
9:10–9:40 am	*Cycles in Sediments of Santa Barbara Basin: Is there a Solar Signal?* Wolf Berger (SIO)
9:40–10:10 am	*The 400-Yr Wet-Dry Climate Cycle in Interior North America and Its Solar Connection* Zicheng Yu (Lehigh University) and E. Ito
10:10–10:30 am	Break
10:30–11:00 am	*Stratigraphic Evidence in Polar Ice of Variations in Solar Activity* Gisela Dreschhoff (Univ. Kansas)
11:00–11:30 am	*Cyclic Variations in Rainfall and Riverflow on the West Slope of the Sierra Madre, Mexico* Walt Dean (USGS)
11:30–12:00 pm	*Global Average Upper Ocean Temperature Response to Changing Solar Irradiance: Exciting Earth's Internal Decadal Mode* Warren B. White (Scripps Institution of Oceanography) and Michael Dettinger
12:00–1:00 pm	Lunch
1:00–1:30 pm	*Solar Effect on North American Hydroclimatology Through Pacific Sea-Surface Temperatures and Atmospheric Vorticity* Charles Perry (USGS)
1:30–2:15 pm	*Causes of Climate Changes Since 1850* Fred Singer (Univ. Virginia)
2:15–2:30 pm	*Now That We Know—What Do We Do About It?* Gary Sharp (Center for Climate/Ocean Resources Study)
2:30–3:00 pm	Break

Tuesday Afternoon, March 5

Past Climates
Moderator: Scott Starratt

3:00–3:30 pm — *Frequency-Dependent Climate Signal in Upper and Lower Forest Border Trees in the Mountains of the Great Basin*
Malcolm K. Hughes and Gary Funkhouser (Univ. Arizona Tree-Ring Lab)

3:30–4:00 pm — *Western Colorado Snowpack Reconstructed from Tree Rings*
Connie Woodhouse (NOAA Paleoclimatology Program)

4:00–4:30 pm — *High Resolution Stable Isotope Record in Holocene Lake Cahuilla Tufa: Evidence of Paleoclimatic Change and/or Episodic Colorado River Delta Switching?*
Richard Peters (Loma Linda Univ.), H. Li, H.P. Burchheim, and L.D. Stott

4:30–5:00 pm — *Central Valley Precipitation Based on 400 Years of Blue Oak Records*
Kelly Redmond (WRCC), Dave Stahle, Matt Therrell, Mike Dettinger, and Dan Cayan

5:00–5:30 pm — *Late Holocene Climate Change and Mesoamerican Prehistory: A Highland-Lowland Comparison*
Roger Byrne (UCB)

6:00–7:00 pm — Dinner

Tuesday Evening, March 5

Poster Sessions

7:00 pm — Posters and Discussion (Over Refreshments)

Wednesday Morning, March 6

7:30–8:30 am	Breakfast
	Modern Climate Applications and Change **Moderator: Peggy Lehman**
8:30–9:00 am	*Climatic Impacts on Fijian Coral Reefs During the 1990s* Richard Casey and A. Casey (Ocean Research International)
9:00–9:30 am	*Use of Paleoclimate Proxy Data to Enhance Drought Planning and Response* Stephen Gray (Univ. Wyoming), S.T. Jackson, and C.L. Fastie
9:30–10:00 am	*Climate Science and Services: Some Lessons from CLIMAS* Andrew Comrie (Univ. Arizona), M.C. Lemos, M.K. Hughes, and J.T. Overpeck
10:00–10:30 am	Break
10:30–11:00 am	*Climate Trends in the Pacific Northwest in the Last 100 Years* George Taylor (Oregon State Univ.)
11:00–11:30 am	*Climatic Causes of Historical Runoff-Timing Changes in Western North America* Iris Stewart (SIO), Dan Cayan, and Mike Dettinger
11:30–12:00 pm	*Suggested Research on the Effect of Climate Change on California Water Resources* Maury Roos (California DWR)
12:00–1:00 pm	Lunch and Exit

Appendix B: Poster Presentations

A 2000-Yr Long Record of Climate from the Gulf of California
John A. Barron, D. Bukry, and J.L. Bischoff (USGS)

Framework for Assessing Risk of Using Climate-Based Streamflow Forecasts in California Reservoir Operations
Levi Brekke and J.A. Dracup (UCB)

Exciting the Delayed-Action Oscillator of the Tropical Pacific Climate with Decadal Changes in the Sun's Irradiance
Mike Dettinger (USGS) and Warren White

Sensitivity of California Vegetation to CO2-Induced Climate Change: A Regional Modeling Study
Noah Diffenbaugh, L.S. Sloan, M.A. Snyder, and J.L. Bell (UCSC)

Looking for Recent Climatic Trends and Patterns in California's Central Sierra
Gary Freeman (PG&E)

History of the Atmosphere and Recent Weather Trends as an Indicator of Climate Trends
Jim Goodridge (Mendicino)

Decadal to Centennial Variability in the California Current: Patterns from High-Resolution Laminated Sediments
J.C. Herguera (CICESE), B.Olivier-Salome, M.A. Esparza-Alvarez, C. Lange, and S. Ramos-Sanchez

Teleconnections in the Southern Hemisphere and Their Influence on Australian Hydrology
Hugo Hidalgo and J.A. Dracup (UCB)

A Lagrangian Trans-Pacific Drift Index, 1967-1998
Jim Ingraham (NMFS)

Hydrologic Controls on Proxy Climate Records in Northern Great Plains Lakes
Emi Ito (Univ. Minnesota), Z. Yu, D.R. Engstrom, S.C. Fritz, A.J. Smith, and J.J. Donovan

The Empirical Search for Clues to Process and Dynamics of Climate Change
Thor Karlstrom (USGS)

Characterization of Drought in California Using the New Multivariate Drought Index
John Keyantash and John Dracup (UCB)

Historical Lapse Rates in the Sierra: the Key to California's Climate Change Sensitivities
Noah Knowles (Scripps Inst. Oceanography)

Cyclic Climate Change and Forecasts for Major Pacific Commercial Fish Stock Fluctuations
Leonid Klyashtorin (Fed. Instit. Fisheries and Oceanography, Russia)

The Influence of Climate on Lower Food Web Production in Northern San Francisco Bay
Peggy Lehman (California DWR)

Recent Changes in Snowpack Conducive Factors in the Mountainous Western United States
Mark Losleben (INSTAAR, Univ. Colorado)

Climate Variability and Plant Migration
Mark Lyford (Univ. Wyoming), S.T. Jackson, and J.L. Betancourt

Changes in Streamflow Statistics in the Conterminous U.S.
Greg Mccabe and D.M. Wolock (USGS)

San Joaquin River Flow Reconstructed to AD 901 from Tree Rings
Dave Meko (Univ. Arizona Tree-Ring Lab), R. Touchan, M.K. Hughes, and A.C. Caprio

The Effects of Galactic Cosmic Rays on Weather and Climate on Multiple Time Scales
Ed Mercurio (Hartnell College)

Solar and Ocean-Related Signals of Climate in the Tropics: Evidence From Lake Turkana, East Africa
Patrick Ng'ang'a (TAMU-Commerce), T.C. Johnson, and M.D. Dettinger

Teleconnective Controls on Yellowstone Riverflow During the Past Three Centuries
Michael Pisaric and L.J. Graumlich (Montana State Univ.)

Extreme Paleofloods in Northern and Southern California: Evidence for a Matching Pattern
Arndt Schimmelmann (Indiana Univ.), C.B.Lange, D. Drake, and C.K. Sommerfield

Spatial Patterns of U.S. Winter Temperature Since 1600 AD
Louis Scuderi (Univ. New Mexico)

Estimating Climate and Unsaturated Zone Moisture Flux for the Past 24,000 Years at the Nevada Test Site
Saxon Sharpe, M.H. Young, C.A. Cooper, and J.J. Miller (DRI)

A Holocene Record from Medicine Lake, Siskiyou County, California: Preliminary Diatom, Pollen, Geochemical, and Sedimentological Data
Scott Starratt (USGS), John Barron, J.L. Bischoff, T. Kneeshaw, R.L. Phillips, and J.A. Wanket

Northern Hemisphere Circulation Variability for the 20th Century
Zbigniew Ustrnul (Institute of Meteorology and Water Management, Cracow, Poland)

Overture to A Landslide—A Seasonal Moisture Prerequisite
Ray Wilson (USGS)

Appendix C: Participants

Vera Agnostini
University of Washington
SAFS-UW Box 355020
Seattle WA 98195

Roger Y. Anderson
Department of Earth and Planet Sciences
University of New Mexico
Albuquerque NM 87131

Edmund Andrew
U.S. Geological Survey
3215 Marine St.
Boulder CO 80303

Ken Baltz
NOAA/NMFS
Santa Cruz Lab
110 Shaffer Rd
Santa Cruz CA 95060

John Barron
U.S. Geological Survey
345 Middlefield Road MS910
Menlo Park CA 94025

Wolf H. Berger
Scripps Institution of Oceanography
University of California, San Diego
La Jolla CA 92093

Steven Bogard
NOAA/NMFS
Pacific Fisheries Environ. Lab
1352 Lighthouse Ave.
Pacific Grove CA 93950

Levi Brekke
Civil and Environmental Engineering Department
University of California, Berkeley
385 Alcatraz Ave.
Oakland CA 94618

Canie Brooks
Long Beach City College
4901 East Carson Street
Long Beach CA 90808

Nancy Burnett
Sea Studios Foundation
810 Cannery Row
Monterey CA

Roger Byrne
Geography Department
University of California, Berkeley
Berkeley CA 94720

Annette Casey
Ocean Research Intl.
650 Loring Street
San Diego CA 92109

Richard Casey
Ocean Research Intl.
650 Loring Street
San Diego CA 92109

Dan Cayan
Scripps Institution of Oceanography
Dept. 0224
University of California, San Diego
9500 Gilman Drive
La Jolla CA 92093

John Chiang
JISAO
University of Washington
Box 354235
Seattle WA 98195-4235

Elaine J. Dorward-King
Rio Tinto Plc
6 St. James's Square
London SW1Y 4LD

Walter E. Dean
U.S. Geological Survey MS 980
Federal Center
Box 25046
Denver CO 80225

Andrew Comrie
University of Arizona
Department of Geography
409 Harvill
Tucson AZ 85721-0076

Michael Dettinger
U.S. Geological Survey
Scripps Institution of Oceanography
Dept. 0224
9500 Gilman Drive
La Jolla CA 92093

Noah Diffenbaugh
University of California, Santa Cruz
Department of Earth Science
Santa Cruz CA 95064

John Dracup
Civil and Environmental Engineering Department
University of California, Berkeley
533 Davis Hall M.C. 1710
Berkeley CA 94720-1710

Karin Forney
NOAA/NMFS
Southwest Fisheries Center
110 Shaffer Rd
Santa Cruz CA 95060

Charlene Frontiera
Hartnell College
156 Homestead Ave.
Salinas CA 93901

Gary J. Freeman
Pacific Gas & Electric Company RM 1308
Mail Code N13C
San Francisco CA 94105-1702

Alexander Gershunov
Climate Reseach Division
Scripps Institution of Oceanography
University of California, San Diego
9500 Gilman Dr.
La Jolla CA 92093-0224

Jim Goodridge
California Department of Water Resources
P0 Box 750
Mendocino CA 95460

Stephen Gray
Department of Botany, University of Wyoming
P0 Box 3165
Laramie WY 82071

Ann Marie Harris
Hydrologic Sciences Program
University of Nevada, Reno M5175
Reno NV 89557

Juan-Carlos Herguera
Division De Oceanologia CICESE
P0 Box 434844
San Diego CA 92143-4844

Hugo Hidalgo
Department of Civil and Environmental Engineering
University of California, Berkeley
631 Davis Hall M.C. 1710
Berkeley CA 94720-1710

Malcolm Hughes
University of Arizona
Laboratory of Tree-Ring Research
105 West Stadium
Tucson AZ 85721

Jim Ingraham, Jr.
NOAA-NMFS-Alaska Fisheries Science Center
7600 Sand Point Way NE
Seattle WA 98115-0070

Caroline Isaacs
U.S. Geological Survey MS 969345
Middlefield Road
Menlo Park CA 94025

Emi Ito
Geology and Geophysics
University of Minnesota
310 Pillsbury Dr. SE
Minneapolis MN 55455

Alexey Kaplan
LDEO at Columbia University
PO Box 1000/61 Route 9W
Palisades NY 10964

Thor Karlstrom
U.S. Geological Survey
4811 SW Brace Pt. Drive
Seattle WA 98136

Charles D. Keeling
Scripps Institution of Oceanography
University of California, San Diego
9500 Gilman Drive
La Jolla CA 92093

John Keyantash
University of California, Los Angeles
Dept. of Civil and Environmental Engineering
5731 Boelter Hall
Box 951593
Los Angeles CA 90095-1593

Leonid Klyashtorin
Federal Research Institute for Fisheries and Oceanography
VNIRO

Tara Kneeshaw
U.S. Geological Survey MS 910
345 Middlefield Rd
Menlo Park CA 94025

Noah Knowles
Scripps Institution of Oceanography
Dept. 0224
University of California, San Diego
9500 Gilman Drive
La Jolla CA 92093

Lydia B. Ladah
CICESE Division of Oceanography
Department of Ecology
PO Box 434844
San Diego CA 92143-4844

Peggy Lehman
California Department of Water Resources
3251 S Street
Sacramento CA 95816

Mark Losleben
Mountain Research Station INSTAAR
University of Colorado
818 County Road 116
Nederland CO 80466

Debby Luchsinger
University of Denver
Department of Geography
2050 E. Iliff Ave.
Denver CO 80208

Sam Luoma
CALFED/U.S. Geological Survey
345 Middlefield Rd MS 465
Menlo Park CA 94028

Mark Lyford
Department of Botany, University of Wyoming
Box 3165
Laramie WY 82071

Greg McCabe
U.S. Geological Survey
Denver Federal Center MS 412
Denver CO 80225

John A McGowan
Scripps Institution of Oceanography
Dept. 0224
University of California, San Diego- 0227
9500 Gilman Drive
La Jolla CA 92093

Nate Mantua
JISAO University of Washington
Box 354235
Seattle WA 98195-4235

Dave Meko
University of Arizona
Laboratory of Tree-Ring Research
105 W. Stadium
Tucson AZ 85721

Ed Mercurio
Hartnell College
647 Wilson St
Salinas CA 93901

Connie Millar
USDA Forest Service
PSW Research Station Box 245
Berkeley CA 94701-0245

Bill Mills
Tetra Tech Inc.
3746 Mt. Diablo Blvd. #300
Lafayette CA 94549-3681

Keith Mootsey
Long Beach City College
4901 East Carson Street
Long Beach CA 90808

Tom Murphree
Naval Postgraduate School, Department of Meteorology
589 Dyer Rd.
Monterey CA 93943-5114

Patrick Ng'ang'a
Texas A&M University - Commerce
Department of Biological and Earth Science
TAMU-C,
Commerce TX 75429

Judit Pap
Goddard Earth and Technology Center
University of Maryland, Baltimore
NASA Goddard Space Flight Center
Code 680-0
Greenbelt MD 20771

Charles Perry
U.S. Geological Survey
Water Resources Division
4821 Quail Crest Place
Lawrence KS 66049

David Pierce
Climate Research Division
Scripps Institution of Oceanography
Dept. 0224
9500 Gilman Drive
La Jolla CA 92093-0224

Michael Pisaric
Big Sky Institute
Montana State University
106 AJM Johnson Hall
Bozeman MT 59717

Kelly Redmond
Western Regional Climate Center
Desert Research Institute
2215 Raggio Parkway
Reno NV 89512-1095

Larry Riddle
Scripps Institution of Oceanography
Climate Research Division 0224
University of California, San Diego
La Jolla CA 92093-0224

Maury Roos
California Department of Water Resources
1305 Lynette Way
Sacramento CA 95831

Arndt Schimmelmann
Indiana University
Department of Geological Sciences-Geology 129
1005 East 10th
Bloomington IN 47405-1403

Frank Schwing
Pacific Fisheries Environmental Lab
1352 Lighthouse Avenue
Pacific Grove CA 93950

Louis Scuderi
Department of Earth and Planet Science
University of New Mexico, Northrup Hall
Albuquerque NM 87131

Jeff Severinghaus
Scripps Institution of Oceanography
University of California, San Diego
9500 Gilman Dr.
La Jolla CA 92093-0224

Gary D. Sharp
Center For Climate/Ocean Resources Study
PO Box 2223
Monterey CA 93940

Saxon Sharpe
Desert Research Institute
2215 Raggio Parkway
Reno NV 89512

Larry Smith
U.S. Geological Survey
7801 Folsom Blvd., Suite 325
Sacramento CA 95826

Paul Smith
NOAA/NMFS
Southwest Fisheries Science Center
La Jolla CA 92038-0271

Mark Snyder
University of California, Santa Cruz
143 Cypress Park
Santa Cruz CA 95060

William Sydeman
PRBO Marine Science Division
4990 Shoreline Hwy.
Stinson Beach CA 94970

Scott Starratt
U.S. Geological Survey
345 Middlefield Rd MS 910
Menlo Park CA 95025

Iris Stewart
Scripps Institution of Oceanography
University of California, San Diego
9500 Gilman Dr.
La Jolla CA 92093-0224

George H. Taylor
Oregon Climate Service
Oregon State University
316 Strand Ag Hall
Corvallis OR 97331-2209

Janice Tomson
Long Beach City College
4901 East Carson Street
Long Beach CA

Zbigniew Ustrnul
Institute of Meteorology, Poland
University of Arizona
Department of Geography
Harvill Bldg. Box#2,
PO Box 210076
Tucson AZ 85721 -0076

Elmira Wan
U.S. Geological Survey
345 Middlefield Rd MS 975
Menlo Park CA 94025

James West
U.S. Bureau of Reclamation
3429 Oyster Bay
Davis CA 95616

Anthony Westerling
Scripps Institution of Oceanography
Climate Research Division
University of California, San Diego
9500 Gilman Dr.
La Jolla CA 92093-0224

Bob Westfall
Pacific Southwest Research Station
U.S. Forest Service
PO Box 245
Berkeley CA 94701

Warren White
Scripps Institution of Oceanography
Climate Research Division 0224
University of California-San Diego
La Jolla CA 92093

Ray Wilson
U.S. Geological Survey MS 977
345 Middlefield Rd.
Menlo Park CA 94025

Richard Wilson
Columbia University
1001 B. Ave. #2
Coronado CA 92118

Connie Woodhouse
NOAA Paleoclimatology Program NGDC
325 Broadway
Boulder CO 80305

Zicheng Yu
EES Department, Lehigh University
31 Williams Drive
Bethlehem PA 18015-3188

*U.S. GPO 2003-0-583-792